ITU Journal
Future and evolving technologies

FREE I FAST I FOR ALL

Special issue

Internet of Bio-Nano Things for health applications

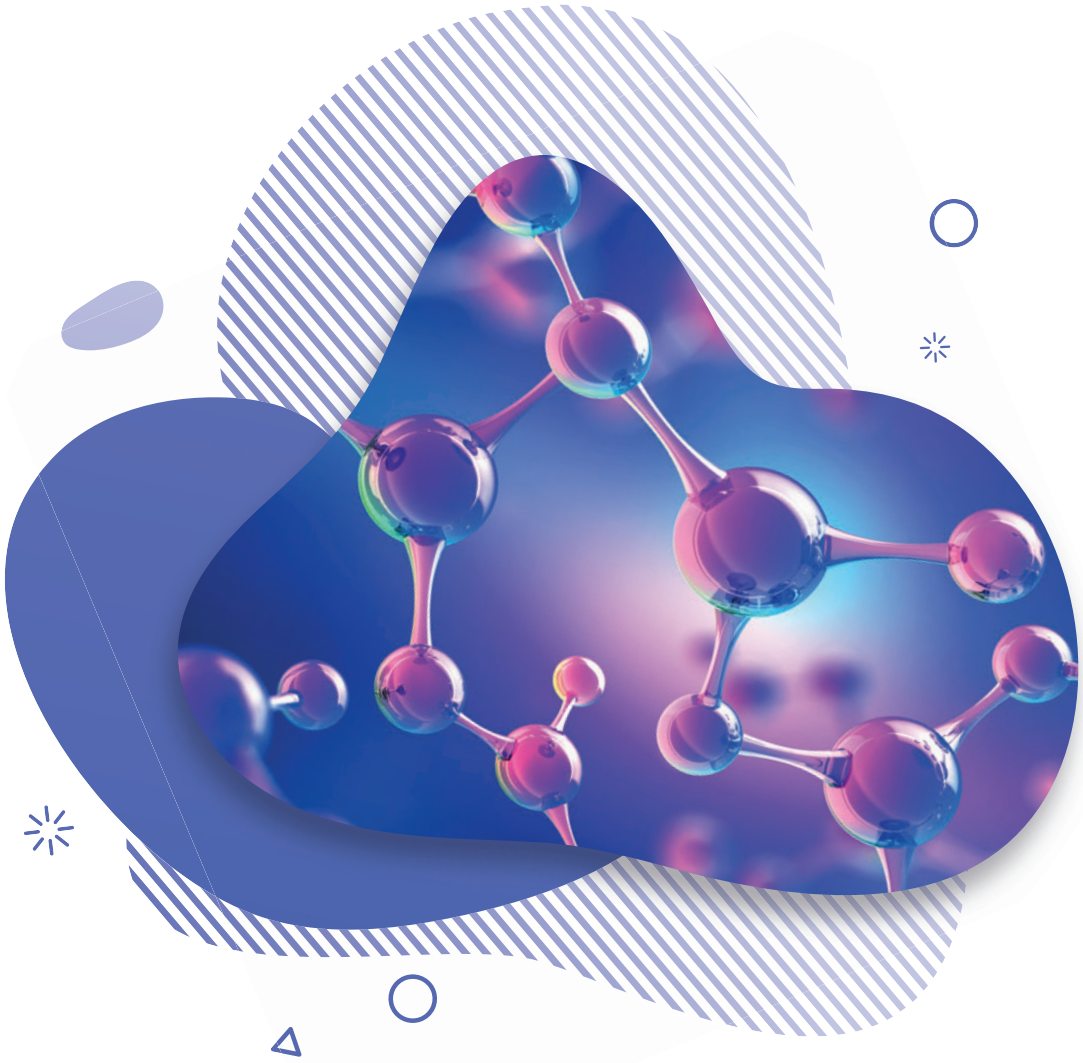

Volume 2 (2021), Issue 3

ITU Journal
Future and evolving technologies

Volume 2 (2021), Issue 3

Internet of Bio-Nano Things for health applications

ITU Journal
Future and evolving technologies

FREE I FAST I FOR ALL

The ITU Journal on Future and Evolving Technologies (ITU J-FET) is an international journal providing complete coverage of all communications and networking paradigms, free of charge for both readers and authors.

The ITU Journal considers yet-to-be-published papers addressing fundamental and applied research. It shares new techniques and concepts, analyses and tutorials, and learnings from experiments and physical and simulated test beds. It also discusses the implications of the latest research results for policy and regulation, legal frameworks, and the economy and society. This publication builds bridges between disciplines, connects theory with application, and stimulates international dialogue. Its interdisciplinary approach reflects ITU's comprehensive field of interest and explores the convergence of ICT with other disciplines.

The ITU Journal welcomes submissions at any time, on any topic within its scope.

Publication rights

SUGGESTED CITATION: ITU Journal on Future and Evolving Technologies, Volume 2 (2021), Issue 3.

ADDITIONAL INFORMATION
Please visit the ITU J-FET website at
https://www.itu.int/en/journal/j-fet/Pages/default.aspx

Inquiries should be addressed to
Alessia Magliarditi at: journal@itu.int

EDITORIAL BOARD

TABLE OF CONTENTS

LIST OF ABSTRACTS

Internet of Bio-Nano Things: A review of applications, enabling technologies and key challenges

Pages 1-24

Murat Kuscu, Bige Deniz Unluturk

Internet of Bio-Nano Things (IoBNT) is envisioned to be a heterogeneous network of nanoscale and biological devices, so called Bio-Nano Things (BNTs), communicating via non-conventional means, e.g., molecular communications (MC), in non-conventional environments, e.g., inside human body. The main objective of this emerging networking framework is to enable direct and seamless interaction with biological systems for accurate sensing and control of their dynamics in real time. This close interaction between bio and cyber domains with unprecedentedly high spatio-temporal resolution is expected to open up vast opportunities to devise novel applications, especially in healthcare area, such as intrabody continuous health monitoring. There are, however, substantial challenges to be overcome if the enormous potential of the IoBNT is to be realized. These range from developing feasible nanocommunication and energy harvesting techniques for BNTs to handling the big data generated by IoBNT. In this survey, we attempt to provide a comprehensive overview of the IoBNT framework along with its main components and applications. An investigation of key technological challenges is presented together with a detailed review of the state-of-the-art approaches and a discussion of future research directions.

View Article

Enabling molecular communication through chirality of enantiomers

Pages 25-32

Valeria Loscrí, Anna Maria Vegni

With the advancement of nanotechnology, there has been fervid research activity on new communication paradigms suitable for new challenging contexts, such as biological systems. Among different approaches, the most considered has been artificial Molecular Communication, where entities such as synthetic molecules, enzymes, hormones, bacteria etc. are functionalized in order to implement information exchange with the surrounding system and with other entities. In this context, it is interesting to analyze specific features that could be exploited for effective communication paradigms. In this paper, we focus on chiral molecules (a.k.a. enantiomers) as novel enablers for a molecular communication paradigm. Chirality is an interesting and appealing feature existing in nature and that can be replicated with strong emphasis in new types of materials, such as metasurfaces and metamaterials. A deep knowledge of chirality features and how chiral molecules interact with each other or with achiral molecules provides insights into designing a new molecular communication technique suitable for biological environments. In this contribution, we will highlight the main applications of chiral molecules and we will present chiral features as the viable way for realizing a nanocommunication system.

View Article

Transmission and detection techniques for Internet of Bio-Nano Things applications with static and mobile molecular communication: A survey

Pages 33-78

Amit K. Shrivastava, Debanjan Das, Neeraj Varshney, Rajarshi Mahapatra

Recent studies have shown that designing communication systems at nanoscale and microscale for the Internet of Bio-Nano Things (IoBNT) applications is possible using Molecular Communication (MC), where two or multiple nodes communicate with each other by transmitting chemical molecules. The basic steps involved in MC are the transmission of molecules, propagation of molecules in the medium, and reception of the molecules at the receiver. Various transmission schemes, channel models, and detection techniques have been proposed for MC in recent years. This paper, therefore, presents an exhaustive review of the existing literature on detection techniques along with their transmission schemes under various MC setups. More specifically, for each setup, this survey includes the transmission and detection techniques under four different environments to support various IoBNT applications: (i) static transmitter and receiver in a pure-diffusive channel, (ii) static transmitter and receiver in a flow-induced diffusive channel, (iii) mobile transmitter and receiver in a pure-diffusive channel, (iv) mobile transmitter and receiver in a flow-induced diffusive channel. Also, performances and complexities of various detection schemes have been compared. Further, several challenges in detection and their possible solutions have been discussed under both static and mobile scenarios. Furthermore, some experimental works in MC are presented to show realistic transmission and detection procedures available in practice. Finally, future research directions and challenges in the practical design of the transmitter and receiver are described to realize MC for IoBNT health applications.

View Article

Brainwave assistive system for paralyzed individuals

Pages 79-89

Md Ahnaf Shariar, Syeda Maliha Monowara, Md. Shafayat Ul Islam, Muhammed Junaid Noor Jawad, Saifur Rahman Sabuj

The Brain-Computer Interface (BCI) is a system based on brainwaves that can be used to translate and comprehend the innumerable activities of the brain. Brainwave refers to the bioelectric impulses invariably produced in the human brain during neurotransmission, often measured as the action potential. Moreover, BCI essentially uses the widely studied Electroencephalography (EEG) technique to capture brainwave data. Paralysis generally occurs when there is a disturbance in the central nervous system prompted by a neurodegenerative or unforeseen event. To overcome the obstacles associated with paralysis, this paper on the brainwave-assistive system is based on the BCI incorporated with Internet-of-things. BCI can be implemented to achieve control over external devices and applications. For instance, the process of cursor control, motor control, neuroprosthetics and wheelchair control, etc. In this paper, the OpenBCI Cyton-biosensing board has been used for the collection of the EEG data. The accumulated EEG data is executed subsequently to obtain control over the respective systems in real-time. Hence, it can be concluded that the experiments of the paper support the idea of controlling an interfaced system through the real-time application of EEG data.

View Article

Rate control for therapeutic applications in Internet of Bio-Nano Things using molecular communication: A survey

Pages 91-99
Shirin Salehi, Naghmeh Sadat Moayedian, Mohammad Taghi Shafiee

Molecular communication is transmitting and receiving chemical signals using molecules and is an interdisciplinary field between nanotechnology, biology, and communication. Molecular communication can be used for connecting bio-nano things. The connected nano-things build a nano-network. Transport mechanisms in molecular communication include free diffusion, gap junction channels, molecular motors, self-propelling microorganisms like bacteria and random collision of mobile nano-things. Free diffusion is the most widely used transport mechanism in the literature. Brownian motion is always available and its energy consumption is zero. This paper explores the therapeutic applications of rate control in the Internet of Bio-Nano Things and reviews the recent trends and advancements in the field of molecular communication. These methods aim to guarantee the desired rate of drug molecules at the target site and overcome the side effects of excessive emission.

View Article

Information theoretic modeling of paranodal regions in myelinated axons

Pages 101-110
Caglar Koca, Ozgur Ergul, Meltem Civas, Ozgur B. Akan

As a natural form of nanoscale communication, neuro-spike communication inspires the deployment of nanomachines inside the human body for healthcare. To this end, the identification of failure mechanisms in normal and diseased connections of nervous nano-networks is crucial. Thus, in this paper, we investigate the information transmission through a single myelinated axon segment. We introduce a realistic multi-compartmental model for a single myelinated segment by incorporating the axon's paranodal regions to the model. Next, we characterize the myelinated segment communication channel in terms of attenuation over the range of frequencies. Based on this, we derive the rate per channel use and upper bound on the information capacity. The performance evaluations reveal that our approach provides dramatic correction regarding frequency response. We believe that this result could have a significant effect on the characterization of demyelinated axons from the information and communication technology (ICT) perspective.

View Article

Evolutionary game theoretic resource allocation simulation for molecular communication

Pages 111-119
Caglar Koca, Meltem Civas, Ozgur B. Akan

Molecular Communication (MC) is an emerging technology using molecules to transfer information between nanomachines. In this paper, we approach the resource allocation problem in Molecular Nano-networks (MCN) from the perspective of evolutionary game theory. In particular, we consider an MCN as an organism having three types of nodes acting as a sensor, relay, and sink, respectively. The resources are distributed among the nodes according to an evolutionary process, which relies on the selection of the most successful organisms followed by creating their offspring iteratively. In this regard, the success of an organism is measured by the total number of dropped messages during its life cycle. To illustrate the evolution procedure, we design a toy problem, and then solve it analytically and using the evolution approach for comparison. We further simulate the performance of the evolution approach on randomly generated organisms. The results reveal the potential of evolutionary game theory tools to improve the transmission performance of MCNs.

View Article

Electric manifestations and social implications of bacteria aggregation from the Bessel-Keller-Segel equation

Pages 121-128
Huber Nieto-Chaupis

This paper proposes a fair extension of Keller-Segel equation based in the argument that bacteria exhibit properties electric in their composition. The new mathematical form of this extension involves the integer-order Bessel functions. With this one can go through the electrodynamics of the representative scenarios in order to understand the social behavior of bacteria. From the theoretical side this paper demonstrates that, charged electrically, aggregation of bacteria would give rise to electric currents that hypothetically are the reasons for social organization and disruption among them. The electrical properties of bacteria from this mathematical proposal might be relevant in a prospective implementation of so-called Internet of Bio-Nano Things network, that aims to be characterized for having a very high signal/noise.

View Article

INTERNET OF BIO-NANO THINGS: A REVIEW OF APPLICATIONS, ENABLING TECHNOLOGIES AND KEY CHALLENGES

Murat Kuscu[1] and Bige Deniz Unluturk[2]
[1]Department of Electrical and Electronics Engineering, Koc University, Rumelifeneri Yolu 34450, Sariyer, Istanbul, Turkey, [2]Department of Electrical & Computer Engineering and Biomedical Engineering, 775 Woodlot Dr., East Lansing, 48823, MI, USA

NOTE: Corresponding author: mkuscu@ku.edu.tr

Abstract *– Internet of Bio-Nano Things (IoBNT) is envisioned to be a heterogeneous network of nanoscale and biological devices, so called Bio-Nano Things (BNTs), communicating via non-conventional means, e.g., molecular communications (MC), in non-conventional environments, e.g., inside human body. The main objective of this emerging networking framework is to enable direct and seamless interaction with biological systems for accurate sensing and control of their dynamics in real time. This close interaction between bio and cyber domains with unprecedentedly high spatio-temporal resolution is expected to open up vast opportunities to devise novel applications, especially in healthcare area, such as intrabody continuous health monitoring. There are, however, substantial challenges to be overcome if the enormous potential of the IoBNT is to be realized. These range from developing feasible nanocommunication and energy harvesting techniques for BNTs to handling the big data generated by IoBNT. In this survey, we attempt to provide a comprehensive overview of the IoBNT framework along with its main components and applications. An investigation of key technological challenges is presented together with a detailed review of the state-of-the-art approaches and a discussion of future research directions.*

Keywords – Internet of Bio-Nano Things, molecular communications, nanonetworks, bio-cyber interfaces, THz-band nanocommunications, nanomachines, nanobiosensors, molecular machines, nanoscale energy harvesting

1. INTRODUCTION

As Internet of Things (IoT) approaches technological maturity with growing number of applications on the market, new integrative ideas emerge to push the current boundaries of IoT and extend its application range. One such approach follows a holistic view and regards the universe as an interconnected entity which is to be observed, understood, and manipulated with new information and communication technologies (ICT). At the center of this approach lies an emerging ICT framework, the Internet of Bio-Nano Things (IoBNT), envisioning the heterogeneous collaborative networks of natural and artificial nano-biological functional devices (e.g., engineered bacteria, human cells, nanobiosensors), seamlessly integrated to the Internet infrastructure [1]. IoBNT is positioned to extend our connectivity and control over non-conventional domains (e.g., human body) with unprecedented spatio-temporal resolution, enabling paradigm-shifting applications, particularly in the healthcare domain, such as intrabody continuous health monitoring and theranostic systems with single molecular precision. The broad application prospects of IoBNT have attracted significant research interest at the intersection of ICT, bionanotechnology, and medical sciences, with the great ma- jority of studies directed towards (i) the design and implementation of Bio-Nano Things (BNTs) [2, 3], (ii) the understanding of natural IoBNTs (e.g., nervous nanonet- work) [4, 5], (iii) the development of communication and networking methods for IoBNT (e.g., molecular communications) [6, 7, 8], (iv) the design of bio/cyber and nano/macro interfaces [9], and (v) the development of new IoBNT applications [10, 11, 12].

Along the aforementioned directions, this survey presents the most recent advances with respect to the theoretical foundations and practical implementation of IoBNT. To this end, we first attempt to provide a big picture of the IoBNT framework. Our discussion starts with the natural IoBNT systems, which inspire the researchers in designing artificial IoBNT systems. These include biological human-body nanonetworks, such as nervous nanonetwork, bacterial nanonetworks, and plant communication networks. Interfacing these systems with artificial IoBNT systems that monitor and control their biochemical states is expected to enable novel IoBNT applications. We extend our discussion of the IoBNT framework with the investigation of various types of BNTs, including engineered-cell based BNTs and artificial molecular and nanomachines, which ultimately determine the capabilities of IoBNT. This is followed by a review of potential IoBNT applications. Although most of them concern healthcare, there are many novel environmental and industrial applications promised by IoBNT, such as smart agriculture, food quality control, monitoring of toxic agents and pollutants, which are reviewed in this paper.

We also provide a comprehensive review of the key technical challenges in realizing the IoBNT applications, and overview the state-of-the-art solutions and future

research directions that can target them. Developing new communication methods for IoBNT is the foremost challenge, as the conventional electromagnetic (EM) techniques are either not feasible for the size- and energy-constrained BNTs or not performing well in the envisioned IoBNT application environments, such as intra-body. Molecular communications have emerged as the most promising technique to enable IoBNT, as it is already utilized by natural BNTs in a ridiculously energy-efficient and robust manner. In addition to the detailed review of MC research, we also look into other emerging communication methods proposed for IoBNT, such as those based on acoustic waves, terahertz (THz)-band EM waves, and Fö rster Resonance Energy Transfer (FRET). The emerging idea of using human body as an IoBNT infrastructure is also discussed through an overview of thrubody haptic communications, vagus nerve-based communication and microbiome-gut-brain-axis-based communication proposed to connect BNTs within human body.

Bio-cyber interfaces lie at the heart of IoBNT applications, which consist in the seamless interconnection of heterogeneous technologies in diverse application environments. We provide an extensive review of electrical and optical bio-cyber interfacing technologies including biosensing-, redox-, optogenetics- and fluorescence-based techniques as well as the newly emerging magnetic and THz-based methods. IoBNT applications with high spatio-temporal resolutions in control and monitoring are expected to generate and handle significant amount of heterogeneous data, imposing critical challenges of big data processing, storage, and transfer, which are also reviewed in this paper. Self-sustaining BNTs are key to the success of IoBNT applications. Although engineered cell-based BNTs might have an inherited metabolism for energy management, artificial BNTs such as those based on nanomaterials should have dedicated mechanisms for energy harvesting (EH) and storage for continuous operation. We review various EH technologies that are suitable for the envisioned BNT architectures and IoBNT application environments. Wireless power transfer (WPT) techniques and energy storage technologies are also reviewed to provide a broader perspective on the energy challenges of IoBNT. We also discuss the security, privacy, biocompatibility and co-existence challenges of IoBNT originating from the unprecedentedly close interaction with the complex biological systems, including our own human body.

Although there are many recent survey articles focused on particular aspects of IoBNT [7, 13, 3, 6, 14, 15, 9, 16], this comprehensive review is aimed at providing a broader snapshot of the state-of-the-art in the entire IoBNT field in order to contribute to an holistic understanding of the current technological challenges and potential research directions.

2. FRAMEWORK

2.1 Natural IoBNT

In the last several billion years, most basic single cell organisms evolved into complex systems of multi-cellular organisms composed of living nanoscale building blocks, i.e., cells, to perform the most intricate tasks in an optimized fashion. This highly coordinated structure of multicellular organisms are indeed a result of self-organized networks of cells communicating at various scales. Hence, these networks can be considered as natural IoBNTs and many lessons can be drawn in terms of effective techniques of communications and networking at nanoscale by observing the behavior of these natural IoBNTS. Here, we will describe some of the most natural IoBNTS, namely, human body nanonetworks, bacterial nanonetworks, and plant networks.

2.1.1 Human-body nanonetworks

Biological systems in the human body are connected to each other and communicate primarily through molecular interactions and action potentials. These communication pathways enable the coordination of various types of cells, which are basic building blocks of life, and organization into tissues, organs, and systems with different structures and functions. The dense network of interconnected cells use signaling at various scales such as juxtracrine (signaling among cells in contact with each other), paracrine (signaling among cells in the vicinity of each other, but not in contact), or endocrine (signaling among cells distant from each other). The performance and reliability of this intrabody networks ensures the health of the human body by preserving the equilibrium state, i.e., homeostasis, achieved by tight control of nervous system reacting to molecular and electrical inputs coming from all parts of the body and environmental cues coming through five senses. Any failure in communication in these networks will deteriorate the health and lead to diseases [4]. For example, i) problems in electrical signaling of heart cells cause arrhythmia, i.e., irregular heartbeat, which can end in heart failure, stroke or sudden death; ii) communication problems between the brain and the body arising from the damage to protective sheath (myelin) that cover nerve fibers by immune system attacks which is the Multiple Sclerosis (MS) disease potentially causing paralysis; iii) irresponsiveness of cells to insulin which is a molecule carrying information re-gulating metabolism in endocrine pathways leads to diabetes; iv) irregular signaling in the microbiome-gut-brain axis, where microbes in gut and brain cells exchange information through endocrine and nervous pathways, is shown to affect mood, neuro-development, and obesity. The most advanced and complex human-body network is the nervous system [5], composed of a very large scale network of neurons interconnected through neuro-spike [17] and synapse [18] communication channels. The nervous nanonetwork distributed throughout the body

transfers information about external stimuli to the brain, which is a dense network of highly complex neuron cells. The brain processes all this information and sends back commands to the body accordingly to control the vital functions, behavior and physical activities. Other networks spanning the whole body yet carrying information on a slower scale than the electrochemical pulses of nervous nanonetworks, are cardiovascular system and the endocrine system both composed of vessels carrying information in molecular form in blood and lymph, respectively[4].

2.1.2 Bacterial nanonetworks

Besides the IoBNT in multicellular organisms such as human body, single cell organisms such as bacteria show coordination and group behavior enabled by intercellular signaling. The first communication mechanism among bacteria discovered is quorum sensing (QS), the ability to detect and respond to cell population density represented by the concentration of the signaling molecules called auto-inducers [19]. QS controls biofilm formation, virulence factor expression, production of secondary metabolites and stress adaptation mechanisms. Using this mechanism, unicellular bacteria coordinate their behavior and act as if they are a unified multicellular organism. Recently, besides the molecular means of QS, electrical means of communication among bacteria has been shown [20]. The bacterial membrane potentials creating potassium waves through bacterial biofilms synchronize the behavior of bacteria in biofilms. In case of nutrient depletion in the center of the biofilm, this signaling mechanism warns the outer circle of bacteria in the biofilm to slow down growth allowing more nutrients to penetrate to the center. Using the above-mentioned communication mechanisms, bacteria form spatio temporally organized community structures optimizing the growth and fitness of the whole colony which resembles a decentralized decision-making system of millions of interconnected nodes. Studies also show that bacterial colonies engage in social behavior such as competition, collaboration, and cheating during the production of public goods [21]. Despite the limited resources of a single bacterium, tight coordination in the bacterial populations containing this sheer number of bacteria can be established. Hence, bacterial nanonetworks provide lots of clues to IoBNT researchers that are looking to form networks of large numbers of BNT devices with limited power and communication resources [22, 23, 24, 25].

2.1.3 Plant networks

Among the natural IoBNTs, plant networks are the most counterintuitive since plants seem to be immobile and solitary. However, the growth and development of plants are highly dependent on the communication both within a plant itself, among different plants, and between plants and micro organisms in soil. Although there is no physical nervous system in plants, electrical communications have been observed between the roots and the body of plants [26], and capillary networks carry molecular information to the various parts of the plant along with water and nutrients. Furthermore, nearby plants use pheromone communication to coordinate their behavior to avoid overgrowth and shadowing each other and to warn each other against attacks from animals and bugs [27, 28]. Considering the many species of plants in a forest, various weed and grass on top of the soil, ivies and the trees on which they live symbiotically, plant networks enable a high level coordination to share the resources and optimize growth of each plant. Another element helping this coordination is the presence of rhizobiome, i.e., the root associated microbiome, which are shaped by the plant signaling primary and secondary root metabolites [29]. In turn, the rhizobiome consisting of multiple species of bacteria helps the roots to reach necessary nutrients from the soil and protects the plant against pathogens. This rhizobiome-plant interaction significantly affects the health and growth of the plant.

2.2 Bio-Nano Things

In IoBNT framework, Bio-Nano Things are defined as basic structural and functional units operating at nanoscale within the biological environment [1]. BNTs are expected to have typical functionalities of the embedded computing devices in IoT, such as sensing, processing, actuation, and communication.

To build BNTs, one approach is miniaturizing electrical devices with nanotechnology and encapsulating these devices for biocompatibility. However, at such a small size, miniaturized electrical BNTs suffer from lack of space for batteries to provide sufficient power and antenna generating usable frequencies. Another approach to build BNTs is utilizing biological units as substrates such as cells which can be considered standalone devices that can harvest its energy from the environment. Another important class of BNTs is molecular and nanomachines, which are tiny artificial devices with feature sizes between 1 and 100 nm, that can perform a useful task at nanoscale [30, 31]. Recent years have observed the design and implementation of molecular and nanomachines with increasing complexity and sophistication, expanding the range of their applications, which now include molecular factories, self-propelling cargo carriers, nanosensors, and molecular computation [32]. At a coarse-grained level, molecular and nanomachines can be categorized into three main groups: molecular machines, self-assembled nanomachines, and hybrid inorganic nanomachines.

Molecular machines are synthetic molecular systems consisting of single or a few molecules that can undergo a mechanical movement upon stimulation resulting in a useful task [33]. This class of BNTs can be further divided into two categories: molecular motors and switches.

Molecular motors are molecular devices, typically implemented with rotaxane- or catenane-type mechanically-interlocked molecular architectures, that can perform work that in turn influences the system as a function of trajectory with chemical, light or electrochemical energy inputs [34, 35]. Molecular motors are promising for biomimicking applications such as synthesizing new molecules from individual atoms and molecules in a programmable manner, just as their biological counterparts, such as ribosome. On the other hand, molecular switches reversibly change the state of the system upon the application of stimuli by producing no net work. Molecular switches are being utilized for high-resolution molecular sensing applications and promising for future molecular computer architectures capable of both digital and analog computing [32].

Self-assembled nanomachines are nanoscale devices that are built based on autonomous or programmed organization of constituent molecules, and can perform similar functions to molecular machines, such as switching, logic gating, active propulsion, typically at larger length scales [32]. Self-assembled DNA nanomachines have particularly attracted research interest due to the high-level control of their assembly through DNA origami techniques, which enable the selective folding of DNA strands into particular designs with the use of short staple strands [36, 37]. Selective targeting and versatile functionalization of DNA nanomachines have expanded their application areas, which involve bio-inspired dynamic DNA walkers, cargo-carrying DNA boxes with stimuli-responsive logic gate-based opening mechanisms, and stimuli-responsive DNA switches [38].

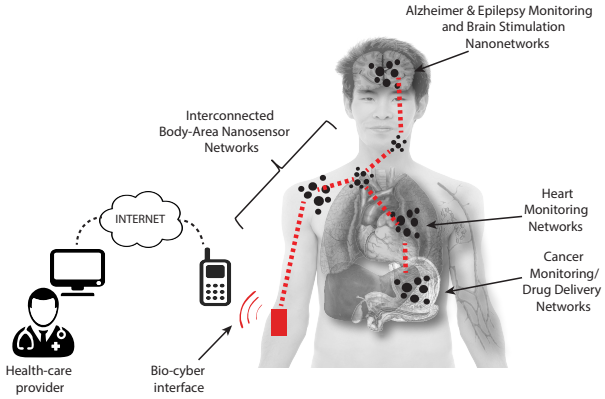

Fig. 1 – Conceptual drawing of a continuous health monitoring application of IoBNT.

Hybrid inorganic nanomachines are sub-100-nanometer devices that can be made of metal, metal oxide or hybrid Nanoparticles (NPs) [32]. In comparison to self-assembled nanomachines and molecular machines, which involve soft biomolecular components, they tend to be more structurally rigid, however, less biocompatible. Additionally, their interaction with external stimuli, such as light, magnetic and electric fields, tend to be much stronger, which makes them attractive for externally controlled applications [32]. Janus nanomachines, which are made of Janus Nanoparticles (JNPs), nanostructures with two chemically distinct parts, are the most popular inorganic nanomachines due to their anisotropic structures that give rise to exceptional propulsion capabilities [39]. This anisotropy results in a chemical potential or thermal gradient in JNPs upon chemical catalysis or external light irradiation, which in turn, leads to the phoretic flow of surrounding fluid around the entire JNP surface. As a result of this phoretic flow, JNPs actively move in the opposite direction. There are also proposed architectures of self-propelled Janus nanomotors working based on the decomposition of hydrogen peroxide into oxygen as a driving force. Moreover, the use of mesoporous silica nanoparticles (MSNs) as JNPs has opened up new biomedical opportunities which involve the targeted delivery and controlled release of therapeutic and diagnostic agents encapsulated in their porous structure [40]. Although much has been done to devise exquisite and complex molecular and nanomachine architectures that can perform sensing, cargo transport, and switching operations, the potential of interconnecting these tiny machines for a wider range of biomedical applications has only recently attracted significant attention. Seveeral communication modalities have already been considered to enable controlled interaction and coordination of these devices, such as diffusion-mediated communication, which is based on the exchange of small molecules, e.g., glucose, through the signaling cascades triggering enzymatic reactions that fuel the movement of the receiver devices, and cell or cell-free genetic circuits that trigger the expression of a certain kind of protein, e.g., green fluorescent protein (GFP), in the receiver BNTs [41, 42, 43, 44]. External energy-mediated communications have also been widely studied to enable the small networks of molecular and nanomachines. This form of interaction occurs through several biophysical phenomena, such as pore formation and modulation of enzyme cascade re- actions, which are triggered by external stimuli such as light, chemicals, temperature, and electric and magnetic fields, and provides higher level of spatiotemporal control compared to the diffusion-mediated communication [41]. Non-covalent interactions considered for molecular and nanomachines involve the short-range electrostatic and hydrophobic/hydrophilic interactions, as well as complex formation through reversible ligand-receptor binding interactions. Lastly, inducing dynamic collective behaviors of active nanomachines, such as Janus nanomachines, through external stimuli, e.g., light, electric and magnetic fields, has also attracted great attention due to their emergent out-of-equilibrium properties resembling natural systems [45, 46, 47]. Incorporation of these interacting molecular and nanomachines into the larger IoBNT framework as heterogeneous BNTs can enable unprecedented therapeutic and diagnostic applications via

exquisite external, distributed, or programmed control with high spatiotemporal resolution.

2.3 IoBNT Applications

The IoBNT will enable a plethora of applications in many fields where the connection of biological entities and nanodevices to the Internet leads to unprecedented ways of interfacing with biology due to IoBNT's inherent biocompatibility, reduced invasiveness, and low power consumption. In the rest of this section, we discuss the potential of IoBNT in biomedical applications, smart agriculture, and environmental applications.

2.3.1 Biomedical Applications

The most promising applications of IoBNT are envisioned to be in the biomedical field where IoBNT would play a crucial role in healthcare. IoBNT comprising nanonetworks of biosensors and actuators operating near, on, or in the body, will enable real-time remote monitoring and control of patients' health.

A nanosensor network deployed in cardiovascular system monitoring vital signs such as heart rate, blood pressure, EEG signals, and blood oxygen and carbon dioxide levels may reveal abruptly occurring diseases such as heart attack and automatically alert healthcare providers. Meanwhile, continuous long-term monitoring of these vital signs may be used for management of chronic diseases as well as data collection to predict future attacks. Recently, researchers also considered applying IoBNT concept for detection and mitigation of infectious diseases [15] where bio-hybrid BNTs constantly monitors for biomarkers released by infectious microorganisms. Other biomarkers that would be interesting to monitor by IoBNT would be glucose. A sudden changes in glucose levels can be deadly for diabetic patients, IoBNT can alert the patient against low/high glucose levels and can help adjust precise and timely administration of insulin automatically. Similarly, IoBNTs can be used for hormonal therapy management in cancer treatments or hormone replacement therapies in sex change [48].

Besides monitoring applications, IoBNT can also lead the realization of next generation smart drug delivery applications. To spare the non-target organs and tissues from the side effects of drugs, BNTs can deliver medicine to targeted regions in human body. BNTs encapsulating drug molecules can either actively search for or be directed externally to target cells and release the drugs only on target location.

2.3.2 Smart Agriculture

Humans are not the only organisms that can benefit from remote health monitoring with IoBNT. The health of animals such as cattle and poultry can be also interrogated by IoBNT to ensure the health of the animals and the quality of their products such as meat, milk, and eggs. Another benefit of IoBNT to agriculture would be through monitoring of plants by measuring their health through BNTs deployed on the plants or in the soil. This can be also supported by BNTs monitoring and controlling smart irrigation systems, actively fertilizing the soil, and deterring bugs and wildlife damaging crops.

2.3.3 Environmental Applications

Another promising area for IoBNT applications is environmental monitoring. By deploying IoBNT networks in water supply and distribution systems, it might be possible to detect pollutants in the water and use nano-filters to remove harmful substances and toxic agents contained in it. A similar system can be deployed to combat air pollution in crowded cities. Another environmental application can be listed as handling the growing problem of waste management where IoBNTs can be used to sort and process waste. Nanosensors can sense and tag different materials and nanoactuators can biodegrade the tagged materials or alert service providers to remove potentially toxic waste that might pollute water or soil.

3. CHALLENGES

3.1 Communication Methods for IoBNT

Conventional forms of electromagnetic (EM) communications are deemed not suitable for connecting BNTs, mainly due to the antenna size limitations, biocompatibility concerns, and the severe attenuation of EM signals in physiological media relevant for IoBNT applications [1]. Because of these challenges, researchers have started a quest for alternative communication methods to extend our connectivity to nanoscales. We can classify the proposed nanocommunication methods into two main types: (i) Molecular communications (MC), (ii) THz-band EM. Other techniques based on magnetic coupling, Förster Resonance Energy Transfer (FRET), heat transfer and acoustic energy transfer have also been proposed for nanonetworks. In the rest of this section, these techniques will be briefly overviewed, with a particular focus on MC, which is considered as the most promising nanocommunication method to enable IoBNT.

3.1.1 Molecular Communications

Molecular communications is a bio-inspired communication technique, that uses molecules to transfer information. More specifically, a physically distinguishable feature of molecules, such as their type and concentration, is used to encode information, and random molecular motion in a fluidic channel is exploited as a means of signal propagation for information transfer. MC is radically different from conventional communication paradigms, e.g., EM communications, in various aspects such as the size and type of network entities, information transmission mechanisms, noise sources and fundamental performance limits including transmission delay, achievable data rates, coverage and power consumption.

Example MC scenarios between pairs of nanomachines are depicted in Fig. 2, where the messages are encoded into the concentration of molecules, and then transmitted to the receiver via molecular propagation in a fluidic channel. The information can also be encoded into the type, release time, or the electronic state of the molecules [8]. Different kinds of propagation methods for molecular messages are investigated in the literature, such as passive diffusion, active transport with molecular mo- tors [49], convection, and transport through gap junctions [50]. Among these, passive diffusion is the most promis- ing, as it does not require energy consumption, and thus perfectly suits the energy limitations of the envisioned nanomachines.

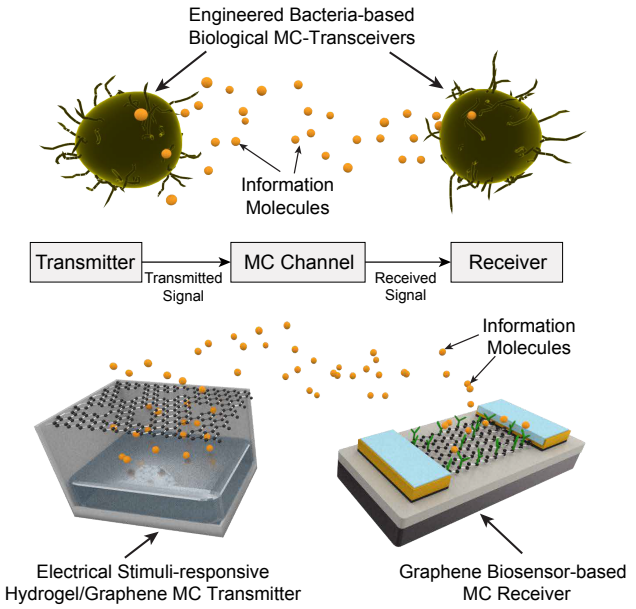

Fig. 2 – Components of an MC system with biological and nanomaterial-based MC transmitter and receiver design approaches.

MC channel has many peculiar characteristics. For example, the discrete nature of information carriers, i.e., molecules, results in molecular counting noise, which is of similar nature with the shot noise occurring in photonic devices [51]. The stochastic nature of the ligand-receptor binding process occurring at the receiver gives rise to colored noise, also leading to a strong correlation between molecular propagation process and reception [52]. The slow nature of diffusion leads to a substantial amount of channel memory, which in turn, causes severe inter-symbol interference (ISI), and limits the achievable data transmission rates [53]. The same reason also causes a significant delay in the transmission [54].

Deviations from the conventional means of communications necessitate radically different ideas for the design of transmitter and receiver architectures, and communication techniques for MC, and new approaches to channel modeling.

a) Transmitter and Receiver Architectures for MC:
There are mainly two design approaches considered for artificial nanomachines that can perform MC and form MC nanonetworks within the IoBNT framework. The first approach is to build the components of nanomachines using newly discovered nanomaterials, such as two-dimensional graphene, and one-dimensional silicon nanowire (SiNW) and carbon nanotube (CNT), which all manifest extraordinary characteristics at the interface of biology and electronics [55]. The other approach relies on synthetic biology, and envisions the use of engineered, i.e., genetically modified, bacteria as artificial nanomachines with communication functionalities wired into their intracellular signaling networks [24]. The physical nature of the BNTs determines the potential transmitter and receiver architectures. The MC transmitter of a BNT should perform the modulation of MC signals, and the release of molecules into the channel upon a stimulation by an external source, or as a result of an internal biochemical or electrical process. The receiver of a BNT is responsible for detecting the incoming molecular mes- sages, transducing them into a processable signal, and extracting the encoded information through signal processing. The decoded information can then be used by the BNT to perform a prescribed operation, e.g., modulation of gene expression or translocation. Therefore, the performance of the transmitter and receiver is critical for the proper operation of a BNT within an IoBNT application. Nanomaterial-based design approaches for MC transmitter mainly draw on the existing drug delivery technologies, such as stimuli-responsive hydrogels, molecule release rate of which is controlled by an electrical or chemical stimuli. Synthetic biology-based approaches, on the other hand, rely on making use of the already existing molecule release mechanisms of living cells, and tailoring these functionalities through genetic modifications to realize the desired MC modulation schemes. There are also theoretical MC transmitter designs that exploit stimuli-responsive ion channels to trigger the release of molecules in an externally controllable fashion [56]. Nanomaterial-based receiver designs are widely inspired by nanobiosensors, which share a common objective with MC receivers, that is to transduce biomolecular signals into a signal form suitable for processing. Although there are many nanobiosensor designs differing in their transducing mechanisms and the resulting signal form at the output, field-effect-transistor (FET)-based nanobiosensors have attracted the most attention for MC receiver design due to their scalability, simple design similar to conventional FETs, internal signal amplification by electrical field-effect, label-free operation, and the electrical output signals that allow fast processing of received signals. More importantly, FET-based nanobiosensors provide a wide range of design options. For example, they can accommodate different types of nanomaterials, e.g., graphene, SiNW, CNT, as the transducer channel, the conductivity of which is modulated by the molecular concentration in its proximity through the alteration of the surface potential and electrical field-effect. FET-

based nanobiosensors have also a biorecognition layer, which replaces the gate electrode in conventional FETs, and consists of receptor molecules selectively binding target molecules via affinity-based ligand-receptor interactions. Depending on the transducer channel material, the biorecongition layer can host a wide range of receptor molecules, ranging from proteins to DNAs. Among other options, graphene FET (GFET) biosensors provide unique advantages for the practical design of MC receiver. The main advantage of graphene is its high sensitivity to the charged analytes, e.g., proteins and DNAs, due to its extremely high carrier mobility and one-atom thickness, exposing all its atoms to the environment. The advent of new types of receptors, e.g., aptamers, has broadened the target range of nanoscale FET biosensors from ions to proteins, peptides, and even whole cells. Aptamers are short functional oligonucleotides (typically 20-60 nucleotides). Their base sequences for specific targets are identified from an oligonucleotide library with an in vitro process called systematic evolution of ligands by exponential enrichment (SELEX). Their application in biosensors has gained momentum due to their wide target range, chemical stability, and ease of production. Combined with the exceptional properties of graphene and aptamers, the ability of nanoscale FET biosensors to provide selective, label-free and continuous detection makes GFET aptamer-based biosensors, i.e., GFET aptasensors, very promising candidates for the design of MC receiver.

Biological MC receiver designs are based on the enhancement of biosensing and biochemical signal processing functionalities of livings cells with synthetic biology tools for the receiver operation. This approach consists in the design of new synthetic receptors that can provide more sensitivity and selectivity in physiological environments, for example, through kinetic proof reading mechanisms [57], and the implementation of new chemical reaction networks within the cell that can realize the required computations for decoding the received MC signals. Synthetic biology is already mature enough to allow performing complex digital computations, e.g., with networks of genetic NAND and NOR gates, as well as analog computations, such as logarithmically linear addition, ratiometric and power-law computations, in synthetic cells [58]. Synthetic gene networks integrating computation and memory is also proven feasible [59]. More importantly, the technology enables implementing BNTs capable of ob- serving individual receptors, as naturally done by living cells. Hence, it stands as a suitable domain for practi- cally implementing more information-efficient MC detec- tors based on the binding state history of individual receptors.

b) MC Channel Modeling: To design effective and efficient MC systems addressing the needs of the envisioned IoBNT applications, it is important to have a theoretical framework which can be used to optimize the physical components of the system with ICT performance metrics. Because of this, there has been tremendous interest in modeling the MC channels to find the ultimate performance limits in terms of information theoretical capacity and data rate. In majority of studies, MC channel is usually assumed to be unbounded where information-carrying molecules propagate through free diffusion with the underlying phenomenon of Brownian motion [60, 61]. In a few studies, diffusion is accompanied by a flow which directs the propagating molecules to a distant receiver [62, 63, 64], whereas some studies also consider the existence of reactive molecules within the channel which can chemically degrade the information carrier molecules and reduce the intersymbol interference. A few studies consider bounded MC channels, for example microfluidic channels where molecules propagate through convection-diffusion. In majority of these studies, it is assumed that the molecules are transmitted from a hypothetical point source, which is capable of releasing a known number of molecules to the channel in the form of an impulse signal at a given time instant. On the other hand, the receiver is typically assumed to be a transparent instrument, which is capable of counting every single molecule in a hypothetically defined space [63], or an ideal absorbing instrument capable of counting each molecule that is absorbed [65]. Common to these studies is the ignorance of the impact of the physical architectures of the transmitter and receiver on the communication channel. As such, researchers have been able to adopt the EM-inspired simplifications in modeling, such as linear and time-invariant (LTI) channel characteristics with additive white Gaussian noise, neglecting the effects of interactions and correlations resulting from transmitter and receiver architectures and channel geometry. This leads to a serious discrepancy between theory and practice, as revealed by the initial MC experiments performed with 'macroscale' sensors and dispensers utilized as MC transmitter and receiver, respectively, showing that the nonlinearity and time-variance caused by the operation of transmitter and receiver invalidate the models built upon these assumptions [66, 67].

On the other hand, some research groups have studied MC receivers that rely on ligand-receptor binding reactions, the common molecular sensing method in natural MC [68, 69]. Deterministic models, assuming free diffusion and point transmitter, have been developed for a virtual MC receiver with ligand receptors. Although the consideration of ligand receptors has advanced the accuracy of the models one step further, the employed assumptions about the transmitter and channel strictly limit the applicability of these models. Additionally, stochastic receiver models are developed for FET nanobiosensor-based MC receivers [69]. In [62], a model for MC with 2D biosensor-based receivers in microfluidic channels is provided. However, these initial models also rely on unrealistic assumptions, e.g., equilibrium conditions in ligand-receptor binding reaction, and ignore the implications of the receiver geometry.

Therefore, there is still a need for a bottom-up physical modeling approach originating from first principles, capturing all interactions in practical transmitter, channel and receiver architectures, causing nonlinear and time-varying behavior and unconventional noise and interference that may have decisive impacts on the development of MC techniques for IoBNT.

c) Experimental MC System Testbeds and Practical Demonstrations: Testbeds are crucial for validating theoretical models, and practically evaluating the performance of new communication techniques. However, research for building experimental MC systems has just recently gained momentum. Few studies in MC literature have focused on 'macroscale' implementation of MC systems with off-the-shelf components. For example, in [66, 70], the isopropyl alcohol (IPA) is used as airborne information carriers, and commercially available metal oxide semiconductor alcohol sensors are used as the MC receiver. The transmission of molecules is realized by electrically-controlled spray nozzles. In [71], the information is encoded in pH level of the transmitted fluid instead of molecular concentration or type. The acidic and basic fluids are injected into off-the-shelf flexible tubes via peristaltic pumps, and a macroscale pH meter is used as the MC receiver. In another testbed [67], magnetic nanoparticles (MNs) are employed as information carriers, which are injected into off-the-shelf mm-scale flexible tubes by flow pumps, and propagate through convection and diffusion. In this study, for the detection of messages encoded into MN concentration, the authors designed bulky detector coils placed around the tubes coupled with capacitors to form a resonator circuit, which informs about the concentration through a change in inductance and shift in resonance frequency. In this implementation, the designed receiver acts only as an observer, and does not physically interact with the information carrier molecules. The focus of the aforementioned studies is on macroscale MC using commercially available channels, and off-the-shelf sensors or bulky detectors as receivers that are not physically relevant for the application domain of MC and IoBNT.

Recently, the first micro/nanoscale demonstration of an MC system is reported in [72]. In this study, the authors provide the results of MC experiments using a custom-made microfluidic testbed with a graphene FET DNA biosensor-based MC receiver integrated into a microfluidic channel. A commercially available microfluidic flow control system is used to pump single-stranded DNA (ssDNA) molecules of different molecular concentrations into the microfluidic channel. Graphene transducer chan- nel of the receiver functionalized with complementary ss- DNAs transduces the real-time concentration of the propagating DNA molecules into electrical signals, which are then used for detection. The authors of the study report nM-level sensitivity and single-base-pair-mismatch selec- tivity for the receiver. However, they also note the very low communication rates on the order of 1 bit/minute, mainly resulting from the slow association-dissociation kinetics of DNA hybridization.

Biological MC testbeds have also been reported by many research groups. For example, in [73] and [74], authors implement a microfluidic MC testbed with genetically en- gineered Escherichia coli (E. coli) bacteria acting as receiver nanomachines. The bacteria in these studies have been engineered to respond to certain biomolecules, e.g., N-(3-Oxyhexanoyl)-L-homoserine lactone (C6-HSL) and N-Acyl homoserine lactone (AHL), by expressing green fluorescent proteins (GFP), which can later be detected via fluorescent microscopy upon excitation with light of certain wavelengths. Both studies report extremely low communication rates on the order of 1 bit/hour due to the lengthy process of gene expression required for each bit transmission. In [75], the authors prefer a different approach by exploiting the light-responsive proton pump gloeorhodopsin (GR) located in the bacterial membrane to obtain an optically controlled MC transmitter that can export protons into the fluidic channel upon the application of external light stimuli. Accordingly, protons are used as information carriers, which propagate through structural diffusion in water, and are detected by a pH sensor acting as the receiver. Using this testbed, the authors report communication rates on the order of 1 bit/minute. Although biological designs have been demonstrated individually for both MC transmitter and receiver, there is yet to be any practical implementation of an entirely biological testbed for end-to-end MC.

d) Development of MC Techniques: The unconventional characteristics of MC, such as discrete nature of information carriers and slow nature of propagation mechanisms, which bear no similarity to conventional EM communications, lead to various challenges, such as high channel memory causing severe ISI, non-Gaussian noise sources, time-variance, and very low communication rates, as revealed by several theoretical investigations [62, 13]. The initial experimental studies performed on both macro- and micro-scales also demonstrated the high level of nonlinearity mainly resulting from the characteristics of sensors utilized as receivers [66, 70, 72]. One can expect that practical MC system implementations for IoBNT applications may face many more challenges, such as molecular interference due to existence of different types of molecules in the channel, environmental fluctuations, such as those in flow velocity and temperature, ionic screening in physiologically relevant environments preventing the receiver from detecting the electrical charges of information molecules, and new noise sources such as electronic 1/f noise in nanomaterial-based MC receivers. Therefore, MC requires new communication methods that account for these peculiarities, and overcome their detrimental effects on the communication performance. Considering physical limitations of the envisioned BNTs, these techniques should be also low-complexity and low-energy, i.e., low-molecule-use.

We summarize some of the major problems stemming from the limitations associated with the physical proper-

ties of the MC channel, transmitter and receiver architectures as follows:

- **Intersymbol Interference (ISI):** Due to the slow nature of molecular diffusion in MC channel, severe ISI occurs in both forward and backward direction, which is the main factor limiting the communication rate. The effect of ISI is less pronounced in flow-based MC channels; however, the slow reaction kinetics at the receiver surface might compound the ISI, as revealed in [72]. Therefore, MC techniques should account for ISI, either removing it or reducing its effects.

- **Nonlinearity and Time-variance:** The nonlinearity of the MC system results from the nonlinear transmission and propagation dynamics, and the reaction-based receiver mechanisms. On the receiver side, in particular, the saturation of the receiver could have substantial effect on the detection performance. Therefore, the developed modulation and detection techniques should account for nonlinearity. Time-variance can result from the fluctuations in the flow conditions, as well as from the time-varying molecular interference level in the channel.

- **Molecular Interference:** The existence of other molecules in the MC channel can originate from an irrelevant biological process, or another MC system co-existing in the same channel. The interference manifests itself on the receiver side, as the selectivity of receptors against information molecules is far from ideal in practice, and thus, many different types of molecules having finite affinity with the receptors, could also bind the same receptors, resulting in considerable interference at the received signal. To overcome this problem, new detection methods exploiting the frequency-domain characteristics of the receiver reaction and transducing processes can be developed to increase the selectivity [57]. Moreover, the receptor cross-talk resulting from multiple types of molecules can be exploited to develop new modulation techniques to boost the communication rate.

- **Noise:** In addition to particle counting noise and ligand-receptor binding noise, which are well investigated in the MC literature, the physical architecture of the receiver can lead to new noise sources. For example, in nanomaterial-based designs, thermal noise and electronic noise, e.g., 1/f noise, of the receiver can be expected to severely undermine the reliability of communication.

- **Ionic Screening:** One of the main problems particularly observed at FET biosensor-based receivers is the ionic screening in physiologically relevant fluids, which decrease the SNR tremendously. The ions in the channel fluid can cause the screening of electrical charges of information molecules, resulting in reduced effective charge per molecule that can be detected by the receiver via field-effect. The strength of ionic screening depends exponentially on the distance of bound information molecules from the surface of the receiver's transducer channel. Numerous solutions exist in the biosensing literature that partially overcome this widely-observed problem. For example, using small-size receptors, e.g., aptamers, can allow the bound information molecules to approach the receiver surface, increasing their effective charge [76, 77]. Alternatively, high-frequency AC biasing at the receiver, exploiting the oscillating dipole moments of the bound information molecules, can be employed to overcome the ionic strength in exchange for increased complexity on the receiver side [78].

- **Low Communication Rate:** Slow diffusion and reaction kinetics of molecules might result in very low-communication rates, as shown in some of the recent practical MC demonstrations. These physical limitations call for new modulation and detection techniques that simultaneously exploit multiple properties of molecules, e.g., concentration and type, to boost the communication rate for MC systems.

Modulation techniques in MC fundamentally differ from that in conventional EM communications, as the modulated entities, i.e., molecules, are discrete in nature, and the developed techniques should be robust against highly time-varying characteristics of the MC channel, as well as inherently slow nature of the propagation mechanisms [8]. Exploiting the observable characteristics of molecules, researchers have proposed to encode information into the concentration, type, or release time of the molecules [13, 79]. The simplest modulation method proposed for MC is on-off keying (OOK) modulation, where a binary symbol is represented by releasing a number of molecules or not releasing any [80]. Similarly, using a single type of molecule, concentration shift keying (CSK), that is analogous to amplitude shift keying (ASK) in traditional wireless channels, is introduced in order to increase the number of transmitted symbols by encoding information into molecular concentration levels [81]. Molecular information can also be encoded into the type of molecules, i.e., molecule shift keying (MoSK) [79], or into both the type and the concentration of molecules to boost the data rate [82]. Additionally, the release order of different types of molecules [83], and the release time of single type of molecules [84] can be modulated to encode information in MC. Finally, in [85], authors propose the isomer-based ratio shift keying (IRSK), where the information is encoded into the ratio of different types of isomers in a molecule, i.e., molecule ratio-keying.
To overcome the noisy and ISI-susceptible nature of MC channels, several channel coding techniques which are adopted from EM communications, e.g., block and convolution codes, or developed specifically for MC, such as the ISI-free coding scheme employing distinguishable molecule types, have been studied. Detection is by far

the most studied aspect of MC in the literature. Several methods varying in complexity have been proposed to cope with the ISI, noise, and even the nonlinearity of the channel, such as optimal Maximum Likelihood (ML)/Maximum A Posteriori (MAP) detection methods, noncoherent detection, sequence detectors with Viterbi algorithm [86, 87, 63, 88, 13]. Synchronization problem is addressed by both developing self-synchronizing mod- ulation techniques and asynchronous detection methods. However, these methods are developed based on existing theoretical models of MC, which largely lack physical correspondence. Therefore, the performance of the proposed methods is not validated, which poses a major problem before practical MC systems and IoBNT applications.

3.1.2 Human Body as IoBNT Infrastructure

MC can typically support only very low communication rates due to the slow diffusion dynamics of molecules. Moreover, MC is prone to errors because of high level of noise and molecular interference in crowded physiological media, as well as due to attenuation of molecular signals as a result of degradation via various biochemical processes, making it reliable only at very short ranges [8]. On the other hand, human body has a large-scale complex communication network of neurons extending to various parts of the body and connecting different body parts with each other through electrical and chemical signaling modalities [4]. A part of the nervous system also senses external stimuli via sensory receptors and transmits the sensed information to the central nervous system, where a reaction is decided [5]. In that regard, the nervous system provides a ready infrastructure that can potentially connect nanomachines in distant parts of the body with each other and with the external devices. In fact, there are many proposal in this direction that both theoretically and experimentally investigate the idea of using the nervous system as an IoBNT backbone inside human body. In [89], authors consider a thru-body haptic communication system, where the information encoded into tactile stimulation is transmitted to the brain through the nervous system, resulting in a discernible brain activity which is detected by ElectroEncephaloGraphy (EEG) and used to decode the transmitted information. An analytical framework based on the computational neuroscience models of generation and propagation of somatosensory stimulation from skin mechanoreceptors is developed for the analysis of the achievable data rate on this communication system. Authors show that the system can support bit rates of 30-40 bit per second (bps) employing an OOK modulation of tactile stimulation taps at the index finger. In [90], the authors practically demonstrate a controlled information transfer through the nervous system of a common earthworm, which stands as a simple model system for bilaterian animals including humans. In the demonstrated setup, authors use external macroscale electrodes to interface with the earthworm's nervous system. Accordingly, the stimulation carrying the encoded information is applied at one end of the nerve cord, and the resulting nerve spikes are recorded at the other end. Through the application of different modulation schemes, e.g., OOK, frequency shift keying (FSK), the authors demonstrate data rates up to 66.61 bps with 6.8×10^{-3} bit error rate.

In [91], the authors propose to use vagus nerve to deliver instructions to an implanted drug delivery device near the brainstem via compound action potentials (CAP) generated by the application of electrical impulses at the neck, known in the literature as the vagus nerve stimulation (VNS). Applying an OOK modulation, the authors theoretically show that the vagus nerve can support data rates up to 200 bps and unidirectional transmission ranges between 60 mm and 100 mm, which is promising for enabling the communication of distant BNTs at a rate that is much higher than the typical MC rates.

A different approach to make use of the natural human body networks for IoBNT is investigated in [92], where authors propose to use Microbiome-Gut-Brain-Axis (MGBA) to connect distant BNTs. MGBA is a large scale heterogeneous intrabody communication system composed of the gut microbial community, the gut tissues, and the enteric nervous system. In MGBA, a bidirectional communication between the central nervous system and the enteric nervous system surrounding the gastrointestinal track (GI track) is realized via the transduction of electrical signals in the nervous system into molecular signals in the GI track, and vice versa. The axis has recently attracted significant research interest due to the discoveries underlining the relation of MGBA signaling with some neurological and gut disorders such as depression and irritable bowel syndrome (IBS). In the research roadmap proposed in [92], the authors envision BNTs as electrical biomedical devices, e.g., cardiac pacemaker, brain implants, insulin pumps, and biological devices, e.g., synthetic gut microbes and artificial organs, interconnected through the MGBA. They also investigate the possibility of a link between the IoBNT and the external environment via molecular (alimentary canal) and electrical (wireless data transfer through skin) interfaces.

3.1.3 Other Nanocommunication Modalities for IoBNT

a) THz-band Electromagnetic Nanocommunication: Conventional electromagnetic (EM) communication is not deemed suitable for IoBNT because the size of BNTs would demand extremely high operating frequencies [93]. Fortunately, graphene-based nanoantennas based on surface plasmon polariton (SPP) waves have been shown to support frequencies down to 0.1 THz, much lower than their metallic counterparts, promising for the development of high-bandwidth EM nanonetworks of nanomaterial-based BNTs using the unutilized THz-band (0.1-10 THz) [94]. In this direction, several plasmonic transceiver antenna designs using graphene and

related nanomaterials (e.g., CNT), whose properties can be tuned by material doping and electric field, have been investigated [95, 96]. However, several challenges exist for the practical implementation of THz-band nanonetworks, such as the very limited communication range resulting from high propagation losses due to molecular absorption, and low transmission power of resource-limited nanodevices. These challenges are being addressed by developing new very-short-pulse-based modulation schemes to overcome the limitations of THz transceivers in terms of power [97, 98], and designing directional antennas and dynamic beamforming antenna arrays to overcome the propagation losses [99]. High density of BNTs in envisioned IoBNT applications also pose challenges regarding the use of the limited spectrum, which are addressed by new medium access protocols for dense THz nanonetworks [100, 101].

b) Acoustic Nanocommunication: Ultrasonic nanocommunication has also been considered for connecting robotic BNTs inside the fluidic environment of human body due to its well-known advantages over its RF counterpart in underwater applications [102, 103, 104]. In [102], it is shown that the best trade-off between efficient acoustic generation and attenuation is realized when the acoustic frequency is between 10 MHz and 300 MHz for distances around 100 μm. The authors also show that the power harvested from ambient oxygen and glucose can be sufficient to support communication rates up to 10^4 bps. In [105], the authors provide a testbed design for ultrasonic intrabody communications with tissue-mimicking materials and as a result of extensive experiments, they report communication rates up to 700 kbps with a BER less than 10^{-6}.

An alternative approach proposed in [106] suggests the use of optoacoustic effect for the generation and detection of ultrasonic waves via a laser and an optical resonator, respectively. It is shown that optoacoustic transduction brings multiple advantages for ultrasonic nanocommunications, such as higher miniaturization, bandwidth and sensitivity over traditional piezoelectric/capacitive transduction methods.

c) FRET-based Nanocommunication: Single molecular BNTs are not capable of performing active communications, as in the case of MC and THz-band EM communications. On the other hand, external stimuli can supply the necessary means of information transfer. One such method is based on Förster Resonance Energy Transfer (FRET), which is a non-radiative and high-rate energy transfer between fluorescent molecules, such as fluorescent proteins and quantum dots (QDs) [107]. The method requires an external optical source for the initial excitation of donor molecules, which then transfer their energy to ground-state acceptor molecules in their close proximity. Encoding information into the excited state of molecules, short-range (5-10 nm) but very high-rate (on the order of Mbps) information transfer can be realized by this method [108]. Additionally, bioluminescent molecules can be utilized as donors that are excited upon binding specific target molecules, promising for single molecular sensor networks within an IoBNT application [109, 110]. It is shown that the limited range of FRET-based nanocommunication can be extended to 10s of nanometers by multi-step energy transfer processes and multi-excitation of donor molecules [111, 112]. Lastly, an experimental study demonstrated a high rate data transfer (250 kbps with a BER below 2×10^{-5}) between fluorescent-dye nanoantennas in a MIMO configuration [113].

3.2 Bio-Cyber and Nano-Macro Interfaces

Most of the envisioned IoBNT applications require a bidirectional nano-macro interface that can seamlessly connect the intrabody nanonetworks to the external macroscale networks, and vice versa [114, 115]. Considering that the MC is the most promising method for intrabody IoBNT, the interface should be capable of performing the conversion between biochemical signals and other signal forms that can be easily processed and communicated over conventional networks, such as electromagnetic, electrical, and optical. Several techniques are considered for enabling such a nano-macro interface.

3.2.1 Electrical Interfaces

These are the devices that can transduce molecular signals into electrical signals, and vice versa. Electrical biosensors can readily serve the function of converting MC signals into electrical signals (see Section 3.1.1 for the use of electrical biosensors as MC receivers). The literature on biosensors is vast, and the first practical demonstration of graphene bioFET-based MC receiver shows promising results in terms of sensitivity, selectivity, and reliability in electrical detection of MC signals [72]. However, challenges posed by physiological conditions should be overcome before employing biosensors as electrical interfaces, as detailed in [55, 13]. Conversion from electrical signals into molecular signals is more challenging due to the problem of maintaining continuous molecule generation or supply. Existing electrical stimuli-responsive drug delivery systems rely on limited-capacity reservoirs or polymer chains, e.g., hydrogel, that can store certain types of molecules and release them upon stimulation with a modulated rate. However, these systems are typical irreversible, i.e., they cannot replenish their molecular stock unless they are replaced or reloaded externally [13]. In [116], a redox-based technique is proposed and practically demonstrated for interfacing biological and electronic communication modalities, which can be used to connect a conventional wireless network with engineered bacterial BNTs communicating via molecular signals. The authors introduced the concept of electronically-controlled biological local area network (BioLAN), which includes a biohybrid electrode that

transduces information-encoded electronic input signals into biologically-recognized signals in the form of hydrogen peroxide through an oxygen reduction reaction. These signals are recognized by bacterial cells that are attached to the biohybrid electrode, and then biologically propagated across a microbial population with quorum sensing molecules. The overall electronic-biology link is bidirectional such that a microbial subpopulation in the BioLAN generates specific molecules that can be detected by the electrode via an electrochemical oxidation reaction.

Wearable and epidermal tattoo biosensors and transdermal drug-delivery systems, which have attracted a significant research interest for various healthcare applications, can also be targeted for an macro-nano interface that can connect intrabody IoBNT to the external communication networks, with the integration of communication antennas, such as radio-frequency-identification (RFID)-tag-antennas [117, 118, 119, 120]. The challenges lie in the further miniaturization of these devices as well as their continuous operation, since biosensors exposed to physiological fluids suffer contamination, and drug delivery systems require periodic replenishment of their reservoir.

3.2.2 Optical Interfaces

Light represents an alternative modality to interface the intrabody IoBNT with external networks. In the case that MC is utilized in IoBNT, such an optical interface can be realized with the help of light-sensitive proteins and bioluminescent/fluorescent proteins.

Optical control of excitable cells, e.g., neurons and muscle cells, can be achieved through a well-known technique called optogenetics [121]. The method relies on the genetic modification of natural cells for enabling them to express light-sensitive transmembrane ion channel proteins, e.g., channelrhodopsin. The resulting light-sensitive ion channels open or close depending on the wavelength of the incident photons. The technique enables specificity at the level of single cells in contrast to conventional electrical interfacing techniques, which generally suffer from low level of specificity. It is shown in [122, 123] that bacteria can also be engineered to express specific light-sensitive proteins, e.g., bacteriorhodopsin, that pump out protons under illumination, and thus, change the pH of its close environment.

In [56], the authors propose that optical control of engineered cells with light-sensitive ion channels can be exploited to enable an optical macro-to-nanoscale interface that can modulate the molecular release of MC transmitters. The authors in [124], experimentally demonstrate that synthetic bacteria expressing bacteriorhodopsin can convert external optical signals to chemical signals in the form of proton concentration at 1 bit/min conversion rate. They use the same technique to enable an experimental MC testbed in [75]. Similarly, in [125], the authors propose an implantable bio-cyber interface architecture that can enable the *in vivo* optical stimulation of brain cells to control neuronal communications based on external EM signals. Their device architecture includes a wireless antenna unit that connects the implanted device to external networks, an ultrasonic energy harvester, and a micro light emitting diodes (μ- LED) for optical stimulation.

Fluorescent molecules, such as fluorescent proteins, quantum dots, and organic dyes, can also be used to realize a wavelength-selective optical interface. In [113], organic dye molecules have been used as nanotransceiver antennas for FRET-based molecular nanonetworks. They act as single molecular optical interfaces that receive optical control signals from an external source and non-radiatively transmit them into a FRET-based nanonetwork. They enable an nano-to-macro interface as well, since the excited fluorescent molecules return to their ground state by releasing a photon at a specific wave-length that can be detected by an external photodetector. Similarly, in [75, 126], it is suggested that a nano-to- macro interface can be realized with engineered bacteria receivers expressing pH-sensitive green fluorescent proteins (GFPs) that change excitation/emission characte-ristics depending on the pH of the environment. Bioluminescent molecules that are excited upon reaction with a target molecule can also be used for the direct conversion of MC signals to optical signals to enable a nano-to-macro interface, as proposed in [127, 108].

3.2.3 Other Interfacing Methods

Depending on the communication modality utilized in intrabody IoBNT, there are some other nano-macro interfacing methods proposed in the literature. For example, in [128], the authors consider the use of magnetic nanoparticles (MNs) as information carriers in a MC system. They propose a wearable magnetic nanoparticle detector in the form of a ring to connect the intrabody MC to an RF-based backhaul. In a follow-up study [129], they also demonstrate the control of MN-based MC signals in microfluidic channels with external magnetic fields, that could potentially evolve to a bidirectional interface for IoBNT.

In light of the emerging reports on the EM-based wireless control of cellular functions via specific proteins that are responsive to electromagnetic fields [130], a wireless link is proposed to connect THz-band EM and MC modalities, that can translate into an EM-based nano-macro interface [131]. The authors in [132], develop an information theoretical model for the mechanotransduction communication channel between an implantable THz nanoantenna acting as the transmitter and a biological protein as the receiver undergoing a conformational change upon stimulation by the THz waves. Although THz-waves are theoretically shown to reliably control the conformational states of proteins, it remains as a challenge to investigate the use of the same modality in sensing the protein states to enable bidirectional wireless interface.

3.3 Energy Harvesting, Power Transfer, and Energy Efficiency

Supply, storage and efficient use of energy is one of the most crucial challenges towards realizing the envisioned IoBNT applications. The energy challenge is currently being addressed through the development of energy harvesting (EH) and wireless power transfer (WPT) techniques to continuously power BNTs, the development of high-capacity energy storage devices at micro/nanoscale, and the design of low-complexity and energy-efficient communication methods for IoBNT.

For BNTs based on engineered cells, the challenge of energy management is relatively straightforward, as living cells have been evolved over billions of years to make the most efficient use of biochemical energy for realizing vital functionalities. Nonetheless, energy budget requirements of engineered cells may be extended with the introduction of new computation and communication functionalities that are demanded by complex IoBNT applications. On the other hand, there are only a few studies that consider the overall energy requirements of MC for only very simple scenarios [133, 134]. The problem is, of course, more challenging for artificial BNTs, such as those that are made up of nanomaterials and missing an inherited metabolism for energy management.

3.3.1 Energy Harvesting

Leaving aside the continuous efforts to reduce the complexity of communication methods for IoBNT, such as modulation and detection techniques [13], in the hope of increasing energy efficiency, the most promising solution to enable self-sustaining IoBNT is the integration of EH modalities into BNTs. EH has recently received tremendous research interest partly due to the energy requirements set by emerging applications of IoT and IoE. Depending on the application environment and device architectures, various natural energy sources have been considered for harvest by IoT devices [135, 136]. For example, solar energy, vibration sources, electromagnetic sources, e.g., ambient RF EM waves, and metabolic sources have been deemed feasible for harvesting [137]. Concerning the intrabody and body area applications, human body stands as a vast source of energy in the form of mechanical vibrations resulting from body movements, respiration, heartbeat, and blood flow in vessels, thermal energy resulting from body heat, and biochemical energy resulting from metabolic reactions and physiological processes [138]. Literature now includes a multitude of successful applications of human body EH to power miniature biomedical devices and implants, such as thermoelectric EH from body heat for wearable devices [139], vibrational EH from heartbeats [140] and respiratory movements [141] to power pacemakers, as well as biochemical EH from human perspiration [142]. These together with EH from chemical reactions within the body, such as glucose uptake, lactate release, and pH variations [138, 143], can be exploited to power the BNTs in an intrabody IoBNT. Among the potential EH mechanisms for intrabody IoBNT, mechanical EH has attracted the most interest. Research in this field has gained momentum with the use of flexible piezoelectric nanomaterials, such as ZnO nanowires and lead zirconate titanate (PZT), in nanogenerators, enabling energy harvesting from natural and artificial vibrations with frequencies ranging from very low frequencies (< 1 Hz) up to several kHz [144, 145].

3.3.2 Wireless Power Transfer

Another way of powering BNTs and IoBNT applications can be WPT from external sources. WPT has seen significant advances in recent years due to increasing need for powering battery-less IoT devices as well as wearable and implantable devices. Various forms of WPT have been considered for powering medical implants [146, 147]. For example, near-field resonant inductive coupling (NRIC)-based WPT, the oldest WPT technique, has been in use for widely-used implants, such as cochlear implants [148, 149]. Other techniques include near-field capaci- tive coupling, midfield and far-field EM-based WPT, and acoustic WPT. Power transfer via near-field capacitive and inductive coupling, however, is only efficient for dis- tances on the order of transmitting and receiving device sizes, and for the right alignment of devices, and there- fore, might not be suitable for powering micro/nanoscale BNTs [148]. On the other hand, radiative mid-field and far-field EM-based WPTs can have looser restrictions depending on the frequency of EM waves.

Recent research on mm-wave and THz rectennas suggests the use of high-frequency EM WPT techniques to power BNTs [150]. However, for intrabody applications, the higher absorption with increasing frequency and power restrictions should be taken into account. Nonetheless, simultaneous wireless information and power transfer techniques (SWIPT) utilizing THz-band have been investigated for EM nanonetworks [151, 152]. Similar SWIPT applications have been considered for MC, where the receiving BNTs use the received molecules for both decoding the information and energy harvesting [153, 154]. There are also applications of acoustic WPT for biomedical implants using external ultrasonic devices [155, 156]. Although not implemented yet, ultrasonic EH has been also considered for powering BNTs with piezoelectric transducers [157, 158, 125].

An interesting research direction in parallel with the wider IoE vision is towards hybrid EH systems that can exploit multiple energy sources. Prototypes have been implemented for ZnO nanowire-based hybrid cells for concurrent harvesting of solar and mechanical energies [159], and piezoelectric PVDF-nanofiber NG based hybrid cells for biomechanical and biochemical EH from bodily fluids [160]. A hybrid EH architecture is also proposed for IoE comprising modules for EH from light, mechanical, thermal, and EM sources [161]. The same hybrid architectures could be considered for IoBNT as well to main-

tain the continuous operation of BNTs. EH from multiple resources can reduce the variance at power output with the addition of alternative complementary procedures in a modular fashion as investigated in [161].

3.3.3 Energy Storage

Storage of energy is also important when BNTs cannot continuously satisfy their power requirements via EH and WPT techniques. There has been considerable interest in miniaturizing the energy storage technologies to make them size-compatible with MEMS and NEMS devices. Some of the efforts have been devoted to develop micro-batteries, miniaturized versions of conventional thin-film lithiumion batteries, benefiting from novel nanomaterials [162]. There are even a few studies focusing on nanoscale versions of lithium batteries [163, 145]. However, they suffer from low energy density, short lifetimes, and potential toxicity in *in vivo* applications. More promising solution is micro-supercapacitors (MSCs), which provide significantly higher energy storage capacity, higher charge/discharge rates, and more importantly, scalability and flexibility, which are crucial for their integration into BNTs [164, 165, 166].

Several types of materials have been considered for the design of MSC electrode to improve the energy density. Carbon nanomaterials, such as CNTs and graphene, are the most widely researched materials due to their abundance and stability, which is reflected to an extended lifetime [164]. Due to its extremely high surface-to-volume ratio, high mobility and flexibility, graphene has attracted particular attention [167, 168]. Additionally, conducting polymers, such as PEDOT/PSS, and graphene/conducting polymer heterostructures are also considered as flexible electrodes for MSCs [164]. The research in MSCs is still at early stages; however, we believe that with the increase of energy density and further reduction of sizes, they can be a viable candidate for energy storage units in BNTs.

3.4 Biocompatibility and Co-existence

Biological processes are complex, and intertwined, often through intricate relationships that are yet to be uncovered. Perturbation of homeostasis maintained by these relationships may result in serious disorders. Even more complicated is the fact that the composition of the physiological environment and the interactome may have a large variance among different members of the same species. For example, gut microbiome is known to be composed of different types of bacteria in different people [169]. Therefore, the evaluation of *in vivo* IoBNT applications in terms of biocompatibility is very challenging, however, must be considered seriously. Biocompatibility constraints for IoBNT can be viewed from two angles [170]. First, an IoBNT application, along with all the communication methods and devices therein, should not disrupt the homeostasis of the organism it is implemented in. Such disruption might occur when the introduced application has toxic, injurious, or adverse effects on the living cells and biochemical processes. Second, an implanted IoBNT application should be able to operate without its performance being degraded by the co-existing biochemical processes. Performance degradation usually follows when an IoBNT application alters the metabolic activities, because such alternation invokes the immune response that might in turn lead to the *rejection* of the deployed application. Rejection can occur in the form of expulsion of the IoBNT application from the organism, encapsulation of the BNTs with biological cells and tissues, or inflammation or death of the surrounding tissues. In the case of MC, performance degradation may also happen as a result of cross-talk caused by the natural biochemical signaling. Biocompatibility concerns both materials used in the physical architecture of BNTs, and the networking, energy harvesting, power transfer, and interfacing processes of the IoBNT. In terms of materials, synthetic biology-based BNTs can be considered highly biocompatible, as they adopt living cells and cellular components as the substrate [24]. Likewise, fluorescent protein- and DNA-based BNTs are also of biological origins, and thus, can be expected to offer similar levels of biocompatibility [108]. However, depending on their exact biological origin and their overall amount in the body, they may still trigger the immune response. For example, a virus-based synthetic BNT can be labeled as foreign agent and attacked by the immune system, unless it is designed to possess a kind of stealth proteins that help escape the immune control [171]. For artificial BNTs based on nanomaterials, biocompatibility is more challenging. There is still no consensus on a universal test of biocompatibility for nanomaterials, leading to conflicting results in the literature about almost all materials. Complexity of the biological systems and reproducibility problem for *in vivo* and *in vitro* tests are the main causes of the ongoing ambiguity. Nonetheless, many polymers (e.g., PMMA, Parylene), gold, titanium, and some ceramics are widely known to be biocompatible [172, 173, 174]. Carbon-based materials, e.g., CNT and graphene, have been reported as both biocompatible and toxic in different works, preventing a generalization over these nanomaterials. This is attributed to large variations in their physicochemical properties, e.g., size, shape, surface characteristics, adopted in different works [175, 176]. However, it has been repeatedly re- ported that their biocompatibility can be modulated with chemical manipulation [175]. For example, surface functionalization with dextran is shown to reduce the toxicity of graphene oxide (GO), hinting at strategies to make carbon-based nanomaterials suitable for safe *in vivo* applications [177, 176]. Similarly, nanoparticles are shown to be detoxified upon the functionalization of their surfaces with smart/benign ligands [178].

In terms of processes, attention must be paid to the communication, bio-cyber interfacing, energy harvesting, transfer and storage processes. In EM-based and acoustic communication and power transfer processes, for ex-

ample, the biocompatibility is crucial for preventing the damage on biochemical structures, e.g., tissue damage by heating, and closely linked to the frequency and power of the EM or acoustic waves. For human body applications, the exposure limits are regulated by the Food and Drug Administration (FDA) in US, as 100 μW/mm^2 for RF waves and 7.2 mW/mm^2 for ultrasound waves, [125, 179]. These limits should be taken into account in the design of IoBNT technologies.

In the cases that MC is adopted in IoBNT applications, the concentration and type of molecules used for communications is very critical for biocompatibility. First, the information-carrying molecules should not invoke the immune response. The degradation of information molecules by enzymes should also be taken into account to prevent performance degradation. Also, the MC signals should not interfere with the inherent biological systems. The type of information molecules must be orthogonal to the molecules involved in biological processes to prevent interference, or their concentration should be low enough not to disrupt these processes. This so-called co-existence challenge has recently attracted close attention of MC researchers, who suggest different solution strategies [180, 181, 182]. For example, in [182], a cognitive radio-inspired transmission control scheme is proposed to overcome interference between MC networks and co-existing biological networks. In [57], various channel sensing methods inspired from the spectrum sensing techniques in EM cognitive radio are proposed to estimate the instantaneous composition of the MC channel with ligand receptors in terms of molecule types. The effect of biological cross-talk on the MC is also investigated in [183], where the performance of several detection methods are investigated in terms of their ability to ensure reliability under such biological interference.

4. CONCLUSION

In this survey, a comprehensive overview of IoBNT framework along with its main components and applications is provided to contribute to an holistic understanding of the current technological challenges and potential research directions in this emerging field. In light of rapid advances in synthetic biology, nanotechnology, and non-conventional communications made possible by inter-disciplinary approaches, we believe that the enormous potential of the IoBNT will soon be realized with high-impact medical, environmental and industrial applications.

ACKNOWLEDGEMENT

The work of Murat Kuscu was supported in part by the European Union's Horizon 2020 Research and Innovation Programme through the Marie Skłodowska-Curie Individual Fellowship under Grant Agreement 101028935 and by The Scientific and Technological Research Council of Turkey (TUBITAK) under Grant #120E301.

REFERENCES

[1] Ian F Akyildiz, Max Pierobon, Sasi Balasubramaniam, and Y Koucheryavy. "The internet of bio-nano things". In: *IEEE Communications Magazine* 53.3 (2015), pp. 32–40.

[2] Murat Kuscu, Ergin Dinc, Bilgesu A. Bilgin, Hamideh Ramezani, and Ozgur B Akan. "Transmitter and Receiver Architectures for Molecular Communications: A Survey on Physical Design with Modulation, Coding and Detection Techniques". In: *Proc. IEEE* 107.7 (2019), pp. 1302–1341. DOI:10.1109/JPROC.2019.2916081.

[3] Dadi Bi, Apostolos Almpanis, Adam Noel, Yansha Deng, and Robert Schober. "A survey of molecular communication in cell biology: Establishing a new hierarchy for interdisciplinary applications". In: *IEEE Communications Surveys & Tutorials* (2021).

[4] Derya Malak and Ozgur B Akan. "Molecular communication nanonetworks inside human body". In: *Nano Communication Networks* 3.1 (2012), pp. 19–35.

[5] Derya Malak and Ozgur B Akan. "Communication theoretical understanding of intra-body nervous nanonetworks". In: *IEEE Communications Magazine* 52.4 (2014), pp. 129–135.

[6] Ian F Akyildiz, Massimiliano Pierobon, and Sasitharan Balasubramaniam. "Moving forward with molecular communication: From theory to human health applications [point of view]". In: *Proceedings of the IEEE* 107.5 (2019), pp. 858–865.

[7] Filip Lemic, Sergi Abadal, Wouter Tavernier, Pieter Stroobant, Didier Colle, Eduard Alarcón, Johann Marquez-Barja, and Jeroen Famaey. "Survey on terahertz nanocommunication and networking: A top-down perspective". In: *IEEE Journal on Selected Areas in Communications* (2021).

[8] Ozgur B Akan, Hamideh Ramezani, Tooba Khan, Naveed A Abbasi, and Murat Kuscu. "Fundamentals of molecular information and communication science". In: *Proceedings of the IEEE* 105.2 (2017), pp. 306–318.

[9] Yevgeni Koucheryavy, Anastasia Yastrebova, Daniel P Martins, and Sasitharan Balasubramaniam. "A Review on Bio-Cyber Interfaces for Intrabody Molecular Communications Systems". In: *arXiv preprint arXiv:2104.14944* (2021).

[10] Sasitharan Balasubramaniam and Jussi Kangasharju. "Realizing the internet of nano things: challenges, solutions, and applications". In: *Computer* 46.2 (2013), pp. 62–68.

[11] Luca Felicetti, Mauro Femminella, Gianluca Reali, and Pietro Liò . "Applications of molecular communications to medicine: A survey". In: *Nano Communication Networks* 7 (2016), pp. 27–45.

[12] Qammer H Abbasi, Ke Yang, Nishtha Chopra, Josep Miquel Jornet, Najah Abed Abuali, Khalid A Qaraqe, and Akram Alomainy. "Nano-communication for biomedical applications: A review on the state-of-the-art from physical layers to novel networking concepts". In: *IEEE Access* 4 (2016), pp. 3920–3935.

[13] Murat Kuscu, Ergin Dinc, Bilgesu A Bilgin, Hamideh Ramezani, and Ozgur B Akan. "Transmitter and receiver architectures for molecular communications: A survey on physical design with modulation, coding, and detection techniques". In: *Proceedings of the IEEE* 107.7 (2019), pp. 1302–1341.

[14] Ke Yang, Dadi Bi, Yansha Deng, Rui Zhang, Muhammad Mahboob Ur Rahman, Najah Abu Ali, Muhammad Ali Imran, Josep Miquel Jornet, Qammer H Abbasi, and Akram Alomainy. "A comprehensive survey on hybrid communication in context of molecular communication and terahertz communication for body-centric nanonetworks". In: *IEEE Transactions on Molecular, Biological and Multi-Scale Communications* 6.2 (2020), pp. 107–133.

[15] Ian F Akyildiz, Maysam Ghovanloo, Ulkuhan Guler, Tevhide Ozkaya-Ahmadov, A Fatih Sarioglu, and Bige D Unluturk. "PANACEA: An internet of bio-nanothings application for early detection and mitigation of infectious diseases". In: *IEEE Access* 8 (2020), pp. 140512–140523.

[16] Michael Taynnan Barros, Mladen Veletić, Masamitsu Kanada, Massimiliano Pierobon, Seppo Vainio, Ilangko Balasingham, and Sasitharan Balasubramaniam. "Molecular Communications in Viral Infections Research: Modelling, Experimental Data and Future Directions". In: *IEEE Transactions on Molecular, Biological and Multi-Scale Communications* (2021).

[17] Eren Balevi and Ozgur B Akan. "A physical channel model for nanoscale neuro-spike communications". In: *IEEE Transactions on Communications* 61.3 (2013), pp. 1178–1187.

[18] Tooba Khan, Bilgesu A Bilgin, and Ozgur B Akan. "Diffusion-based model for synaptic molecular communication channel". In: *IEEE Transactions on Nanobioscience* 16.4 (2017), pp. 299–308.

[19] Christopher M Waters and Bonnie L Bassler. "Quorum sensing: cell-to-cell communication in bacteria". In: *Annu. Rev. Cell Dev. Biol.* 21 (2005), pp. 319–346.

[20] Arthur Prindle, Jintao Liu, Munehiro Asally, Jordi Garcia-Ojalvo, and Gürol M Süel. "Ion channels enable electrical communication in bacterial communities". In: *Nature* 527.7576 (2015), pp. 59–63.

[21] Bernard J Crespi. "The evolution of social behavior in microorganisms". In: *Trends in ecology & evolution* 16.4 (2001), pp. 178–183.

[22] Sasitharan Balasubramaniam et al. "Multi-hop conjugation based bacteria nanonetworks". In: *IEEE Transactions on nanobioscience* 12.1 (2013), pp. 47–59.

[23] Sasitharan Balasubramaniam et al. "Opportunistic routing through conjugation in bacteria communication nanonetwork". In: *Nano Communication Networks* 3.1 (2012), pp. 36–45.

[24] Bige D Unluturk, A Ozan Bicen, and Ian F Akyildiz. "Genetically engineered bacteria-based biotransceivers for molecular communication". In: *IEEE Transactions on Communications* 63.4 (2015), pp. 1271–1281.

[25] Bige D Unluturk, Sasitharan Balasubramaniam, and Ian F Akyildiz. "The impact of social behavior on the attenuation and delay of bacterial nanonetworks". In: *IEEE transactions on nanobioscience* 15.8 (2016), pp. 959–969.

[26] Hamdan Awan, Raviraj S Adve, Nigel Wallbridge, Carrol Plummer, and Andrew W Eckford. "Information theoretic based comparative analysis of different communication signals in plants". In: *IEEE Access* 7 (2019), pp. 117075–117087.

[27] Max Teplitski, Jayne B Robinson, and Wolfgang D Bauer. "Plants secrete substances that mimic bacterial N-acyl homoserine lactone signal activities and affect population density-dependent behaviors in associated bacteria". In: *Molecular Plant-Microbe Interactions* 13.6 (2000), pp. 637–648.

[28] Bige D Unluturk and Ian F Akyildiz. "An end-to-end model of plant pheromone channel for long range molecular communication". In: *IEEE transactions on nanobioscience* 16.1 (2016), pp. 11–20.

[29] Oluwaseyi Samuel Olanrewaju, Ayansina Segun Ayangbenro, Bernard R Glick, and Olubukola Oluranti Babalola. "Plant health: feedback effect of root exudates-rhizobiome interactions". In: *Applied microbiology and biotechnology* 103.3 (2019), pp. 1155–1166.

[30] David A Leigh. "Genesis of the nanomachines: The 2016 Nobel prize in chemistry". In: *Angewandte Chemie International Edition* 55.47 (2016), pp. 14506–14508.

[31] Kyle Lund, Anthony J Manzo, Nadine Dabby, Nicole Michelotti, Alexander Johnson-Buck, Jeanette Nangreave, Steven Taylor, Renjun Pei, Milan N Stojanovic, Nils G Walter, et al. "Molecular robots guided by prescriptive landscapes". In: *Nature* 465.7295 (2010), pp. 206–210.

[32] Elizabeth Ellis, Suresh Moorthy, Weng-I Katherine Chio, and Tung-Chun Lee. "Artificial molecular and nanostructures for advanced nanomachinery". In: *Chemical Communications* 54.33 (2018), pp. 4075–4090.

[33] Ivan Aprahamian. "The future of molecular machines". In: *ACS central science* 6.3 (2020), pp. 347–358.

[34] Euan R Kay, David A Leigh, and Francesco Zerbetto. "Synthetic molecular motors and mechanical machines". In: *Angewandte Chemie International Edition* 46.1-2 (2007), pp. 72–191.

[35] Wesley R Browne and Ben L Feringa. "Making molecular machines work". In: *Nanoscience and Technology: A Collection of Reviews from Nature Journals* (2010), pp. 79–89.

[36] Masayuki Endo and Hiroshi Sugiyama. "DNA origami nanomachines". In: *Molecules* 23.7 (2018), p. 1766.

[37] Marcello DeLuca, Ze Shi, Carlos E Castro, and Gaurav Arya. "Dynamic DNA nanotechnology: toward functional nanoscale devices". In: *Nanoscale Horizons* 5.2 (2020), pp. 182–201.

[38] Hamid Ramezani and Hendrik Dietz. "Building machines with DNA molecules". In: *Nature Reviews Genetics* 21.1 (2020), pp. 5–26.

[39] Samuel Sánchez, Lluís Soler, and Jaideep Katuri. "Chemically powered micro-and nanomotors". In: *Angewandte Chemie International Edition* 54.5 (2015), pp. 1414–1444.

[40] Mingjun Xuan, Jingxin Shao, Xiankun Lin, Luru Dai, and Qiang He. "Self-propelled janus mesoporous silica nanomotors with sub-100 nm diameters for drug encapsulation and delivery". In: *ChemPhysChem* 15.11 (2014), pp. 2255–2260.

[41] Jiabin Luan, Danni Wang, and Daniela A Wilson. "Leveraging synthetic particles for communication: from passive to active systems". In: *Nanoscale* (2020).

[42] Beatriz de Luis, Angela Morellá-Aucejo, Antoni Llopis-Lorente, Tania M Godoy-Reyes, Reynaldo Villalonga, Elena Aznar, Félix Sancenón, and Ramón Martínez-Máñez. "A chemical circular communication network at the nanoscale". In: *Chemical Science* 12.4 (2021), pp. 1551–1559.

[43] Chuanrui Chen, Xiaocong Chang, Hazhir Teymourian, Doris E Ramírez-Herrera, Berta Esteban-Fernández de Ávila, Xiaolong Lu, Jinxing Li, Sha He, Chengcheng Fang, Yuyan Liang, et al. "Bioinspired chemical communication between synthetic nanomotors". In: *Angewandte Chemie International Edition* 57.1 (2018), pp. 241–245.

[44] Antoni Llopis-Lorente, Paula Díez, Alfredo Sánchez, María D Marcos, Félix Sancenón, Paloma Martínez-Ruiz, Reynaldo Villalonga, and Ramón Martínez-Máñez. "Interactive models of communication at the nanoscale using nanoparticles that talk to one another". In: *Nature communications* 8.1 (2017), pp. 1–7.

[45] Hong Wang and Martin Pumera. "Coordinated behaviors of artiicial micro/nanomachines: from mutual interactions to interactions with the environment". In: *Chemical Society Reviews* 49.10 (2020), pp. 3211–3230.

[46] Jing Yan, Ming Han, Jie Zhang, Cong Xu, Erik Luijten, and Steve Granick. "Reconiguring active particles by electrostatic imbalance". In: *Nature materials* 15.10 (2016), pp. 1095–1099.

[47] Krishna Kanti Dey. "Dynamic coupling at low Reynolds number". In: *Angewandte Chemie International Edition* 58.8 (2019), pp. 2208–2228.

[48] Ozgur B Akan, Hamideh Ramezani, Tooba Khan, Naveed A Abbasi, and Murat Kuscu. "Fundamentals of molecular information and communication science". In: *Proceedings of the IEEE* 105.2 (2016), pp. 306–318.

[49] Michael Moore, Akihiro Enomoto, Tadashi Nakano, Ryota Egashira, Tatsuya Suda, Atsushi Kayasuga, Hiroaki Kojima, Hitoshi Sakakibara, and Kazuhiro Oiwa. "A design of a molecular communication system for nanomachines using molecular motors". In: *Pervasive Computing and Communications Workshops, 2006. PerCom Workshops 2006. Fourth Annual IEEE International Conference on*. IEEE. 2006, 6–pp.

[50] Deniz Kilinc and Ozgur B Akan. "An information theoretical analysis of nanoscale molecular gap junction communication channel between cardiomyocytes". In: *IEEE Transactions on Nanotechnology* 12.2 (2013), pp. 129–136.

[51] Massimiliano Pierobon and Ian F Akyildiz. "Diffusion-based noise analysis for molecular communication in nanonetworks". In: *IEEE Transactions on signal processing* 59.6 (2011), pp. 2532–2547.

[52] Massimiliano Pierobon and Ian F Akyildiz. "Noise analysis in ligand-binding reception for molecular communication in nanonetworks". In: *IEEE Transactions on Signal Processing* 59.9 (2011), pp. 4168–4182.

[53] Massimiliano Pierobon and Ian F Akyildiz. "Intersymbol and co-channel interference in diffusion-based molecular communication". In: *Communications (ICC), 2012 IEEE International Conference on*. IEEE. 2012, pp. 6126–6131.

[54] Bige D Unluturk, Derya Malak, and Ozgur B Akan. “Rate-delay tradeoff with network coding in molecular nanonetworks”. In: *IEEE Transactions on Nanotechnology* 12.2 (2013), pp. 120–128.

[55] Murat Kuscu and Ozgur B Akan. “On the physical design of molecular communication receiver based on nanoscale biosensors”. In: *IEEE Sensors Journal* 16.8 (2016), pp. 2228–2243.

[56] Christian A Söldner, Eileen Socher, Vahid Ja- mali, Wayan Wicke, Arman Ahmadzadeh, Hans- Georg Breitinger, Andreas Burkovski, Kathrin Castiglione, Robert Schober, and Heinrich Sticht. “A survey of biological building blocks for synthetic molecular communication systems”. In: *IEEE Communications Surveys & Tutorials* 22.4 (2020), pp. 2765–2800.

[57] Murat Kuscu and Ozgur B Akan. “Channel Sensing in Molecular Communications with Single Type of Ligand Receptors”. In: *IEEE Transactions on Communications* 67.10 (2019), pp. 6868–6884.

[58] Ramiz Daniel, Jacob R Rubens, Rahul Sarpeshkar, and Timothy K Lu. “Synthetic analog computation in living cells”. In: *Nature* 497.7451 (2013), p. 619.

[59] Oliver Purcell and Timothy K Lu. “Synthetic analog and digital circuits for cellular computation and memory”. In: *Current Opinion in Biotechnology* 29 (2014), pp. 146–155.

[60] Ignacio Llatser, Eduard Alarcó n, and Massimiliano Pierobony. “Diffusion-based channel characterization in molecular nanonetworks”. In: *Computer Communications Workshops (INFOCOM WK- SHPS), 2011 IEEE Conference on*. IEEE. 2011, pp. 467–472.

[61] Massimiliano Pierobon and Ian F Akyildiz. “Capacity of a diffusion-based molecular communication system with channel memory and molecular noise”. In: *IEEE Transactions on Information Theory* 59.2 (2013), pp. 942–954.

[62] Murat Kuscu and Ozgur B Akan. “Modeling convection-diffusion-reaction systems for microluidic molecular communications with surface-based receivers in Internet of Bio-Nano Things”. In: *PloS One* 13.2 (2018), e0192202.

[63] Adam Noel, Karen C Cheung, and Robert Schober. “Optimal receiver design for diffusive molecular communication with lo w and additive noise”. In: *IEEE Transactions on Nanobioscience* 13.3 (2014), pp. 350–362.

[64] A Ozan Bicen and Ian F Akyildiz. “System-theoretic analysis and least-squares design of microluidic channels for lo w-induced molecular communication”. In: *IEEE Transactions on Signal Processing* 61.20 (2013), pp. 5000–5013.

[65] H Birkan Yilmaz, Akif Cem Heren, Tuna Tugcu, and Chan-Byoung Chae. “3-d channel characteristics for molecular communications with an absorbing receiver”. In: *IEEE Communications Letters* 18.6 (2014), pp. 929–932.

[66] Nariman Farsad, Weisi Guo, and Andrew W Eckford. “Tabletop molecular communication: Text messages through chemical signals”. In: *PloS One* 8.12 (2013), e82935.

[67] Harald Unterweger, Jens Kirchner, Wayan Wicke, Arman Ahmadzadeh, Doaa Ahmed, Vahid Jamali, Christoph Alexiou, Georg Fischer, and Robert Schober. “Experimental molecular communication testbed based on magnetic nanoparticles in duct lo w”. In: *2018 IEEE 19th International Workshop on Signal Processing Advances in Wireless Communications (SPAWC)*. IEEE. 2018, pp. 1–5.

[68] Yansha Deng, Adam Noel, Maged Elkashlan, Arumugam Nallanathan, and Karen C Cheung. “Modeling and simulation of molecular communication systems with a reversible adsorption receiver”. In: *IEEE Transactions on Molecular, Biological and Multi-Scale Communications* 1.4 (2015), pp. 347–362.

[69] Murat Kuscu and Ozgur B Akan. “Modeling and analysis of SiNW FET-based molecular communication receiver”. In: *IEEE Transactions on Communications* 64.9 (2016), pp. 3708–3721.

[70] Bon-Hong Koo, Changmin Lee, H Birkan Yilmaz, Nariman Farsad, Andrew Eckford, and Chan-Byoung Chae. “Molecular MIMO: From theory to prototype”. In: *IEEE Journal on Selected Areas in Communications* 34.3 (2016), pp. 600–614.

[71] Nariman Farsad, David Pan, and Andrea Goldsmith. “A novel experimental platform for in-vessel multi-chemical molecular communications”. In: *GLOBECOM 2017-2017 IEEE Global Communications Conference*. IEEE. 2017, pp. 1–6.

[72] Murat Kuscu, Hamideh Ramezani, Ergin Dinc, Shahab Akhavan, and Ozgur B Akan. “Fabrication and microluidic analysis of graphene-based molecular communication receiver for Internet of Nano Things (IoNT)”. In: *Scientific reports* 11.1 (2021), pp. 1–20.

[73] Bhuvana Krishnaswamy, Caitlin M Austin, J Patrick Bardill, Daniel Russakow, Gregory L Holst, Brian K Hammer, Craig R Forest, and Raghupathy Sivakumar. “Time-elapse communication: Bacterial communication on a microluidic chip”. In: *IEEE Transactions on Communications* 61.12 (2013), pp. 5139–5151.

[74] A Ozan Bicen, Caitlin M Austin, Ian F Akyildiz, and Craig R Forest. "Eficient sampling of bacterial signal transduction for detection of pulse-amplitude modulated molecular signals". In: *IEEE Transactions on Biomedical Circuits and Systems* 9.4 (2015), pp. 505–517.

[75] Laura Grebenstein, Jens Kirchner, Wayan Wicke, Arman Ahmadzadeh, Vahid Jamali, Georg Fischer, Robert Weigel, Andreas Burkovski, and Robert Schober. "A Molecular Communication Testbed Based on Proton Pumping Bacteria: Methods and Data". In: *IEEE Transactions on Molecular, Biological and Multi-Scale Communications* 5.1 (2019), pp. 56–62.

[76] Yasuhide Ohno, Kenzo Maehashi, and Kazuhiko Matsumoto. "Label-free biosensors based on aptamer-modified graphene field-effect transistors". In: *Journal of the American Chemical Society* 132.51 (2010), pp. 18012–18013.

[77] Roey Elnathan, Moria Kwiat, Alexander Pevzner, Yoni Engel, Larisa Burstein, Artium Khatchtourints, Amir Lichtenstein, Raisa Kantaev, and Fernando Patolsky. "Biorecognition layer engineering: overcoming screening limitations of nanowire-based FET devices". In: *Nano letters* 12.10 (2012), pp. 5245–5254.

[78] Girish S Kulkarni and Zhaohui Zhong. "Detection beyond the Debye screening length in a high-frequency nanoelectronic biosensor". In: *Nano letters* 12.2 (2012), pp. 719–723.

[79] Mehmet S Kuran, Huseyin Birkan Yilmaz, Tuna Tugcu, and Ian F Akyildiz. "Modulation techniques for communication via diffusion in nanonetworks". In: *Communications (ICC), 2011 IEEE International Conference on*. IEEE. 2011, pp. 1–5.

[80] Mohammad Upal Mahfuz, Dimitrios Makrakis, and Hussein T Mouftah. "On the characterization of binary concentration-encoded molecular communication in nanonetworks". In: *Nano Communication Networks* 1.4 (2010), pp. 289–300.

[81] Mehmet Şü krü Kuran, H Birkan Yilmaz, Tuna Tugcu, and Ian F Akyildiz. "Interference effects on modulation techniques in diffusion based nanonetworks". In: *Nano Communication Networks* 3.1 (2012), pp. 65–73.

[82] Hamidreza Arjmandi, Amin Gohari, Masoumeh Nasiri Kenari, and Farshid Bateni. "Diffusion-based nanonetworking: A new modulation technique and performance analysis". In: *IEEE Communications Letters* 17.4 (2013), pp. 645–648.

[83] Baris Atakan, Sebastia Galmes, and Ozgur B Akan. "Nanoscale communication with molecular arrays in nanonetworks". In: *IEEE Transactions on NanoBioscience* 11.2 (2012), pp. 149–160.

[84] Nora Garralda, Ignacio Llatser, Albert Cabellos-Aparicio, Eduard Alarcó n, and Massimiliano Pierobon. "Diffusion-based physical channel identification in molecular nanonetworks". In: *Nano Communication Networks* 2.4 (2011), pp. 196–204.

[85] Na-Rae Kim and Chan-Byoung Chae. "Novel modulation techniques using isomers as messenger molecules for nano communication networks via diffusion". In: *IEEE Journal on Selected Areas in Communications* 31.12 (2013), pp. 847–856.

[86] Ignacio Llatser, Albert Cabellos-Aparicio, Massimiliano Pierobon, and Eduard Alarcó n. "Detection techniques for diffusion-based molecular communication". In: *IEEE Journal on Selected Areas in Communications* 31.12 (2013), pp. 726–734.

[87] Deniz Kilinc and Ozgur B Akan. "Receiver design for molecular communication". In: *IEEE Journal on Selected Areas in Communications* 31.12 (2013), pp. 705–714.

[88] Bin Li, Mengwei Sun, Siyi Wang, Weisi Guo, and Chenglin Zhao. "Low-complexity noncoherent signal detection for nanoscale molecular communications". In: *IEEE transactions on nanobioscience* 15.1 (2015), pp. 3–10.

[89] Natalie Hanisch and Massimiliano Pierobon. "Digital modulation and achievable information rates of thru-body haptic communications". In: *Disruptive Technologies in Sensors and Sensor Systems*. Vol. 10206. International Society for Optics and Photonics. 2017, p. 1020603.

[90] Naveed A Abbasi, Dilan Lafci, and Ozgur B Akan. "Controlled information transfer through an in vivo nervous system". In: *Scientific reports* 8.1 (2018), pp. 1–12.

[91] Michael Donohoe, Brendan Jennings, and Sasitharan Balasubramaniam. "Deep brain drug-delivery control using vagus nerve communications". In: *Computer Networks* 171 (2020), p. 107137.

[92] Ian F Akyildiz, Jiande Chen, Maysam Ghovanloo, Ulkuhan Guler, Tevhide Ozkaya-Ahmadov, Massimiliano Pierobon, A Fatih Sarioglu, and Bige D Unluturk. "Microbiome-Gut-Brain Axis as a Biomolecular Communication Network for the Internet of Bio-NanoThings". In: *IEEE access* 7 (2019), pp. 136161–136175.

[93] Filip Lemic, Sergi Abadal, Wouter Tavernier, Pieter Stroobant, Didier Colle, Eduard Alarcón, Johann Marquez-Barja, and Jeroen Famaey. "Survey on terahertz nanocommunication and networking: A top-down perspective". In: *arXiv preprint arXiv:1909.05703* (2019).

[94] Josep Miquel Jornet and Ian F Akyildiz. "Fundamentals of electromagnetic nanonetworks in the terahertz band". In: *Foundations and Trends® in Networking* 7.2-3 (2013), pp. 77–233.

[95] Ignacio Llatser, Christian Kremers, Albert Cabellos-Aparicio, Josep Miquel Jornet, Eduard Alarc n, and Dmitry N Chigrin. "Graphene-based nano-patch antenna for terahertz radiation". In: *Photonics and Nanostructures-Fundamentals and Applications* 10.4 (2012), pp. 353–358.

[96] M Rosenau Da Costa, OV Kibis, and ME Portnoi. "Carbon nanotubes as a basis for terahertz emitters and detectors". In: *Microelectronics Journal* 40.4-5 (2009), pp. 776–778.

[97] Josep Miquel Jornet and Ian F Akyildiz. "Femtosecond-long pulse-based modulation for terahertz band communication in nanonetworks". In: *IEEE Transactions on Communications* 62.5 (2014), pp. 1742–1754.

[98] Hakim Mabed. "Enhanced spread in time on-off keying technique for dense Terahertz nanonetworks". In: *2017 IEEE Symposium on Computers and Communications (ISCC)*. IEEE. 2017, pp. 710–716.

[99] Arjun Singh, Michael Andrello, Ngwe Thawdar, and Josep Miquel Jornet. "Design and operation of a graphene-based plasmonic nano-antenna array for communication in the terahertz band". In: *IEEE Journal on Selected Areas in Communications* 38.9 (2020), pp. 2104–2117.

[100] Hakim Mabed and Julien Bourgeois. "A le xible medium access control protocol for dense terahertz nanonetworks". In: *Proceedings of the 5th ACM International Conference on Nanoscale Computing and Communication*. 2018, pp. 1–7.

[101] Anish Prasad Shrestha, Sang-Jo Yoo, Hyoung Jin Choi, and Kyung Sup Kwak. "Enhanced rate division multiple access for electromagnetic nanonetworks". In: *IEEE Sensors Journal* 16.19 (2016), pp. 7287–7296.

[102] Tad Hogg and Robert A Freitas Jr. "Acoustic communication for medical nanorobots". In: *Nano Communication Networks* 3.2 (2012), pp. 83–102.

[103] G Enrico Santagati, Tommaso Melodia, Laura Galluccio, and Sergio Palazzo. "Ultrasonic networking for e-health applications". In: *IEEE Wireless Communications* 20.4 (2013), pp. 74–81.

[104] G Enrico Santagati, Tommaso Melodia, Laura Galluccio, and Sergio Palazzo. "Medium access control and rate adaptation for ultrasonic intrabody sensor networks". In: *IEEE/ACM Transactions on Networking* 23.4 (2014), pp. 1121–1134.

[105] G Enrico Santagati and Tommaso Melodia. "Experimental evaluation of impulsive ultrasonic intra-body communications for implantable biomedical devices". In: *IEEE Transactions on Mobile Computing* 16.2 (2016), pp. 367–380.

[106] G Enrico Santagati and Tommaso Melodia. "Optoultrasonic communications for wireless intrabody nanonetworks". In: *Nano Communication Networks* 5.1-2 (2014), pp. 3–14.

[107] Murat Kuscu and Ozgur B Akan. "A physical channel model and analysis for nanoscale molecular communications with Fö rster resonance energy transfer (FRET)". In: *IEEE Transactions on Nanotechnology* 11.1 (2011), pp. 200–207.

[108] Murat Kuscu and Ozgur B Akan. "The Internet of molecular things based on FRET". In: *IEEE Internet of Things Journal* 3.1 (2015), pp. 4–17.

[109] Murat Kuscu and Ozgur B Akan. "A communication theoretical analysis of FRET-based mobile ad hoc molecular nanonetworks". In: *IEEE transactions on nanobioscience* 13.3 (2014), pp. 255–266.

[110] Murat Kuscu and Ozgur B Akan. "Coverage and throughput analysis for FRET-based mobile molecular sensor/actor nanonetworks". In: *Nano Communication Networks* 5.1-2 (2014), pp. 45–53.

[111] Murat Kuscu and Ozgur B Akan. "Multi-step FRET-based long-range nanoscale communication channel". In: *IEEE Journal on Selected Areas in Communications* 31.12 (2013), pp. 715–725.

[112] Murat Kuscu and Ozgur B Akan. "FRET-based nanoscale point-to-point and broadcast communications with multi-exciton transmission and channel routing". In: *IEEE transactions on nanobioscience* 13.3 (2014), pp. 315–326.

[113] Murat Kuscu, Alper Kiraz, and Ozgur B Akan. "Fluorescent molecules as transceiver nanoantennas: The irst practical and high-rate information transfer over a nanoscale communication channel based on FRET". In: *Scientific reports* 5.1 (2015), pp. 1–6.

[114] Falko Dressler and Stefan Fischer. "Connecting in-body nano communication with body area networks: Challenges and opportunities of the Internet of Nano Things". In: *Nano Communication Networks* 6.2 (2015), pp. 29–38.

[115] Meltem Civas, Oktay Cetinkaya, Murat Kuscu, and Ozgur B Akan. "Universal Transceivers: Opportunities and Future Directions for the Internet of Everything (IoE)". In: *Frontiers in Communi-cations and Networks* 2.50 (2021), pp. 1–20.

[116] Eric VanArsdale, Juliana Pitzer, Gregory F Payne, and William E Bentley. "Redox Electrochemistry to Interrogate and Control Biomolecular Communication". In: *Iscience* 23.9 (2020), p. 101545.

[117] Jayoung Kim, Alan S Campbell, and Joseph Wang. "Wearable non-invasive epidermal glucose sensors: A review". In: *Talanta* 177 (2018), pp. 163–170.

[118] Asimina Kiourti. "RFID antennas for body-area applications: From wearables to implants". In: *IEEE Antennas and Propagation Magazine* 60.5 (2018), pp. 14–25.

[119] Feng Wen, Tianyiyi He, Huicong Liu, Han-Yi Chen, Ting Zhang, and Chengkuo Lee. "Advances in chemical sensing technology for enabling the next-generation self-sustainable integrated wearable system in the IoT era". In: *Nano Energy* (2020), p. 105155.

[120] Morteza Amjadi, Sahar Sheykhansari, Bradley J Nelson, and Metin Sitti. "Recent advances in wearable transdermal delivery systems". In: *Advanced Materials* 30.7 (2018), p. 1704530.

[121] Karl Deisseroth. "Optogenetics". In: *Nature methods* 8.1 (2011), pp. 26–29.

[122] Lucas A Hartsough, Matthew V Kotlajich, Bing Han, Chih-Chun J Lin, Lauren Gambill, Meng Carla Wang, and Jeffrey J Tabor. "Optogenetic control of gut bacterial metabolism". In: *bioRxiv* (2020).

[123] Zedao Liu, Jizhong Zhang, Jiao Jin, Zilong Geng, Qingsheng Qi, and Quanfeng Liang. "Programming bacteria with light—sensors and applications in synthetic biology". In: *Frontiers in microbiology* 9 (2018), p. 2692.

[124] Laura Grebenstein, Jens Kirchner, Renata Stavracakis Peixoto, Wiebke Zimmermann, Florian Irnstorfer, Wayan Wicke, Arman Ahmadzadeh, Vahid Jamali, Georg Fischer, Robert Weigel, et al. "Biological optical-to-chemical signal conversion interface: A small-scale modulator for molecular communications". In: *IEEE transactions on nanobioscience* 18.1 (2018), pp. 31–42.

[125] Sasitharan Balasubramaniam, Stefanus A Wirdatmadja, Michael Taynnan Barros, Yevgeni Koucheryavy, Michal Stachowiak, and Josep Miquel Jornet. "Wireless communications for optogenetics-based brain stimulation: Present technology and future challenges". In: *IEEE Communications Magazine* 56.7 (2018), pp. 218–224.

[126] Tadashi Nakano, Shouhei Kobayashi, Tatsuya Suda, Yutaka Okaie, Yasushi Hiraoka, and Tokuko Haraguchi. "Externally controllable molecular communication". In: *IEEE Journal on Selected Areas in Communications* 32.12 (2014), pp. 2417–2431.

[127] Saied M Abd El-atty, Reda Bidar, and El-Sayed M El-Rabaie. "MolCom system with downlink/uplink biocyber interface for Internet of Bio-NanoThings". In: *International Journal of Communication Systems* 33.1 (2020), e4171.

[128] Steven Kisseleff, Robert Schober, and Wolfgang H Gerstacker. "Magnetic nanoparticle based interface for molecular communication systems". In: *IEEE Communications Letters* 21.2 (2016), pp. 258–261.

[129] Wayan Wicke, Arman Ahmadzadeh, Vahid Jamali, Harald Unterweger, Christoph Alexiou, and Robert Schober. "Magnetic nanoparticle-based molecular communication in microluidic environments". In: *IEEE transactions on nanobioscience* 18.2 (2019), pp. 156–169.

[130] Vijai Krishnan, Sarah A Park, Samuel S Shin, Lina Alon, Caitlin M Tressler, William Stokes, Jineta Banerjee, Mary E Sorrell, Yuemin Tian, Gene Y Fridman, et al. "Wireless control of cellular function by activation of a novel protein responsive to electromagnetic ields" . In: *Scientific reports* 8.1 (2018), pp. 1–12.

[131] Hadeel Elayan, Andrew Eckford, and Raviraj Adve. "Regulating Molecular Interactions Using Terahertz Communication". In: *ICC 2020-2020 IEEE International Conference on Communications (ICC)*. IEEE. 2020, pp. 1–6.

[132] Hadeel Elayan, Andrew W Eckford, and Raviraj Adve. "Information Rates of Controlled Protein Interactions Using Terahertz Communication". In: *IEEE Transactions on NanoBioscience* (2020).

[133] Mehmet Şükrü Kuran, H Birkan Yilmaz, Tuna Tugcu, and Bilge Özerman. "Energy model for communication via diffusion in nanonetworks". In: *Nano Communication Networks* 1.2 (2010), pp. 86–95.

[134] Chenyao Bai, Mark S Leeson, and Matthew David Higgins. "Minimum energy channel codes for molecular communications". In: *Electronics Letters* 50.23 (2014), pp. 1669–1671.

[135] Hrishikesh Jayakumar, Kangwoo Lee, Woo Suk Lee, Arnab Raha, Younghyun Kim, and Vijay Raghunathan. "Powering the internet of things". In: *Proceedings of the 2014 international symposium on Low power electronics and design*. 2014, pp. 375–380.

[136] Ergin Dinc, Murat Kuscu, Bilgesu A. Bilgin, and Ozgur B Akan. "Internet of Everything (IoE) - From Molecules to the Universe". In: *Harnessing the Internet of Everything (IoE) for Accelerated Innovation Opportunities*. IGI, 2018.

[137] Ozgur B Akan, Oktay Cetinkaya, Caglar Koca, and Mustafa Ozger. "Internet of hybrid energy harvesting things". In: *IEEE Internet of Things Journal* 5.2 (2017), pp. 736–746.

[138] Canan Dagdeviren, Zhou Li, and Zhong Lin Wang. "Energy harvesting from the animal/human body for self-powered electronics". In: *Annual review of biomedical engineering* 19 (2017), pp. 85–108.

[139] Vladimir Leonov. "Thermoelectric energy harvesting of human body heat for wearable sensors". In: *IEEE Sensors Journal* 13.6 (2013), pp. 2284–2291.

[140] M Amin Karami and Daniel J Inman. "Powering pacemakers from heartbeat vibrations using linear and nonlinear energy harvesters". In: *Applied Physics Letters* 100.4 (2012), p. 042901.

[141] Qiang Zheng, Bojing Shi, Fengru Fan, Xinxin Wang, Ling Yan, Weiwei Yuan, Sihong Wang, Hong Liu, Zhou Li, and Zhong Lin Wang. "In vivo powering of pacemaker by breathing-driven implanted triboelectric nanogenerator". In: *Advanced materials* 26.33 (2014), pp. 5851–5856.

[142] Wenzhao Jia, Gabriela Valdés-Ramírez, Amay J Bandodkar, Joshua R Windmiller, and Joseph Wang. "Epidermal biofuel cells: energy harvesting from human perspiration". In: *Angewandte Chemie International Edition* 52.28 (2013), pp. 7233–7236.

[143] Bojing Shi, Zhou Li, and Yubo Fan. "Implantable energy-harvesting devices". In: *Advanced Materials* 30.44 (2018), p. 1801511.

[144] Zhong Lin Wang and Wenzhuo Wu. "Nanotechnology-enabled energy harvesting for self-powered micro-/nanosystems". In: *Angewandte Chemie International Edition* 51.47 (2012), pp. 11700–11721.

[145] Ian F Akyildiz and Josep Miquel Jornet. "Electromagnetic wireless nanosensor networks". In: *Nano Communication Networks* 1.1 (2010), pp. 3–19.

[146] Kush Agarwal, Rangarajan Jegadeesan, Yong-Xin Guo, and Nitish V Thakor. "Wireless power transfer strategies for implantable bioelectronics". In: *IEEE reviews in biomedical engineering* 10 (2017), pp. 136–161.

[147] John S Ho, Alexander J Yeh, Evgenios Neofytou, Sanghoek Kim, Yuji Tanabe, Bhagat Patlolla, Ramin E Beygui, and Ada SY Poon. "Wireless power transfer to deep-tissue microimplants". In: *Proceedings of the National Academy of Sciences* 111.22 (2014), pp. 7974–7979.

[148] Sadeque Reza Khan, Sumanth Kumar Pavuluri, Gerard Cummins, and Marc PY Desmulliez. "Wireless power transfer techniques for implantable medical devices: A review". In: *Sensors* 20.12 (2020), p. 3487.

[149] Mohamed Manoufali, Konstanty Bialkowski, Beadaa Jasem Mohammed, Paul C Mills, and Amin Abbosh. "Near-field inductive-coupling link to power a three-dimensional millimeter-size antenna for brain implantable medical devices". In: *IEEE Transactions on Biomedical Engineering* 65.1 (2017), pp. 4–14.

[150] Zhichao Rong, Mark S Leeson, Matthew D Higgins, and Yi Lu. "Nano-rectenna powered body-centric nano-networks in the terahertz band". In: *Healthcare technology letters* 5.4 (2018), pp. 113–117.

[151] Li Feng, Amjad Ali, Muddesar Iqbal, Farman Ali, Imran Raza, Muhammad Hameed Siddiqi, Muhammad Shaiq, and Syed Asad Hussain. "Dynamic Wireless Information and Power Transfer Scheme for Nano-Empowered Vehicular Networks". In: *IEEE Transactions on Intelligent Transportation Systems* (2020).

[152] Zhichao Rong, Mark S Leeson, Matthew D Higgins, and Yi Lu. "Simultaneous wireless information and power transfer for AF relaying nanonetworks in the Terahertz Band". In: *Nano communication networks* 14 (2017), pp. 1–8.

[153] Weisi Guo, Yansha Deng, H Birkan Yilmaz, Nariman Farsad, Maged Elkashlan, Andrew Eckford, Arumugam Nallanathan, and Chan-Byoung Chae. "SMIET: Simultaneous molecular information and energy transfer". In: *IEEE Wireless Communications* 25.1 (2017), pp. 106–113.

[154] Yansha Deng, Weisi Guo, Adam Noel, Arumugam Nallanathan, and Maged Elkashlan. "Enabling energy eficient molecular communication via molecule energy transfer". In: *IEEE Communications Letters* 21.2 (2016), pp. 254–257.

[155] Teimour Maleki, Ning Cao, Seung Hyun Song, Chinghai Kao, Song-Chu Ko, and Babak Ziaie. "An ultrasonically powered implantable micro-oxygen generator (IMOG)". In: *IEEE transactions on Biomedical Engineering* 58.11 (2011), pp. 3104–3111.

[156] Patrick J Larson and Bruce C Towe. "Miniature ultrasonically powered wireless nerve cuff stimulator". In: *2011 5th International IEEE/EMBS Conference on Neural Engineering*. IEEE. 2011, pp. 265–268.

[157] Michael Donohoe, Sasitharan Balasubramaniam, Brendan Jennings, and Josep Miquel Jornet. "Powering in-body nanosensors with ultrasounds". In: *IEEE Transactions on Nanotechnology* 15.2 (2015), pp. 151–154.

[158] Michael Donohoe, Brendan Jennings, Josep Miquel Jornet, and Sasitharan Balasubramaniam. "Nanodevice arrays for peripheral nerve fascicle activation using ultrasound energy-harvesting". In: *IEEE Transactions on Nanotechnology* 16.6 (2017), pp. 919–930.

[159] Chen Xu, Xudong Wang, and Zhong Lin Wang. "Nanowire structured hybrid cell for concurrently scavenging solar and mechanical energies". In: *Journal of the American Chemical Society* 131.16 (2009), pp. 5866–5872.

[160] Benjamin J Hansen, Ying Liu, Rusen Yang, and Zhong Lin Wang. "Hybrid nanogenerator for concurrently harvesting biomechanical and biochemical energy". In: *ACS nano* 4.7 (2010), pp. 3647–3652.

[161] Ozgur B Akan, Oktay Cetinkaya, Caglar Koca, and Mustafa Ozger. "Internet of hybrid energy harvesting things". In: *IEEE Internet of Things Journal* 5.2 (2018), pp. 736–746.

[162] F Albano, YS Lin, D Blaauw, DM Sylvester, KD Wise, and AM Sastry. "A fully integrated microbattery for an implantable microelectromechanical system". In: *Journal of Power Sources* 185.2 (2008), pp. 1524–1532.

[163] Fride Vullum, Dale Teeters, Anton Nytén, and Josh Thomas. "Characterization of lithium nanobatteries and lithium battery nanoelectrode arrays that beneit from nanostructure and molecular self-assembly". In: *Solid State Ionics* 177.26-32 (2006), pp. 2833–2838.

[164] Hongxi Zhang, Yudong Cao, Mason Oliver Lam Chee, Pei Dong, Mingxin Ye, and Jianfeng Shen. "Recent advances in micro-supercapacitors". In: *Nanoscale* 11.13 (2019), pp. 5807–5821.

[165] Swati Patil and Dong-Weon Lee. "Status review on the MEMS-based le xible supercapacitors". In: *Journal of Micromechanics and Microengineering* 29.9 (2019), p. 093001.

[166] Yao Lu, Kai Jiang, Di Chen, and Guozhen Shen. "Wearable sweat monitoring system with integrated micro-supercapacitors". In: *Nano Energy* 58 (2019), pp. 624–632.

[167] Chenguang Liu, Zhenning Yu, David Neff, Aruna Zhamu, and Bor Z Jang. "Graphene-based supercapacitor with an ultrahigh energy density". In: *Nano letters* 10.12 (2010), pp. 4863–4868.

[168] Zhong-Shuai Wu, Xinliang Feng, and Hui-Ming Cheng. "Recent advances in graphene-based planar micro-supercapacitors for on-chip energy storage". In: *National Science Review* 1.2 (2014), pp. 277–292.

[169] Taichi A Suzuki and Ruth E Ley. "The role of the microbiota in human genetic adaptation". In: *Science* 370.6521 (2020).

[170] Malcolm Egan, Trang C Mai, Trung Q Duong, and Marco Di Renzo. "Coexistence in molecular communications". In: *Nano communication networks* 16 (2018), pp. 37–44.

[171] Markus Schmid, Patrick Ernst, Annemarie Honegger, Maarit Suomalainen, Martina Zimmermann, Lukas Braun, Sarah Stauffer, Cristian Thom, Birgit Dreier, Matthias Eibauer, et al. "Adenoviral vector with shield and adapter increases tumor specificity and escapes liver and immune control". In: *Nature communications* 9.1 (2018), p. 450.

[172] Hong Chen, Lin Yuan, Wei Song, Zhongkui Wu, and Dan Li. "Biocompatible polymer materials: role of protein–surface interactions". In: *Progress in Polymer Science* 33.11 (2008), pp. 1059–1087.

[173] Mukta Kulkarni, A Mazare, E Gongadze, Š Perutkova, V Kralj-Igli , I Milošev, Patrik Schmuki, A Igli , and M Mozeti . "Titanium nanostructures for biomedical applications". In: *Nanotechnology* 26.6 (2015), p. 062002.

[174] Laura Treccani, Tanja Yvonne Klein, Fabian Meder, Karoline Pardun, and Kurosch Rezwan. "Functionalized ceramics for biomedical, biotechnological and environmental applications". In: *Acta biomaterialia* 9.7 (2013), pp. 7115–7150.

[175] Alberto Bianco. "Graphene: safe or toxic? The two faces of the medal". In: *Angewandte Chemie International Edition* 52.19 (2013), pp. 4986–4997.

[176] Andrea C Ferrari, Francesco Bonaccorso, Vladimir Fal'Ko, Konstantin S Novoselov, Stephan Roche, Peter Bøggild, Stefano Borini, Frank HL Koppens, Vincenzo Palermo, Nicola Pugno, et al. "Science and technology roadmap for graphene, related two-dimensional crystals, and hybrid systems". In: *Nanoscale* 7.11 (2015), pp. 4598–4810.

[177] Shuai Zhang, Kai Yang, Liangzhu Feng, and Zhuang Liu. "In vitro and in vivo behaviors of dextran functionalized graphene". In: *Carbon* 49.12 (2011), pp. 4040–4049.

[178] Alaaldin M Alkilany and Catherine J Murphy. "Toxicity and cellular uptake of gold nanoparticles: what we have learned so far?" In: *Journal of nanoparticle research* 12.7 (2010), pp. 2313–2333.

[179] Michael Okwori, Ali Behfarnia, Phanikumar Vuka, and Ali Eslami. "A Micro-Scale Mobile-Enabled Implantable Medical Sensor". In: *arXiv preprint arXiv:1806.06163* (2018).

[180] Bayram Cevdet Akdeniz and Malcolm Egan. "A Reactive Signaling Approach to Ensure Coexistence Between Molecular Communication and External Biochemical Systems". In: *IEEE Transactions on Molecular, Biological and Multi-Scale Communications* 5.3 (2019), pp. 247–250.

[181] Malcolm Egan, Valeria Loscri, Ido Nevat, Trung Q Duong, and Marco Di Renzo. "Estimation and Optimization for Molecular Communications with a Coexistence Constraint". In: *Proceedings of the Sixth Annual ACM International Conference on Nanoscale Computing and Communication*. 2019, pp. 1–6.

[182] Malcolm Egan, Valeria Loscri, Trung Q Duong, and Marco Di Renzo. "Strategies for coexistence in molecular communication". In: *IEEE transactions on nanobioscience* 18.1 (2018), pp. 51–60.

[183] Murat Kuscu and Ozgur B Akan. "Detection in molecular communications with ligand receptors under molecular Interference". In: *Digital Signal Processing* (2021), p. 103186.

AUTHORS

Murat Kuscu received his PhD degrees in engineering from University of Cambridge, UK, in 2020, and in electrical and electronics engineering from Koç University, Turkey, in 2017. He is currently an Assistant Professor with the Department of Electrical and Electronics Engineering, Koç University. His current research interests include the Internet of Bio-Nano Things, bio/chemical information and communication technologies, graphene and related two-dimensional nanomaterials, biosensors, bio-cyber interfaces, and microluidic sensors. He has received the Marie Skłodowska-Curie Actions Individual Fellowship 2020, University of Cambridge CAPE Acorn Post-graduate Research Award 2019, IEEE Turkey Ph.D. Thesis Award 2018, and Koç University Post-graduate Academic Excellence Award 2018.

Bige Deniz Unluturk received her Ph.D. degree in Electrical and Computer Engineering from the Georgia Institute of Technology, Atlanta, GA, in August 2020. In 2013, she received her M.Sc. degree from Koc University, Istanbul, Turkey. In 2011, she graduated from Electrical and Electronics Engineering at Middle East Technical University, Ankara, Turkey. She is currently an assistant professor in the Departments of Electrical & Computer Engineering and Biomedical Engineering at Michigan State University. Her research is in the areas of wireless communication and networking, more specifically Molecular Communications and Internet of Bio-NanoThings, and their applications to healthcare.

ENABLING MOLECULAR COMMUNICATION THROUGH CHIRALITY OF ENANTIOMERS

Valeria Loscrí[1] and Anna Maria Vegni[2]
[1]Inria Lille - Nord Europe, Lille, France, [2]Roma Tre University, Rome, Italy

NOTE: Corresponding author: Valeria Loscrí, valeria.loscri@inria.fr

Abstract *– With the advancement of nanotechnology, there has been fervid research activity on new communication paradigms suitable for new challenging contexts, such as biological systems. Among different approaches, the most considered has been artificial Molecular Communication, where entities such as synthetic molecules, enzymes, hormones, bacteria etc. are functionalized in order to implement information exchange with the surrounding system and with other entities. In this context, it is interesting to analyze specific features that could be exploited for effective communication paradigms. In this paper, we focus on chiral molecules (a.k.a. enantiomers) as novel enablers for a molecular communication paradigm. Chirality is an interesting and appealing feature existing in nature and that can be replicated with strong emphasis in new types of materials, such as metasurfaces and metamaterials. A deep knowledge of chirality features and how chiral molecules interact with each other or with achiral molecules provides insights into designing a new molecular communication technique suitable for biological environments. In this contribution, we will highlight the main applications of chiral molecules and we will present chiral features as the viable way for realizing a nanocommunication system.*

Keywords – Chiral molecules, chirality transfer, enantiomers, molecular communications, optical activity

1. INTRODUCTION

A Molecular Communication (MC) paradigm consists of using molecules to encode, transmit and receive information. It has recently received a lot of attention by the research community since it is considered as the viable alternative of electromagnetic (EM) communications, thanks to the specific features of biocompatibility. MC is mostly inspired by existing communication mechanisms occurring between biological entities and is developed by considering small molecules, peptides, lipids, as well as bacteria, viruses, pheromones and so on [1].

An MC paradigm is based on the transmission and reception of information encoded into molecules (*i.e.*, messenger molecules) [2, 3]. These entities freely propagate in the medium by connecting a transmitter with a receiver nanomachine. Typical molecular communication systems are based on the free diffusion process of molecules, such as calcium signaling, microtubules, pheromone signaling, and bacterium-based communications [4]. Different biological entities allow reaching different communication ranges and performance. For instance, the use of pheromones (*i.e.*, molecules of chemical compounds released by plants, insects, and other animals) triggers specific behaviors among the receptor members and reaches long-range communications *i.e.*, approximately one meter. On the other side, both flagellated bacteria and catalytic nanomotors are able to carry DNA messages and allow short-range communications. The use of DNA as information messages allows achieving an information rate that is relatively high (*i.e.*, up to several kilobits per second). In contrast, the propagation of information by means of guided bacteria or catalytic nanomotors is relatively very slow (*i.e.*, a few millimeters per hour).

A special type of molecules that is expected to be very promising in the field of molecular communications is the *chiral molecule*. Chiral molecules show the chirality effect *i.e.*, a physical phenomenon that pervades the universe. The term chirality was introduced in 1884 and refers to objects that are not equivalent to their mirror images, and the two images are not superposed to each other. A typical example of such a geometrically chiral object is the human hand, so that the left and the right hands are mirror images of each other, but it is impossible to superpose them.

Chiral molecules, a.k.a. *enantiomers*, can show their different handedness in many ways, including the way they affect human beings. For instance, one enantiomeric form of a compound called limonene is primarily responsible for the odor of oranges, while the other enantiomer, for the odor of lemons. Molecules of the amino acids of which our proteins are built have the property of being non-superposable on their mirror image. In contrast, objects (and molecules) that are superposable on their images are achiral. The chirality of molecules can be demonstrated with relatively simple compounds. For instance, consider a 2-butanol molecule *i.e.*, an organic compound with formula $CH_3CH(OH)CH_2CH_3$. The structure of 2-butanol is chiral, that means that there are actually two different 2-butanols and they are enantiomers. Another example is the amino acid alanine, which is in the form of left-handed and right-handed enantiomers *i.e.*, (S)-alanine and (R)-alanine, respectively. Fig. 1 depicts

the two enantiomers, whose mirror images are not equivalent and non-superposable on each other. Another example of enantiomers are the molecules of natural sugars, almost all classified as being right handed, including the sugar that occurs in DNA. Also DNA is a chiral structure, since its two helixes are not superposable to each other, as well depicted in Fig. 1 (b).

In this paper we address how to exploit chiral molecules as messenger molecules for molecular communications. The use of similar molecules *i.e.*, isomers, as enablers of molecular communications has already been investigated in [5], where Kim and Chae proposed three novel modulation techniques, *i.e.*, concentration-based, molecular-type-based, and molecular-ratio-based. However, in [5] it did not emerge the main features of such special molecules and how it is possible to exploit them for molecular communications by means of their inner features. For example, one of the main features of chiral molecules is their behavior towards plane-polarized light. When a beam of plane-polarized light passes through an enantiomer, the plane of polarization rotates. Also, separate enantiomers rotate the plane of plane-polarized light at equal amounts but in opposite directions. Then, separate enantiomers are optically active compounds.

In this paper, we focus on the features of chiral molecules such as (*i*) the rotation of the polarization plane of the impinging EM wave and (*ii*) the chirality transfer effect, in order to model a chiral channel comprised of enantiomers that forward data information via a multi-hop protocol. Specifically, in our vision, data information is represented by exploiting the chirality phenomenon with a chiral molecule emitting a rotated EM wave when a light input impinges on an initial transmitter node after a steady state is achieved. Dissemination of data information inside a chiral medium occurs through the *chirality transfer* mechanism that considers the non-covalent bonds between a chiral and an achiral molecule. Chirality is exploited to encode the information in the chiral molecules, and it is decoded at the receiver as a 1 bit when an EM wave (*i.e.*, an optical signal) is applied. When no EM wave is applied, the information is decoded as a bit 0.

This paper is organized as follows. Section 2 introduces the concept of chirality effect and describes the main enantiomers that can be found in nature, specifically in the biological context. The features of chiral molecules are then presented in Subsection 2.1. In Section 3 we characterize the chiral transfer effect from a chiral molecule to an achiral molecule. In Section 4, we define a chiral medium as a channel for molecular communications. Data information is encoded in the chiral molecules that transport the chirality effect, which can be forwarded hop-by-hop in the overall system. Finally, conclusions are drawn at the end of this paper.

Fig. 1 – Examples of chiral molecules in case of (a) alanine amino-acid, and (b) DNA chains. Enantiomers are non-superposable mirror images to each other.

2. CHIRAL MOLECULES

A chiral molecule shows the chirality effect that makes the molecule not equivalent to its mirror image. The chiral molecule and its mirror image are enantiomers, and the relationship between the chiral molecule and its mirror image is defined as enantiomeric. The word chiral comes from the Greek, and means "hand". Indeed, a classic example of chiral objects are the hands, since the mirror image of the left hand is exactly the right hand. However, the left hand is not superposable on the right hand.

From the etymology of chiral, chiral objects are said to possess "handedness". Although both mirror image forms are theoretically possible, such as those for the amino acid alanine, they have evolved in a way that amino acids are mainly of the mirror image said to be "left-handed" (see Fig. 1 (a)). The reason that most amino acids are of the left-handed form is not known, however.

Chirality is an important phenomenon in the universe. Several plants show chirality, by winding around supporting structures. The human body is structurally chiral and it is not clear why, but most people are right-handed. Usually, only one form of chiral occurs in a given species. Just as an example, the molecules of white sugars are right handed. Enantiomers of a chiral molecule have identical physico-chemical properties, and also the same electrochemical behavior. The enantioselective electrochemistry represents the ability of discriminating enantiomers of chiral molecules (*i.e.*, electroanalysis), or to selectively activate or achieve a given enantiomer of a chiral molecule (*i.e.*, electrosynthesis) and is an issue particularly important in the biological and pharmaceutical fields [6].

2.1 Features of chiral molecules

The specific rotation is a property of a chiral molecule. It is defined as the change in orientation of monochromatic plane-polarized light, per unit distance-concentration product, as the light passes through a sample of a compound in solution. Fig. 2 describes the property of rotation of the polarization plane of an EM field that impinges on a chiral channel. At the output of the channel, the polarization plane has been rotated. Specifically, chiral molecules can rotate the plane of polarization of an

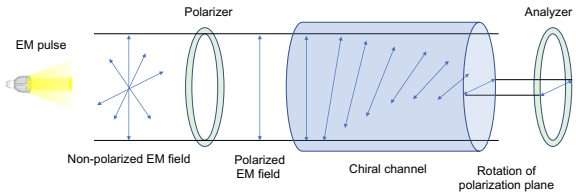

Fig. 2 – Property of rotation of the polarization plane of an EM pulse impinging a chiral channel.

EM field both clockwise and counterclockwise. If the rotation is clockwise, chiral molecules are said to be *dextrorotary*, and correspond to positive rotation values, while chiral molecules rotating the plane of polarization counterclockwise are said to be *levorotary*, and correspond with negative values of the specific rotation.

Another important feature of chiral molecules is the *chirality transfer* that occurs when a chiral molecule encounters an achiral molecule. In such a scenario, the chirality effect is extended over the whole molecular system *i.e.*, it propagates from a chiral to an achiral molecule, which becomes chiral. The induction of the chirality in the achiral components is of utmost importance. In order to induce the chirality of the achiral components, the interaction between the chiral molecules and the achiral molecules plays a very important role.

The induced chirality generally refers to those chiral supramolecular systems where chirality is induced in an achiral guest molecule as a result of asymmetric information transfer from a chiral host *e.g.*, a chiral molecule or a chiral nanostructure. In order to produce the induced chirality, it is necessary for the achiral molecule to have a strong interaction with the chiral host through a noncovalent bond. A typical example of induced chirality is the encapsulation of a chromophore into the cavity of cyclodextrin [7]. Finally, a very important aspect related to chirality is the *chiral communication* that is a common phenomenon occurring in many biological processes [8], strictly tied with the chirality transfer property.

In this paper, we will exploit the chirality transfer effect by the means of diffusion of chiral molecules which come into contact with achiral molecules in a biological solution.

3. CHIRALITY TRANSFER EFFECT

As already introduced in Subsection 2.1, the chirality transfer effect is observed between organic and inorganic molecular structures. The modeling of macroscopic chi- rality emerged from the chiral molecular elements is a challenge for theory, computations, and experiments. Nu- merous experimental results demonstrated the transfer of chirality among different length scales ranging from di- mensions of the elementary particles to the macro-scale (*i.e.*, the length of the axon). In particular, it was shown that the chirality at the molecular scale (*i.e.*, amino acids, proteins, and polysaccharides) could be transferred to the macroscopic and macro level (*i.e.*, neurofilaments and in-organic crystals).

In general, chirality transfer occurs through chemical bonds, but recently it has been observed that chiral biomolecules may impart some of their optical properties to a spatially separated achiral dye [9]. Knof and von Zelewsky [10] have characterized the chiral transfer as through the use of organic ligands chiral information can be transferred.

In the context of chirality transfer it is important to highlight chiroptical properties. Among the most important properties are the chiral luminescent lanthanide complexes used as probes for the characterization of chiral environments [11, 12, 13] or as chiral luminescent complexes [14, 15, 16, 17]. Lanthanides are ideal candi- dates as luminescent probes, based on specific features such as their long lifetimes and large Stokes shifts. CP luminescence has great potential to investigate the configurational, as well as conformational changes, in biological systems in solution, since it combines the gen- eral sensitivity of luminescence measurements and the high specificity of the signal for the chiral environment. Furthermore, using very simple chiral ligands and lanthanide ions, chiral nanoballs were obtained where the array of lanthanide ions are arranged as in the ferritin biological molecule [18, 19]. With very simple chiral ligands used as synthons (*i.e.*, a synthon is a component of a molecule to be synthesized, playing an active role in synthesis) in coordination chemistry, it is possible to obtain sophisticated chiral assemblies which mimic biological systems. These considerations are encouraging in the development of "artificial" molecular communication systems.

Chirality is also important in molecular switches [20, 21]. A switch is a molecule that can reversibly interconvert be- tween two stable states upon an external stimulus. In [22] Dai *et al.* described a chiroptical switch based on pho- tochromes that exhibit two different states with signifi- cantly different optical rotations. Finally, chiral transfer phenomena can be used for sensing chirality of a wide range of chiral molecules, as well as for developing novel chiroptical devices and chiral materials. The wider application of chiral sensing continues to be hampered by the involved chiral signals being inherently weak. To avoid this issue, plasmonic and dielectric nanostructures have recently been shown to offer a viable route for enhancing weak circular dichroism (CD) effects. Re- cently, in [23] Mohammadi *et al.* presented an analytical study of the problem of substrate CD spectroscopy for an arbitrary nanophotonic substrate (either, chiral or achi- ral, plasmonic or dielectric) and clarify the interplay be- tween key affecting parameters, such as the thickness and chirality of the substrate, as well as the near-field optical chirality enhancement. From the telecommunications point of view, chirality transfer can be exploited by the means of a diffusion process of the chiral molecules. When the "chirality effect" is transferred to an achiral molecule and an optical signal is applied, it will be able to

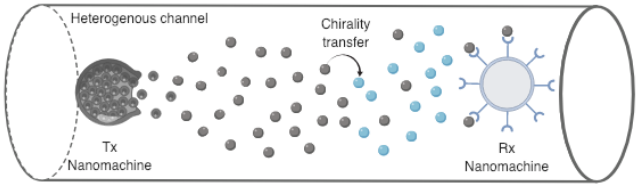

Fig. 3 – Chirality transfer property of chiral molecules (*black circles*) towards achiral molecules (*light blue molecules*).

show an optical activity, and become a chiral molecule. As a result, the chirality transfer works as point-to-point data forwarding among heterogeneous molecules (*i.e.*, from chiral to achiral molecules).

Specifically, when a chiral molecule encounters an achiral component, it forms a non-covalent bond and the chirality effect is transferred into the achiral molecule, which becomes chiral. Finally, the chirality transfer propagates in the whole system.

Fig. 3 depicts the chirality transfer feature of chiral molecules in a heterogeneous channel (*i.e.*, comprised of both chiral and achiral molecules). In this scenario, the chiral molecules are used as messenger molecules released by a transmitter nanomachine (*e.g.*, a eukaryotic cell) through the medium via diffusion (*i.e.*, Brownian motion). They are used as messengers, since they allow the transmission of a light signal applied to a transmitter molecule and transferred from a molecule to the neighbors through the chiroptical properties when the system will reach a steady state. The motion is basically driven by diffusion, meaning that the particles move from areas of higher concentration to areas of lower concentration, and the displacement of messenger molecules follows a normal distribution with zero mean.

The overall chiral molecule concentration flux is given by the sum of the N chiral molecules concentration gradients, with N as the number of apertures of the Tx nanomachine. The flux of chiral molecule concentration depends on both time and position through the Fick's first law *i.e.*,

$$J\left(x,t\right) = -D\sum_{i=1}^{N}\nabla C_{i,CM}\left(x,t\right), \qquad (1)$$

where ∇ is an operator used in vector calculus as a vector differential operator, $C_{i,CM}$ [mol/cm^3] is the i-th chiral molecule concentration with $i = \{1, 2, \ldots, N\}$, and D [cm^2/s] is the diffusion coefficient, assumed as a constant value for a given fluidic medium as:

$$D = \frac{k_B T}{3\pi\eta d}, \qquad (2)$$

where k_B is the Boltzmann constant equal to $1.38 \times 10^{-23}[J/K]$, T is the temperature $[K]$, η is the viscosity of the liquid $[mPa{\cdot}s]$, and d is the size of the chiral molecules expressed in $[nm]$. Finally, Eq. *(1)* can be rewritten as:

$$J\left(x,t\right) = \frac{Q_{CM} + Q_{AM}Pr(AM \rightarrow CM)}{\sqrt{\left(4\pi Dt\right)^3}} e^{-\frac{x^2}{4Dt}} \qquad (3)$$

where Q_{CM} is the initial concentration of chiral molecules, Q_{AM} is the initial concentration of achiral molecules and $J(x,t)$ represents the Brownian particles at time t at point x, with first moment as:

$$x^2 = 2Dt, \qquad (4)$$

and standard deviation:

$$\sigma = \sqrt{2Dt}. \qquad (5)$$

In Eq. *(3)*, we account for the achiral molecules that are "inducted" to become chiral with a certain probability that is proportional to the helical twisting power of the chiral molecules, *i.e.*:

$$Pr(AM \rightarrow CM) \backsim \beta, \qquad (6)$$

where β is the helical twisting power and is expressed as [24]

$$\beta = \frac{\Delta\mu}{8\pi K_2 k}, \qquad (7)$$

where Δu is the chemical potential difference between a chiral molecule and its enantiomer when they are placed in the solution, K_2 is twist elastic constant, the wavevector $k = 2\pi/P$ and P is the elical pitch, which is inversely proportional to the concentration of chiral molecules injected by the transmitter.

4. CHIRAL OPTICAL CHANNEL

In the context of molecular communication, we envision that chiral molecules will be expected to be largely exploited [25]. Due to the feature of changing the polarization plane of an impinging optical signal, data information can be encoded into chiral molecules, and carried out via the chiral transfer mechanism. Specifically, when an optical pulse impinges a (biological) chiral channel, an optical activity as output of the channel will be observed. The optical activity is expressed as a rotation of the polarization plane of the impinging EM wave. On the other side, if no pulse impinges the chiral channel, no optical activity will be observed at the output of the chiral channel, and then, there will be no rotation of the polarization plane of the EM wave.

In Fig. 4 we show how the chiral molecules are arranged after the diffusion process, in a steady state. We assume that a certain concentration of chiral molecules is injected in the system and these molecules diffuse in the solution and "transfer" their chirality to other achiral molecules. Specifically, a Tx nanomachine releases a concentration of chiral molecules that transfer chirality to neighboring achiral molecules, which become chiral as well. Blue circles represent chiral molecules (both enantiomers), while gray circles are the achiral molecules. In this work, we treat chiral molecules as chiral optical antennas and we focus on some specific parameters allowing the characterization of the chiral optical field generated. In particular, as demonstrated in [26], we consider the chirality flux

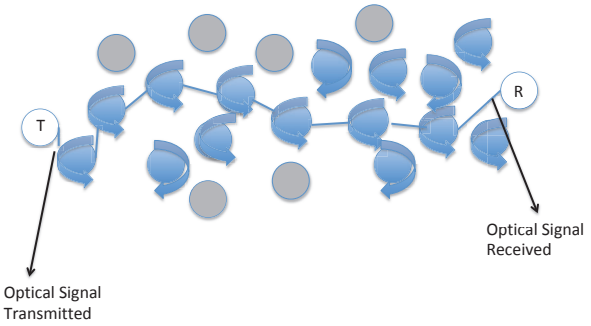

Fig. 4 – Representation of the chiral molecular channel after the diffusion process. The blue (gray) circles represent chiral (achiral) molecules.

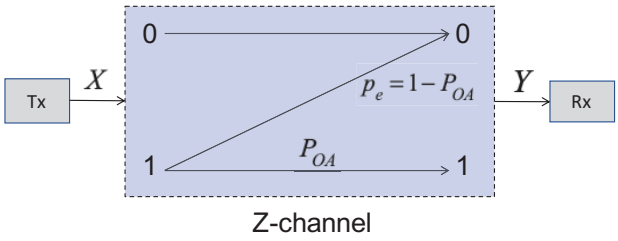

Fig. 5 – Z-channel model for the chiral medium.

efficiency, that describes the ability of our molecules to scatter chiral optical fields, that will be considered as the input for the neighbor chiral molecule as shown in Fig. 4. In particular, the chiral flux efficiency can be written as [26]:

$$\eta_{\tilde{F},d} = \mathrm{Re}(\alpha_c)\frac{3}{8\mu_0}\frac{|\varepsilon_0|^2}{P_{tot}}\frac{1}{\sqrt{r^2+\zeta^2}}, \qquad (8)$$

with r and ζ as radial and longitudinal cylindrical coordinates, μ_0 and $|\ \varepsilon_0\ |^2$ the amplitude of the complex electric field in the point 0 and P_{tot} is the total power of the outgoing light. Most important is the parameter α_c representing the coupled magneto-electric polarizability, to which chiral optical properties are attributed to. Of course, we have to consider that in molecules chiral optical signals are lower than in chiral metallic nanostructures, but there are recent research activities showing how it is possible to improve the quality of the signal [27].

The chiral channel can be then designed as a Z-channel, as depicted in Fig. 5. The output of the channel is expressed in terms of rotation of the polarization plane in case of an optical wave impinging the biological chiral channel.

From the telecommunications point of view, the optical activity due to the effect of chirality can be decoded as a 1 bit, while the absence of rotation of the polarization plane will be decoded as a 0 bit. Fig. 5 describes a chiral channel comprised of chiral molecules. A source node (*i.e.*, Tx node) emits a bit stream modulated through an On Off Keying (OOK) scheme. Specifically, the variable X represents the bit 1 or 0 transmitted along the channel, while Y is the received bit (*i.e.*, 1 or 0), based on a probabilistic approach. The presence of a bit 1 at the receiver means that a bit 1 has been transmitted with conditional probability $\Pr(Y = 1|X = 1)$, while a bit 0 at the receiver side can be affected by errors in the channel corresponding to the error probability $p_e = \Pr(Y = 0|X = 1)$, in case of a bit 1 transmitted with errors. Notice that, different to traditional OOK-based communication schemes for molecular communications, in this paper the OOK modulation is not based on the concentration variation of the molecules, but on the optical activity generated by the chiral molecules. In practice, a bit 1 is associated to the optical activity occurrence, while a bit 0 is associated to no optical activity at the output of the channel.

Furthermore, we assume a time-based synchronization scheme at the transmitter side, and then the transmission of a bit 1 corresponds to an EM wave that excites the chiral channel at the beginning of a time slot, while no excitation corresponds to the emission of a bit 0. The probability of sending a bit 0 in the case of No Excitation at the beginning of the time slot is defined as P_{NE}. If no excitation is provided to the Tx node, then no optical activity will occur (*i.e.*, from the information theory point of view, no transmission errors will occur, while transmitting bit 0). The probability that the bit 1 is correctly received by the receiver corresponds to the probability of optical activity experienced by the chiral molecules, namely P_{OA}. This probability can be considered depending on the specific optical rotation *i.e.*, $[\alpha]^T_\lambda$, that is a physical constant of a chiral molecule, expressed as:

$$[\alpha]^T_\lambda = \frac{\alpha}{l \cdot \rho}, \qquad (9)$$

where α is the optical rotation expressed in degrees, l is the optical path length $[dm]$, and ρ is the concentration of sample in $[g/mL]$, that we can derive from (*(3)*). In Eq. *(9)*, we notice that the specific rotation depends on the wavelength λ [nm] of the impinging EM wave and the temperature T [Celsius]. Usually, the wavelength of the light used is 589 nm (*i.e.*, the sodium D line), and the symbol D is used *i.e.*, $[\alpha]^T_D$. The specific rotation can be either positive or negative, if the chiral molecules are dextrotary or levorotary, respectively.

The probability of optical activity occurrence is intrinsically not equal to 1, *i.e.*, $P_{OA} \neq 1$, and can be expressed as:

$$P_{OA} = \Pr\left\{[\alpha]^T_\lambda > +0^\circ\right\}, \qquad (10)$$

that means that if the specific rotation is greater than $+0^\circ$, then it is likely to have optical activity at the output of the chiral channel. Notice that the specific rotation depends on the enantiomers that will rotate the plane of the polarized light of the same magnitude but in opposite directions (*i.e.*, $+$ or $-$). Without loss of generality, herein we assumed a positive rotation of the polarization plane, *i.e.*, we are assuming that the biological medium is comprised of a mixture of enantiomers $(+/-)$ but the overall contribution of the specific rotation will be positive. On the

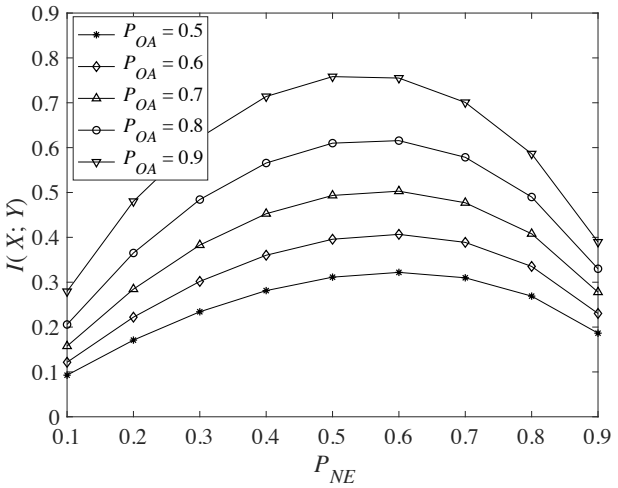

Fig. 6 – Mutual information related to the enantiomer Z-channel model.

other side, the channel will be optically inactive if the specific rotation will be null *i.e.*, there will be both $50\%(+)$ and $50\%(-)$ of enantiomers. This configuration is a racemate or racemic mixture.

According to the transmission probabilities of the Z-channel, the associated transition matrix is

$$\mathbf{P} = \begin{bmatrix} 1 & 0 \\ 1 - P_{OA} & P_{OA} \end{bmatrix}, \qquad (11)$$

and then we can derive the mutual information between X and Y as:

$$I(X;Y) = H(P_{OA}(1-P_{NE})) - (1-P_{NE})\, H(1-P_{OA}), \qquad (12)$$

where $H(\cdot)$ represents the binary entropy. From Eq. *(12)*, we can compute the channel capacity of the chiral medium as the maximum of the mutual information *i.e.*,

$$C_{chiral} = \max_{P_{OA}} [H(P_{OA}(1-P_{NE})) - (1-P_{NE})\, H(1-P_{OA})], \qquad (13)$$

where the probability distribution of input that maximizes the capacity will change according to specific chiral molecule concentrations.

Finally, Fig. 6 depicts the mutual information versus the probability of no excitation, for different values of P_{OA}. Notice that we consider only values of P_{OA} higher than 0.5, as it depends on the concentration of positive/negative enantiomers that comprise the channel. As expected, the highest value of the capacity (*i.e.*, 0.758 bit) is obtained for a high value of P_{OA}.

5. CONCLUSIONS

This paper presents an overview of the chirality effect in biomolecules. Chiral molecules *i.e.*, enantiomers, are present in nature everywhere, and therefore the main applications range from pharmaceutical to chemical and biological fields, including also communications and electronics. Apart from natural enantiomers, artificial chiral materials (*i.e.*, chiral metamaterials) can be accordingly designed in order to exhibit an enhanced optical activity *i.e.*, the Giant Optical Activity (GOA) effect.

In the context of communications, the use of natural chiral molecules, as well as chiral metamaterials, is envisioned as a potential enabler for novel communication techniques. Specifically, in an MC paradigm, chiral molecules have been analyzed as viable candidates for chiral communications, where information is encoded into chiral molecules. The features of rotation of the polarization plane and the chirality transfer have been exploited in order to derive a communication model based on chiral molecules. Information is represented by the optical activity, which can propagate inside a chiral medium by means of chirality transfer.

REFERENCES

[1] I. F. Akyildiz, J. M. Jornet, and M. Pierobon. "Nanonetworks: a New Frontier in Communications". In: *Communications of the ACM* 54 (11 Nov. 2011), pp. 84–89.

[2] Ian F. Akyildiz, Fernando Brunetti, and Cristina Blázquez. "Nanonetworks: A new communication paradigm". In: *Computer Networks* 52.12 (2008), pp. 2260–2279. ISSN: 1389-1286. DOI: https://doi.org/10.1016/j.comnet.2008.04.001. URL: http://www.sciencedirect.com/science/article/pii/S1389128608001151.

[3] M. Pierobon and I. F. Akyildiz. "A physical end-to-end model for molecular communication in nanonetworks". In: *IEEE Journal on Selected Areas in Communications* 28.4 (May 2010), pp. 602–611. ISSN: 0733-8716. DOI: 10.1109/JSAC.2010.100509.

[4] T. Nakano, M. J. Moore, F. Wei, A. V. Vasilakos, and J. Shuai. "Molecular Communication and Networking: Opportunities and Challenges". In: *IEEE Transactions on NanoBioscience* 11.2 (June 2012), pp. 135–148. ISSN: 1536-1241. DOI: 10.1109/TNB.2012.2191570.

[5] N. Kim and C. Chae. "Novel Modulation Techniques using Isomers as Messenger Molecules for Nano Communication Networks via Diffusion". In: *IEEE Journal on Selected Areas in Communications* 31.12 (Dec. 2013), pp. 847–856. ISSN: 0733-8716. DOI: 10.1109/JSAC.2013.SUP2.12130017.

[6] Serena Arnaboldi, Mirko Magni, and Patrizia Romana Mussini. "Enantioselective selectors for chiral electrochemistry and electroanalysis: Stereogenic elements and enantioselection performance". In: *Current Opinion in Electrochemistry* 8 (2018), pp. 60–72. ISSN: 2451-9103. DOI: https://doi.org/10.1016/j.coelec.2018.01.002. URL: http://www.sciencedirect.com/science/article/pii/S2451910317301588.

[7] Michael M. Bobek, Daniel Krois, and Udo H. Brinker. "Induced Circular Dichroism of Cyclodextrin Inclusion Complexes: Examining the Cavity with a Bilateral Probe". In: *Organic Letters* 2.14 (2000). PMID: 10891214, pp. 1999–2002. DOI: 10.1021/ol005923d.

[8] T. Chen, S.Y. Li, D. Wang, M. Yao, and L.J. Wan. "Remote Chiral Communication in Coadsorber Induced Enantioselective 2D Supramolecular Assembly at a Liquid/Solid Interface". In: *Wiley Angewandte Chemie, GDCh* (Feb. 2015). DOI: https://doi.org/10.1002/anie.201410927.

[9] X. Li and M. Shapiro. "Communications: Spatial separation of enantiomers by coherent optical means". In: *The Journal of Chemical Physics* 132.4 (2010), p. 041101. DOI: 10.1063/1.3298585.

[10] Ulrich Knof and Alex von Zelewsky. "Predetermined Chirality at Metal Centers". In: *Angewandte Chemie International Edition* 38.3 (1999), pp. 302–322. DOI: 10.1002/(SICI)1521-3773(19990201)38:3<302::AID-ANIE302>3.0.CO;2-G.

[11] D. Parker, R. S. Dickins, H. Puschmann, C. Crossland, and J. A. K. Howard. "Being excited by lanthanide coordination complexes: aqua species, chirality, excited-state chemistry, and exchange dynamics". In: *Chem Rev* 102.6 (Feb. 2002), pp. 1977–2010.

[12] Helen C. Aspinall. "Chiral Lanthanide Complexes: Coordination Chemistry and Applications". In: *Chemical Reviews* 102.6 (2002). PMID: 12059255, pp. 1807–1850. DOI: 10.1021/cr010288q.

[13] Hiroshi Tsukube and Satoshi Shinoda. "Lanthanide Complexes in Molecular Recognition and Chirality Sensing of Biological Substrates". In: *Chem. Rev.* 102.6 (June 2002), pp. 2389–2404.

[14] D. Parker. "Excitement in f block: structure, dynamics and function of nine-coordinate chiral lanthanide complexes in aqueous media". In: *NCBI, Chem. Soc. Rev.* 33.3 (Mar. 2004), pp. 156–165.

[15] J.I. Bruce, D. Parker, S. Lopinski, and R.D. Peacock. "Survey of factors determining the circularly polarised luminescence of macrocyclic lanthanide complexes in solution". In: *NCBI* 14.7 (July 2002), pp. 562–7.

[16] J.I. Bruce, D. Parker, S. Lopinski, and R.D. Peacock. "Synthesis and characterisation of highly emissive and kinetically stable lanthanide complexes suitable for usage "in cellulo"". In: *NCBI, Org. Biomol. Chem.* 3.6 (Mar. 2005), pp. 1013–24.

[17] Jean-Claude G. Benzli. "Benefiting from the Unique Properties of Lanthanide Ions". In: *Accounts of Chemical Research* 39.1 (2006). PMID: 16411740, pp. 53–61. DOI: 10.1021/ar0400894. eprint: https://doi.org/10.1021/ar0400894.

[18] Sushobhan Ghosh and Partha Sarathi Mukherjee. "Self-Assembly of Molecular Nanoball: Design, Synthesis, and Characterization". In: *The Journal of Organic Chemistry* 71.22 (2006). PMID: 17064013, pp. 8412–8416. DOI: 10.1021/jo061311g.

[19] Kyung Seok Jeong, Young Shin Kim, Yun Ju Kim, Eunsung Lee, Ji Hye Yoon, Won Hwa Park, Young Woo Park, Seung-Joon Jeon, Zee Hwan Kim, Jaheon Kim, and Nakcheol Jeong. "Lanthanitin: A Chiral Nanoball Encapsulating 18 Lanthanum Ions by Ferritin-Like Assembly". In: *Angewandte Chemie International Edition* 45.48 (2006), pp. 8134–8138. DOI: 10.1002/anie.200603622. eprint: https://onlinelibrary.wiley.com/doi/pdf/10.1002/anie.200603622. URL: https://onlinelibrary.wiley.com/doi/abs/10.1002/anie.200603622.

[20] Ben L. Feringa, Richard A. van Delden, Nagatoshi Koumura, and Edzard M. Geertsema. "Chiroptical Molecular Switches". In: *Chemical Reviews* 100.5 (2000). PMID: 11777421, pp. 1789–1816. DOI: 10.1021/cr9900228.

[21] Elisa Murguly, Tyler B. Norsten, and Neil R. Branda. "Nondestructive Data Processing Based on Chiroptical 1,2-Dithienylethene Photochromes". In: *Angewandte Chemie International Edition* 40.9 (2001), pp. 1752–1755. DOI: 10.1002/1521-3773(20010504)40:9<1752::AID-ANIE17520>3.0.CO;2-W.

[22] Zhaohua Dai, Jennifer Lee, and Wenyao Zhang. "Chiroptical Switches: Applications in Sensing and Catalysis". In: *Molecules* 17.2 (2012), pp. 1247–1277. ISSN: 1420-3049. DOI: 10.3390/molecules17021247. URL: http://www.mdpi.com/1420-3049/17/2/1247.

[23] Ershad Mohammadi, Kosmas Tsakmakidis, Amir-Nader Askarpour, Parisa Dehkhoda, Ahad Tavakoli, and Hatice Altug. "Nanophotonic Platforms for Enhanced Chiral Sensing". In: *ACS Photonics* (May 2018). DOI: 10.1021/acsphotonics.8b00270.

[24] Mark R. Wilson and David J. Earl. "Calculating the helical twisting power of chiral dopants". In: *Journal of Materials Chemistry* 11 (2001), pp. 2672–2677. DOI: 10.1039/b103520g.

[25] Y. Zhao, A. N. Askarpour, L. Sun, J. Shi, X. Li, and A. Alú. "Chirality detection of enantiomers using twisted optical metamaterials". In: *Nature Communications* 8 (2017).

[26] Lisa V. Poulikakos, Prachi Thureja, Alexia Stollmann, Eva De Leo, and David J. Norris. "Chiral Light Design and Detection Inspired by Optical Antenna Theory". In: *ACS Nano Letters* 18 (2018), pp. 4633–4640. DOI: 10.1021/acs.nanolett.8b00083.

[27] VE Bochenkov and TI Shabatina. "Chiral Plasmonic Biosensors". In: *Biosensors (Basel)* 8 (4 2018).

AUTHORS

Valeria Loscrí is a permanent researcher of the FUN Team at Inria Lille-Nord Europe since Oct. 2013. From Dec. 2006 to Sept. 2013, she was Research Fellow in the TITAN Lab of the University of Calabria, Italy. She received her MSc and PhD degrees in Computer Science in 2003 and 2007, respectively, from the University of Calabria and her HDR (Habilitation a diriger des recherches) in 2018 from Université de Lille (France). Her research interests focus on emerging technologies for new communication paradigms such as Visible Light Communication and TeraHertz bandwidth and cooperation and coexistence of wireless heterogeneous devices. She has been involved in the activity of several European Projects (H2020 CyberSANE, FP7 EU project VITAL, the FP6 EU project MASCOT, etc.), Italian and French projects. She is in the editorial board of IEEE COMST, Elsevier ComNet, JNCA, IEEE Trans. on Nanobioscience. Since 2019, she is Scientific International Delegate for Inria Lille-Nord Europe.

Anna Maria Vegni (Senior member, IEEE) is a tenure-track Assistant Professor in the Department of Engineering at Roma Tre University (Italy), since March 2020. She received the Ph.D. degree in Biomedical Engineering, Electromagnetics and Telecommunications from the Department of Applied Electronics, Roma Tre University, in March 2010. She received the 1st and 2nd level Laurea Degree cum laude in Electronics Engineering at Roma Tre University, in July 2004, and 2006, respectively. In 2009, she was a visiting researcher in the Multimedia Communication Laboratory, directed by Prof. Thomas D.C. Little, at the Department of Electrical and Computer Engineering, Boston University, Boston, MA. Her research activity focused on vehicular networking supported by heterogeneous wireless networks and optical wireless communications. She a member of ACM and an IEEE Senior Member. In March 2018, she got the Italian Habilitation (Abilitazione Scientifica Nazionale) for Associate Professorship in Telecommunication Engineering. She is involved in the organization of several IEEE and ACM international conferences and is a member of the editorial board of IEEE Communications Magazine, Ad Hoc Networks, Journal of Networks and Computer Applications, Nanocomnet Elsevier journals, IEEE JCN, ITU J-FET and ETT Wiley journal.

TRANSMISSION AND DETECTION TECHNIQUES FOR INTERNET OF BIO-NANO THINGS APPLICATIONS WITH STATIC AND MOBILE MOLECULAR COMMUNICATION: A SURVEY

Amit K. Shrivastava[1], Debanjan Das[1], Neeraj Varshney[2], Rajarshi Mahapatra[1]
[1]Department of Electronics & Communication Engineering, International Institute of Information Technology Naya Raipur, [2]Wireless Networks Division, National Institute of Standards and Technology, Gaithersburg, MD 20899 USA

NOTE: Corresponding author: Neeraj Varshney, neeraj.varshney@nist.gov

Abstract – *Recent studies have shown that designing communication systems at nanoscale and microscale for the Internet of Bio-Nano Things (IoBNT) applications is possible using Molecular Communication (MC), where two or multiple nodes communicate with each other by transmitting chemical molecules. The basic steps involved in MC are the transmission of molecules, propagation of molecules in the medium, and reception of the molecules at the receiver. Various transmission schemes, channel models, and detection techniques have been proposed for MC in recent years. This paper, therefore, presents an exhaustive review of the existing literature on detection techniques along with their transmission schemes under various MC setups. More specifically, for each setup, this survey includes the transmission and detection techniques under four different environments to support various IoBNT applications: (i) static transmitter and receiver in a pure-diffusive channel, (ii) static transmitter and receiver in a flow-induced diffusive channel, (iii) mobile transmitter and receiver in a pure-diffusive channel, (iv) mobile transmitter and receiver in a flow-induced diffusive channel. Also, performances and complexities of various detection schemes have been compared. Further, several challenges in detection and their possible solutions have been discussed under both static and mobile scenarios. Furthermore, some experimental works in MC are presented to show realistic transmission and detection procedures available in practice. Finally, future research directions and challenges in the practical design of the transmitter and receiver are described to realize MC for IoBNT health applications.*

Keywords – Detector design, Internet of Bio-Nano Things, modulation schemes, molecular communication, micro-scale and nanoscale communication

1. INTRODUCTION

Molecular Communication (MC) is one of the fastest emerging research fields in the recent times where chemical signals are used to communicate between the transmitter and the receiver. It is worth noting that MC is a natural phenomenon and has been used by micro-organisms such as bacteria to communicate among themselves [1]. However, recent advancements in the field of nanotechnology enable the development of nano-scale devices that can also utilize MC to support several potential applications where conventional wireless communication using Electromagnetic (EM) waves is not feasible. Apart from this, biological cells can also be synthetically modified or generated to develop bio-nanomachines to support various applications within Internet-of-Bio-Nano Things (IoBNT) where the information can be easily encoded using the concentration, release time, and type of molecules.

It is important to note that since the capabilities of individual bio-nanomachines may be limited to simple sensing and actuation, the IoBNT [2] is envisioned to enable the interconnection of several bio-nanomachines to perform complex tasks. Applications of IoBNT include intra-body sensing and actuation, gene therapy, intra-body connectivity control, artificial blood cell production, and human body monitoring by an external healthcare provider [2]. This paradigm also poses several research challenges in terms of communication and networking using biochemical infrastructure while enabling an interface to the Internet. Development of efficient and safe techniques for information exchange, interaction, and networking between the biological nano-machines within the IoBNT, is one of the major research challenges. In this context, MC has attracted significant research attention to support several health applications. Some of the other important applications of MC i.e., Lab-on-a-Chip (LOC) devices [3], [4], Targeted Drug Delivery (TDD) [5], [6], and the diagnosis and mitigation of infectious diseases at the cellular level [7], [8], [9] are described below.

The detection of biomolecules for LOC has been proposed in [3] using the Radio Frequency inductance capacitance (RF LC) resonator. The principle behind the biomolecule detection was detecting the changes in the RF signal due to the permeability and the resistance of the biomolecule. For LOC application, a relay-assisted MC based on dielectrophoresis was proposed in [4] where the molecules propagate from the transmitter to the receiver under the influence of a periodic electric field generated inside the relay. In this work, the inter-relay segment is modeled using the transmission line technique in which the relay provides drift to the molecules in the direction of the intended receiver. In [10], a wearable susceptometer (on finger) for detecting magnetic nanoparticles has been

proposed. In this work, a nano-machine beneath the finger (inside body) could sense one type of molecule and release another type of molecule (i.e., magnetic nanoparticles), which can be detected by the wearable susceptometer. The principle behind this system is that the current through the coil changes if the magnetic nanoparticles pass through it. The equivalent circuit for this detector using the induction and the operational amplifier has also been presented therein.

A novel method was proposed in [11] to transmit the digitally encoded Deoxyribonucleic Acid (DNA) using the bacteria-based nano-networks. In this work, motile bacteria moved towards non-motile bacteria that stored the digital information using plasmid (a DNA molecule). The motile bacteria then conjugates with the non-motile bacteria to pick up the stored information. Finally, the motile bacteria deliver the information to another location. The movement of the motile bacteria was governed through a molecular positioning system containing trilateral beacons, emitting chemo-attractants.

For TDD applications, the authors in [5] proposed a method for target delivery of nano-sensors by using the bacteria-based coordination. Their proposed method utilized multi-hop communication along with two different chemicals for guiding the nano-sensors in a particular direction. This setup can be useful in TDD applications where drug delivery inside the cancerous tumor is required. Further, for TDD and monitoring the drug concentration, an implantable drug delivery system was proposed in [6] where the anti-cancer drug molecules were released by the transmitter towards the cancer cells that may form a lump or tumor. The drug molecules are assumed to propagate inside the Extracellular Space (ECS). For analysis purposes, spherical transmitter and receiver models are considered and the Channel Impulse Response (CIR) is derived and verified through particle-based simulation. In this work, the drug concentration profile at any point inside the tumor is also obtained by solving the convolution of the release rate and the derived CIR.

Furthermore, a scheme for reducing the effect of propagation delay in a simultaneous drug delivery system was proposed in [12], where a controller nano-machine sent signaling molecules to the drug-carrying nano-machines which could be at unequal distances from the controller nano-machine. Upon receiving the signaling molecules, the drug-carrying nano-machines were expected to release the drug molecules simultaneously. However, due to unequal distances from the controller nano-machine, the drug-carrying nano-machines could not release the drugs simultaneously. Apart from the TDD applications, various MC systems for health monitoring in IoBNT are also present in the literature. For example, the work in [8] proposed an MC-based health monitoring system which detects the biomarkers of heartattacks through the implanted nano-sensors. The nano-sensors were designed to sense the endothelial cells circulating in the body.

Also, the early detection of neurogenerative diseases such as Alzheimer's was presented in [13] considering the MC. This work considered an intercellular communication system where the calcium molecules were used as signaling molecules and their oscillation patterns were different in the astrocyte (biological tissue) of a person suffering from dementia in comparison to a healthy person. The difference between the other metrics such as the molecular delay, the channel gain as a function of distance (i.e., the number of cells between the transmitter and receiver), and the calcium oscillations were also presented. Further, a Microbiome-Gut-Brain-Axis IoBNT communication network was studied in [14]. Note that the MGBA refers to the bidirectional communication network between the brain and the gastrointestinal tract, which in general includes central, autonomic, and enteric nervous systems of the body, the gastrointestinal tract, and its microbiome (human microbiomes are responsible for launching the immune system, affecting inflammatory homeostasis and immune regulation). Also, electrical and molecular infrastructure to realize the communication through MGBA has been discussed in [14].

For monitoring the viscosity of blood, a wearable smart device was presented in [9] where a transmitter released molecules (in particular aptamers) inside the blood vessel through a needle and these molecules were received by the sensors. These sensors then sense the level of absorption and differentiate between the levels of absorption for high and normal viscosity scenarios. Further, a method for detecting cancer using mobile nano-sensors in the blood vessels was proposed in [15]. In this work, mobile nano-sensors are used to detect the presence of cancer biomarkers in the blood vessels. Finally, these mobile nano-sensors reach a fusion center (FC), which decides the presence or absence of an anomaly after detecting the concentration of biomarkers and comparing against the threshold using the Log-Likelihood Ratio (LLR) test. In all the above studies, the transmitter and receiver were either static or mobile under pure diffusive or flow-induced diffusive channels. Also, the scenarios and applications of MC systems differ in each of the works. Hence, a structured survey of transmission and detection under different scenarios and applications is required.

1.1 Related works

A survey on recent advancements in MC was presented in [16] in which microscale and macroscale communication along with modulation techniques, channel modeling, error correction codes, and simulation tools have been discussed. In [17], an MC-based nano-network has been studied for TDD applications. Particularly, the communication between different entities in a simple nano-network based TDD has been highlighted. Apart from this, several challenges in modeling the cardiovascular system, extracellular space, and cellular surface as a communication channel were presented. Apart from this, an

overview of transmitter and receiver nano-systems has been provided in [17]. A survey related to transmitter and receiver architectures has been published in [18], where some of the modulation, coding, and detection techniques have been discussed. In addition to these techniques, a Graphene-based transmitter and bio-Field Effect Transistor (bio-FET)-based receiver have been described to realize the MC based systems.

A cooperative drug delivery system was discussed in [19] where multiple mobile nano-machines communicate and deliver drugs in cooperative manner. More specifically, the leader nano-machines sense the presence of a target and release the attractant molecules in the environment. The follower nano-machines subsequently sense the attractant molecules and move towards the target for releasing drugs. Channel modeling for an MC-based system considering different types of transmitters (e.g., point, volume and ion channel based), and receivers (e.g., passive, fully absorbing and reactive) has been studied in [20]. A survey on biological building blocks for MC has been presented in [21] where the transmitter and receiver for different types of signaling particles (i.e., cations, neurotransmitters, and phosphopeptides) have been described. This work also discussed the biological approach for Inter-Symbol Interference (ISI) mitigation. Further, a survey on modulation techniques for molecular communication has been presented in [22]. In [22], the modulation techniques have been classified as concentration-based, type-based, release-time-based, spatial techniques and higher order modulations. Moreover, the metrics used for evaluating the performance of modulation schemes are also presented therein.

In contrast to these existing survey papers, this survey paper comprehensively focuses only on the transmission and detection techniques present in the existing literature under different channel conditions. It is worth noting that the modeling of the channel is different for different applications. Therefore, this paper also classifies the transmission and detection techniques based on the applications. Broadly we discuss four different scenarios as shown in Fig. 1: (i) static nano-machines communicating in pure-diffusive channel without drift or flow, (ii) static nano-machines under a flow-induced diffusive channel which experiences diffusion as well as drift, (iii) mobile nano-machines under a pure-diffusive channel, and (iv) mobile nano-machines under the flow-induced diffusive channel. Further, we discuss the transmission and detection for relay-assisted-based MC systems, cooperative or distributed-detection-based MC systems, MIMO-based MC systems, and machine-learning-based MC systems under all four possible scenarios described above.

The first static transmitter and receiver scenario is shown in Fig. 2, where nano-machines reach the cell surface receptor and can communicate over the cell surface. Such a configuration of nano-machines is present in the application of TDD over a cell surface [23], [24]. Here the drugs can be delivered to the malignant cell while minimizing the drug delivery to healthy cells. Fig. 3 shows the static nano-machines bound to the endothelial cells. However, the signaling molecules reach the receiver via drift and diffusion inside the blood vessel. This case can be found in the application of blood viscosity monitoring [9] and other health monitoring applications. In Fig. 4 the nano-machines and the signaling molecules are mobile and follow Brownian motion (free diffusion). This scenario can arise in the TDD application within the Extracellular Fluid (ECF) [25] as the movement of transmitter/receiver within ECF is governed by free diffusion. Fig. 5 shows that the nano-machines and signaling molecules are mobile under the influence of drift and diffusion inside the blood vessel. Mobile nano-machines inside the blood vessels can be used for early detection of biomarkers released by cancer cells in the blood vessels [15]. This is also a health monitoring application.

Also, different types of MC systems have been proposed in the literature in which the simplest case considers a single transmitter and receiver. An example of a single transmitter and receiver communicating in a flow-based channel is shown in Fig. 6. A wearable device with a transmitter and receiver is implanted over human skin for monitoring the blood viscosity. The transmitter releases molecules through a needle and these molecules pass through the blood vessel. On the other hand, the statistics of the received signal are monitored at the receiver since the diffusion coefficient of the released molecules varies with viscosity of blood which in turn change the statistics of the received signal. This setup can be useful for detecting the hyper-viscosity syndrome [9].

This simple case is further extended for the Multiple-Input Multiple-Output (MIMO) scenario to enhance the data rate by dividing the bit stream among multiple transmit antennas. As shown in Fig. 7, these MIMO-MC systems can also be used for improving the rate of drug delivery by using multiple transmitters and receivers. Here a transmitter (e.g., controller nano-machine) can sense the amount of drug required over the cell surface and sends a signal to the receiver for drug delivery [26]. The receiver carrying drug molecules can deliver the drug molecules at the cell surface after receiving the signaling molecules from the transmitter. This process can be faster if more than one transmitter and receiver are used for drug delivery. Further, note that in diffusion-based MC, the range of communication is limited due to the loss of molecules caused by the random Brownian motion. Therefore, to increase the range of communication, an intermediate relay node is introduced in between the transmitter and the receiver.

On the other hand, cooperative or distributed detection is proposed mostly for abnormality detection problems, where multiple receivers send their individual decision to a Fusion Center (FC) to make a global decision.

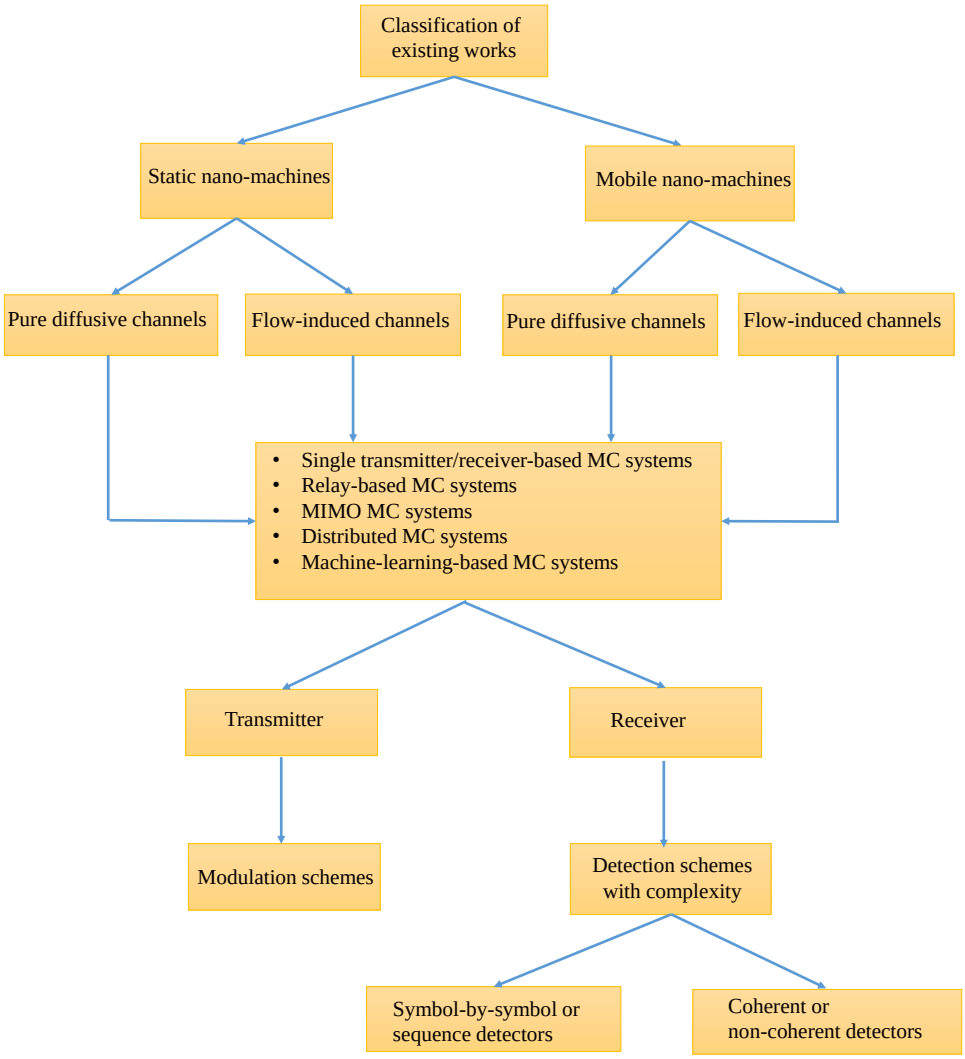

Fig. 1 – Various aspects of MC systems discussed in this paper.

An example of abnormality detection [15] has been shown in Fig. 8. This is a cooperative MC system for detecting the presence of a cancer cell. The cancer cell releases biomarkers inside the blood vessel. The concentration of biomarkers are sensed by multiple nano-sensors and finally the FC placed at a suitable location inside the blood vessel collects the reading of nano-sensors to decide whether cancer cells are present or not. For a global decision at FC, various decision rules at FC (e.g., AND, OR, and K out of N rules) have been proposed in the literature. In the AND rule, the FC makes a positive decision if all the receivers send a positive decision. In the OR rule, if any one of the receivers sends a positive decision then the FC makes a positive decision. In the K out of N rule, the FC makes a positive decision if K out of N receivers send a positive decision. Note that each of the decision rules results in different system performance.

Further, various machine-learning-based MC systems [27], [28], [29], [30] are also proposed in the literature. The advantage of machine-learning-based MC systems is that the receiver does not need any channel knowledge since it can directly learn from the data [31]. These machine learning based algorithms are particularly suitable for detection in a complex environment e.g., more than two receivers in 3-D medium.

Furthermore, every MC system discussed above is intended for different applications. An example showing the possible applications of the different MC systems in IoBNT has been shown in Fig. 9. In this example, if an abnormality detection system detects an abnormality such as cancer cells, it can send molecular signals to the bio-cyber interface. The bio-cyber interface can be a wearable device that can convert molecular signals to electromagnetic (EM) signals [17] and vice versa. The bio-cyber interface further sends the signal to an access point.

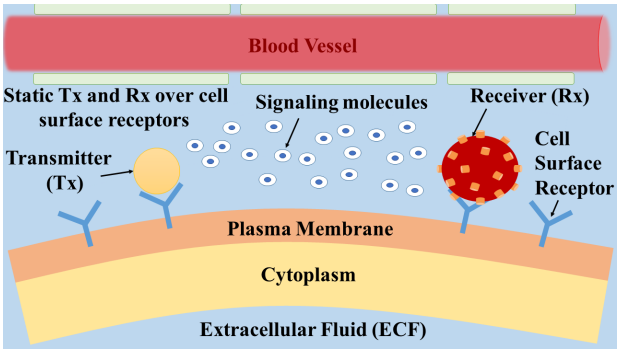

Fig. 2 – Schematic diagram of static transmitter and receiver over cell surface receptors.

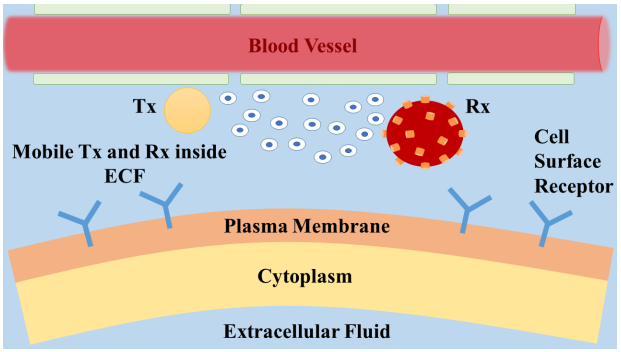

Fig. 4 – Schematic diagram of mobile transmitter and receiver inside extracellular fluid.

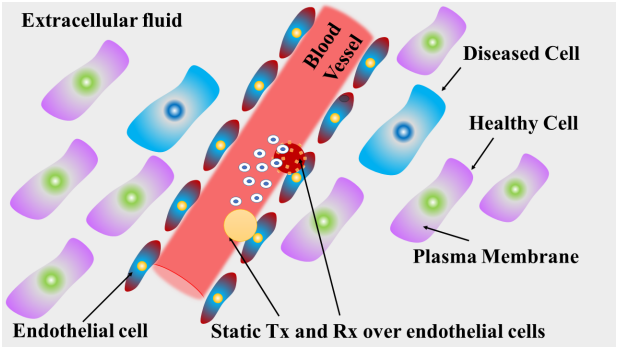

Fig. 3 – Schematic diagram of static transmitter and receiver bound to endothelial cells. Signaling molecules undergo drift and diffusion.

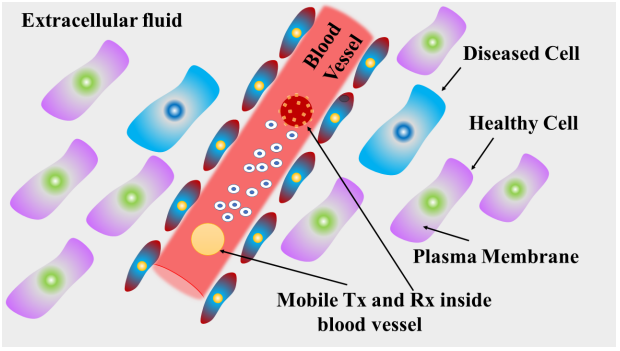

Fig. 5 – Schematic diagram of mobile transmitter and receiver inside the blood vessel. Transmitter, receiver, and signaling molecules propagate under the influence of drift and diffusion.

The signal reaches the medical personnel at a remote place through the Internet. The medical personnel can initiate the drug delivery process by sending appropriate commands to the drug delivery system inside the body. The signal propagates in the reverse order for this case. Further, different MC systems have to be used for the aforementioned scenario.

For example, cooperative MC systems are most suitable for abnormality detection and MIMO-MC systems can be used for drug delivery. The requirement of a router to send signals between different networks is also mentioned in [17]. Further, machine-learning-based MC system can be used at the FC and the bio-cyber interface as the computational complexity of machine learning algorithms may not be feasible to implement on the nano-machines with limited computational complexity. Irrespective of the complexity, this survey also covers the transmission and detection schemes proposed for all the aforementioned MC-based systems. Further, the performances and the complexities of some important detection schemes have also been discussed and compared in this survey.

The rest of the paper is organized as follows: Section 2 describes the transmission and detection techniques when communicating nano-machines are static. Section 3 discusses the transmission and detection techniques for mobile nano-machines. Transmission and detection used in some of the experimental works are presented in Section 4. Challenges of practical transmitter and receiver design as well as future research directions are presented in Section 5. Finally, Section 6 concludes the paper. Also, the complete list of acronyms used in this paper is given in Table 1.

Table 1 – List of Acronyms

Acronym	Description	Acronym	Description
Ach	Acetylcholine	MAP	Maximum A posteriori Probability
ANN	Artificial Neural Network	MC	Molecular Communication
ASK	Amplitude Shift Keying	MF	Matched Filter
AWGN	Additive White Gaussian Noise	MIMO	Multiple-Input Multiple-Output
BA	Biological Agent	MISO	Multiple-Input Single-Output
BCDA	Block Coordinate Descent Algorithm	MMC	Mobile Molecular Communication
BCZ	Bovine serum albumin protein conjugated ZnO nano-sphere	MMSE	Minimum Mean Square Error
BER	Bit Error Rate	MoSK	Molecule Shift Keying
BFGS	Broyden-Fletcher-Goldfarb-Shanno	mRNA	Messenger Ribonucleic acid
BSA	Bovine Serum Albumin	MSSK	Molecular Space Shift Keying
CDF	Cumulative Distribution Function	MTSK	Molecule Transition Shift Keying
CIR	Channel Impulse Response	NP	Neyman-Pearson
CNT	Carbon Nano-Tube	OOK	On-Off keying
CSI	Channel State Information	OSK	Order Shift Keying
CSK	Concentration Shift Keying	PAM	Pulse Amplitude Modulation
CTAT	Count-To-A-Threshold	PDF	Probability Density Function
CTMP	Continuous Time Markov Process	PDMS	Polydimethylsiloxane
DFE	Decision Feedback Equalizer	PMF	Probability Mass Function
DFF	Decision Feedback Filter	PNN	Probabilistic Neural Network
DNA	Deoxyribonucleic acid	PPM	Pulse Position Modulation
ECF	Extracellular Fluid	PSO	Particle Swarm Optimization
ECS	Extracellular Space	QMSSK	Quadrature Molecular Space Shift Keying
EGFETs	Electrolyte-Gated Field-Effect Transistors	RF LC	Radio Frequency inductance capacitance
FC	Fusion Center	RKHS	Reproducing Kernel Hilbert Space
FCM	Fuzzy C-mean	RNN	Recurrent Neural Network
FET	Field-Effect Transistor	RS	Reed-Solomon
FRET	Forster Resonance Energy Transfer	RTSK	Release Time Shift Keying
G-LOD	Generalized-Local Optimum Detector	SBRNN	Sliding Bidirectional Recurrent Neural Network
G-LRT	Generalized-Likelihood Ratio Test	SEP	Symbol Error Probability
HCl	Hydrochloric acid	SIMO	Single-Input Multiple-Output
IG	Inverse Gaussian	SINR	Signal-to-Interference plus Noise Ratio
ILI	Inter-Link Interference	Si-NW	Silicon-Nano Wire
IoBNT	Internet-of-Bio-Nano Things	SISO	Single-Input Single-Output
ISI	Inter-Symbol Interference	SNR	Signal-to-Noise Ratio
LED	Light Emitting Diode	SPIONs	Super-Paramagnetic Iron Oxide Nanoparticles
LLR	Log-Likelihood Ratio	SVM	Support Vector Machine
LM	Levenberg-Marquardt	SWCNT	Single-Walled Carbon Nano-Tube
LMS	Least Mean Square	TDD	Targeted Drug Delivery
LOC	Lab-on-a-Chip	TS	Takagi-Sugeno
LSTM	Long Short Term Memory	ZF	Zero Forcing

2. TRANSMISSION AND DETECTION WITH STATIC NANO-MACHINES

2.1 Static nano-machines in pure diffusive channel

2.1.1 Single transmitter and single receiver-based MC systems

In [32], authors employed an On-Off Keying (OOK) modulation scheme at the transmitter where a fixed number of molecules were transmitted for bit-1 and no molecules were transmitted for bit-0. For this setup, optimal and suboptimal detection schemes[1] were derived by maximizing the mutual information between transmitted and received symbols in the presence of ISI. In this work, perfect synchronization between the transmitter and the receiver is assumed to simplify the analysis. In contrast to OOK, the work in [33] considered a Molecule Shift Keying (MoSKmodulation scheme in which different types of molecules are sent to transmit different symbols. In this work, a linear and time-invariant model for signal propagation is assumed and the noise is modeled as the additive, uncorrelated, and non-stationary random variable with zero mean and variance dependent on the magnitude of the signal.

[1]In contrast to suboptimal detection scheme, optimal detection scheme requires a priori probability.

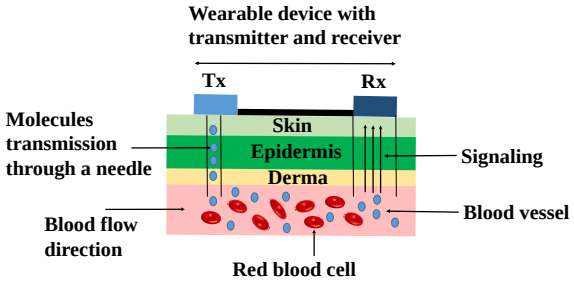

Fig. 6 – Wearable device for monitoring blood viscosity.

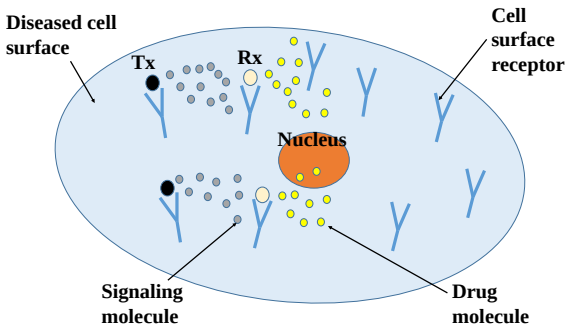

Fig. 7 – Drug delivery over a cell surface using MIMO-MC system.

A general block diagram of an MC system proposed in [33] has been shown in Fig. 10, where $y(t)$ is the received signal, N_{tx} is the number of transmitted molecules, $p(t)$ is the pulse shaping filter, $h(t)$ is the CIR, and $n(t)$ is the signal-dependent noise (other external noise sources can also be included). The received number of molecules is assumed to be binomial which is approximated as a Gaussian distributed random variable to derive the maximum likelihood detector. In addition to the maximum likelihood-based detector, a sequence detection scheme (i.e., Viterbi detector) is also derived since the channel with ISI adds memory to the signal which is similar to a convolutional encoder using the shift registers.

For improving the BER performance compared to [33], the authors in [34] introduced a noise whitening filter at the receiver for binary MoSK modulation-based transmission. In this work, the reception process was modeled as a Low Pass Filtering (LPF) operation where the LPF transfer function was derived using the ligand-receptor binding equation at the receiver. Moreover, the Brownian and residual noises corrupting the signal have been assumed to be signal-dependent. Finally, the system bit error rate performance is shown to improve by using a noise whitening filter.

The work in [35] derived an energy-based detector considering the binary Pulse Amplitude Modulation (PAM) based transmission using a square pulse instead of an impulse of molecules. For this setup, the mean and variance of the number of received molecules have been calculated by integrating the propensity function of concentration signal intensity over a symbol duration. Finally, at the receiver, the threshold-based detection was performed where the test statistic[2] was shown to be composed of a constant, two Normal random variables, and a Chi-square random variable. Further, in [36], binary and 3-ary PAM transmission schemes have been used. In this work, the detection at the receiver was carried out based on the response generated by the bacteria to the input molecular signals. Four different sampling strategies of the response were studied. These strategies were based on the total response, peak response, positive and negative slopes in which the BER for positive slope sampling was found to be the worst.

In [37], the performance of NP and matched filter (MF) detectors were analyzed for the detection of a nanobiosensor signal corrupted with thermal and shot noises. It is shown that these two detectors result in identical performance in the presence of thermal noise only. However, as the shot noise increases, the NP-based test outperforms the MF detector. Also, when the binary signals to be differentiated, are very close or farther from each other, both NP and MF detectors have identical performance otherwise the NP rule outperforms. Further, binary and quaternary ASK were used as the transmission schemes in [38] and the receiver based on an NP test was proposed. In addition to this, suboptimal detection schemes with reduced complexity were also reported.

On the other hand, OOK modulation and two different methods of detection based on pulse amplitude and pulse energy with fixed threshold have been proposed in [39]. In this work, analytical expressions of communication metrics such as pulse delay (i.e., peak time), pulse amplitude (i.e., the concentration at peak time), and pulse width (i.e., the time difference between two points when concentration falls to 50% of its peak value) were derived for the pulse amplitude-based detector. Similarly, the analytical expressions of pulse energy (i.e., the integral of concentration with respect to time) and pulse duration (i.e., the time when the energy becomes a specified fraction of total energy) have been derived for a pulse energy-based detector. It is observed therein that the pulse amplitude and energy-based detectors are suitable for a high transmission rate and large transmission distance, respectively.

In [40] the transmitter used a rectangular pulse of concentration. Four different methods of detection have been proposed at the receiver. More specifically, Maximum A posteriori Probability (MAP) and maximum likelihood-based sequence detection schemes were proposed, which maximize the joint Probability Density Function (PDF) of received samples and the transmitted bits, and use the Viterbi algorithm. Let b_j denote the information bit trans-

[2]The test statistic is derived by taking the logarithm of the likelihood ratio that uses the Neyman-Pearson (NP) formula.

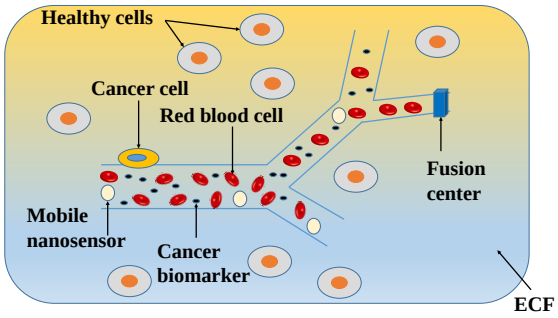

Fig. 8 – Cooperative MC system of mobile nano-sensors and fusion center using biomarker concentration inside blood vessels for detecting cancer cell.

mitted in the jth bit interval. The MAP sequence detection corresponding to the transmitted bit sequence of length $N+1$ can be done according to the following equation

$$\hat{\boldsymbol{b}}_{\boldsymbol{0}}^{\boldsymbol{N}} = \underset{\boldsymbol{b}_{\boldsymbol{0}}^{\boldsymbol{N}}}{\text{argmax}}\, f(\boldsymbol{y}_{\boldsymbol{0}}^{\boldsymbol{N}}, \boldsymbol{b}_{\boldsymbol{0}}^{\boldsymbol{N}}), \tag{1}$$

where $\hat{\boldsymbol{b}}_{\boldsymbol{0}}^{\boldsymbol{N}}$ represents the estimated sequence (of length $N+1$) for the transmitted sequence $\boldsymbol{b}_{\boldsymbol{0}}^{\boldsymbol{N}}$, and $f(\boldsymbol{y}_{\boldsymbol{0}}^{\boldsymbol{N}}, \boldsymbol{b}_{\boldsymbol{0}}^{\boldsymbol{N}})$ is the joint PDF of the received signal samples $\boldsymbol{y}_{\boldsymbol{0}}^{\boldsymbol{N}}$ and the transmitted bits $\boldsymbol{b}_{\boldsymbol{0}}^{\boldsymbol{N}}$, which can be expressed as

$$f(\boldsymbol{y}_{\boldsymbol{0}}^{\boldsymbol{N}}, \boldsymbol{b}_{\boldsymbol{0}}^{\boldsymbol{N}}) = \prod_{k=0}^{N} \mathrm{P}(b_k) \prod_{k=0}^{N} f(y_k | \boldsymbol{b}_{\boldsymbol{k-I}}^{\boldsymbol{k}}), \tag{2}$$

if b_k's are independent, I is the ISI length, $\mathrm{P}(b_k)$ is the PMF of the transmitted bit b_k, and $f(y_k|\boldsymbol{b}_{\boldsymbol{k-I}}^{\boldsymbol{k}})$ denotes the conditional PDF of y_k.

Further, in [40], a linear equalizer based on the Minimum Mean Square Error (MMSE) criterion and a nonlinear Decision Feedback Equalizer (DFE) were also proposed. Performance was evaluated for time-invariant and time-varying[3] channels. It is shown that the maximum likelihood-based detector performed better than DFE, and the MMSE equalizer performed the worst among all other detectors. On the other hand, different concentration levels of molecules for binary and quaternary Amplitude Shift Keying (ASK) transmission schemes have been proposed in [41]. At the receiver, a signal detection rule based on NP tests has been derived for both schemes. Performance of both detectors was evaluated with increasing ISI and BER was found to be lower in the case of binary ASK than the quaternary ASK transmission.

A method of ISI mitigation using enzymes in the environment was presented in [24]. For system setup, OOK at the transmitter and a single sample-based detector with a fixed threshold at the receiver were employed. In this work, a lower bound on the number of received molecules in the presence of enzymes was derived. Moreover, it was shown that ISI, as well as useful signals, reduce by using enzymes. For analysis purposes, the number of received molecules was shown to be binomial distributed and its approximation as Poisson distribution was shown to be more accurate than the Gaussian distribution when calculating the detection probability at the receiver.

Similar to [24], the work in [42] also used an OOK modulation scheme. However, the number of molecules released by the transmitter was modeled as a random variable whose mean was known to both transmitter and receiver. For signal detection at the receiver, a one-shot detector with three different signal processing schemes based on sampling, correlation (multiplying the received concentration by a correlation function which was constant or based on MF), and ISI cancellation (the difference between the peak concentration or concentration at symbol end time whichever is minimum and the concentration at starting time of the received concentration) were proposed. Each of the schemes results in a different test statistic. In this work, the ISI cancellation approach was found to perform better than the schemes based on sampling and correlation techniques.

In [43], a transmission scheme similar to Release Time Shift Keying (RTSK) was proposed to send a pattern of molecules based on different time-instants. For example, the pattern $\delta_{t,1} + \delta_{t,1.5} + 3\delta_{t,5}$ can be used for transmission of bit-1. As shown in Fig. 11, this pattern implies that one molecule is sent at $t = 1$ s and $t = 1.5$ s time-instant, and three molecules are sent at $t = 5$ s time-instant. In this work, transmission, diffusion of molecules, and reception were modeled using the Continuous-Time Markov Process (CTMP). For the reception, a MAP demodulator has been employed which maximizes the posterior probability that a symbol was sent given the history of ligand-receptor complexes formed at the receiver.

Further, the bit transmission based on the release time of the molecule was proposed in [44]. In [44], three different detection schemes based on the maximum likelihood detector, linear detector, and the detector based on the first arrival were considered. The propagation time of a particle was assumed to be Lévy distributed for a pure-diffusive channel and inverse Gaussian (IG) for a flow-induced diffusive channel. The performance of each detection scheme was evaluated for different propagation profiles where arrival time is modeled as (i) uniformly, (ii) exponentially, (iii) IG, and (iv) Lévy distributed random variable. Further, it is shown that the detection based on the first arrival achieved the performance close to the maximum likelihood-based detection if the noise density has zero mode[4].

Further, for reducing ISI, a novel transmission scheme based on Molecule Transition Shift Keying (MTSK) was

[3] Two different cases of time-varying diffusion coefficient were selected: i) $D(t)$=$2.2\times10^{-9}+0.8\times10^{-9}\cos(2\pi t)$ m^2/s, ii) $D(t)$=$2.2\times10^{-9}+0.8\times10^{-9}\cos(10\pi t)$ m^2/s. The channel variation is 5 times faster in the latter case.

[4] The value of a random variable where the PDF is maximum is defined as the mode.

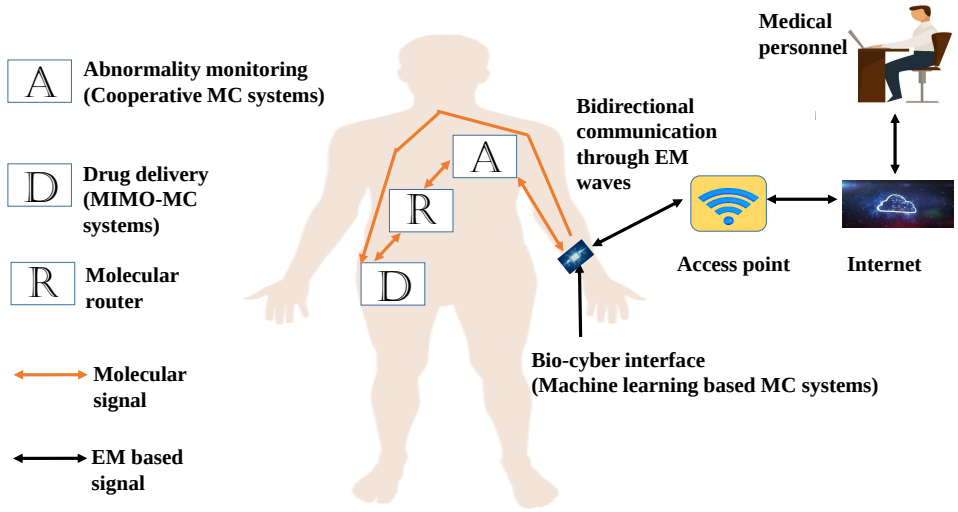

Fig. 9 – Different MC systems for different applications in IoBNT [17].

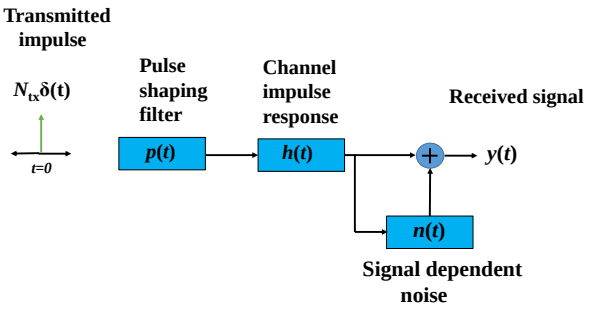

Fig. 10 – A general block diagram of an MC system.

proposed in [45], where type-A and type-B molecules were used for bit-1 and no molecule for bit-0. As shown in Fig. 12, in contrast to the OOK modulation scheme, type-B molecules were released for bit-1 before each bit-0 to reduce the effect of ISI. In addition to the MTSK modulation scheme, receiver-based ISI mitigation using a Decision Feedback Filter (DFF) was proposed where the computational complexity of DFF was independent of the number of filter taps. Further, the DFF is less complex than the conventional DFE and MMSE equalizers. The results showed that DFF significantly reduced the ISI from the received signal before comparing it with a threshold for detection. On the other hand, Impulse Transmission (IM) and pulse transmission (PAM) schemes were proposed in [46]. In this work, the energy-based detection using the binary hypothesis testing was proposed in the presence and absence of ISI. The results therein demonstrated that the IM transmission scheme has a higher probability of detection in comparison to PAM.

A low complexity adaptive threshold detection scheme has been proposed in [47] where the received signal in the current bit-interval was compared with the received signal in the previous bit-interval to decide in the favor of bit-1 or bit-0, which was transmitted using the OOK modulation scheme. Further, in [48], memory-less and memory-based receiver designs based on a MAP rule were proposed for OOK modulated symbols. In this work, the received signal PDF was considered as a Gaussian mixture model in presence of ISI and the detection threshold was evaluated iteratively by minimizing the probability of error. Furthermore, the authors in [49] considered rectangular pulse transmission using an OOK modulation scheme, where a non-coherent[5] detection was proposed which utilized the difference between the accumulated concentration of molecules in successive bit-intervals. This scheme also provides ISI mitigation capability. Further, this scheme gives better BER performance than the coherent MAP and MMSE schemes if channel memory length is restricted to 10.

In [50], an OOK modulation scheme has been employed at the transmitter, while asynchronous peak detection and energy detection schemes with and without decision feedback were proposed at the receiver. In an asynchronous peak detector without decision feedback, all the samples within a symbol interval were compared to find the maximum value, and the maximum value was compared against the threshold for detection. Further, in the case of detection with decision feedback, the expected ISI was subtracted from the total received signal and then asynchronous peak detection was performed. A similar procedure was considered for energy detection with and without decision feedback. It is shown that the energy-based detection with ISI cancellation outperforms the other proposed schemes.

A convex optimization problem that minimizes the error probability for determining the detection threshold

[5] In contrast to the coherent detector, a non-coherent detector does not require Channel State Information (CSI) at the receiver nano-machine.

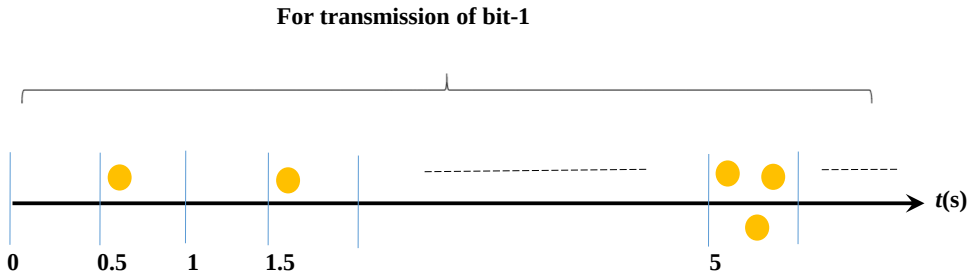

Fig. 11 – Modulation scheme similar to Release Time Shift Keying (RTSK), where the pattern $\delta_{t,1} + \delta_{t,1.5} + 3\delta_{t,5}$ is used for transmission of bit-1.

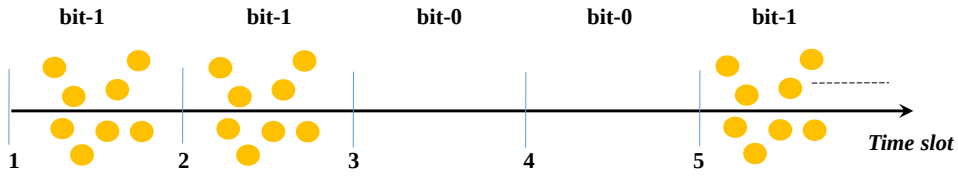

(a) Traditional OOK modulation based transmission

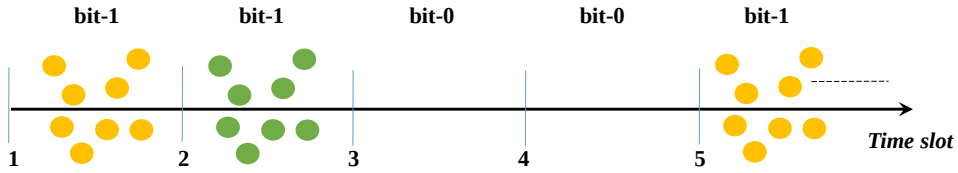

(b) MTSK modulation based transmission

Fig. 12 – MTSK modulation scheme, where two different colors represent two types of molecule.

was proposed in [51]. The logarithmic barrier function was used in optimization. Further, the Newton-Raphson method was employed for updating the threshold in each iteration. Authors in [52] proposed a non-linear and non-coherent signal detection scheme for amplitude modulated symbols, where a combination of different decision metrics was used for detection. The first decision metric was constructed using the convex property of the filtered signal, whereas the second decision metric was constructed using energy[6] difference between the successive symbols. In Fig. 13, the convex nature of the signal for bit-1 transmission can be observed. Further, in Fig. 14, the energy difference is positive if bit-1 is transmitted (e.g., energy difference of 2nd and 1st bit-intervals) and negative if bit-0 is transmitted (e.g., energy difference of 3rd and 2nd bit-intervals). Most importantly, the detection threshold at the receiver is obtained adaptively. The proposed scheme was shown to achieve BER performance

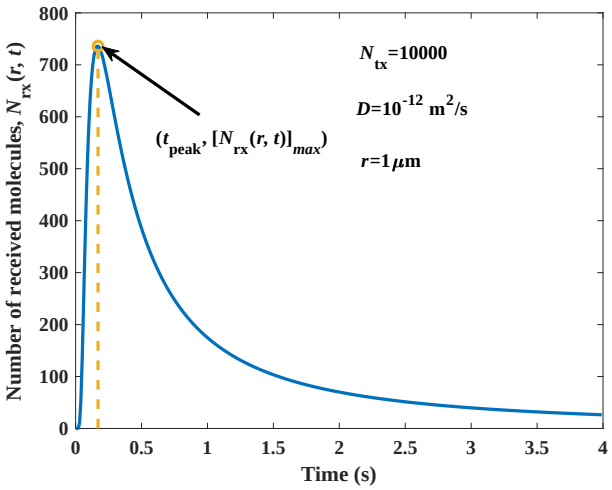

Fig. 13 – Received signal without noise considering MC-based transmission between two nano-machines.

[6]Energy in a bit-interval is defined as the sum of all samples within a considered bit-interval.

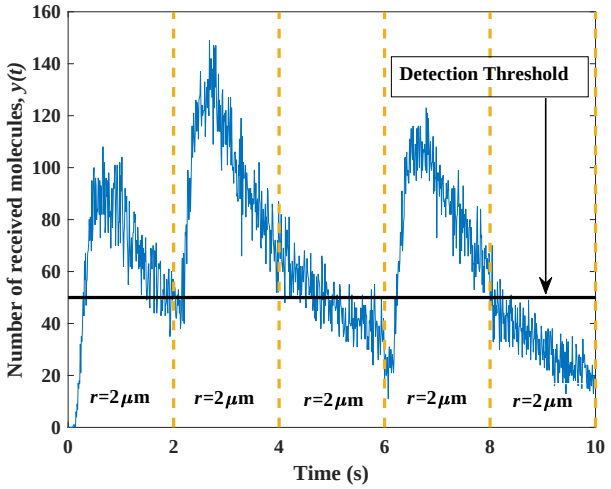

Fig. 14 – Received signal including noise and ISI for the transmitted sequence [1 1 0 1 0]. The maximum signal is above the threshold in 3rd and 5th-bit durations leading to incorrect detection.

identical to MAP and MMSE detection schemes at a significantly low Signal-to-Noise-Ratio (SNR) range.

In [53], OOK was used at the transmitter and an adaptive threshold-based detection in presence of noise and ISI was proposed at the receiver. Half of the total received molecules in the previous bit-interval was used as the threshold for detection in the current bit-interval. It is shown that the fixed threshold scheme does not work well since a varying number of molecules (depending on previous bit transmissions) due to ISI is added in the current bit-interval. A transmission scheme similar to [53] was also considered in [54]. However, at the receiver, the authors proposed energy-based and sampling-based detection schemes. For the energy-based detection scheme, an optimal time-interval was determined to minimize the error rate at the receiver. For sampling-based detection, the total number of samples and the sampling point were optimized to minimize the error rate.

The Pulse Position Modulation (PPM) scheme was proposed in [55] where molecules were released at the beginning and middle of the bit-interval in case of bit-1 and bit-0, respectively. A novel low complexity MAX detection scheme was proposed where the time at which the maximum concentration occurs is determined. In the case of bit-1 and bit-0, the maximum concentration occurs before and after the midpoint of the bit-interval, respectively. The performance of the MAX detector was close to the maximum likelihood detector except for scenarios that experience significant ISI. Further, similar to [55], the work in [56] also employed PPM modulation scheme at the transmitter. However, in contrast to [55], two asynchronous detectors were proposed in [56], where the first detection scheme approximated the observation vector to a linear weighted quantity and used a maximum likelihood estimate for detection. In the second method, only the first arriving molecule was considered for detection. Thus, the first element of the observation vector was set to one, and the rest of the entries were set to zero. Based on this observation vector, a maximum likelihood estimation was carried out at the receiver.

The Reed-Solomon (RS) coding scheme for MC was introduced in [57] to enhance the error rate performance at the receiver. In this work, the system using RS coding was shown to achieve better BER than the system which uses hamming codes. The work in [58] proposed constant weight codes along with a maximum likelihood sequence detection scheme at the receiver. This detection scheme was non-coherent, i.e., CSI free detection.

A soft detection scheme using subtraction and genetic amplifier circuits modeled via chemical reactions was presented in [59]. In this work, LLR was computed assuming noise as Poisson (or Gaussian) distributed random variable. It was found that BER performance under both Poisson and Gaussian models was identical thereby justifying the Gaussian assumption. A sequence detection scheme for OOK modulation has been proposed in [60]. Two-layered detection was performed where the first layer found the number of bit-1 in the received sequence of 7-bits. A different group of 7-bit patterns was divided into zones based on a logarithmic metric. Zones containing more number of bit-1 had a higher metric. Then the second layer found the locations of bit-1 in a specific zone by using a Pearson correlation metric. This process need not search all the 7-bit states thereby reducing the complexity.

On the other hand, a detector based on the derivative of the received signal considering the OOK-based transmission was proposed in [61]. More specifically, for detection of bit b_j at the receiver, all the derivative values within jth time slot of duration T were calculated using the received signal $y(t)$, and then the maximum of these derivative values was compared against the fixed threshold ω as shown below.

$$\hat{b}_j = \begin{cases} 1 & \text{if } \max \frac{y(kT_s) - y((k-1)T_s)}{T_s} \geq \omega, \\ 0 & \text{otherwise,} \end{cases} \qquad (3)$$

where $jN_s \leq k < (j+1)N_s$, sampling time T_s is defined as $T_s = T/N_s$ and N_s is the number of samples taken in a bit interval. Note that the threshold ω can be determined empirically, where minimum BER is achieved. Simulation results showed that the proposed detector performed better than the MAP detector at a high data rate or small bit duration.

Further, a preprocessing scheme based on higher order derivatives has been proposed in [62]. Note that higher order derivatives can be used if a high transmission rate is required compared to the first order derivative used in [61]. This is because of the fact that the peak time reduces with an increase in the derivative order. Also, higher order derivative processing offers better ISI mitigation since

the amplitude of the signal reduces quickly. However, higher order derivatives may amplify the noise. Hence the optimal derivative order is required for a trade-off between the noise amplification and ISI mitigation. For decoding, maximum likelihood sequence detection with reduced channel memory was used in [62].

In [63], a variant of OOK was proposed in which two different types of molecules were considered for transmission of bit-1, and no molecules were released for bit-0. For bit-1, the type-A molecule was transmitted at the beginning of a bit-interval, and the type-B molecule was transmitted at the peak time of the type-A molecule. Further, in [63], another modulation scheme was the Order Shift Keying (OSK) in which type-A molecule was transmitted at the beginning of a bit-interval, and the type-B molecule was transmitted at the peak time of type-A molecule for bit-1 and the order of molecules transmission was reversed for sending bit-0. These procedures reduced the ISI at the receiving nano-machine as type-A and type-B molecules were assumed to react together. The schemes proposed are shown in Fig. 15. In addition to these schemes, a suboptimal maximum likelihood detection scheme and ISI neglecting detection scheme were also proposed.

The authors in [64] proposed an optimal detection scheme based on Accelerated-Particle Swarm Optimization (A-PSO). This scheme used an acceleration factor to find the optimal weights $\boldsymbol{w} = [w_{jN_s}, w_{jN_s+1}, \cdots, w_{(j+1)N_s}]$, such that the error probability is minimum as described below.

$$\boldsymbol{w} = \underset{\boldsymbol{w}}{\operatorname{argmin}}\, P_e. \tag{4}$$

Finally, using these optimal weights, a weighted sum detector was employed at the receiver i.e., each sample within a bit-interval was multiplied by a weight and all the weighted samples were added to compare against the threshold θ for detection,

$$\hat{b}_j = \begin{cases} 1 & \text{if } \sum_{k=jN_s}^{(j+1)N_s} w_k y_k \geq \theta; \\ 0 & \text{otherwise}, \end{cases} \tag{5}$$

where $w_k \geq 0$. This detector was shown to perform better than the MF detector.

Further, a suboptimal detection scheme was presented in [65], where the CSI was modeled as a Gamma distributed random variable. A non-coherent decision feedback detection was also proposed therein, which utilizes statistical CSI. The proposed decision feedback detector considered a fixed detection window of size K where a constant CSI was assumed. Further, a blind CSI estimation-based detection was also proposed in which CSI estimates were found by averaging over the expected positions of bit-1 and bit-0.

In [66], two different detection schemes based on the maximum likelihood criterion were presented for a ligand-receptor type communication. The first technique considered the likelihood of observing bound receptor molecules given the current transmitted bit and the estimate of ISI bits. The other one considered the likelihood of observing the unbound time of receptors for detection. The latter technique experienced better BER performance because the bound state of receptors can provide little information when the receiver saturates due to the ISI.

Further, three different detection techniques based on the number of bound receptors, unbound time (around the sampling time) of the receptors, and bound time of the receptors were proposed in [67]. The detection based on the bound time of the receptors was better in performance than the other two schemes. In this work, an estimator based on the log-likelihood of the ratio of ligand and total concentration was also proposed for the detection. In [68], chemical reaction networks for detecting binary MoSK signals were proposed. In this work, sampling was based on transcription networks and the demodulation process used an integral feedback controller that senses whether a chemical signal is above the threshold or not. The demodulator output is used for detecting symbols using the biological XOR gate.

In [69], OOK with rectangular pulse shaping was used at the transmitter. The transmitted pulse was convolved with the CIR to obtain the received signal. Further, at the receiver, the detection process was carried out in three steps: (i) stochastic resonance-based nonlinear filtering (processing based on local transient features), (ii) calculation of the non-coherent metric, and (iii) threshold-based detection. The decision metric was constructed by adding the metrics of the convex property of the filtered signal, transient shape among the symbols, and the energy difference between the successive symbols.

The derivation of an event (e.g. presence of a cancer cell) detection probability was presented in [70], where the event was defined as the hitting of a single molecule at any one of the multiple receivers within a certain period. The detection probabilities were derived for both degradable and non-degradable molecules. In this work, the centers of the receivers were assumed to be distributed as a Poisson point process. Also, the number of molecules to be transmitted for a specified probability of event detection was derived.

Rectangular pulse-based OOK was used as the modulation in [71]. Further, a weighted sum method with optimal weights was proposed for detection and ISI mitigation at the receiver. Optimal weights were obtained by maximizing the Signal-to-Interference-plus-Noise Ratio (SINR) i.e., differentiating SINR with respect to weights and setting it equal to zero. Also, a block-wise data detection-based iterative method for ISI mitigation was proposed where the expected ISI was subtracted from the total received signal. Simulation results showed that the iterative method outperformed the weighted sum method for ISI mitigation.

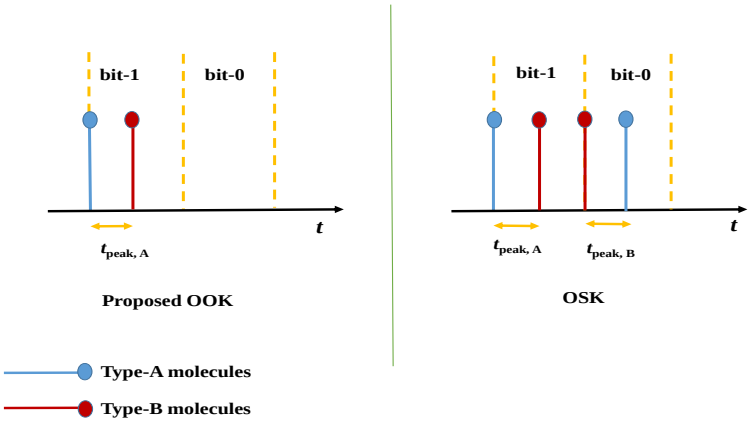

Fig. 15 – A variant of OOK and OSK modulation schemes.

For better ISI mitigation in comparison with [71], a scheme based on non-linear mapping was proposed in [72]. This scheme first calculated the peak time of the CIR and then the CIR before peak time was multiplied by a factor such that the peak value of the CIR should increase. Also, for ISI mitigation, the CIR after peak time was multiplied by a different factor to reduce the CIR tail. Further, for OOK-based transmission, a threshold-based detection was performed using signal energy as a decision metric. In this case, the threshold at the receiver was selected as the mean of the signal energies of the previous P bit-intervals. Note that this selection of threshold is valid only if P is significantly large. Simulation results demonstrated that this non-linear mapping scheme had better BER performance compared to the scheme proposed in [71].

In [73] CSK modulation similar to [74] was used at the transmitter. The detection was done by maximizing the Probability Mass Function (PMF) of the number of received molecules. A similar detection procedure was also presented considering the presence of an additional source. This additional source generated interference which was modeled using a uniformly distributed random variable for mathematical analysis. Also, an optimal detection interval was found, which minimized the error probability. It was shown that the optimal detection interval was less than the transmission bit-interval. Authors in [75] proposed coded modulation for binary OOK and 4-ary CSK. Moreover, at the receiver, threshold-less detection of data symbols was proposed since the threshold was set to zero due to the orthogonal coding scheme. However, the data rate was limited[7] for the proposed system due to channel coding.

Further, a generalized MoSK modulation was proposed in [76] to improve the data rate using less types of molecules compared to the conventional MoSK modulation [33]. The generalized MoSK can transmit $\lfloor \log_2(M!/(M_I!(M - M_I!)) \rfloor$ bits per symbol where M_I out of M types of molecules were required to send a symbol. While the MoSK scheme can only transmit $\lfloor \log_2(M) \rfloor$ bits per symbol using M types of molecules. For example, M=16 is required in MoSK while M=6 and M_I=3 is required in generalized MoSK to achieve a data rate of 4 bits per symbol. Apart from this, maximum likelihood detection considering the presence/absence of ISI from previous one symbol duration was used at the receiver. The simulation results demonstrated that the proposed modulation scheme with a maximum likelihood detector achieves better error performance compared to MoSK, CSK and D-MoSK schemes.

2.1.2 Relay-assisted-based MC systems

The work in [74] proposed CSK modulation where Q_1 molecules were emitted to transmit bit-1 and $Q_0 (< Q_1)$ molecules were emitted to transmit bit-0. This reduces the Peak-to-Average-Molecule Ratio that is suitable for nano-machines having limited storage. Further, an estimate-and-forward relaying scheme was proposed, which was shown to perform better than the decode-and-forward, and amplify-and-forward relaying schemes. In contrast to decode-and-forward relaying, this improvement arises since the estimate-and-forward relay transmits a soft decision. Also, the estimate-and-forward relay does not amplify the noise as seen in the amplify-and-forward relaying scheme. The maximum likelihood estimation of the number of transmitted molecules was performed at the intermediate relay node which was also used to find the error probability at the destination receiver. The optimization of the decision threshold in [74] was similar to the one proposed in [51].

The work in [77] considered an amplify-and-forward relaying scheme to increase the communication range. In this work, a detection scheme based on the MAP rule has been proposed for OOK modulated transmission. The detection threshold was determined by differentiating the

[7] Since the channel coding schemes append some coded bits to the information bits, the amount of information transmitted in a given time is reduced in comparison to the scenario which does not consider channel coding.

expected error probability with respect to the threshold and substituting the resulting expression equal to zero. Further, in [78], equal gain combining was used at the final destination which could sense the molecules sent by both the transmitter and the decode-and-forward relay node. In this work, the optimal position of the relay and optimal detection threshold at each of the receivers were derived by using a Block Coordinate Descent Algorithm (BCDA) which minimizes the end-to-end probability of error. Note that single type of molecules transmission at both the nodes causes ILI that in turn decreases the channel capacity. Thus, to improve the channel capacity of a decode-and-forward relay-assisted-based MC system, different types of molecules were used for transmission at the source and the relay in [79]. For decoding, a joint optimal detection threshold problem was also solved using the Gradient Descent algorithm, which minimizes the error probability with respect to thresholds at the intermediate relay and the final destination.

2.1.3 MIMO-based MC systems

The work in [80] proposed a binary ASK modulation scheme for the MIMO-MC system. For the proposed system, a Zero-Forcing (ZF)-based equalizer, as well as fixed and adaptive threshold-based detection schemes, have been proposed. Simulation results demonstrated that both ZF and adaptive threshold-based detectors had identical BER performance, however, the fixed threshold-based detection experienced the worst BER performance at the receiver.

Derivative-based detection for 2×2 MIMO-MC considering OOK modulation was proposed in [81]. In this work, the detection was based on the premise that when a bit-1 was transmitted the received signal had consecutive positive derivative values due to an initial rise in the number of received molecules, and in the case of bit-0, the received signal either had consecutive negative slope values or small positive values due to a weak rising edge caused by the Inter-Link Interference (ILI). Further, for detection in a severe ILI scenario, a ZF detection scheme was proposed in [82] assuming asymmetric topology (different number of transmit/receive antennas). The received signal was multiplied by the Moore-Penrose pseudo inverse of the channel matrix to counter the ILI and also to yield an estimate of the transmitted signal. Simulation results showed that ZF detection with signal sampling at peak times of respective receive antennas achieved lower BER than the ZF detection with signal sampling at the same time for all receive antennas.

A MIMO-MC system where a transmitter could send different types of molecules was proposed in [83]. In this work, optimizing the drug dosage (i.e., number of molecules emitted by the transmitter) was considered. For performance analysis, BER was evaluated for four different configurations i.e., Single-Input Single-Output (SISO), Single-Input Multiple-Output (SIMO), Multiple-Input Single Output (MISO), and MIMO. Further, the work in [84] derived approximate analytical expression of hitting probability considering the the presence of two fully absorbing receivers in 3-D medium. Based on this expression, authors demonstrated that a signaling molecule has higher hitting probability if two fully absorbing receivers at a distant location are used instead of a single fully absorbing receiver. Further, considering null and alternative hypotheses with OOK modulated symbols, the area under the ROC curve was derived to analyze the detection performance at both receivers. The insights developed in this work can be further used for designing the detection schemes with two receivers.

2.1.4 Distributed detection-based MC systems

The work in [85] considered cooperative detection where more than one receiver detects the OOK modulated transmitted bit and send their decision to an FC, which makes a global decision using the majority, AND, and OR rules. Simulation results demonstrated that the error probability for the majority rule was the lowest. In the noisy scenario, the OR rule performed better for high threshold values. A square pulse transmission based on OOK was proposed in [86] for abnormality detection. In this work, the abnormality detection scheme considered a two-tier structure, where several sensor nano-machines sensed the abnormality and sent their decisions to an FC to decide the presence or absence of abnormality. The NP criterion-based generalized likelihood ratio test was used for detection in the first tier and the OR-based fusion rule [85] was used at FC in the second tier.

Authors in [87] formulated a convex optimization problem to determine the threshold at each of the receivers and FC, which minimizes the expected end-to-end probability of error. The performance of the system was evaluated under perfect and noisy reporting by the receivers to the FC. A similar system of sensor nano-machines sending molecular signals to an FC for cooperative abnormality detection was proposed in [88]. In this work, two different transmission schemes emitting the same type of molecules and different types of molecules by sensors to the FC were considered. For detection, LLR was compared against the threshold to decide whether an abnormality is present or not. In addition to this, suboptimal detection schemes for different types of molecules were proposed, where only the maximum value inside the logarithm function was considered. Moreover, the maximal ratio combining of the sensor outputs and two-stage detection were also proposed therein.

Further, to reduce the number of samples and subsequently decision delay at the FC, a detection technique was proposed in [89]. This technique used a sequential average probability ratio test, which employed two different thresholds for binary hypothesis testing. A decision was made in favor of the first hypothesis if LLR was less than the lower threshold otherwise the second hypothesis

was chosen if LLR was greater than the upper threshold. If the LLR was in between the lower and the upper thresholds, then only one more sample was collected and LLRT was repeated again. A communication system similar to [85] was proposed in [90]. In this case, multiple receivers emitted the same type of molecules to convey information to the FC and at the FC, a simple detection based on a constant threshold was proposed for decoding information bits. This scheme was slightly inferior to the majority rule considered in [85], which however had low complexity.

A communication system based on several nano-sensors sending information to the FC was proposed in [91]. This system was for detecting the presence or absence of target (malignant tissue) considering the unknown secretion rate of biomarkers and unknown location of the malignant tissue. In this work, the LLR test was used at the nano-sensors for detection, whereas the Generalized-Likelihood Ratio Test (G-LRT) and Generalized-Local Optimum Detector (G-LOD) were proposed at the FC. In contrast to G-LRT, G-LOD was less computationally complex since it maximized the decision variable with respect to target location only. A MIMO communication system was proposed in [92] where multiple transmitters sent different molecules to the receivers. A signal processing scheme to find the global peak out of various impulse responses received at a single receiver was presented. Further, an NP test was performed at each of the receivers to decide in favor of bit-1 or bit-0. Finally, the central node i.e., FC collected all the individual decisions from each receiver and made the decision using K out of N rule i.e., if K or more than K receivers decide bit-1 then FC decides bit-1.

On the other hand, three different variations of maximum likelihood detection were proposed in [93]. In a perfect reporting scenario: i) the FC assesses each observation by the receiver to calculate the likelihood. This is termed as Full-maximum likelihood. ii) The FC assigns equal weight to all the samples within a bit-interval at each receiver. This is Limited-maximum likelihood detection. In noisy reporting, the FC adds all the observations that arrive from different receivers and finds the likelihood. All the receiver's use single molecule and decode-and-forward strategy to send information to the FC. Hence this technique was termed as SD-maximum likelihood. SD-maximum likelihood had the worst performance and the Full-maximum likelihood detection performed the best.

Abnormality detection and monitoring schemes using sensor networks with FC have been presented in [94]. Sensors used the OOK modulation scheme to transmit information to the FC. After collecting observations from all the sensors, the FC makes a final decision on the state of abnormality. Note that this system was based on a partially observable Markov decision process (non-homogeneous Markov model). In this model, the system state was defined as the location and time of occurrences of abnormalities at multiple sites, and how they propagate. Different situations in the system were mapped to some states of the Markov process. Further, the probability for each state was calculated and updated. Based on these probabilities, the changes in the system were monitored. More specifically, the spreading of changes in the environment (e.g. gradual tumor growth) was studied for monitoring. On the other hand, suboptimal detectors based on myopic policy were proposed. For detection, the aim was to minimize the delay in reporting to the FC. Furthermore, binary and non-binary stopping time scenarios were investigated.

In [95], two maximum likelihood detection schemes (single molecule type and multiple molecule types) at FC based on decode-and-forward relaying and an maximum likelihood detection scheme based on amplify-and-forward relaying was proposed. It was shown that the multiple molecule type scheme outperformed the other two proposed schemes for the considered cooperative MC system.

2.1.5 Machine-learning-based MC systems

An adaptive threshold-based detection using an Artificial Neural Network (ANN) was proposed in [27]. In this work, the Gradient-Descent algorithm was used for weight optimization. Moreover, elements of the output vector of the neural network were used as an adaptive threshold for detecting the bits, e.g., if the number of received molecules in jth bit duration was N_{rx_j} and o_j was the corresponding output of ANN then $N_{\text{rx}_j} > o_j$ was the rule for detecting bit-1 and vice-versa. In this work, BER performance better than state-of-the-art detectors was claimed at a reduced number of transmitted molecules.

In [96], curve fitting for the received molecules is done, where the Least Mean Square (LMS) method is used to update the polynomial coefficients. Moreover, the weighted sum of polynomial coefficients is used as the adaptive threshold for detecting the information in the presence of ISI. Further, Takagi-Sugeno (TS) fuzzy model has been employed, which can approximate complex nonlinear systems with fewer rules and higher modeling accuracy, and express the local dynamics of each fuzzy rule. The TS model, which is comprised of an optimized structure (the number of rules and inputs), optimized parameters for membership function. This strategy can minimize the error between the fuzzy output and the desired output. This work also proposed an ANN detector with two hidden layers, which combines the adaptive fuzzy threshold (in the first hidden layer) and polynomial approximation (in the second hidden layer).

Further, for a CSK-based modulation scheme, a deep learning-based detector was proposed in [28] that minimized the difference between detected and transmitted symbol vectors. The detector had 70 neurons in the first hidden layer and 10 neurons in the second hidden layer. This detector performed well at SNR values of 18 dB and

15 dB for ISI and ISI free scenarios respectively. Furthermore, to reduce the number of hidden layer neurons, a different architecture of the feed-forward ANN detector has been proposed in [29] where the training of a neural network was carried out for zero-bit, one-bit, and K-bit memory receivers using the number of received particles and the corresponding transmitted bit. The number of hidden layers was 10 with 5 neurons in each layer. Moreover, the Levenberg-Marquardt (LM) optimization algorithm has been used for updating the weights. The detection was based on whether the probability of observing a bit-1 given the number of received particles and previously estimated bits was greater or less than 0.5.

Further, two different detectors using feed-forward NN having one hidden layer of 16 nodes and RNN having one Long Short-Term Memory (LSTM) layer of 16 nodes at a fusion center in a distributed detection system was proposed in [97]. This system was proposed for a binary hypothesis testing to detect the presence or absence of an abnormality considering OOK-based transmission. These detectors were trained using the received signal at the FC from all the sensors and the corresponding hypothesis. Adam optimizer and Gradient Descent with momentum were used for feed-forward NN and RNN, respectively. These schemes avoid the requirement of an analytical channel model and CSI estimation particularly for distributed MC systems. It was shown that an RNN detector performed well than the feed-forward NN. Table 2 summarizes the modulation and detection techniques in static MC without drift in the channel.

2.2 Static nano-machines in flow-induced diffusive channel

2.2.1 Single transmitter and single receiver-based MC systems

In [98], a MAP rule-based signal detection scheme with ISI cancellation was presented for binary and M-ary transmissions. The ISI cancellation was achieved by subtracting the expected ISI molecules from the number of received molecules in the current bit-interval. In this work, positive drift velocity has been assumed and the PDF of first hitting time of a molecule is considered as IG. The maximum likelihood sequence detection along with two variations of a weighted sum detector i.e., equal weight detector and MF detector were proposed in [99] for different types of flow present in the environment. It is shown that the maximum likelihood sequence detection outperformed the other two detectors for most of the scenarios. However, both weighted detectors performed well if a mild flow was present opposite to the direction of information flow. Further, the work in [105] considered OOK modulation and proposed an MF detector which maximizes the SINR to calculate the optimal weights to be multiplied by each sample within a bit-interval. However, the selection of the detection threshold was not specified therein.

In [112], binary and 4-ary amplitude modulation schemes have been presented. Apart from these two schemes, authors also proposed a third modulation scheme where symbols 01 and 10 were considered as 1, and 00 and 11 were considered as 0 and 2, respectively. For each scheme, Symbol Error Probability (SEP) expression was derived considering maximum likelihood detection at the receiver. Authors demonstrated that in positive drift scenario, SEP for all three schemes decreased with an increase in flow velocity. Moreover, SEP performance of the third modulation scheme was in between the other two modulation schemes. Extending the previous work [99], the authors in [113] proposed Viterbi sequence detection to obtain a lower bound on the BER. Further, a family of weighted sum detectors (i.e., MF and equal weight detectors) were also proposed and their BER performances were compared with the Viterbi detector. Analytical expressions were also derived for different weighted sum detectors. Further, ISI mitigation by using the enzymes in the environment was also included to enhance the performance at the receiver.

In [100], an OOK modulation scheme was considered for transmission. However, for detection, the variance of the propagation time of molecules was calculated and subtracted from the current time to find the emitting time of the molecules. This detection process was asynchronous. In this work, the PDF of propagation time for superior vena cavae at 120 mm/s blood flow velocity and capillaries at 790 μm were shown. Further, for performance analysis, the error probability expression in terms of the Chi-square Cumulative Distribution Function (CDF) is derived. Finally, the authors showed that the variance of propagation time PDF was lesser in superior vena cavae than the capillaries. Therefore, the communication in superior vena cavae was slightly more reliable than in capillaries. In [101], MoSK modulation was used for transmission where N molecules of type-A and type-B were released for sending bit-1 and bit-0, respectively. A novel asynchronous detector named Count-To-A-Threshold (CTAT) was designed which counted both types of molecules and then decided in favor of a particular bit if the number of molecules corresponding to that bit was above a predefined threshold. In the presence of ISI, this detector resulted in a better performance than the simple binary detector, which compared the number of type-A received molecules with type-B received molecules.

The work in [103] proposed a binary timing-based modulation scheme for conveying the information between two communicating nodes. Also, three different detection schemes were proposed at the receiver. The first detection scheme was based on MAP criteria where a conditional PDF of output was maximized for detection; however, it was very complex as the multiplication of several IG distributions were required. The second technique was

Table 2 – Summary of transmission and detection in static MC without drift

Reference	Modulation	Detection	Symbol-by-symbol (Sbs)/Sequence (Seq) detector	Coherent/ Non-coherent detection	Complexity
[33]	MoSK	i) MAP detection without ISI ii) Viterbi detection with ISI	Sbs for i) and Seq for ii)	Coherent	i) High ii) Very high
[35]	Binary PAM	Log LRT for energy detection scheme	Sbs	Coherent	High
[37]	OOK	NP test (for separating very close binary signals) and MF detector	Sbs	Coherent	Low
[39]	OOK	Amplitude and energy detection with fixed threshold	Sbs	Non-coherent	Low
[34]	MoSK	MAP detection with noise whitening filter	Sbs	Coherent	High
[40]	Rectangular pulse based OOK	Adaptive receiver based on steepest descent algorithm for i) MAP detection ii) Maximum likelihood detection iii) MMSE equalizer iv) DFE	Seq for i), ii) and Sbs for iii), iv)	Coherent	i) Very high ii) High iii) Low iv) Moderate
[41]	Binary and quaternary ASK	Log LRT for binary and M-ary detection	Sbs	Coherent	High
[43]	Modulation based on chemical reaction rate	MAP rule using CTMP	Sbs	Coherent	Moderate
[45]	MTSK	DFF	Sbs	Coherent	High
[86]	OOK	Cooperative detection with GLRT at 1st tier and OR fusion rule at 2nd tier	Sbs	Coherent	High
[52]	Rectangular pulsed based OOK	Nonlinear adaptive threshold detection based on local geometry and energy difference of received signal	Sbs	Non-coherent	Low
[60]	Rectangular pulsed based OOK	Two layered detection for reducing the number of sequences to be searched	Seq	Non-coherent	High
[27]	OOK	ANN with Gradient-Descent optimization for weights	Seq	Non-coherent	High
[61]	OOK	Derivative based detection	Sbs	Non-coherent	Moderate
[63]	OOK and OSK	Suboptimal maximum likelihood detector and ISI neglecting detector	Sbs	Non-coherent	Moderate
[96]	OOK	ANN with fuzzy threshold detection and polynomial approximation	Sbs	Non-coherent	High
[29]	OOK	ANN detection with LM optimizer	Sbs	Non-coherent	Moderate
[71]	Rectangular pulse based OOK	Binary detection with iterative method of ISI mitigation	Sbs	Non-coherent	Moderate

average detection i.e., an average of the output was calculated then fed to the MAP detector for reducing the complexity of the receiver. In the third technique, first-order arrival time was used as the test statistic.

In [104], the transmitter emitted molecules using the OOK modulation scheme. In this work, the channel was similar to the vein and at the receiver, maximum likelihood sequence detection was used. The BER performance was evaluated in the presence of a periodic force generated due to heart pumping, where periodic force was modeled as a sinusoidal wave. Also, the performance evaluation was done considering different sinusoidal phases and the different size of transmitted molecules. Simulation results demonstrated that performance improvement can be achieved by the appropriate selection of release time of molecules and their size.

Synchronous and asynchronous sensing techniques were proposed in [114]. In this work, two different nanonetworks (each consisting of a single transmitter and receiver pair) were assumed inside a blood vessel. At the receiver, energy detection was employed for detecting the molecules. Besides, sensing based on long and short sensing windows in the case of synchronous sensing was also proposed. Moreover, the Bayesian approach was used to derive the likelihood ratio test in the case when the two networks were not synchronized. In [115], sampling time i.e., the number of samples taken at the receiver was optimized to minimize the error probability with OOK modulated transmission. For decoding, an energy detector was used at the receiver.

Table 3 – Summary of transmission and detection in static MC with drift

Reference	Modulation	Detection	Symbol-by-symbol (Sbs)/Sequence (Seq) detector	Coherent/ Non-coherent detection	Complexity
[98]	Binary and M-ary quantity based modulation	MAP detection	Sbs	Coherent	High
[99]	Binary PAM	Weighted sum detector	Sbs	Coherent	Low
[100]	OOK	Detection based on variance of arrival times of molecules	Sbs	Coherent	Moderate
[101]	MoSK	CTAT	Sbs	Coherent	Low
[102]	OOK	i) Optimal distributed detection using weighted Log LRT ii) K out of N fusion rule at FC	Sbs	Coherent	i) High ii) Low
[103]	Binary timing based modulation	i) MAP detection ii) Average detection iii) Order statistic detection	Sbs	Coherent	i) High ii) Low iii) Moderate
[104]	OOK	Maximum likelihood sequence detection	Seq	Coherent	Very high
[105]	OOK	MF detector	Sbs	Coherent	Low
[106]	OOK	SBRNN with ADAM optimizer	Seq	Non-coherent	High
[107]	MSSK and QMSSK	i) Maximum count decoding ii) Maximum likelihood sequence detection iii) Maximum likelihood detection	Seq for i), ii) and Sbs for iii)	Non-coherent in i) and Coherent in ii), iii)	i) Low ii) High iii) Moderate
[108]	Release time shift keying with convolutional coding	Viterbi detection with asymmetric metric	Seq	Coherent	High
[30]	OOK	Parzen-PNN based detection	Sbs	Non-coherent	High
[109]	OOK	Detection based on i) MAP criterion ii) Mean square error iii) Error probability minimization	Sbs	Non-coherent	i) Moderate ii) Low iii) High
[110]	Rectangular pulse based OOK	Sparse dictionary learning and Kernel LMS algorithm	Sbs	Non-coherent	High
[111]	CSK	Fuzzy C-means clustering	Sbs	Non-coherent	Moderate

The channel modeling for active and passive receivers was proposed in [116], where reception probability for a passive receiver and the PDF of first hitting time at an absorbing point located on an infinite plane were derived. In addition to this, the reception probability of a molecule was also derived for a receptor on an absorbing wall. Also, maximum likelihood sequence detection using hard decision Viterbi decoding was used at the receiver. In [122], maximum likelihood detection and the detection based of first arrival time of molecules were considered for release time modulation at the transmitter. Authors showed that for the scenarios when the number of released molecules is small, the detector based on first arrival performed very close to the maximum likelihood detector. On the other hand, if the number of released molecules are large, the maximum likelihood detector outperformed the first arrival-time-based detector.

The maximum likelihood sequence detection has been proposed for the M-ary transmission scheme in [123]. In this work, it is shown that the performance can be enhanced by using a shift register of $\log_2$M bits at the transmitter. The state of shift register determined the number of molecules to be emitted by the transmitter. A sliding bidirectional recurrent neural network has been proposed in [106] for sequence detection. This procedure can be useful when the channel model is unknown. In this work, a sliding window is used over which the estimated PMFs are averaged to find the final PMF.

Super-Paramagnetic Iron Oxide Nanoparticles (SPIONs) were used as the information particles in [124]. In this work, OOK modulation and simple threshold-based detection were used at the transmitter and receiver, respectively. Interestingly, an external magnetic field was used to guide the particles towards the receiver. Thus, the movement of particles was studied under different magnetic field gradients and the system performance was characterized in terms of error rate under different particle size distributions. It is worth noting that this scheme

Table 4 – Comparison of different modulation schemes proposed in the literature

Reference	Modulation	Abbreviation	Based on	ISI mitigation	Types of molecule
[32], [39], [24], [50], [61], [77], [117], [118], [119]	On-off keying	OOK	Concentration	No	1
[73], [74], [75], [120]	Concentration shift keying	n-CSK	Concentration	No	1
[33], [68], [101]	Molecular shift keying	n-MoSK	Molecule type	Medium	n
[35], [36]	Pulse amplitude modulation	PAM	Concentration	No	1
[55], [56]	Pulse position modulation	PPM	Molecule release time	No	1
[45]	Molecular transition shift keying	n-MTSK	Concentration and molecule type	Yes	2n
[63]	Order shift keying	OSK	Order of molecules	Yes	2
[107]	Molecular space shift keying	MSSK	Spatial position	Yes	1
[107]	Quadrature molecular space shift keying	QMSSK	Spatial position and molecule type	Yes	2
[121]	Depleted-molecular shift keying	D-MoSK	Molecule type	Yes	$n/\log_2 n$

can be useful in a negative drift environment where the molecules move away from the receiver. In [108], release time shift keying combined with convolution coding and Viterbi decoding based on asymmetric distance metric was proposed. The basic premise of employing this new metric was the asymmetry of the molecular channel, unlike the symmetric Additive White Gaussian Noise (AWGN) channel. In this work, encoders and decoders based on biological circuits were also proposed, where liposomes capable of receiving and sending molecules were used.

A release time-based modulation scheme was used in [125] for a microfluidic channel with drift. In this scheme, a molecule generator for synthesizing molecules and an oscillator to control their release time were used at the transmitter. On the other hand, the receiver used an oscillator that was not synchronized to the transmitter and NAND gate which could be designed using messenger Ribonucleic acid (mRNA) cells for generating any logical function. For decoding, the receiver employed a maximum likelihood-based detection scheme. The authors demonstrated that in the case of negligible background noise, the variance of the arrival time of molecules follows a non-central Chi-squared distribution. However, for the case when the background noise was present, the PDF of the sample variance of the arrival time was shown to be a linear weighted function of non-central Chi-squared distributions, where the weighting factors followed a hypergeometric distribution.

In [120], three-dimensional molecular cooperative communication system performance was analyzed under the flow-induced diffusive channel. In this work, binary CSK has been used at the transmitter and the equal gain combining was used at the receiver, which combined the signals received from the transmitter and the intermediate cooperative nano-machine. The LRT-based rule was used to determine the detection threshold at the cooperative nano-machine. Moreover, the detection threshold at the final destination was obtained by minimizing the end-to-end error probability using the Gradient-Descent algorithm. In addition to decision thresholds, the optimal number of molecules to be transmitted by the source and the cooperative nano-machine was also determined using the Gradient-Descent algorithm. A method for estimating various system parameters in the presence of drift was proposed in [126]. In this work, maximum likelihood estimation was used where the log-likelihood function was maximized to find the diffusion coefficient, the distance between the transmitter and the receiver, and the drift velocity of the medium. The Cramer-Rao lower bound as well as the mean-squared error in the estimation of different parameters were also determined.

A linear filter-based receiver design was proposed in [127] for the time-varying Poisson channel. In this work, a sampled average of expected observed molecules for bit-1 and bit-0 was found over all permutations of sequences. Then, the ratio of these sampled average values was calculated to evaluate filter coefficients. A worst-case filter design was also proposed therein where all previous bits were either 1 or 0. Finally, filter design based on linear programming was also discussed for a high transmission rate. A fuzzy clustering algorithm called Fuzzy C-mean (FCM) was proposed in [111] where each bit was detected based on its closeness to the center of a particular cluster. The metrics used in this work for calculating the center of the clusters were similar to the ones considered in [69].

2.2.2 Relay-assisted-based MC systems

An MC system based on decode-and-forward relaying was analyzed in [128] considering positive drift velocity. For communication and also to avoid interference at the intermediate relay node, type-A molecules were used by the transmitter in the first phase and type-B molecules were used by a relay node in the second phase. The error proba-

bility expression at the destination was derived which was shown to be a function of detection thresholds employed at the relay and destination nodes. Therefore, the authors determined: (i) the threshold at the relay node by using the likelihood-ratio test and (ii) the threshold at the destination by minimizing the end-to-end error probability. This end-to-end error probability minimization problem was formulated as a quasi-convex optimization problem, which was solved using the bisection method.

The work in [129] proposed an estimate-and-forward relaying scheme under the flow-induced diffusive channel. In this scheme, estimating the number of transmitted molecules at the relay node was done by maximizing the joint PDF of all observations. The Newton-Raphson method was used for this purpose. Moreover, the analytical expression of error probability was derived considering maximum likelihood and energy detectors at the receiver. Simulation results demonstrated that the decode-and-forward relaying achieves low BER if the relay is located close to the source. On the other hand, estimate-and-forward relaying works better if the relay is located close to the destination. The work in [109] considered an amplify-and-forward relaying scheme to increase the range of communication. Three different detection techniques were presented considering OOK-based transmission. In particular, the detection based on mean-squared error, the detection based on MAP, and the decision rule which minimized the error probability were considered.

2.2.3 MIMO-based MC systems

In [130], the MISO system has been considered where multiple transmitters were assumed to send information in different time slots using OOK modulation. Apart from ISI, ILI was also considered while analyzing system performance. In this work, symbol duration and the number of transmitted molecules were jointly optimized. For this purpose, multi-objective optimization was transformed to a single objective optimization by using the weighted sum method. This system was claimed to be useful for drug release management where the requirement of various drugs in different dosages was present.

Various index modulation schemes utilizing antenna separation were proposed in [107]. The first scheme considered Molecular Space Shift Keying (MSSK) modulation, where the transmitter uses each of its antennas to transmit different bit-streams. The second scheme considered Quadrature Molecular Space Shift Keying (QMSSK) where two different MSSK modulators were used at the transmitter and each modulator sent a different type of molecule thus providing channels orthogonal to each other. The schematic representation of both MSSK and QMSSK schemes are given in Fig. 16. Also, a combination of MSSK and QMSSK was proposed as the third modulation scheme. Three different detection schemes i.e., maximum-count decoding, maximum likelihood sequence detection, and symbol-by-symbol maximum likelihood detection were studied.

In maximum-count decoding, one receiver antenna index is found that receives the maximum number of molecules. Corresponding to that antenna index, an n-bit sequence is decoded where $n = \log_2(n_t)$ and n_t is the number of transmit antennas. In maximum likelihood sequence detection, the likelihood function corresponding to a particular symbol sequence is maximized. Towards this, the maximum likelihood sequence detector generates the trellis to obtain the likelihood of n_r^L antenna index vectors, where n_r and L represent the number of receiver antennas and channel memory length, respectively. On the other hand, the symbol-by-symbol maximum likelihood detection decodes the symbol by maximizing the sum of likelihood functions at each of the receiver antennas.

2.2.4 Distributed detection-based MC systems

A distributed detection scheme was proposed in [131] and [102], where many sensors sent molecules to an FC to decide the presence or absence of a biological agent (BA). In this work, the emission by the BA was modeled as the Kolmogorov-Feller diffusion process (colloidal Brownian motion under drift). The weighted log-likelihood ratio test was the optimal fusion rule for binary hypothesis testing. This rule is called the Chair-Varshney rule under both the NP and Bayesian framework. Further, a suboptimal fusion rule was also presented therein. Event detection in anomalous diffusion with drift was studied in [132] for an FC-based distributed nano-network. Considering OOK modulated transmission, the detection at FC was carried out using the binary hypothesis testing with LLR. In this work, time-slot optimization based on reinforcement learning was also proposed to increase the throughput of the network.

2.2.5 Machine-learning-based MC systems

High-dimensional metric combining was proposed in [30] for a non-coherent detection scheme. In this work, the first metric was constructed using the rising edge property of the signal, the second metric was the minimum inflection considering successive time slots and the third metric was the energy difference in successive time slots. At the receiver, the sum of these metrics was used for detection, which was shown to be insensitive to ISI and imperfect synchronization. Parzen-probabilistic Neural Network (PNN) was trained using the high-dimensional metric and corresponding symbols to obtain the approximate likelihood PDFs instead of exact likelihood PDFs for detection. Also, Parzen-PNN was claimed to be less complex than the back-propagation based ANNs and radial basis function-based neural networks.

A non-linear equalizer, which mitigates ISI and counters the non-linearity of the channel has been proposed in [110]. In this work, lower-to-higher dimensional mapping was carried out using a machine learning algo-

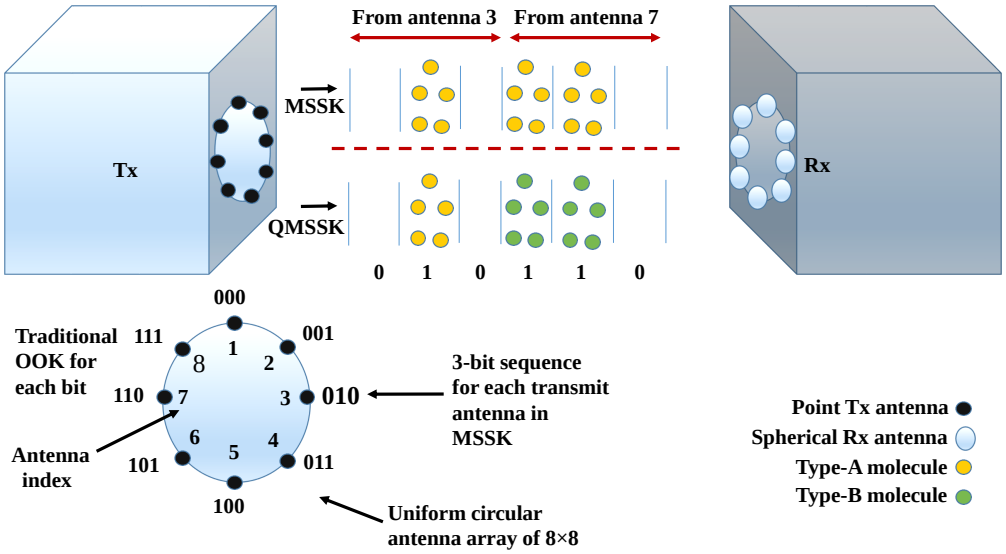

Fig. 16 – MSSK and QMSSK modulation schemes. In n_t-QMSSK scheme, first $\log_2 n_t$ bits sent using type-A molecules and last $\log_2 n_t$ bits sent using type-B molecules. $n_t = 8$ is used.

rithm, Reproducing Kernel Hilbert Space (RKHS). Moreover, sparse dictionary learning and the Kernel LMS algorithm were used by the receiver for detection. Also, the stochastic Gradient-Descent approach was used for updating the weights.

2.3 Performance and complexity comparison of different detection techniques for static MC

If N_s denotes the total number of samples taken by the receiver in a bit interval then the computational complexity of the linear MMSE method is $O(N_s^3)$. The complexity of the coherent MAP method [40], [98] is $O(2^{N_s})$. The derivative-based detector [61] offers less complexity and better BER than the MAP detector [40]. Further, the non-coherent detector based on concentration difference in [49] has a computational complexity of $O(N_s^2)$. Furthermore, the non-linear detector in [69] offers less computational complexity than the coherent MAP and MMSE detectors. With the channel coding scheme used in [58], the complexity of maximum likelihood sequence detection is $O(K\log(\log(S)))$ where K is the codeword length and S is the number of available symbols at the transmitter. To reduce the complexity of decoding the convolutional codes, Viterbi detector with asymmetric distance metric has been proposed in [108]. The complexity of the receiver in [75] is $O(K/2)$.

Both decision feedback and the blind detectors had a linear complexity in n in [65] but the blind detector is less complex than the decision feedback detector since it does not needs the calculation of the complex decision metric and the statistical CSI. Here n denotes the sequence length to be decoded. The CSI free detector proposed in [69] gives a complexity of $O(SN_s)$. The MSSK modulation helps to mitigate the ILI while the QMSSK mitigates ISI significantly in MIMO systems [107]. Further, a simple maximum count decoding introduced in [107] offers less computational complexity than other existing detection schemes for MIMO systems. Also, the complexity of estimate-and-forward relaying is the highest but it gives improved performance than decode-and-forward, amplify-and-forward relaying. The complexity of decode-and-forward relaying increases with the modulation order [74] while amplify-and-forward relaying offers the least computational complexity.

Further, the non-linear receiver based on sparse dictionary learning and the Kernel LMS algorithm [110] gives a complexity of $O(|D_m|)$ where $|D_m|$ is the number of observations present in the dictionary at convergence. Furthermore, a low complexity detection $\approx O(N_s^2)$ was proposed in [72]. In [111], the non-coherent detection based on Fuzzy-C means clustering gives a computational complexity of $O(SN_k)$ that is significantly less than the coherent MAP detection. Here N_k is the number of data points in a cluster. Time complexity of the ANN based detector proposed in [27] was shown as $O(\sum_{i=1}^{d} n_{i-1} s_i^2 f_i m_i^2)$ where i is the index of a layer, d is the number of layers, n_{i-1} is the number of input channels of the ith layer, s_i is the spatial size of filter, f_i is the number of filters in the ith layer, and m_i is the spatial size of the output feature. Further, in the Parzen-PNN technique proposed by [30], the complexities related to computation, time and storage are $O(dN_s)$, $O(d)$, and $O(dN_s)$, respectively. Here, d denotes the dimension of the metrics and $d = 3$ was used in [30]. The Parzen-PNN-based detector is less complex than the ANN-based detectors. Table 3 summarizes the modulation and detection techniques in static MC with drift in the channel.

Further, Table 4 compares the various modulation schemes in terms of their ISI mitigation capability and the types of molecules required. In traditional OOK, no ISI mitigation is possible while the MoSK modulation suppresses the ISI moderately. The types of the molecule required in MoSK increase with the modulation order n. The MTSK [45] modulation also mitigates the ISI but the types of the molecule required are larger than MoSK. Further, OSK [63] has a good ISI mitigation capability and the types of molecules required are only 2. D-MoSK [121] is a modified version of MoSK modulation that needs fewer types of the molecule than MoSK for a given modulation order. Also, MSSK and QMSSK [107] modulations use antenna separation to suppress the ISI and the ILI, and the types of the molecule required are less than most of the modulation schemes.

2.4 Challenges in detection and possible solutions

2.4.1 Noise and ISI in diffusive MC channel

The major challenge in detection arises due to noise and ISI experienced in the diffusing MC channel even for the static scenario where the distance between transmitter and receiver is constant. The number of received molecules $N_{\text{rx}}(r,t)$ at time t and at a distance r from a point transmitter is given by [133]

$$N_{\text{rx}}(r,t) = \frac{N_{\text{tx}} V_{\text{rx}}}{(4\pi D t)^{3/2}} e^{-r^2/4Dt}, \qquad (6)$$

where N_{tx} represents the number of transmitted molecules, V_{rx} is the volume of the receiver, D is the diffusion coefficient of a signaling molecule. Since the distance r between the communicating nano-machines is constant, the time at which $N_{\text{rx}}(r,t)$ is maximum, can be obtained by differentiating *(6)* with respect to t and set it equal to zero, as

$$t_{\text{peak}} = \frac{r^2}{6D}. \qquad (7)$$

Also, the peak amplitude can be obtained by substituting *(7)* in *(6)*

$$[N_{\text{rx}}(r,t)]_{\max} = \left(\frac{3}{2\pi e}\right)^{3/2} \frac{N_{\text{tx}}}{r^3}. \qquad (8)$$

It can be observed from *(8)* that the peak amplitude is independent of the diffusion coefficient D; however, varies inversely as the third power of distance r. For the case when r and D are constant, and the noise and ISI are absent, as shown in Fig. 13, then detection at the receiver can be easily performed by sampling at a fixed peak time t_{peak} and comparing $N_{\text{rx}}(r, t_{\text{peak}})$ against a threshold.

The threshold can be obtained by applying MAP-based rule [80] to the PDF of the received signals, as shown in Fig. 17. According to the MAP-based rule, the optimal threshold required for detection in jth bit-interval for Gaussian distributed signals is given by

$$\lambda_j = 0.5\frac{\mu_{j1} + \mu_{j0}}{\mu_{j1} - \mu_{j0}}\sigma^2 \ln\left(\frac{\text{P}(b_j = 1)}{\text{P}(b_j = 0)}\right), \qquad (9)$$

where σ^2 is the AWGN variance. Further, for Poisson distributed signals, the detection threshold in jth bit-interval [133] can also be obtained by substituting PDF/PMF equations in LRT expression (shown in Fig. 17) as

$$\lambda_j = \frac{\ln\left(\frac{\text{P}(b_j=1)}{\text{P}(b_j=0)}\right) + \mu_{j1} - \mu_{j0}}{\ln(\mu_{j1}) - \ln(\mu_{j0})}. \qquad (10)$$

In *(9)* and *(10)*, the quantities μ_{j1} and μ_{j0} denote the mean of received signals corresponding to the transmission of bit-1 and bit-0, respectively. The probabilities $\text{P}(b_j = 1)$ and $\text{P}(b_j = 0)$ represent the a priori probabilities for bit-1 and bit-0, respectively. For the case when the noise and ISI are present, as shown in Fig. 14, sampling at t_{peak} can cause incorrect detection. The received signal including ISI (for OOK at transmitter) is given as

$$y(t) = \sum_{j=0}^{\infty} b_j N_{rx}(r, t - jT_b) + n(r,t), \qquad (11)$$

where $b_j \in \{0,1\}$ is transmitted bit in jth bit-interval, T_b is the bit duration and $n(r,t)$ is the signal dependent noise whose variance is given as [39]

$$\sigma^2[n(r,t)] = \frac{3}{4\pi r_{\text{rx}}^3} N_{\text{rx}}(r,t), \qquad (12)$$

where r_{rx} is the radius of the receiver.

Fig. 14 shows the received signal perturbed by the noise and ISI for the transmitted bit sequence [1 1 0 1 0]. In the 3rd and 5th bit-intervals the transmitted bit was 0, but the maximum signal in those bit-intervals is above the threshold that lead to incorrect decoding if we employ an asynchronous peak detector. In the MC channel, the noise can be filtered out, as shown in [34] and maximum likelihood sequence-based detection can be used at the receiver to enhance the system performance under ISI. Also, MMSE equalizer and DFE can be considered for ISI mitigation [40, 45]. It is worth noting that these equalizers are less complex than the maximum likelihood sequence-based detection. Moreover, the detection in the presence of time varying diffusion coefficient[8] can also be done by using a channel estimator proposed in [40].

2.4.2 Unknown channel model

If the channel model is not known at the receiver then non-coherent detection schemes such as [52] can be employed, which relies on the local geometry of the received signal and the energy difference between received signals

[8] A time-varying diffusion coefficient can exist in multilayered channels such as alveolar-blood barrier [134].

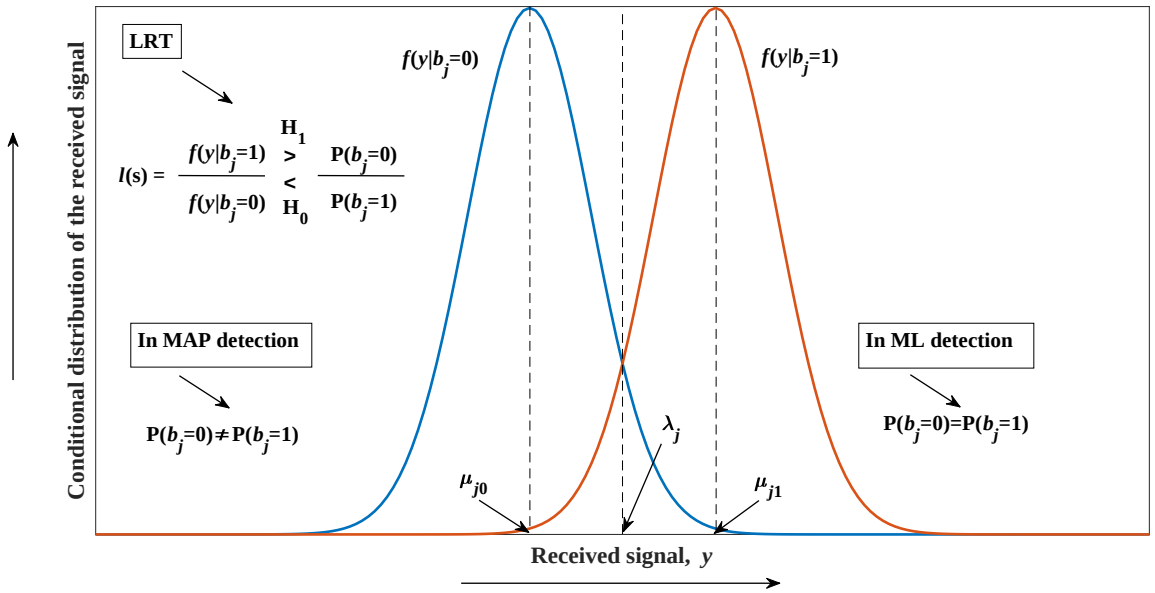

Fig. 17 – Conditional distribution of the received signal.

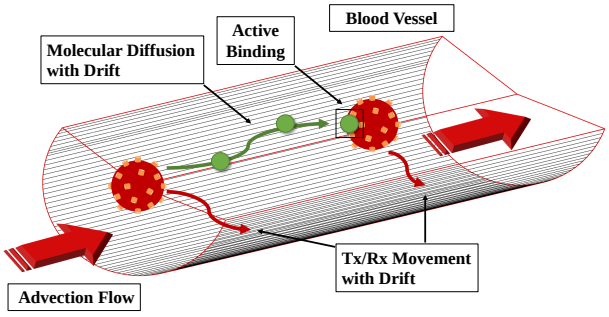

Fig. 18 – Mobile nano-machines under drift and diffusion inside the blood vessel.

in consecutive bit intervals. Further, ANN-based detectors can also be very robust [106] under unknown channel conditions. These detectors can be trained on the transmitted bit sequence and the corresponding received signal or features extracted from the received signal. Also, unsupervised clustering [111] based on a fuzzy clustering algorithm can be useful in unknown channel conditions.

3. TRANSMISSION AND DETECTION WITH MOBILE NANO-MACHINES

This section presents various transmission and detection schemes for mobile nodes. Performance and complexity comparison of the detection schemes are also discussed. An illustration of mobile nano-machines inside the blood vessel is shown in Fig. 18.

3.1 Mobile nano-machines in pure diffusive channel

3.1.1 Single transmitter and receiver-based mobile MC systems

A single sample detector at a fixed sampling time in each bit-interval was proposed in [117] for diffusion-based MMC, where the OOK modulation scheme was considered at the transmitter. In this work, dynamic CIR was modeled by using the effective diffusion coefficient value[9] in the expression of static CIR. No noise and ISI were considered while analyzing the system performance in terms of error rate. The error probability of the order of 10^{-4} was obtained in the case of the low diffusion coefficient of the transmitter (i.e., 10^{-12} m^2/s). However, an increase in the diffusion coefficient by 100 times led to degradation in BER performance by approximately 100 times indicating that the fixed sampling time does not work well for MMC.

A non-coherent detection scheme based on the local convexity of the received signal has been proposed in [135]. In this work, the received signal was filtered using a moving average filter. Three convexity metrics have been found and added together to yield the final decision metric. This decision metric was compared with a threshold to decide in favor of bit-1 or bit-0. Note that the convexity metric was higher in the case of bit-1. Also, the upper and lower bounds on the detection threshold were evaluated. Finally, the authors showed that the complexity of the convexity-based detector was lower than the MAP and MMSE detection schemes, however, the proposed detection scheme achieved the identical BER values as the MAP and MMSE detectors at a higher SNR regime.

[9]Effective diffusion coefficient is calculated as the sum of diffusion coefficients of signaling molecules and the receptors.

Two methods of adaptive threshold detection for OOK transmission were proposed in [118]. The adaptive threshold calculation was based on determining the average distance variation within a symbol interval. The distance was calculated using the diffusion equation *(6)*. The first adaptive detection scheme was based on a comparison of received concentration with the adaptive threshold. In this scheme, the adaptive threshold was selected as half of the maximum value of the reconstructed signal during the interval where the last bit-1 was detected. Thus, the decision rule to detect the transmitted bit in the jth bit interval can be expressed as

$$\hat{b}_j = \begin{cases} 1 & \text{if } h_{j,peak} \geq h_{*,peak}/2, \\ 0 & \text{otherwise}, \end{cases} \qquad (13)$$

where $*$ denotes the index of the last bit-1 detected, and $h_{j,peak}$ is the peak value of reconstructed signal using average distance between the transmitter and the receiver in jth bit interval.

The second detection scheme was peak time-based detection in which the peak time of the current bit-interval was compared with 1.6 times the peak time of the reconstructed signal where the last bit-1 was detected. Moreover, ISI mitigation was also performed by subtracting the reconstructed signals of previous bit-intervals from the total received signal in the current bit-interval. Simulation results demonstrated that these detection schemes perform well if the coherence time of the channel is large, however they fail to give satisfactory performance if the coherence time is small (i.e., around 1-bit interval).

To overcome the limitations of this work, another detection scheme was proposed in [136] in which modified concentration shift keying was used where some molecules for bit-0 were also transmitted. This could help the receiver to find the distance using the diffusion equation even when bit-0 was transmitted and the adaptive threshold was calculated based on the reconstructed signals of previous bit duration unlike [118] where the threshold calculation based on the bit duration in which the last bit-1 was transmitted. The detection rule in [136] is given by

$$\hat{b}_j = \begin{cases} 1 & \text{if } \max(x_{r_k,k}[j]) \geq \frac{f_{1,\max}(j-1,t) - f_{0,\max}(j-1,t)}{\ln \frac{f_{1,\max}(j-1,t)}{f_{0,\max}(j-1,t)}}; \\ 0 & \text{otherwise.} \end{cases} \qquad (14)$$

where $x_{r_k,k}[j]$ is the ISI mitigated signal in jth bit interval, r_k is the distance between the transmitter and the receiver at kth sample, $f_{1,\max}(j-1,t)$ and $f_{0,\max}(j-1,t)$ are the peak values of the reconstructed signals for bit-1 and bit-0 respectively in $(j-1)$th bit interval. It is shown that the detection scheme in [136] performs well for a coherence time of $\approx$ 2-bit duration.

Further, a signal detection scheme with initial distance estimation was proposed in [137]. In this scheme, a pilot signal was released before information transmission which assisted to estimate the stochastic distance based on maximizing the likelihood of the received signal in the first step. In the second step, maximum likelihood estimation was used to find the initial distance by maximizing the likelihood function based on the PDF of distance. Authors employed a MAP-based detection scheme at the receiver and based on this, the expression for optimal threshold was obtained. Furthermore, an adaptive detection scheme for OOK modulation was proposed in [138], where the decision threshold in the current bit-interval was selected as the weighted sum of the received signals in the previous two bit-intervals. The weights were obtained by minimizing the error rate at the receiver nano-machine. Also, a pre-coding scheme was presented to combat ISI, where the transmitter scaled the number of released molecules if two consecutive bit-1 were transmitted. The probability of error was further minimized to determine the optimal scaling factor. The proposed technique outperformed the fixed threshold technique and the one presented in [47] where the received signal in the previous bit-interval was considered as an adaptive threshold.

Optimal LLR based decision rule was derived at the receiver in [139]. Based on the derived optimal rule, the probability of error with respect to the number of transmitted molecules and channel capacity with increasing external interference was also evaluated. A detection scheme based on slope values within a symbol interval was proposed in [140] considering OOK based transmission at the transmitter. In this work, Einsteins' law of diffusion was used to find the CIR. Moreover, the detection threshold was set to zero as the slope value was positive for bit-1 and negative for bit-0. Cell-to-cell communication based on calcium signaling was proposed in [141]. In this work, intra-cellular and intercellular calcium signaling was studied for mobile cells in an environment composed of cytoplasm. Based on the external diffusion model of calcium, the transmission of calcium-based on concentration and waveform was also studied. Moreover, the decay of calcium signals in the environment and the number of activated cells as a percentage of sender cells were analyzed.

The work in [142] studied cluster formation by a set of mobile nano-machines using the attractant molecules. This work considered that the angular movement of nano-machines was in the direction of the maximum concentration gradient and the concentration sensed by nano-machines was governed by their sensitivity. The number and size of clusters were shown to be controlled by the sensitivity of nano-machines to the concentration of attractants. An MMC system for drug delivery was proposed in [143] where drug carriers and diseased cells were considered as transmitters and receivers, respectively. Using the PDF of stochastic CIR and the reception probability

of a single molecule, the authors demonstrated that the controlled drug release mechanism was shown to be better than the constant drug release. Moreover, the PDF of the dynamic distance between the transmitter and the receiver was used to optimize the release profile at the transmitter, the time duration of a frame, and the detection threshold at the receiver.

A non-coherent iterative detection has been proposed in [144] considering the 1-D motion of transmitter and receiver, where the PDF of first hitting time was obtained in terms of effective diffusion coefficient [117]. In this work, ISI mitigation was also implemented by subtracting the average ISI concentration from the total received signal in the current symbol-interval. Another non-coherent detection scheme for OOK was proposed in [145], where the decision metric was calculated as the difference of the signal energies received in current and previous bit-intervals. This technique is useful for the scenarios that experience strong ISI because it makes the energy difference positive in the case of bit-1 and negative in the case of bit-0.

In [133], the statistical nature of CIR in the case of MMC was investigated, where the mean and variance of the noiseless and noisy received signal were derived. The noisy received signal was shown to be Poisson-Log normal distributed which could be approximated as Poisson distributed in some cases. In this work, the PDF of the dynamic distance was also found. Moreover, binary hypothesis testing was done at the receiver for three different detection thresholds i.e. fixed threshold, half threshold, and optimal threshold according to MAP rule for Poisson distributed signals. Simulated results demonstrated that the MAP-based optimal thresholding scheme achieved the lowest BER and on the other hand, the half threshold scheme performed the worst.

In [146], two transmission techniques based on CSK and Manchester coding were presented, where bit-1 and bit-0 were represented as symbol [1 0] and [0 1], respectively. Moreover, at the receiver, a concentration difference-based detection was proposed which used the maximum concentration difference within a bit-interval for detection of the transmitted bit using CSK. For Manchester coding at the transmitter, the detector employed a decision metric based on concentration difference between successive bits and the detection threshold was found using the MAP rule.

In [119], OOK modulation has been used at the transmitter and an adaptive detection scheme based on local convexity of the received signal in the case of bit-1 and concavity of the received signal in the case of bit-0 was proposed for the receiver. In this work, the average of the received signal was found where the average was calculated for the two sampling times within which the signal was convex. For example, 0.1 s and 0.3 s in Fig. 13. This average value was later subtracted from the peak received signal within a bit-interval for designing a convexity metric. Moreover, an adaptive threshold was obtained as the weighted sum of convexity metrics of the bit-intervals in which the last, the second last, and the third last bit-1 were detected.

3.1.2 Relay-assisted-based mobile MC systems

Forster Resonance Energy Transfer (FRET[10])-based MMC has been proposed in [147] for detecting tumors. In this work, authors considered two different types of network configuration: (i) FRET-based mobile sensor and actuator network in which molecular sensing and actuating tasks were carried out at the molecular level, (ii) FRET-based mobile ad-hoc network with source, relay, and destination nodes, where the source transmits information to the relay node or destination in a probabilistic manner. Detection probability and detection time of a single message were analyzed, where message propagation is modeled using the Markov-chain process.

3.1.3 MIMO-based mobile MC systems

In [148], MIMO-MC was proposed for both static and dynamic transmitter and receiver scenarios. Before sending a block of data, a training sequence was sent for channel estimation. Channel estimation was done using the maximum likelihood CIR and the least square CIR estimators, where the latter was less complex to implement. In this work, the training sequence was selected which maximized the Cramer-Rao bound of the CIR. The authors also studied the performance of DFE, MMSE-DFE, and ZF-DFE equalizers for ISI/ILI mitigation. Moreover, to avoid cross-talk, time interleaving was used, where different gates at the transmitter released molecules at different time intervals within a bit duration. For performance evaluation, the authors showed that MSEs for the least-squares CIR estimator and maximum likelihood CIR estimator were 16 dB and 14 dB, respectively, at a training sequence of length 250 bits. Further, with a decrease in training sequence length from 250 bits to 16 bits, the MSEs for least squares and maximum likelihood CIR estimators increased to 25 and 23 dB, respectively.

3.1.4 Machine-learning-based mobile MC systems

Various symbol-by-symbol and sequence detectors based on neural network[11] for binary and M-ary amplitude modulation schemes were proposed in [31]. Specifically, Recurrent Neural Network (RNN), Bidirectional RNN (BRNN), and Sliding BRNN (SBRNN) with LSTM cells were used, where SBRNN was shown to perform well for a coherence time of $\approx$ 1-bit duration.

[10] FRET is an energy transfer mechanism observed in fluorophores.

[11] A significant advantage of neural network-based detectors is that they can perform well in time-varying channels where CSI is difficult to obtain at the receiving node.

Besides, a comparison with Viterbi sequence detection was also presented in [31].

Further, the work in [149] proposed an ANN-based detection scheme using Broyden–Fletcher–Goldfarb–Shanno (BFGS) algorithm where received signal was filtered then the filtered signal, slope values and the concentration difference values of the filtered signal were used for training and detection by the NN. Filtering the received signal was done by partitioning the bit interval into P equal subintervals and averaging the signal in each partition as described below.

$$\phi_i = \frac{1}{N_p} \sum_{k=jN_s+low}^{jN_s+high} y_j[k], \qquad (15)$$

where $i = 0, 1, 2, \cdots, P-1$ and N_p is the number of samples within a partition. The low and $high$ parameters are defined as, $low = iN_p$ and $high = (i+1)N_p - 1$ for ϕ_i. Using *(15)*, the filtered signal in jth bit interval can be written as $\boldsymbol{\phi_j} = [\phi_0, \phi_1, \cdots, \phi_{P-1}]$. Based on this filtered signal, the slope vector $\boldsymbol{s_j}$ and concentration difference [146] vector $\boldsymbol{d_j}$ can be obtained as $\boldsymbol{s_j} = [s_0, s_1, \cdots, s_{P-2}]$, where $s_i = \phi_{i+1} - \phi_i$ and $\boldsymbol{d_j} = [d_0, d_1, \cdots, d_{P-2}]$, where $d_i = \phi_{i+1} - \phi_0$. Thus, the features $\boldsymbol{z_j}$ (input to the detector) for the three different techniques were based on (a) the filtered signal, (b) slope, and (c) concentration difference:

$$\boldsymbol{z_j} = \begin{cases} \boldsymbol{\phi_j} & \text{for (a)}, \\ [s_0, s_1, \cdots, s_{P-2}, E(\boldsymbol{s_j}), \text{var}(\boldsymbol{s_j})] & \text{for (b)}, \\ [d_0, d_1, \cdots, d_{P-2}, E(\boldsymbol{d_j}), \text{var}(\boldsymbol{d_j})] & \text{for (c)}, \end{cases} \qquad (16)$$

where $E(\cdot)$ and $\text{var}(\cdot)$ denote the expectation and the variance. In this work, the transmitted bits are represented in the following manner. For bit-0, $\boldsymbol{p_j} = [0 \quad 1]^T$ and for bit-1, $\boldsymbol{p_j} = [1 \quad 0]^T$. Note that the values inside $\boldsymbol{p_j}$ represent the Probability Mass Function (PMF) of the transmitted bit. If L consecutive bits are transmitted then $\boldsymbol{P_L} = [\boldsymbol{p_1}, \boldsymbol{p_2}, \cdots, \boldsymbol{p_L}]$ represents the sequence of transmitted bits and $\boldsymbol{Z_L} = [\boldsymbol{z_1}, \boldsymbol{z_2}, \cdots, \boldsymbol{z_L}]$ be the corresponding features then the training data set is represented by $(\boldsymbol{P_L}, \boldsymbol{Z_L})$. The output of the NN is the vector $\hat{\boldsymbol{p}}_{\boldsymbol{j}} = NN(\boldsymbol{z_j}; \boldsymbol{W})$, where $\boldsymbol{W}$ represents the weights and biases in the NN. Finally, the bits are estimated according to the following criterion

$$\hat{b}_j = \arg\max_{b_j \epsilon S} \hat{\boldsymbol{p}}_{\boldsymbol{j}}, \qquad (17)$$

where $\hat{\boldsymbol{p}}_{\boldsymbol{j}} = [\Pr(b_j = 1|\boldsymbol{z_j}) \;\; \Pr(b_j = 0|\boldsymbol{z_j})]^T$ is the estimated PMF vector.

Furthermore, a detection scheme based on Generative-Adversarial-Network (GAN) has been proposed in [150]. This network learned from the channel transition probability. For fine tuning the transition probabilities, the scheme in [150] combined the use of pilot symbols and generating training data in real time to track time-varying channels. Most importantly, this scheme avoids retraining the network from the beginning.

3.2 Mobile nano-machines in flow-induced diffusive channel

3.2.1 Single transmitter and single receiver-based mobile MC systems

A quaternary modulation scheme for reducing ISI was proposed in [121], where type-A and type-B molecules were used for transmission. In this scheme, no molecules were sent for symbol [0 0], type-A molecules were sent for [0 1], type-B molecules were sent for [1 0], and both types molecules were sent for symbol [1 1]. This scheme was termed as Depleted-MoSK (D-MoSK). For decoding purposes, maximum likelihood detection was used at the receiver. Individual thresholds for both types of molecules were used at the receiver e.g. if the number of type-A molecules was above a certain threshold t_a and the number of type-B molecules was less than the threshold t_b then the transmitted symbol was decoded as [0 1].

On similar lines, other symbols were decoded. Simulation results showed that the D-MoSK modulation scheme resulted in a better BER performance than MoSK. Further, a novel modulation based on permutation of different molecules was proposed in [153] to achieve better performance than D-MoSK in the presence of strong ISI. In this modulation scheme, different types of molecules were sent at different instants within a symbol duration. If M different types of molecules are chosen then $M!$ permutations exist and in this case a total $\lfloor \log_2 M! \rfloor$ bits per symbol can be sent. At the receiver, maximum likelihood detection was performed. This modulation scheme achieved better BER performance than MoSK and D-MoSK schemes for a large ratio of number of transmitted molecules to information bits per symbol.

In [154], a nano-sensor network for in-body applications has been proposed in which various nano-machines used repellent molecules to move away from one another. This process is suitable for searching a target inside the body. Further, attractant molecules were used by the nano-machines to come closer once the target is detected. In this work, a non-diffusion[12]-based MC has been assumed and the gradient of adhesive molecules which could bind to the inner wall of the blood vessel were used for guiding the mobile nano-machines. This kind of coordination can be useful where loss of molecules due to diffusion is high. More specifically, the aim of this work was to evaluate the number of nano-machines near to the target and the number of nano-machines hitting the target.

Furthermore, a leader follower-based MMC has been discussed in [155]. After finding the target location, the leader nano-machines released adhesive molecules which could be sensed by the follower nano-machines for moving towards a target (e.g., cancer cells) for various purposes such as drug delivery etc. Maximum likelihood esti-

[12] In non-diffusion-based MC, molecules disperse quickly in the environment, which has dominant flow and limited diffusion.

Table 5 – Summary of transmission and detection in MMC with and without drift

Reference	Modulation	Detection	Symbol-by-symbol (Sbs)/Sequence (Seq) detector	Coherent/ Non-coherent detection	Complexity
[117]	OOK	Single sample detection	Sbs	Non-coherent	Low
[135]	OOK	Local convexity detection	Sbs	Non-coherent	Moderate
[118]	OOK	Adaptive threshold-based detection with distance estimation in intervals with bit-1 (Valid for large coherence time)	Sbs	Coherent	Very high
[136]	MCSK	Adaptive threshold detection with distance estimation in every bit-interval (Valid for small coherence time)	Sbs	Coherent	Very high
[31]	Binary and M-ary amplitude modulation	Recurrent neural network detection schemes	Sbs and Seq	Non-coherent	High
[144]	OOK	Iterative detector	Sbs	Non-coherent	High
[139]	OOK	LLR test	Sbs	Coherent	Moderate
[148]	OOK (MIMO-MC)	i) DFE, ii) MMSE-DFE, iii) ZF-DFE, and iv) Least squares DFE detector	Sbs	Coherent	i) Very high ii) High iii) High iv) Very high
[138]	OOK	Adaptive threshold detector	Sbs	Non-coherent	Moderate
[145]	OOK	Energy difference based detector	Sbs	Non-coherent	Low
[133]	CSK	Binary detector with i) Fixed threshold, ii) Half threshold, iii) Optimal threshold obtained using MAP rule	Sbs	Non-coherent	i) Low ii) Low iii) High
[146]	MCSK, Manchester coded MCSK	Concentration difference detector based on i) Difference within a bit-interval, ii) Difference in successive bit-intervals	Sbs	Non-coherent	Low
[137]	OOK	Single sample detector with initial distance estimation based on pilot signal	Sbs	Coherent	Very high
[119]	OOK	Convexity detector with detection threshold as weighted sum of earlier convexity metrics	Sbs	Non-coherent	High
[151]	OOK	Cooperative detection with OR/AND fusion rules at FC	Sbs	Coherent	High
[152]	OOK	Log LRT	Sbs	Coherent	High
[121]	OOK, Depleted-MoSK (D-MoSK)	Maximum likelihood detection	Sbs	Coherent	Moderate

mate of various parameters was also obtained. These parameters were related to resistance offered to the motion of nano-machines, noise effects on the motion and the impact of gradient of attractants' concentration.

3.2.2 Relay-assisted-based mobile MC systems

In [152], a decode-and-forward relaying scheme was proposed for MMC in the presence of drift. In this work, Log LRT was used at the receiver and relay to determine the detection threshold. Also, an optimal number of transmitted molecules at each of the transmitting nodes was found to minimize the end-to-end error probability. A relay-assisted MMC in the presence of drift was studied in [156]. In this work, optimal LRT-based detection was performed at the receiver in each time slot. Further, for performance analysis through the analytical framework, a closed-form expression for channel capacity was also derived, where a decrease in capacity was reported with an increase in interference due to other sources of transmission and due to an increase in the diffusion coefficient of the receiver.

Table 6 – BER performance of different detection schemes

Reference	Modulation	Detection	Lowest BER	SNR/Number of transmitted molecules	Distance between transmitter and receiver
[33]	MoSK	i) MAP detection without ISI ii) Viterbi detection with ISI	i) 5×10^{-3} ii) $\approx 10^{-5}$	4 dB/10^3	100 μm
[34]	MoSK	MAP detection with noise whitening filter	7×10^{-6}	10 dB/2.5×10^4	600 μm
[40]	Rectangular pulse based OOK	Adaptive receiver based on steepest descent algorithm for i) Maximum likelihood sequence detection ii) MMSE equalizer iii) DFE with decision metric iv) DFE with quantizer	i) 0 ii) 3×10^{-5} iii) 10^{-6} iv) 3×10^{-6}	16 dB/4×10^9	0.05 μm
[45]	MTSK	i) MMSE equalizer ii) DFF	i) $\approx 10^{-4}$ ii) 3×10^{-4}	500	5 μm
[52]	Rectangular pulsed based OOK	Non linear adaptive threshold detection based on local geometry and energy difference of received signal	2×10^{-4}	8 dB	9 nm
[60]	Rectangular pulsed based OOK	Two layered detection for reducing the number of sequences to be searched	10^{-5}	9 dB/10^4	3 μm
[29]	OOK	ANN detection with LM optimizer	$\approx 10^{-4}$	31 dB	0.5 μm
[105]	OOK	MF detector	2×10^{-4}	4×10^4	0.5 μm
[30]	OOK	Parzen-PNN based detection	5×10^{-4}	10 dB	2 μm
[111]	CSK	Fuzzy C-means clustering	$\approx 10^{-3}$	11 dB/3×10^4	0.5 μm
[135]	OOK	Local convexity detection	2×10^{-4}	31 dB	0.065 μm
[31]	Binary and M-ary amplitude modulation	Recurrent neural network detection schemes	5×10^{-4}	-	-
[137]	OOK	Single sample detector with initial distance estimation based on pilot signal	4×10^{-3}	3×10^4 for pilot signal and 4×10^4 for information	1 μm

3.2.3 Distribution detection-based mobile MC systems

In [157], 1-D MMC with drift was considered, where multiple cooperative nano-machines were used between the source and the destination. Channel capacity and the probability of bit error expressions were derived at the destination using the probabilities of detection and false alarm. Authors' analysis demonstrated that the optimal decision threshold at the destination depends on the probabilities of detection and false alarm of the last cooperative nano-machine.

A cooperative detection strategy was presented in [151], where several cooperative nano-machines sent their decisions to an FC about the presence or absence of an abnormality inside the blood vessel. In this work, each of the nano-machines and the FC were assumed to be mobile under the influence of both diffusion and drift. For performance analysis, the PDF of the first hitting time of molecule at the FC was also described, where the concept of effective diffusion coefficient was used as described in [117]. OR (if one of the nano-machines sent a positive report) and AND (if all the nano-machines sent a positive report) rules were used at the FC for making the global decision about the presence or absence of abnormality. Authors demonstrated that for a higher probability of false alarm, OR rule performed better than AND rule and vice-versa. This is because in case of high chances of error, all the nano-machines may not be able to make the correct decision, and hence performance of the AND rule degrades. Further, to reduce the error probability, a cooperative abnormality detection scheme was proposed in [158]. In this scheme, a sensor could be activated if it detects an abnormality itself or it receives signaling molecules from other sensors that detected abnormality. Finally, an FC collected responses from all the sensors and checked the activation flag of all the sensors to decide the presence or absence of abnormality. Optimal threshold at the FC was derived by minimizing the error probability.

3.3 Performance and complexity comparison of different detection techniques for mobile MC

Computational complexity of the non-coherent detector proposed in [145] is $O(N_s)$ that is much less than the detection schemes such as coherent MAP method and MMSE [40], [98].

The complexity of the local convexity detector proposed in [135] is given by $O(l) + O(l^2)$, where l is the length of a convexity metric. $O(l)$ is due to the calculations of the convexity metric and the threshold, $O(l^2)$ is the complexity due to the moving average operation. Further, the computational complexity of maximizing the likelihood in [137] was $O(log(N))$. This was based on the Newton-Raphson method. This technique for detection was less complex than [118] (complexity is $O(S^3)$), as the CIR reconstruction and threshold determination in every bit interval was not required for detection. Instead authors in [137] used statistical characteristics of the CIR to estimate the initial distance and set the threshold for all bit intervals in advance for detection. Furthermore, the complexity in [119] was $O(S)$ that is also less than the technique presented in [118].

In [148], ZF-DFE and MMSE-DFE have computational complexity of $O(BMn_t^2)$, where B is the block length, M is the number of channel taps in an $n_t \times n_t$ MIMO system. Whereas a least squares DFE detector has a complexity of $O(BM2^{n_t})$. Thus, a least squares DFE detector has higher complexity but better BER performance than ZF-DFE and MMSE-DFE. If channel memory is denoted as M, n denotes the length of the sequence to be decoded, L is the window length of SBRNN. N is the number of states with highest log-likelihood values among 2^M states that are kept at each time instance in the beam search Viterbi algorithm. Then, as discussed in [31], $N = 2^M$. Computational complexities of the Viterbi detector, RNN and SBRNN are given by $O(Nn)$, $O(n)$, and $O(L(n-L+1))$, respectively. It can be observed that RNN is most efficient in terms of computational complexity. SBRNN and beam search VD can have similar complexity. Complexity of traditional VD grows exponentially with memory length M.

The ANN detector proposed in [29] is less complex than the ANN-based detector in [31] as the number of hidden layers' neurons in the former technique are significantly less compared to the latter technique. Further, DFF proposed in [45] has a complexity of $O(M)$ whereas MMSE equalizer has a complexity of $O(M^3)$. Table 5 summarizes the modulation and detection techniques in MMC with or without drift in the channel. Further, Table 6 shows the lowest BER obtained in different detection schemes at a particular SNR. The distance between the transmitter and the receiver is also mentioned.

3.4 Challenges in detection and possible solutions

3.4.1 Tracking the dynamic distance and determining the adaptive threshold

It can be seen from *(7)* and *(8)* that both peak time and peak amplitude depend on the distance between the transmitter and the receiver. One can also notice in Fig. 19 that the peak time decreases and peak amplitude increases as the distance between communicating nanomachines decreases. When the distance is 1 μm, the peak time and peak amplitude are around 0.017 s and 735, respectively. However, when the distance is 2 μm, the peak time and amplitude are around 0.675 s and 92, respectively. Hence, sampling at a fixed time (c.f. *(7)*) [117] is not suitable for detection under varying (or dynamic) distance over time, which arises due to mobility. For example, sampling at t_{peak} in case of r = 1 μm gives maximum signal but amplitude of signal becomes very less at the same time for r = 2 μm, as shown in Fig. 19. The impact of distance on the received signal (perturbed by the noise and ISI) has been shown in Fig. 20. The received signal is given by

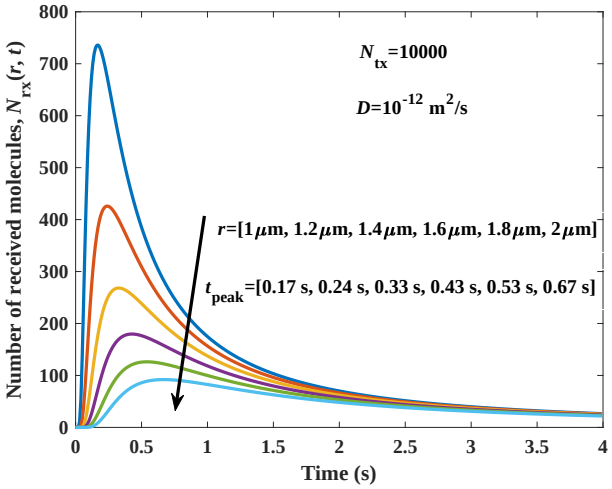

Fig. 19 – Comparison of the received signal without noise at different distances between the transmitter and the receiver. Respective peak times are also shown.

$$y(r(t),t) = \sum_{j=0}^{\infty} b_j N_{rx}(r(t), t - jT_b) + n(r(t),t). \quad (18)$$

In *(18)*, the distance $r(t)$ is assumed to be time-varying, unlike *(11)* where distance $r(t) = r \; \forall t$ is constant. For this simulation, the transmitted sequence is considered as [1 1 0 1 0] and the distance in each bit-interval is progressively increasing. It can be observed that in the 4th bit-interval, the received signal for the transmitted bit-1 goes below the threshold, that causes incorrect detection. Hence, the threshold at the receiver should not be fixed (as considered in static MC). To address this issue, the decision threshold should be adaptive and dependent upon the dynamic distance. Moreover, for detection, the estimation of distance at the receiver under static and mobile conditions is also an important issue, which has been addressed in some of the works such as [118], [136], [137], [159], [160].

Under a mobility condition, as described in [135], the detection based on local convexity of the received signal (in case of bit-1 transmission) can be used since the convexity persists even if the peak time and peak amplitude change (c.f. Fig. 19).

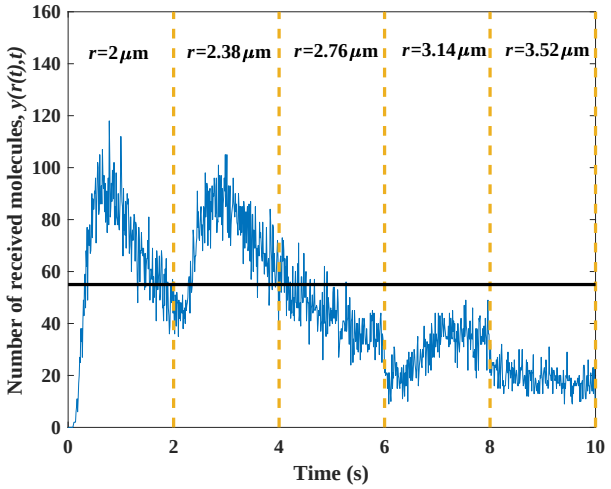

Fig. 20 – Received signal including noise and ISI for the transmitted sequence [1 1 0 1 0]. The maximum signal is below the threshold in 4th bit duration for bit-1 leading to incorrect detection.

The detection based on the convexity metric is also suitable for the system experiencing only ISI, where noise can be filtered by using a moving average filter as described in [135]. Further, to improve the performance, the ISI mitigation technique described in [118] can be considered under mobile scenarios. In this work, dynamic distance is estimated using *(6)* if the number of received molecules $N_{\text{rx}}(r,t)$ is known. This estimated distance is further used to reconstruct the received signal (within a bit-interval) and subtract it from the total received signal for ISI mitigation. Note that the distance estimation using *(6)* in [118] is not correct if bit-0 is transmitted as N_{tx} is zero for bit-0.

Hence, in [118], the adaptive threshold for detection in the current bit-interval was calculated using the distance estimated in the bit-interval when the last bit-1 was detected. If the coherence time of the channel is small then the channel can change considerably between the current bit-interval and the bit-interval in which the last bit-1 was detected. Hence, the detection threshold can be wrong. This problem can be solved by transmitting some molecules for bit-0, as well [136]. Considering the non-zero number of molecules for bit-0, the adaptive threshold in the current bit-interval can be obtained using the distance estimated in the previous bit-interval. Also, for MMC in a drift-based environment, threshold determination has been shown in [152].

3.4.2 *Multiple parameters estimation*

If the number of transmitted molecules N_{tx} and the diffusion coefficient D change along with the distance r then the estimate of these parameters over time is difficult to obtain using *(6)*. In [161], a method for estimating multiple parameters has been shown. If we consider that N_{tx}, D, and r are constant within a bit-interval then three samples of the received signal within a bit-interval will be required as there are three unknown variables to be determined. By solving three different equations similar to *(6)* with three samples of the received signal N_{rx_1}, N_{rx_2}, and N_{rx_3}, three unknown parameters i.e., N_{tx}, D, r can be estimated. However, for a mobile transmitter and receiver, as the distance r changes at each sampling time, we cannot estimate five unknown variables i.e., N_{tx}, D, r_1, r_2, r_3 using three samples of the received signal N_{rx_1}, N_{rx_2}, and N_{rx_3}. Hence, non-coherent detectors [119] and ANN detectors [31] are more suitable in this case.

3.4.3 *Unknown channel model*

If channel model is not known then the adaptive threshold-based detection techniques used in [118] and [136] will not yield good performance because *(6)* can not be used for distance estimation. Therefore, to deal with unknown channel model, non-coherent detection techniques proposed in [145], [146], [119] can be considered. In [146], amplitude difference was used as the decision metric, whereas energy difference was used as the decision metric in [145]. Also, the technique proposed in [145] is suitable for the scenario when the system experiences strong ISI. Further, to improve the detection performance in noisy and unknown channel scenarios, ANN detectors [31] can also be considered as one of the possible solutions.

3.4.4 *Synchronization*

For a static MC scenario, few synchronization techniques such as blind synchronization [161], [162], synchronization using peak observation time and threshold triggering [163], and reference broadcast synchronization considering molecule synthesis time [164] have been proposed. Note that these synchronization schemes proposed for static MC cannot be used in MMC scenarios. Moreover, synchronization is more challenging in mobile MC due to the time-varying distance between the communicating nano-machines. It is also worth noting that joint detection and synchronization have to be done to realize practical mobile MC systems. Recently, two synchronization schemes based on the least-square method and peak time have been proposed for mobile MC in [165]. However, these techniques rely on a known channel model and will not work if extended for unknown channel models e.g., channel model with multiple fully-absorbing receiver nano-machines. Considering limited computational resources for nano-machines, investigation of novel asynchronous detection techniques for mobile MC is required.

4. EXPERIMENTAL WORKS

4.1 Microscale experiments

A microfluidic chip for detecting a Deoxyribonucleic acid (DNA) molecule was proposed in [166]. This chip was fabricated using multilayer soft lithography, which consists of two layers of silicone rubber i.e., Polydimethylsiloxane (PDMS), a flow layer with several micro-wells, and a control layer. Possibilities of nano-resonators made of Graphene sheets and Carbon Nano-Tubes (CNTs) for transportation and detection of molecules at very low concentration were explored in [167]. These materials detect the shift in wave velocity (inside CNT) and resonant frequencies due to the presence of external molecules. The motion of water molecules inside the CNT channel was demonstrated in this work. Moreover, nano-pumping action to initiate the molecule flow was also shown. This setup could be helpful for the design of transmitters in MC.

Silicon-Nano-Wire (Si-NW)-based biomolecule detection was presented in [168]. In [168], a faster response of Si-NW than the Ion-Sensitive Field Effect Transistor (ISFET) was shown. Also, the sensitivity of the Si-NW sensor was revealed to be dependent upon the pH level of the surroundings, the geometry of the sensor, and its doping level. In [169], detection of femtograms of mercury-ion was proposed using Bovine Serum Albumin (BSA) protein conjugated ZnO nano-sphere (BCZ). In this work, a logarithmic variation of conductance of BCZ was demonstrated with the concentration of mercury-ions. Further, the formation of a complex between BCZ and mercury was confirmed through fluorescence spectroscopy. Note that the proposed work in [169] has several biomedical applications such as detection of diseases related to ingestion of mercury and other heavy metals, which are toxic for a human body.

A microscale modulator was proposed in [170], which converted an optical signal from a Light-Emitting Diode (LED) to a chemical signal consisting of protons. The proposed system was similar to one considered in [171], where incident light on bacteria released the H^+ ions. On the other hand, a pH sensor was employed at the receiver. For this system, channel estimation schemes based on short-duration pilot signals and long duration previously detected data were proposed. Moreover, the optimal maximum likelihood detector and suboptimal derivative-based detector were also derived. Simulation results showed that the system can achieve a bit rate of 1 bit per minute. A Graphene-based micro-resonator for individual molecule detection of DNA, dopamine, and nicotine was proposed in [172]. An ingestible pill with the bidirectional wireless interface was proposed in [173] for in-body nucleic acid-sensing. In this work, transmit and received powers of the order of micro-watts was demonstrated. Also, a receiver mode sensitivity of -59 dBm with BER of 10^{-3} was shown at the speed of 1 megabits per second (Mbps).

4.2 Macroscale experiments

An experimental setup was presented in [174] to model the diffusive channel. In this setup, a spray of isopropyl alcohol was used as a transmitter and a metal oxide sensor was used as a receiver that generates a voltage based on the concentration of alcohol received over the air. The distance between the transmitter and the receiver was considered from 2 to 5 meters and spraying duration was also varied from 50 milliseconds to 200 milliseconds under different trials. Moreover, the response of the receiver was averaged over these trials and the unknown coefficients in the diffusion equation were found by minimizing the difference between the experimental observations and the theoretically expected response.

A 2×2 MIMO-MC system was developed in [175] and [176], where two alcohol sprays and two chemical sensors were used at the transmitter and receiver, respectively. In this work, a micro-controller for transmission and two micro-controllers for decoding the text message was used. Simulation results showed a data rate improvement of 1.7 times with respect to the SISO system. Signal-to-inter link interference of 14.567 was calculated using the MIMO test bed when the transmitter and receiver were separated by 90 cm and antenna separation was 40 cm. Such communication systems could be useful for structural high speed health monitoring for smart cities and also for the transmission of signals to robots in a subterranean (i.e, under the earth surface) region where implementing radio frequency communication is challenging.

An experimental setup was demonstrated in [177] in which a peristaltic pump is used as a transmitter and a pH sensor is employed at the receiver. The peristaltic pump used acid to transmit bit-0 and base to transmit bit-1 over the channel which contains water in a silicon tube. In the case of an acidic signal, the receiver generated positive voltage and for the base signal, the receiver generated negative voltage. For detection, two different techniques were proposed in which Support Vector Machine (SVM) and RNN are used. The SVM-based detection scheme uses a linear relationship between the input and the output. Also, a slope-based detector was used which measures the rate of change of pH within a symbol interval. It was shown that RNN[13] performs better among other detectors for a short symbol duration. On the other hand, slope-based detection performed the worst. Hence, training based detectors are suitable for cases where the channel model is not known.

In [178], the authors used a test bed that was similar to [174]. In this setup, isopropyl alcohol spray and metal oxide sensor was used for transmission and reception,

[13] RNN was trained using the slope values and corresponding bit patterns.

respectively. At the transmitter, to control the function (turn on/off spray), an Arduino Uno microprocessor was connected. A computer was used for uploading the control codes to the microprocessor. On the other hand, the receiver consisted of an MQ-3 semiconductor metal oxide gas sensor and a microprocessor, which was used to read the sensor data. Finally, for decoding the transmitted information, the detection algorithm was implemented on the computer connected to the microprocessor. A modified slope-based detection was proposed in [178] in which the number of positive and negative slope values within a bit duration was counted to decide in favor of bit-1 or bit-0. It was shown that in the case of bit-1, 80% of the slope values were positive. In this work, the number of samples within a bit duration was set as 10 and the detection threshold was considered as 8 based on 80% criterion.

An experimental MMC system was proposed in [179] in which the mobile receiver was able to sense the gradient of alcohol molecules formed in the environment. This gradient was formed by spraying the molecules by the target. The mobile receiver was a two-wheeled vehicle controlled by an Arduino-Uno microprocessor. A metal oxide sensor was mounted on the vehicle to sense the concentration of alcohol molecules. A bio-inspired algorithm similar to bacterial chemotaxis was used by the receiver to move towards the target. It was shown that this algorithm was more efficient than a random walk process in terms of the time required to reach the target.

In [180], an ethanol electrical sprayer was used as a transmitter. To create a flow-based channel, a table fan was used to provide velocity to the transmitted molecules. Moreover, at the receiver, the detection was based on an adaptive threshold mechanism where the decision threshold was calculated using the first sample of each time slot. The proposed detection scheme was claimed to be better than the one proposed in [178], which obtains the decision threshold in terms of the number of positive slope values of the received signal. A test bed based on proton pumping bacteria was proposed in [171], where incident light on a plasmid inside bacteria generated protons which were later sensed by a pH sensor at the receiver.

An experimental setup for validating the theoretical models was proposed in [181]. In this work, Hydrochloric acid (HCl) controlled by a solenoid valve was used as the transmitter and a pH sensor was deployed as the receiver. Moreover, a glass pipe containing water was considered as the channel for communication between the transmitter and the receiver. At the receiver, adaptive threshold-based detection was performed considering the channel memory of the previous one bit or two bits. Interestingly, COMSOL simulations of the experimental setup were also carried out to compare against the experimental data. An experiment similar to [174] was also carried out in [182]. However, in this work, multilevel modulation was proposed where different symbols were sent by varying the time duration of releasing the molecules. A slope-based detection along with experimentally validated channel and noise models were also presented. A test bed using SPIONs as the information particles was proposed in [183]. In this work, SPIONs were sent into a pipe containing the water, and a susceptometer was used for detecting the particles. The change in inductance was investigated under the various distribution of particles passing. A MAP demodulator based on chemical reactions has been presented in [184]. It was shown that a gene promoter circuit DCS2 found in yeast can be used for MAP-based demodulation.

A transmitter using acetone and methanol for signaling with N_2 gas as a carrier and a mass spectrometer with a quadrupole mass analyzer as detector were used in [185]. Tangential and longitudinal diffusion coefficients were taken into account for the analysis of amplitude, energy, and SNR of the received signal. An implantable glucose sensor was proposed in [186] in which InGaZnO (IGZO)-based Electrolyte-Gated Field-Effect Transistors (EGFETs) were considered as the sensor material. This material has better field-effect mobility and a large on-off ratio than previously used materials e.g., Graphene and Si-NW. The basic principle of sensing in [186] was to sense the pH value due to the H^+ ions generated by the reaction of glucose (to be sensed) and glucose oxidase (i.e., the material immobilized on the sensor). A test bed showing its effectiveness was also implemented. Also, RNN and module-based decoding where each module consists of ANN were used for the detection of pH value. Simulation results demonstrated that deep learning-based algorithms achieve better BER performance in unknown and noisy channels.

In [187] a channel coding scheme was proposed to mitigate ISI. In the codeword, the following three properties were used: i) Sending consecutive bit-1 was not allowed, ii) The codeword always started with bit-0, and iii) At-least one bit-1 should be present in each codeword. Also, an adaptive threshold was used to decode each codeword, where the threshold scaling factor was estimated by sending the pilot signal before information transmission. The proposed technique was also tested experimentally where alcohol spray and alcohol sensor was employed as the transmitter and receiver, respectively. Authors demonstrated that BER $\approx 5 \times 10^{-2}$ can be obtained with this setup. Particle image velocimetry and planar laser-induced fluorescence were proposed in [188] for tracking the changes in molecular signals as well as the channel parameters responsible for a change in the molecular signal.

A cooperative RNN was proposed in [189] in which RNN had forward and backward components. A merged layer with the time-varying property was designed to combine the outputs of forward and backward RNN components. The proposed network was tested experimentally on a

test bed structure similar to [177]. The BER in training and testing data sets was ≈ 0.032 and ≈ 0.074, respectively. The proposed network achieved BER less than SBRNN and a simple detector, where pH difference of last and first values within a bit-interval was used as the decision metric. Table 7 shows a brief description of the experimental works and concluding remarks on the outcomes of the experiments.

5. CHALLENGES IN PRACTICAL DESIGN OF TRANSMITTER AND RECEIVER, AND FUTURE RESEARCH DIRECTIONS

5.1 Transmitter design

Most of the existing works consider the transmitter to be an ideal point source that can release molecules in the direction of the receiver. This is a very weak assumption, which has been employed for analytical tractability to analyze the system performance. However, for realizing a practical spherical transmitter, the following issues must be taken into consideration:

5.1.1 Energy

The transmitter requires some energy for its operation for example encoding the transmitted information, controlling the number of emitted molecules, etc. Therefore, it should have the capability of harvesting energy. For health applications within IoBNT, this energy harvesting can be done by using the chemical molecules present in the environment. For example, glucose is the natural source of energy in all organisms. Similarly, the transmitter can also use some chemical to energize itself.

5.1.2 Molecule synthesis

The transmitter is expected to release the signaling molecules to communicate with the receiver. Hence, the very first requirement is the synthesis of molecules in the required amount. To achieve this, a controlled chemical reaction is required. On the other hand, the signaling molecules/drug particles can also be loaded beforehand so that there is no requirement for molecule synthesis. Thus, for biomedical applications e.g., drug delivery, the required number of chemical molecules should be calculated before inserting the nano-machine inside the human body.

5.1.3 Modulator

As discussed in the previous sections, various types of modulation schemes have been proposed in the literature, e.g., to transmit information, the number of released molecules is varied, or the release time of the molecules is varied. Hence, a unit at the transmitter is required to control the concentration or release time of the molecules.

5.1.4 Molecule release mechanism

The transmission of molecules requires a pumping action. Therefore, nano-pumps, as described in [167], can be used for this purpose. Moreover, by applying mechanical loads to the CNTs, molecular flows can also be achieved.

5.1.5 Biocompatibility

Since these nano-machines are expected to perform their task inside the human body, they should be biocompatible and should not produce any immunological response or toxic effects while performing their task in an environment of living cells. For example, a biocompatible polymer like chitosan conjugated with anticancer agents is used for gradual drug release in cancerous tissues. Ensuring biocompatibility requires interdisciplinary research.

5.2 Receiver design

The types of receiver considered in the literature are mostly passive receiver, absorbing receiver, and reactive receiver. Passive receivers are assumed to be a hypothetical sphere transparent to the arriving molecules. This implies that the passive receiver can count the number of molecules within its closed boundary without affecting their propagation in the environment. In contrast to the passive receiver, an absorbing receiver can count and absorb the molecules once they hit the surface. On the other hand, reactive[14] receivers have receptors on their surface that can bind to the molecules through a reversible reaction. In such a scenario, counting the number of bound receptors can provide the information of received molecules.

Note that passive and absorbing receivers are difficult to develop in practice. Thus, a reactive receiver can be considered for the practical design of the receiver. It is also important to note that the functioning of the reactive receiver is similar to the cells which can bind respective ligands and provide transduction of extracellular signals to intracellular signals. Bio-FET can also be used as a receiver to realize MC.

5.2.1 Receptor design

Since the receiver is expected to bind the signaling molecules at its receptor, the design of receptors is important. The selectivity and sensitivity of the receptors to the intended molecule can be done by selecting the proper material for the receptor. Selectivity means the receptor should bind only that molecule, which is used for signaling. Sensitivity means the response time of the receptors. The response time should not be very high otherwise it will limit the data rate of the MC system. As discussed in [18], aptamers and DNAs can be appropriate to be used as receptors. Various types of aptamers and corresponding ligand/signaling molecules are available [190], [191], [192].

[14] Binding and unbinding of molecules is possible in such receivers.

Table 7 – System description and important conclusions in experimental works

Reference	System description	Conclusion
[168]	Silicon-nano wire (Si-NW) based biomolecule detection	Faster response of Si-NW than the Ion-Sensitive Field-Effect Transistor (ISFET) was shown.
[169]	Detection of femtograms of Mercury-ion using BSA protein conjugated ZnO nano-sphere (BCZ)	i) Logarithmic variation of conductance of BCZ with the concentration of Mercury-ions. ii) Useful for biomedical applications such as detection of toxic heavy metals in body.
[170]	i) Conversion of optical signal from LED to chemical signal (H^+ ions) ii) Detection of H^+ ions using pH sensor	i) Derivative-based detection was used to obtain a bit rate of 1-bit/min. ii) System can work as microscale modulator.
[174]	i) **Transmitter** - Spray of isopropyl alcohol ii) **Channel** - Air iii) **Receiver** - Metal oxide sensor	i) Study of diffusion over the air ii) Determines and validates the channel model experimentally.
[176]	i) 2×2 MIMO-MC system using two alcohol sprays and two chemical sensors	i) 1.7 times data rate improvement w.r.t. SISO system. ii) Useful for applications like structural high speed health monitoring in smart cities.
[177]	i) **Transmitter** - Peristaltic pump using acid to transmit bit-0 and base to transmit bit-1 ii) **Channel** - Water in a silicon tube iii) **Receiver**- RNN-based detection	Training-based detectors are suitable if channel model is not known.
[179]	i) **Transmitter** - Alcohol spray ii) **Channel** - Air iii) **Mobile receiver** - Metal oxide sensor mounted on a vehicle	Better target (transmitter) detection by the receiver using bio-inspired algorithm than the random walk process.
[186]	i) Implantable glucose sensor is proposed ii) InGaZnO-based EGFET is used as the sensor material iii) Detection of H^+ ions generated by the reaction of glucose using RNN	i) Deep learning-based detection performs better than conventional threshold based detectors in unknown and noisy channels. ii) EGFETs have better field-effect mobility and a large on-off ratio than Si-NW.
[187]	i) **Transmitter** - Alcohol spray ii) **Channel** - Air iii) **Receiver**- Alcohol sensor	i) Channel coding for better ISI mitigation. ii) Adaptive threshold for decoding of the code-word.
[189]	i) **Transmitter** - Peristaltic pump using acid to transmit bit-0 and base to transmit bit-1 ii) **Channel** - Water in a silicon tube iii) **Receiver**- Cooperative RNN-based detection	Better BER performance than SBRNN.

5.2.2 Transduction unit

In bio-FET, the channel between drain and source electrodes is the transduction unit for generating an electrical signal based on the molecular signal at the receptors. Single-Walled CNTs (SWCNTs), Si-NW [168], graphene [167] could be used as the transduction unit. The SWCNT for Acetylcholine (Ach) receptor has been discussed in [193] to detect Ach. Si-NW-based transduction unit for re- ceptor protein in prostate cancer detection has been pre- sented in [194]. The graphene-based transducer channel for a glucose oxidase receptor in a glucose sensing device has been discussed in [195]. The conductivity of trans- ducers such as SWCNT, Si-NW and graphene varies with the number of molecules bound to the receptors. This in turn changes the current flow between source and drain of bio-FET [18] thus providing transduction capability to these materials. SWCNT and Si-NW are one dimensional structures but graphene is a two dimensional material that can provide large spatial coverage leading to an increase in the number of receptors that can be functionalized on its surface.

5.2.3 Signal processing unit

After the transduction unit, the processing of the generated electrical signal is required for the detection of information. Since a nano-machine is expected to be a simple device with limited computational capability, simple and less-complex detectors such as derivative-based detection [61], asynchronous detection [50] are more suitable. However, the limitation of these detectors is that they cannot perform well under high noise and mobile transmitter/receiver scenarios. Moreover, the non-coherent detector can also be used in challenging environments where the channel model is difficult to obtain. A non-coherent detector based on local convexity [135] that uses a moving average operation for noise reduction and ANN-

based detection can be robust detectors [31] as they do not require CSI and are also capable of working in the high noise environment.

5.3 Future research directions

Within IoBNT, multiple transmitters and receivers have to work together to perform complex tasks, including sensing and actuation. However, exact analytical channel models considering multiple fully absorbing receivers in the medium are not available in the existing literature due to mathematical intractability of corresponding diffusion equations. In this context, the work in [196] considered two fully absorbing receivers in a 3-D medium and derived an approximate first hitting time distribution to demonstrate the mutual dependency between receivers. However, this approximation is only valid when $r_1 > 3a$, $r_2 > 3a$, and $R > 3a$, where r_1, r_2, R, and a denote the distance between the transmitter and first receiver, distance between the transmitter and second receiver, distance between the first and second receiver, and the radius of the receiver, respectively. In this derivation, the radius of each receiver is assumed to be identical.

The analysis was further extended for an underlay-based cognitive paradigm in [197] where both primary and secondary link performances were evaluated by employing a simple molecule control mechanism at the secondary transmitter. In this work, the radius of each receiver is assumed to be different and the impact of molecule degradation over time was also considered while analyzing the system performance. However, the analyses in [196] and [197] is restricted only for two fully absorbing receivers and cannot be easily extended for more than two receivers. Thus, development of exact analytical channel models involving multiple fully absorbing receivers in a 3-D medium is still an open problem.

Further, many MC systems [33], [40], [45], [118], [148], [136], [144] that are proposed in the literature are coherent. These coherent MC systems require CSI and suffers from the drawback of complex channel estimation. Note that the channel in these systems can be very unpredictable with very short coherence times. Hence the MC systems that use pilot signal [137], [148], [187] for estimating the CSI, are not very suitable. Also, the receivers that can detect the information for fast-varying channels (i.e., short coherence time) are required to build practical MC systems. Machine/deep learning-based MC systems that do not need CSI and perform well in fast-varying channels [31] are suitable in such complex scenarios. Also, machine/deep learning-based algorithms do not rely on accurate channel models and can be classified as non-coherent schemes. Hence, the possibility of implementing these algorithms should be explored to address IoBNT applications with static [30], [186], [189] and mobile MC [106], [31].

In this context, one of the possible research areas is neural network detection considering the channel model which is not known or difficult to obtain. Further, the performance of different first order and second order algorithms [198] used for optimizing the neural network detectors should be investigated.

On the other hand, most of the detection schemes assume perfect synchronization between the transmitter and the receiver. However, for practical MC systems, joint synchronization and detection or asynchronous detection has to be performed, as shown in [163] and [50], respectively. In this context, novel low-complexity schemes should be devised to perform asynchronous detection or detection with synchronization at the fully absorbing receiver, especially for a flow-induced mobile MC where each of the nano-machines are considered to be mobile in diffusive channel along with drift. Moreover, the state of the art detectors [45], [52], [118], [146] considered perfect synchronization while analyzing the system performance. Thus, the performance evaluation of these detectors considering synchronization error is still lacking in the current literature.

6. CONCLUSION

For the IoBNT applications such as drug delivery, in-body health monitoring, etc, the nanoscale and microscale devices are expected to perform collaborative tasks using MC. However, the MC system performance in these applications significantly depends on the transmission and detection schemes employed at the transmitter and receiver nano-machines (or bio-nano-machines), respectively. This survey, therefore, presented the transmission and detection techniques existing in the current literature for static and mobile nano-machines under pure-diffusive and flow-induced diffusive channels. In each category, different types of MC system such as SISO, MIMO, relay-assisted, and FC-based cooperative detection scheme have been discussed to support several health applications within IoBNT. Various coherent and non-coherent detection schemes are presented under each category. The detectors have also been classified based on symbol-by-symbol detection and sequence detection. Also, the performance and the complexities of some detection techniques are discussed. Further, several challenges in detection have been described under various scenarios. Experimental works related to MC are also presented. At the end of this survey, some major challenges related to the practical design of the transmitter and receiver along with future research directions have been added.

REFERENCES

[1] Tadashi Nakano, Andrew W Eckford, and Tokuko Haraguchi. *Molecular communication*. Cambridge University Press, 2013.

[2] Ian F Akyildiz, Max Pierobon, Sasi Balasubramaniam, and Y Koucheryavy. "The internet of bio-nano things". In: *IEEE Communications Magazine* 53.3 (2015), pp. 32–40.

[3] Young Il Kim, Yoonkwon Park, and Hongkoo Baik. "A novel detection for biomolecule using RF LC resonator". In: *SENSORS, 2007 IEEE*. IEEE. 2007, pp. 728–731.

[4] Puneet Manocha, Gitanjali Chandwani, and Soumen Das. "Characterization of Dielectrophoresis Based Relay-Assisted Molecular Communication Using Analogue Transmission Line". In: *IEEE Access* 8 (2020), pp. 33352–33359.

[5] Wei-Kang Hsu, Xiaojun Lin, and Mark R Bell. "Deep-target delivery of nanosensors with bacteria-inspired coordination". In: *GLOBECOM 2017-2017 IEEE Global Communications Conference*. IEEE. 2017, pp. 1–6.

[6] Muneer M Al-Zu'bi and Ananda Sanagavarapu Mohan. "Modelling of implantable drug delivery system in tumor microenvironment using molecular communication paradigm". In: *IEEE Access* 7 (2019), pp. 141929–141940.

[7] Ian F Akyildiz, Maysam Ghovanloo, Ulkuhan Guler, Tevhide Ozkaya-Ahmadov, A Fatih Sarioglu, and Bige D Unluturk. "PANACEA: An internet of bio-nanothings application for early detection and mitigation of infectious diseases". In: *IEEE Access* 8 (2020), pp. 140512–140523.

[8] Youssef Chahibi and Ilangko Balasingham. "An intra-body molecular communication networks framework for continuous health monitoring and diagnosis". In: *2015 37th Annual International Conference of the IEEE Engineering in Medicine and Biology Society (EMBC)*. IEEE. 2015, pp. 4077–4080.

[9] Luca Felicetti, Mauro Femminella, and Gianluca Reali. "A molecular communications system for live detection of hyperviscosity syndrome". In: *IEEE Transactions on NanoBioscience* (2020).

[10] Steven Kisseleff, Robert Schober, and Wolfgang H Gerstacker. "Magnetic nanoparticle based interface for molecular communication systems". In: *IEEE Communications Letters* 21.2 (2016), pp. 258–261.

[11] Federico Tavella, Alberto Giaretta, Triona-Marie Dooley-Cullinane, Mauro Conti, Lee Coffey, and Sasitharan Balasubramaniam. "DNA molecular storage system: Transferring digitally encoded information through bacterial nanonetworks". In: *IEEE Transactions on Emerging Topics in Computing* (2019).

[12] Tania Islam, Ethungshan Shitiri, and Ho-Shin Cho. "A Simultaneous Drug Release Scheme for Targeted Drug Delivery Using Molecular Communications". In: *IEEE Access* 8 (2020), pp. 91770–91778.

[13] Michael Taynnan Barros, Walisson Silva, and Carlos Danilo Miranda Regis. "The multi-scale impact of the Alzheimer's disease on the topology diversity of astrocytes molecular communications nanonetworks". In: *IEEE Access* 6 (2018), pp. 78904–78917.

[14] Ian F Akyildiz, Jiande Chen, Maysam Ghovanloo, Ulkuhan Guler, Tevhide Ozkaya-Ahmadov, Massimiliano Pierobon, A Fatih Sarioglu, and Bige D Unluturk. "Microbiome-gut-brain axis as a biomolecular communication network for the Internet of Bio-NanoThings". In: *IEEE access* 7 (2019), pp. 136161–136175.

[15] Reza Mosayebi, Arman Ahmadzadeh, Wayan Wicke, Vahid Jamali, Robert Schober, and Masoumeh Nasiri-Kenari. "Early cancer detection in blood vessels using mobile nanosensors". In: *IEEE transactions on nanobioscience* 18.2 (2018), pp. 103–116.

[16] Nariman Farsad, H Birkan Yilmaz, Andrew Eckford, Chan-Byoung Chae, and Weisi Guo. "A comprehensive survey of recent advancements in molecular communication". In: *IEEE Communications Surveys & Tutorials* 18.3 (2016), pp. 1887–1919.

[17] Uche AK Chude-Okonkwo, Reza Malekian, Bodhaswar T Maharaj, and Athanasios V Vasilakos. "Molecular communication and nanonetwork for targeted drug delivery: A survey". In: *IEEE Communications Surveys & Tutorials* 19.4 (2017), pp. 3046–3096.

[18] Murat Kuscu, Ergin Dinc, Bilgesu A Bilgin, Hamideh Ramezani, and Ozgur B Akan. "Transmitter and receiver architectures for molecular communications: A survey on physical design with modulation, coding, and detection techniques". In: *Proceedings of the IEEE* 107.7 (2019), pp. 1302–1341.

[19] Tadashi Nakano, Yutaka Okaie, Shouhei Kobayashi, Takahiro Hara, Yasushi Hiraoka, and Tokuko Haraguchi. "Methods and applications of mobile molecular communication". In: *Proceedings of the IEEE* 107.7 (2019), pp. 1442–1456.

[20] V. Jamali, A. Ahmadzadeh, W. Wicke, A. Noel, and R. Schober. "Channel Modeling for Diffusive Molecular Communication—A Tutorial Review". In: *Proceedings of the IEEE* 107.7 (2019), pp. 1256–1301. DOI: 10.1109/JPROC.2019.2919455.

[21] Christian A Söldner, Eileen Socher, Vahid Jamali, Wayan Wicke, Arman Ahmadzadeh, Hans-Georg Breitinger, Andreas Burkovski, Kathrin Castiglione, Robert Schober, and Heinrich Sticht. "A survey of biological building blocks for synthetic molecular communication systems". In: *IEEE Communications Surveys & Tutorials* (2020).

[22] M. Ş. Kuran, H. B. Yilmaz, I. Demirkol, N. Farsad, and A. Goldsmith. "A Survey on Modulation Techniques in Molecular Communication via Diffusion". In: *IEEE Communications Surveys Tutorials* 23.1 (2021), pp. 7–28. DOI: 10.1109/COMST.2020.3048099.

[23] Bhushan S Pattni and Vladimir P Torchilin. "Targeted drug delivery systems: Strategies and challenges". In: *Targeted drug delivery: Concepts and design*. Springer, 2015, pp. 3–38.

[24] Adam Noel, Karen C Cheung, and Robert Schober. "Improving receiver performance of diffusive molecular communication with enzymes". In: *IEEE Transactions on NanoBioscience* 13.1 (2014), pp. 31–43.

[25] Rakesh K Jain and Triantafyllos Stylianopoulos. "Delivering nanomedicine to solid tumors". In: *Nature reviews Clinical oncology* 7.11 (2010), p. 653.

[26] Mauro Femminella, Gianluca Reali, and Athanasios V Vasilakos. "A molecular communications model for drug delivery". In: *IEEE transactions on nanobioscience* 14.8 (2015), pp. 935–945.

[27] Ghalib H Alshammri, Walid KM Ahmed, and Victor B Lawrence. "Adaptive Batch Training Rule-Based Detection Scheme for ON-OFF-Keying Diffusion-Based Molecular Communications". In: *2018 IEEE 13th Nanotechnology Materials and Devices Conference (NMDC)*. IEEE. 2018, pp. 1–4.

[28] S. Sharma, D. Dixit, and K. Deka. "Deep Learning based Symbol Detection for Molecular Communications". In: *2020 IEEE International Conference on Advanced Networks and Telecommunications Systems (ANTS)*. 2020, pp. 1–6. DOI: 10.1109/ANTS50601.2020.9342782.

[29] X. Qian, M. Di Renzo, and A. Eckford. "Molecular Communications: Model-Based and Data-Driven Receiver Design and Optimization". In: *IEEE Access* 7 (2019), pp. 53555–53565.

[30] Zhuangkun Wei, Weisi Guo, Bin Li, Jerome Charmet, and Chenglin Zhao. "High-dimensional metric combining for non-coherent molecular signal detection". In: *IEEE Transactions on Communications* 68.3 (2019), pp. 1479–1493.

[31] Nariman Farsad and Andrea Goldsmith. "Neural network detection of data sequences in communication systems". In: *IEEE Transactions on Signal Processing* 66.21 (2018), pp. 5663–5678.

[32] Ling-San Meng, Ping-Cheng Yeh, Kwang-Cheng Chen, and Ian F Akyildiz. "Optimal detection for diffusion-based communications in the presence of ISI". In: *2012 IEEE Global Communications Conference (GLOBECOM)*. IEEE. 2012, pp. 3819–3824.

[33] Hoda ShahMohammadian, Geoffrey G Messier, and Sebastian Magierowski. "Optimum receiver for molecule shift keying modulation in diffusion-based molecular communication channels". In: *Nano Communication Networks* 3.3 (2012), pp. 183–195.

[34] Hoda ShahMohammadian, Geoffrey G Messier, and Sebastian Magierowski. "Modelling the reception process in diffusion-based molecular communication channels". In: *2013 IEEE International Conference on Communications Workshops (ICC)*. IEEE. 2013, pp. 782–786.

[35] Mohammad Upal Mahfuz, Dimitrios Makrakis, and Hussein T Mouftah. "Strength based receiver architecture and communication range and rate dependent signal detection characteristics of concentration encoded molecular communication". In: *2012 Seventh International Conference on Broadband, Wireless Computing, Communication and Applications*. IEEE. 2012, pp. 28–35.

[36] A Ozan Bicen, Caitlin M Austin, Ian F Akyildiz, and Craig R Forest. "Efficient sampling of bacterial signal transduction for detection of pulse-amplitude modulated molecular signals". In: *IEEE Transactions on Biomedical Circuits and Systems* 9.4 (2015), pp. 505–517.

[37] Wanzhi Qiu, Thanh Cong Nguyen, and Efstratios Skafidas. "Detection of weak nano-biosensor signals corrupted by shot noise". In: *2013 13th IEEE International Conference on Nanotechnology (IEEE-NANO 2013)*. IEEE. 2013, pp. 305–310.

[38] Mohammad Upal Mahfuz, Dimitrios Makrakis, and Hussein T Mouftah. "A comprehensive analysis of strength-based optimum signal detection in concentration-encoded molecular communication with spike transmission". In: *IEEE Transactions on NanoBioscience* 14.1 (2015), pp. 67–83.

[39] Ignacio Llatser, Albert Cabellos-Aparicio, Massimiliano Pierobon, and Eduard Alarcón. "Detection techniques for diffusion-based molecular communication". In: *IEEE Journal on Selected Areas in Communications* 31.12 (2013), pp. 726–734.

[40] Deniz Kilinc and Ozgur B Akan. "Receiver design for molecular communication". In: *IEEE Journal on Selected Areas in Communications* 31.12 (2013), pp. 705–714.

[41] Mohammad U Mahfuz, Dimitrios Makrakis, and Hussein T Mouftah. "A comprehensive study of sampling-based optimum signal detection in concentration-encoded molecular communication". In: *IEEE Transactions on NanoBioscience* 13.3 (2014), pp. 208–222.

[42] Ling-San Meng, Ping-Cheng Yeh, Kwang-Cheng Chen, and Ian F Akyildiz. "On receiver design for diffusion-based molecular communication". In: *IEEE Transactions on Signal Processing* 62.22 (2014), pp. 6032–6044.

[43] Chun Tung Chou. "A Markovian approach to the optimal demodulation of diffusion-based molecular communication networks". In: *IEEE Transactions on Communications* 63.10 (2015), pp. 3728–3743.

[44] Yonathan Murin, Mainak Chowdhury, Nariman Farsad, and Andrea Goldsmith. "Diversity gain of one-shot communication over molecular timing channels". In: *GLOBECOM 2017-2017 IEEE Global Communications Conference*. IEEE. 2017, pp. 1–6.

[45] Burcu Tepekule, Ali E Pusane, H Birkan Yilmaz, Chan-Byoung Chae, and Tuna Tugcu. "ISI mitigation techniques in molecular communication". In: *IEEE Transactions on Molecular, Biological and Multi-Scale Communications* 1.2 (2015), pp. 202–216.

[46] Mohammad Upal Mahfuz. "Achievable strength-based signal detection in quantity-constrained PAM OOK concentration-encoded molecular communication". In: *IEEE Transactions on NanoBioscience* 15.7 (2016), pp. 619–626.

[47] Martin Damrath and Peter Adam Hoeher. "Low-complexity adaptive threshold detection for molecular communication". In: *IEEE Transactions on NanoBioscience* 15.3 (2016), pp. 200–208.

[48] Yeganeh Zamiri-Jafarian and Saeed Gazor. "Receiver design for diffusion-based molecular communication: Gaussian mixture modeling". In: *2016 IEEE International Conference on Communications (ICC)*. IEEE. 2016, pp. 1–6.

[49] Bin Li, Mengwei Sun, Siyi Wang, Weisi Guo, and Chenglin Zhao. "Low-complexity noncoherent signal detection for nanoscale molecular communications". In: *IEEE Transactions on NanoBioscience* 15.1 (2015), pp. 3–10.

[50] Adam Noel and Andrew W Eckford. "Asynchronous peak detection for demodulation in molecular communication". In: *2017 IEEE International Conference on Communications (ICC)*. IEEE. 2017, pp. 1–6.

[51] Satish K Tiwari, Tadi Ravi Teja Reddy, and Prabhat K Upadhyay. "Error performance optimization using logarithmic barrier function in molecular nanonetworks". In: *IEEE Communications Letters* 21.11 (2017), pp. 2408–2411.

[52] Bin Li, Chenglin Zhao, and Weisi Guo. "Non-linear signal detection for molecular communications". In: *GLOBECOM 2017-2017 IEEE Global Communications Conference*. IEEE. 2017, pp. 1–6.

[53] Ghalib H Alshammri, Mohammed S Alzaidi, Walid KM Ahmed, and Victor B Lawrence. "Low-complexity memory-assisted adaptive-threshold detection scheme for ON-OFF-keying diffusion-based molecular communications". In: *2017 IEEE 38th Sarnoff Symposium*. IEEE. 2017, pp. 1–6.

[54] Georgia D Ntouni, Vasileios M Kapinas, and George K Karagiannidis. "On the optimal timing of detection in molecular communication systems". In: *2017 24th International Conference on Telecommunications (ICT)*. IEEE. 2017, pp. 1–5.

[55] Amin Zare, Ali Jamshidi, and Alireza Keshavarz-Haddad. "Receiver design for pulse position modulation technique in diffusion-based molecular communication". In: *2017 IEEE 4th International Conference on Knowledge-Based Engineering and Innovation (KBEI)*. IEEE. 2017, pp. 0729–0733.

[56] Qingchao Li. "The clock-free asynchronous receiver design for molecular timing channels in diffusion-based molecular communications". In: *IEEE Transactions on NanoBioscience* 18.4 (2019), pp. 585–596.

[57] Maheshi B Dissanayake, Yansha Deng, Arumugam Nallanathan, EMN Ekanayake, and Maged Elkashlan. "Reed solomon codes for molecular communication with a full absorption receiver". In: *IEEE Communications Letters* 21.6 (2017), pp. 1245–1248.

[58] Vahid Jamali, Arman Ahmadzadeh, Nariman Farsad, and Robert Schober. "SCW codes for optimal CSI-free detection in diffusive molecular communications". In: *2017 IEEE International Symposium on Information Theory (ISIT)*. IEEE. 2017, pp. 3190–3194.

[59] Alessio Marcone, Massimiliano Pierobon, and Maurizio Magarini. "The Gaussian approximation in soft detection for molecular communication via biological circuits". In: *2017 IEEE 18th International Workshop on Signal Processing Advances in Wireless Communications (SPAWC)*. IEEE. 2017, pp. 1–6.

[60] Mohammed S Alzaidi, Walid KM Ahmed, and Victor B Lawrence. "A Novel Reduced Complexity Detection Scheme for ON-OFF-Keying Diffusion-Based Molecular Communications". In: *2018 International Conference on Computing, Electronics & Communications Engineering (iCCECE)*. IEEE. 2018, pp. 195–200.

[61] Hao Yan, Ge Chang, Zhongke Ma, and Lin Lin. "Derivative-based signal detection for high data rate molecular communication system". In: *IEEE Communications Letters* 22.9 (2018), pp. 1782–1785.

[62] M. C. Gursoy and U. Mitra. "Higher Order Derivatives: Improved Pre-Processing and Receivers for Molecular Communications". In: *GLOBECOM 2020 - 2020 IEEE Global Communications Conference*. 2020, pp. 1–6. DOI: 10.1109/GLOBECOM42002.2020.9322240.

[63] Vahid Jamali, Nariman Farsad, Robert Schober, and Andrea Goldsmith. "Diffusive molecular communications with reactive molecules: Channel modeling and signal design". In: *IEEE Transactions on Molecular, Biological and Multi-Scale Communications* 4.3 (2018), pp. 171–188.

[64] Georgia D Ntouni, Alexandros E Paschos, Vasileios M Kapinas, George K Karagiannidis, and Leontios J Hadjileontiadis. "Optimal detector design for molecular communication systems using an improved swarm intelligence algorithm". In: *Micro & Nano Letters* 13.3 (2018), pp. 383–388.

[65] Vahid Jamali, Nariman Farsad, Robert Schober, and Andrea Goldsmith. "Non-coherent detection for diffusive molecular communication systems". In: *IEEE Transactions on Communications* 66.6 (2018), pp. 2515–2531.

[66] Murat Kuscu and Ozgur B Akan. "Maximum likelihood detection with ligand receptors for diffusion-based molecular communications in Internet of bio-nano things". In: *IEEE Transactions on NanoBioscience* 17.1 (2018), pp. 44–54.

[67] Giulia Muzio, Murat Kuscu, and Ozgur B Akan. "Selective signal detection with ligand receptors under interference in molecular communications". In: *2018 IEEE 19th International Workshop on Signal Processing Advances in Wireless Communications (SPAWC)*. IEEE. 2018, pp. 1–5.

[68] Malcolm Egan, Trung Q Duong, and Marco Di Renzo. "Biological circuits for detection in MoSK-based molecular communication". In: *IEEE Access* 7 (2019), pp. 21094–21102.

[69] Bin Li, Weisi Guo, Xiang Wang, Yansha Deng, Yueheng Lan, Chenglin Zhao, and Arumugam Nallanathan. "CSI-Independent Non-Linear Signal Detection in Molecular Communications". In: *IEEE Transactions on Signal Processing* 68 (2019), pp. 97–112.

[70] Nithin V Sabu and Abhishek K Gupta. "Detection Probability in a Molecular Communication via Diffusion System with Multiple Fully-absorbing Receivers". In: *IEEE Communications Letters* (2020).

[71] Mahendra S Thakur, Sanjeev Sharma, and Vimal Bhatia. "Iterative Signal Detection for Diffusion-Based Molecular Communications". In: *IEEE Transactions on Molecular, Biological and Multi-Scale Communications* 6.1 (2020), pp. 36–49.

[72] M. S. Thakur, S. Sharma, and V. Bhatia. "Molecular Signal Detection Using Nonlinear Mapping". In: *IEEE Wireless Communications Letters* (2020), pp. 1–1. DOI: 10.1109/LWC.2020.3037184.

[73] Trang Ngoc Cao, Nikola Zlatanov, Phee Lep Yeoh, and Jamie S Evans. "Optimal detection interval for absorbing receivers in molecular communication systems with interference". In: *IEEE Transactions on Molecular, Biological and Multi-Scale Communications* (2020).

[74] Satish K Tiwari and Prabhat K Upadhyay. "Estimate-and-forward relaying in diffusion-based molecular communication networks: Performance evaluation and threshold optimization". In: *IEEE Transactions on Molecular, Biological and Multi-Scale Communications* 3.3 (2017), pp. 183–193.

[75] Sanjeev Sharma, Kuntal Deka, and Vimal Bhatia. "Thresholdless detection of symbols in nano-communication systems". In: *IEEE Transactions on NanoBioscience* 19.2 (2019), pp. 259–266.

[76] X. Chen, Y. Huang, L. -L. Yang, and M. Wen. "Generalized Molecular-Shift Keying (GMoSK): Principles and Performance Analysis". In: *IEEE Transactions on Molecular, Biological and Multi-Scale Communications* 6.3 (2020), pp. 168–183. DOI: 10.1109/TMBMC.2020.3021281.

[77] Jiaxing Wang, Shuo Yuan, and Mugen Peng. "Performance analysis and optimal signal detection for amplify-and-forward relay in diffusion-based molecular communication systems". In: *2017 IEEE/CIC International Conference on Communications in China (ICCC)*. IEEE. 2017, pp. 1–6.

[78] Nooshin Tavakkoli, Paeiz Azmi, and Nader Mokari. "Optimal positioning of relay node in cooperative molecular communication networks". In: *IEEE Transactions on Communications* 65.12 (2017), pp. 5293–5304.

[79] P. Hou, A. W. Eckford, and L. Zhao. "Analysis and Design of Two-Hop Diffusion-Based Molecular Communication With Ligand Receptors". In: *IEEE Access* 8 (2020), pp. 189458–189470. DOI: 10.1109/ACCESS.2020.3032009.

[80] Bon Hong Koo, H Birkan Yilmaz, Chan-Byoung Chae, and Andrew Eckford. "Detection algorithms for molecular MIMO". In: *2015 IEEE International Conference on Communications (ICC)*. IEEE. 2015, pp. 1122–1127.

[81] Yu Huang, Xuan Chen, Miaowen Wen, Lie-Liang Yang, Chan-Byoung Chae, and Fei Ji. "A Rising Edge-Based Detection Algorithm for MIMO Molecular Communication". In: *IEEE Wireless Communications Letters* 9.4 (2019), pp. 523–527.

[82] C. Wu, L. Lin, W. Guo, and H. Yan. "Signal Detection for Molecular MIMO Communications With Asymmetrical Topology". In: *IEEE Transactions on Molecular, Biological and Multi-Scale Communications* 6.1 (2020), pp. 60–70. DOI: 10.1109/TMBMC.2020.3004030.

[83] Hamid Khoshfekr Rudsari, Mohammad Reza Javan, Mahdi Orooji, Nader Mokari, and Eduard A Jorswieck. "Multiple-type transmission multiple-type reception framework on molecular communication". In: *IEEE Wireless Communications Letters* (2020).

[84] N. V. Sabu, N. Varshney, and A. K. Gupta. "3-D Diffusive Molecular Communication With Two Fully-Absorbing Receivers: Hitting Probability and Performance Analysis". In: *IEEE Transactions on Molecular, Biological and Multi-Scale Communications* 6.3 (2020), pp. 244–249. DOI: 10.1109/TMBMC.2020.3031414.

[85] Yuting Fang, Adam Noel, Nan Yang, Andrew W Eckford, and Rodney A Kennedy. "Distributed cooperative detection for multi-receiver molecular communication". In: *2016 IEEE Global Communications Conference (GLOBECOM)*. IEEE. 2016, pp. 1–7.

[86] Siavash Ghavami and Farshad Lahouti. "Abnormality detection in correlated Gaussian molecular nano-networks: Design and analysis". In: *IEEE transactions on nanobioscience* 16.3 (2017), pp. 189–202.

[87] Yuting Fang, Adam Noel, Nan Yang, Andrew W Eckford, and Rodney A Kennedy. "Convex optimization of distributed cooperative detection in multi-receiver molecular communication". In: *IEEE Transactions on Molecular, Biological and Multi-Scale Communications* 3.3 (2017), pp. 166–182.

[88] Reza Mosayebi, Vahid Jamali, Nafiseh Ghoroghchian, Robert Schober, Masoumeh Nasiri-Kenari, and Mahdieh Mehrabi. "Cooperative abnormality detection via diffusive molecular communications". In: *IEEE Transactions on NanoBioscience* 16.8 (2017), pp. 828–842.

[89] Sinem Solak and Mengü ç Öner. "Sequential Decision Fusion for Abnormality Detection via Diffusive Molecular Communications". In: *IEEE Communications Letters* (2020).

[90] Yuting Fang, Adam Noel, Yiran Wang, and Nan Yang. "Simplified cooperative detection for multi-receiver molecular communication". In: *2017 IEEE Information Theory Workshop (ITW)*. IEEE. 2017, pp. 329–333.

[91] Reza Mosayebi, Wayan Wicke, Vahid Jamali, Arman Ahmadzadeh, Robert Schober, and Masoumeh Nasiri-Kenari. "Advanced target detection via molecular communication". In: *2018 IEEE Global Communications Conference (GLOBECOM)*. IEEE. 2018, pp. 1–7.

[92] Pengfeng Hou, Liqiang Zhao, and Andrew W Eckford. "Improving receiver performance of diffusion-based molecular MIMO communication". In: *2018 IEEE 18th International Conference on Nanotechnology (IEEE-NANO)*. IEEE. 2018, pp. 1–4.

[93] Yuting Fang, Adam Noel, Nan Yang, Andrew W Eckford, and Rodney A Kennedy. "Maximum likelihood detection for cooperative molecular communication". In: *2018 IEEE International Conference on Communications (ICC)*. IEEE. 2018, pp. 1–7.

[94] Nafiseh Ghoroghchian, Mahtab Mirmohseni, and Masoumeh Nasiri-Kenari. "Abnormality Detection and Monitoring in Multi-Sensor Molecular Communication". In: *IEEE Transactions on Molecular, Biological and Multi-Scale Communications* 5.2 (2019), pp. 68–83.

[95] Yuting Fang, Adam Noel, Nan Yang, Andrew W Eckford, and Rodney A Kennedy. "Symbol-by-symbol maximum likelihood detection for cooperative molecular communication". In: *IEEE Transactions on Communications* 67.7 (2019), pp. 4885–4899.

[96] Ghalib H Alshammri, Walid KM Ahmed, and Victor B Lawrence. "Receiver Techniques for Diffusion-Based Molecular Nano Communications Using an Adaptive Neuro-Fuzzy-Based Multivariate Polynomial Approximation". In: *IEEE Transactions on Molecular, Biological and Multi-Scale Communications* 4.3 (2018), pp. 140–159.

[97] S. N. Solak and M. Oner. "Neural Network Based Decision Fusion for Abnormality Detection via Molecular Communications". In: *2020 IEEE Workshop on Signal Processing Systems (SiPS)*. 2020, pp. 1–5. DOI: 10.1109/SiPS50750.2020.9195212.

[98] Wei-An Lin, Yen-Chi Lee, Ping-Cheng Yeh, and Chia-han Lee. "Signal detection and ISI cancellation for quantity-based amplitude modulation in diffusion-based molecular communications". In: *2012 IEEE Global Communications Conference (GLOBECOM)*. IEEE. 2012, pp. 4362–4367.

[99] Adam Noel, Karen C Cheung, and Robert Schober. "Diffusive molecular communication with disruptive flows". In: *2014 IEEE International Conference on Communications (ICC)*. IEEE. 2014, pp. 3600–3606.

[100] Jeongman Lee, Minhoe Kim, and Dong-Ho Cho. "Asynchronous detection algorithm for diffusion-based molecular communication in timing modulation channel". In: *IEEE Communications Letters* 19.12 (2015), pp. 2114–2117.

[101] Yang-Kai Lin, Wei-An Lin, Chia-Han Lee, and Ping-Cheng Yeh. "Asynchronous threshold-based detection for quantity-type-modulated molecular communication systems". In: *IEEE Transactions on Molecular, Biological and Multi-Scale Communications* 1.1 (2015), pp. 37–49.

[102] Uri Rogers and Min-Sung Koh. "Parallel molecular distributed detection with Brownian motion". In: *IEEE Transactions on NanoBioscience* 15.8 (2016), pp. 871–880.

[103] Junzhe Xiong and Hui Li. "Receiver design for binary timing-based molecular communication". In: *2016 8th International Conference on Wireless Communications & Signal Processing (WCSP)*. IEEE. 2016, pp. 1–6.

[104] Toshiaki Koike-Akino, Junichi Suzuki, and Philip V Orlik. "Molecular signaling design exploiting cyclostationary drift-diffusion fluid". In: *GLOBECOM 2017-2017 IEEE Global Communications Conference*. IEEE. 2017, pp. 1–7.

[105] Vahid Jamali, Arman Ahmadzadeh, and Robert Schober. "On the design of matched filters for molecule counting receivers". In: *IEEE Communications Letters* 21.8 (2017), pp. 1711–1714.

[106] Nariman Farsad and Andrea Goldsmith. "Sliding bidirectional recurrent neural networks for sequence detection in communication systems". In: *2018 IEEE International Conference on Acoustics, Speech and Signal Processing (ICASSP)*. IEEE. 2018, pp. 2331–2335.

[107] Mustafa Can Gursoy, Ertugrul Basar, Ali Emre Pusane, and Tuna Tugcu. "Index modulation for molecular communication via diffusion systems". In: *IEEE Transactions on Communications* 67.5 (2019), pp. 3337–3350.

[108] Qingchao Li. "The asymmetric-distance metrics for decoding of convolutional codes in diffusion-based molecular communications". In: *IEEE Transactions on NanoBioscience* 18.3 (2019), pp. 469–481.

[109] Jiaxing Wang, Mugen Peng, Yaqiong Liu, Xiqing Liu, and Mahmoud Daneshmand. "Performance Analysis of Signal Detection for Amplify-and-Forward Relay in Diffusion-Based Molecular Communication Systems". In: *IEEE Internet of Things Journal* 7.2 (2019), pp. 1401–1412.

[110] Mahendra S Thakur, Sandesh Jain, Sanjeev Sharma, and Vimal Bhatia. "Nonlinear Receiver for Diffusion-Based Molecular Communications". In: *2019 IEEE 30th Annual International Symposium on Personal, Indoor and Mobile Radio Communications (PIMRC)*. IEEE. 2019, pp. 1–6.

[111] Shenghan Liu, Zhuangkun Wei, Bin Li, and Chenglin Zhao. "Unsupervised Clustering-based Non-Coherent Detection for Molecular Communications". In: *IEEE Communications Letters* (2020).

[112] Amit Singhal, Ranjan K Mallik, and Brejesh Lall. "Molecular communication with brownian motion and a positive drift: performance analysis of amplitude modulation schemes". In: *IET Communications* 8.14 (2014), pp. 2413–2422.

[113] Adam Noel, Karen C Cheung, and Robert Schober. "Optimal receiver design for diffusive molecular communication with flow and additive noise". In: *IEEE Transactions on NanoBioscience* 13.3 (2014), pp. 350–362.

[114] Ardalan Alizadeh, Hamid Reza Bahrami, Mehdi Maleki, Nghi H Tran, and Pedram Mohseni. "On the coexistence of nano networks: Sensing techniques for molecular communications". In: *IEEE Transactions on Molecular, Biological and Multi-Scale Communications* 3.4 (2017), pp. 209–223.

[115] Georgia D Ntouni, Vasileios M Kapinas, and George K Karagiannidis. "Optimization of the detection process timing in molecular communication systems with flow". In: *2017 25th Telecommunication Forum (TELFOR)*. IEEE. 2017, pp. 1–4.

[116] Manav R Bhatnagar et al. "3-D diffusive-drift molecular channel characterization for active and passive receivers". In: *IEEE Transactions on Molecular, Biological and Multi-Scale Communications* 4.2 (2018), pp. 107–117.

[117] Arman Ahmadzadeh, Vahid Jamali, Adam Noel, and Robert Schober. "Diffusive mobile molecular communications over time-variant channels". In: *IEEE Communications Letters* 21.6 (2017), pp. 1265–1268.

[118] Ge Chang, Lin Lin, and Hao Yan. "Adaptive detection and ISI mitigation for mobile molecular communication". In: *IEEE Transactions on NanoBioscience* 17.1 (2017), pp. 21–35.

[119] Xiaodong Mu, Hao Yan, Bin Li, Manhua Liu, Ruifeng Zheng, Yan Li, and Lin Lin. "Low-Complexity Adaptive Signal Detection for Mobile Molecular Communication". In: *IEEE Transactions on NanoBioscience* 19.2 (2020), pp. 237–248.

[120] Lokendra Chouhany, Neeraj Varshney, and Prabhat Kumar Sharma. "On Gradient Descent Optimization in Diffusion-Advection based 3-D Molecular Cooperative Communication". In: *IEEE Transactions on NanoBioscience* (2020).

[121] Jiaxing Wang, Xiqing Liu, Mugen Peng, and Mahmoud Daneshmand. "Performance Analysis of D-MoSK Modulation in Mobile Diffusive-Drift Molecular Communications". In: *IEEE Internet of Things Journal* (2020).

[122] Yonathan Murin, Nariman Farsad, Mainak Chowdhury, and Andrea Goldsmith. "Optimal detection for one-shot transmission over diffusion-based molecular timing channels". In: *IEEE Transactions on Molecular, Biological and Multi-Scale Communications* 4.2 (2018), pp. 43–60.

[123] Manav R Bhatnagar et al. "M-ary Poisson reception in molecular communication". In: *Micro & Nano Letters* 13.4 (2018), pp. 509–513.

[124] Wayan Wicke, Arman Ahmadzadeh, Vahid Jamali, Harald Unterweger, Christoph Alexiou, and Robert Schober. "Magnetic nanoparticle-based molecular communication in microfluidic environments". In: *IEEE Transactions on NanoBioscience* 18.2 (2019), pp. 156–169.

[125] Qingchao Li. "A Novel Time-Based Modulation Scheme in Time-Asynchronous Channels for Molecular Communications". In: *IEEE Transactions on NanoBioscience* 19.1 (2019), pp. 59–67.

[126] Yanbin Chen, Yu Li, Lin Lin, and Hao Yan. "Parameter Estimation of Diffusive Molecular Communication With Drift". In: *IEEE Access* 8 (2020), pp. 142704–142713.

[127] Fardad Vakilipoor, Francesca Ratti, Maurizio Magarini, and Hamdan Awan. "Linear Receiver Design for Time-Varying Poisson Molecular Communication Channels with Memory". In: *2020 IEEE 21st International Workshop on Signal Processing Advances in Wireless Communications (SPAWC)*. IEEE. 2020, pp. 1–5.

[128] Nooshin Tavakkoli, Paeiz Azmi, and Nader Mokari. "Performance evaluation and optimal detection of relay-assisted diffusion-based molecular communication with drift". In: *IEEE Transactions on NanoBioscience* 16.1 (2016), pp. 34–42.

[129] Satish K Tiwari and Prabhat K Upadhyay. "Estimate-and-Forward Relaying in Molecular Communication using Brownian Motion with Drift". In: *2018 International Conference on Signal Processing and Communications (SPCOM)*. IEEE. 2018, pp. 502–506.

[130] Hamid Khoshfekr Rudsari, Nader Mokari, Mohammad Reza Javan, Eduard A Jorswieck, and Mahdi Orooji. "Drug Release Management for Dynamic TDMA-Based Molecular Communication". In: *IEEE Transactions on Molecular, Biological and Multi-Scale Communications* 5.3 (2019), pp. 233–246.

[131] Uri Rogers and Min-Sung Koh. "Exploring molecular distributed detection". In: *2015 9th IEEE International Conference on Nano/Molecular Medicine & Engineering (NANOMED)*. IEEE. 2015, pp. 153–158.

[132] Trang C Mai, Malcolm Egan, Trung Q Duong, and Marco Di Renzo. "Event detection in molecular communication networks with anomalous diffusion". In: *IEEE Communications Letters* 21.6 (2017), pp. 1249–1252.

[133] Shuai Huang, Lin Lin, Hao Yan, Juan Xu, and Fuqiang Liu. "Statistical analysis of received signal and error performance for mobile molecular communication". In: *IEEE Transactions on NanoBioscience* 18.3 (2019), pp. 415–427.

[134] S. Md Mustam, S. K. Syed-Yusof, and S. Zubair. "Capacity and Delay Spread in Multilayer Diffusion-Based Molecular Communication (DBMC) Channel". In: *IEEE Transactions on NanoBioscience* 15.7 (2016), pp. 599–612. DOI: 10.1109/TNB.2016.2631240.

[135] Bin Li, Mengwei Sun, Siyi Wang, Weisi Guo, and Chenglin Zhao. "Local convexity inspired low-complexity noncoherent signal detector for nanoscale molecular communications". In: *IEEE Transactions on Communications* 64.5 (2016), pp. 2079–2091.

[136] Amit Kumar Shrivastava, Debanjan Das, and Rajarshi Mahapatra. "Adaptive Threshold Detection and ISI Mitigation in Mobile Molecular Communication". In: *2020 IEEE Wireless Communications and Networking Conference (WCNC)*. IEEE. 2020, pp. 1–6.

[137] Shuai Huang, Lin Lin, Weisi Guo, Hao Yan, Juan Xu, and Fuqiang Liu. "Initial Distance Estimation and Signal Detection for Diffusive Mobile Molecular Communication". In: *IEEE Transactions on NanoBioscience* (2020).

[138] Arzhang Shahbazi and Ali Jamshidi. "Improving adaptive receivers performance in molecular communication via diffusion". In: *IET Nanobiotechnology* 13.4 (2019), pp. 441–448.

[139] Neeraj Varshney, Aditya K Jagannatham, and Pramod K Varshney. "On diffusive molecular communication with mobile nanomachines". In: *2018 52nd Annual Conference on Information Sciences and Systems (CISS)*. IEEE. 2018, pp. 1–6.

[140] Amit Kumar Shrivastava, Debanjan Das, and Rajarshi Mahapatra. "Slope Based Detection for Mobile Molecular Communication Based on Einstein's Law of Diffusion". In: *2018 15th IEEE India Council International Conference (INDICON)*. IEEE. 2018, pp. 1–6.

[141] Peng He, Bowen Pi, and Qiang Liu. "Calcium signaling in mobile molecular communication networks: From a multimedia view". In: *IEEE Access* 7 (2019), pp. 164825–164834.

[142] Yutaka Okaie. "Cluster Formation by Mobile Molecular Communication Systems". In: *IEEE Transactions on Molecular, Biological and Multi-Scale Communications* 5.2 (2019), pp. 153–157.

[143] Trang Ngoc Cao, Arman Ahmadzadeh, Vahid Jamali, Wayan Wicke, Phee Lep Yeoh, Jamie Evans, and Robert Schober. "Diffusive Mobile MC with Absorbing Receivers: Stochastic Analysis and Applications". In: *IEEE Transactions on Molecular, Biological and Multi-Scale Communications* 5.2 (2019), pp. 84–99.

[144] Mahendra S Thakur, Sanjeev Sharma, and Vimal Bhatia. "Noncoherent Detection for Dynamic Transmitter and Receiver in Molecular Communication". In: *2018 IEEE International Conference on Advanced Networks and Telecommunications Systems (ANTS)*. IEEE. 2018, pp. 1–6.

[145] Chunfu Luo, Xia Wu, Lin Lin, Chao Wang, and Fuqiang Liu. "Non-Coherent Signal Detection Technique for Mobile Molecular Communication at High Data Rates". In: *2019 IEEE Global Communications Conference (GLOBECOM)*. IEEE. 2019, pp. 1–6.

[146] Amit K Shrivastava, Debanjan Das, Rajarshi Mahapatra, and Saraju P Mohanty. "dMole: A Novel Transreceiver for Mobile Molecular Communication Using Robust Differential Detection Techniques". In: *IEEE Transactions on NanoBioscience* 19.4 (2020), pp. 609–621.

[147] Murat Kuscu and Ozgur B Akan. "FRET-based mobile molecular nanonetworks". In: *2013 12th Annual Mediterranean Ad Hoc Networking Workshop (MED-HOC-NET)*. IEEE. 2013, pp. 120–127.

[148] SM Reza Rouzegar and Umberto Spagnolini. "Diffusive MIMO molecular communications: Channel estimation, equalization, and detection". In: *IEEE Transactions on Communications* 67.7 (2019), pp. 4872–4884.

[149] Amit K. Shrivastava, Debanjan Das, and Rajarshi Mahapatra. "Performance Evaluation of Mobile Molecular Communication System using Neural Network Detector". In: *IEEE Wireless Communications Letters* (2021), pp. 1–1. DOI: 10.1109/LWC.2021.3079522.

[150] L. Sun, Y. Wang, A. L. Swindlehurst, and X. Tang. "Generative-Adversarial-Network Enabled Signal Detection for Communication Systems With Unknown Channel Models". In: *IEEE Journal on Selected Areas in Communications* 39.1 (2021), pp. 47–60. DOI: 10.1109/JSAC.2020.3036954.

[151] Neeraj Varshney, Adarsh Patel, Yansha Deng, Werner Haselmayr, Pramod K Varshney, and Arumugam Nallanathan. "Abnormality detection inside blood vessels with mobile nanomachines". In: *IEEE Transactions on Molecular, Biological and Multi-Scale Communications* 4.3 (2018), pp. 189–194.

[152] Lokendra Chouhan, Prabhat Kumar Sharma, and Neeraj Varshney. "Optimal transmitted molecules and decision threshold for drift-induced diffusive molecular channel with mobile nanomachines". In: *IEEE Transactions on NanoBioscience* 18.4 (2019), pp. 651–660.

[153] Y. Tang, M. Wen, X. Chen, Y. Huang, and L. -L. Yang. "Molecular Type Permutation Shift Keying for Molecular Communication". In: *IEEE Transactions on Molecular, Biological and Multi-Scale Communications* 6.2 (2020), pp. 160–164. DOI: 10.1109/TMBMC.2020.3014803.

[154] Takuya Obuchi, Yutaka Okaie, Tadashi Nakano, Takahiro Hara, and Shojiro Nishio. "Inbody mobile bionanosensor networks through non-diffusion-based molecular communication". In: *2015 IEEE International Conference on Communications (ICC)*. IEEE. 2015, pp. 1078–1084.

[155] Tadashi Nakano, Yutaka Okaie, Shouhei Kobayashi, Takako Koujin, Chen-Hao Chan, Yu-Hsiang Hsu, Takuya Obuchi, Takahiro Hara, Yasushi Hiraoka, and Tokuko Haraguchi. "Performance evaluation of leader–follower-based mobile molecular communication networks for target detection applications". In: *IEEE Transactions on Communications* 65.2 (2016), pp. 663–676.

[156] Neeraj Varshney, Adarsh Patel, Werner Haselmayr, Aditya K Jagannatham, Pramod K Varshney, and Weisi Guo. "Impact of cooperation in flow-induced diffusive mobile molecular communication". In: *2018 52nd Asilomar Conference on Signals, Systems, and Computers*. IEEE. 2018, pp. 494–498.

[157] Neeraj Varshney, Adarsh Patel, Werner Haselmayr, Aditya K Jagannatham, Pramod K Varshney, and Arumugam Nallanathan. "Impact of intermediate nanomachines in multiple cooperative nanomachine-assisted diffusion advection mobile molecular communication". In: *IEEE Transactions on Communications* 67.7 (2019), pp. 4856–4871.

[158] L. Khaloopour, M. Mirmohseni, and M. Nasiri-Kenari. "Cooperative Abnormality Detection in Fluidic Medium Molecular Communication". In: *2020 Iran Workshop on Communication and Information Theory (IWCIT)*. 2020, pp. 1–6. DOI: 10.1109/IWCIT50667.2020.9163534.

[159] X. Wang, M. D. Higgins, and M. S. Leeson. "Distance Estimation Schemes for Diffusion Based Molecular Communication Systems". In: *IEEE Communications Letters* 19.3 (2015), pp. 399–402. DOI: 10.1109/LCOMM.2014.2387826.

[160] Z. Luo, L. Lin, Q. Fu, and H. Yan. "An Effective Distance Measurement Method for Molecular Communication Systems". In: *2018 IEEE International Conference on Sensing, Communication and Networking (SECON Workshops)*. 2018, pp. 1–4. DOI: 10.1109/SECONW.2018.8396344.

[161] Z. Luo, L. Lin, W. Guo, S. Wang, F. Liu, and H. Yan. "One Symbol Blind Synchronization in SIMO Molecular Communication Systems". In: *IEEE Wireless Communications Letters* 7.4 (2018), pp. 530–533. DOI: 10.1109/LWC.2018.2793197.

[162] H. ShahMohammadian, G. G. Messier, and S. Magierowski. "Blind Synchronization in Diffusion-Based Molecular Communication Channels". In: *IEEE Communications Letters* 17.11 (2013), pp. 2156–2159. DOI: 10.1109/LCOMM.2013.100713.131727.

[163] V. Jamali, A. Ahmadzadeh, and R. Schober. "Symbol Synchronization for Diffusion-Based Molecular Communications". In: *IEEE Transactions on NanoBioscience* 16.8 (2017), pp. 873–887. DOI: 10.1109/TNB.2017.2782761.

[164] L. Lin, W. Li, R. Zheng, F. Liu, and H. Yan. "Diffusion-Based Reference Broadcast Synchronization for Molecular Communication in Nanonetworks". In: *IEEE Access* 7 (2019), pp. 95527–95535. DOI: 10.1109/ACCESS.2019.2929873.

[165] L. Huang, L. Lin, F. Liu, and H. Yan. "Clock Synchronization for Mobile Molecular Communication Systems". In: *IEEE Transactions on NanoBioscience* (2020), pp. 1–1. DOI: 10.1109/TNB.2020.3041631.

[166] Lin Qiu, Qiangyuan Zhu, Yibo Gao, Bingwen Yu, Hao Ren, Wei Jin, Qinhan Jin, and Ying Mu. "Self-priming compartmentalization digital LAMP for single molecule detection". In: *2012 Asia Communications and Photonics Conference (ACP)*. IEEE. 2012, pp. 1–3.

[167] Quan Wang and Behrouz Arash. "Nanoresonators in sensors and molecular transportation: An introduction to the possibilities of carbon nanotubes and graphene sheets". In: *IEEE Nanotechnology Magazine* 8.4 (2014), pp. 29–37.

[168] Mohiuddin Munna, Md Obidul Islam, Md Kabiruzzaman, and Zahid Hasan Mahmood. "Performance analysis of a Si-NW biosensor for detection of charged biomolecules". In: *2014 International Conference on Informatics, Electronics & Vision (ICIEV)*. IEEE. 2014, pp. 1–5.

[169] Milan Sasmal, Tapas Kumar Maiti, and Tarun Kanti Bhattacharyya. "Conjugation of Bovine Serum Albumin With ZnO Nanosphere-A Novel Approach for Ultra-Low Level Mercury Ion Detection". In: *IEEE Transactions on NanoBioscience* 15.7 (2016), pp. 748–755.

[170] Laura Grebenstein, Jens Kirchner, Renata Stavracakis Peixoto, Wiebke Zimmermann, Florian Irnstorfer, Wayan Wicke, Arman Ahmadzadeh, Vahid Jamali, Georg Fischer, Robert Weigel, et al. "Biological optical-to-chemical signal conversion interface: A small-scale modulator for molecular communications". In: *IEEE Transactions on NanoBioscience* 18.1 (2018), pp. 31–42.

[171] Laura Grebenstein, Jens Kirchner, Wayan Wicke, Arman Ahmadzadeh, Vahid Jamali, Georg Fischer, Robert Weigel, Andreas Burkovski, and Robert Schober. "A Molecular Communication Testbed Based on Proton Pumping Bacteria: Methods and Data". In: *IEEE Transactions on Molecular, Biological and Multi-Scale Communications* 5.1 (2019), pp. 56–62.

[172] Z Cao, C Qin, L Bi, Y Chen, Z Xie, and B Yao. "Graphene enhanced intra-resonator biochemical detection with individual molecule sensitivity and selectivity". In: *2019 18th International Conference on Optical Communications and Networks (ICOCN)*. IEEE. 2019, pp. 1–3.

[173] Chengjie Zhu, Yuhan Wen, Tao Liu, Haw Yang, and Kaushik Sengupta. "A Packaged Ingestible Bio-Pill with 15-Pixel Multiplexed Fluorescence Nucleic-Acid Sensor and Bi-Directional Wireless Interface for In-Vivo Bio-Molecular Sensing". In: *2020 IEEE Symposium on VLSI Circuits*. IEEE. 2020, pp. 1–2.

[174] Na-Rae Kim, Nariman Farsad, Chan-Byoung Chae, and Andrew W Eckford. "A universal channel model for molecular communication systems with metal-oxide detectors". In: *2015 IEEE International Conference on Communications (ICC). IEEE. 2015,* pp. 1054–1059.

[175] Changmin Lee, Bonhong Koo, Na-Rae Kim, Birkan Yilmaz, Nariman Farsad, Andrew Eckford, and Chan-Byoung Chae. "Molecular MIMO communication link". In: *2015 IEEE Conference on Computer Communications Workshops (INFOCOM WKSHPS)*. IEEE. 2015, pp. 13–14.

[176] Bon-Hong Koo, Changmin Lee, H Birkan Yilmaz, Nariman Farsad, Andrew Eckford, and Chan-Byoung Chae. "Molecular MIMO: From theory to prototype". In: *IEEE Journal on Selected Areas in Communications* 34.3 (2016), pp. 600–614.

[177] Nariman Farsad, David Pan, and Andrea Goldsmith. "A novel experimental platform for in-vessel multi-chemical molecular communications". In: *GLOBECOM 2017-2017 IEEE Global Communications Conference*. IEEE. 2017, pp. 1–6.

[178] Haoyang Zhai, Qiang Liu, Athanasios V Vasilakos, and Kun Yang. "Anti-ISI demodulation scheme and its experiment-based evaluation for diffusion-based molecular communication". In: *IEEE Transactions on NanoBioscience* 17.2 (2018), pp. 126–133.

[179] Haoyang Zhai, Liting Yang, Tadashi Nakano, Qiang Liu, and Kun Yang. "Bio-inspired design and implementation of mobile molecular communication systems at the macroscale". In: *2018 IEEE Global Communications Conference (GLOBECOM)*. IEEE. 2018, pp. 1–6.

[180] Padarthi Naga Prasanth, Kakani Pruthvi Sumanth, Vijay K Chakka, and Gouriprasanna Roy. "Experimental Implementation of Molecular Communication System using Sampling based Adaptive Threshold Variation Demodulation Algorithm". In: *2018 IEEE International Conference on Advanced Networks and Telecommunications Systems (ANTS)*. IEEE. 2018, pp. 1–5.

[181] Ladan Khaloopour, Seyed Vahid Rouzegar, Alireza Azizi, Amir Hosseinian, Maryam Farahnak-Ghazani, Nahal Bagheri, Mahtab Mirmohseni, Hamidreza Arjmandi, Reza Mosayebi, and Masoumeh Nasiri-Kenari. "An Experimental Platform for Macro-Scale Fluidic Medium Molecular Communication". In: *IEEE Transactions on Molecular, Biological and Multi-Scale Communications* 5.3 (2019), pp. 163–175.

[182] Na-Rae Kim, Nariman Farsad, Changmin Lee, Andrew W Eckford, and Chan-Byoung Chae. "An experimentally validated channel model for molecular communication systems". In: *IEEE Access* 7 (2019), pp. 81849–81858.

[183] Doaa Ahmed, Harald Unterweger, Georg Fischer, Robert Schobe, and Jens Kirchner. "Characterization of an Inductance-based Detector in Molecular Communication Testbed Based on Superparamagnetic Iron Oxide Nanoparticles". In: *2019 IEEE SENSORS*. IEEE. 2019, pp. 1–4.

[184] Chun Tung Chou. "Designing molecular circuits for approximate maximum a posteriori demodulation of concentration modulated signals". In: *IEEE Transactions on Communications* 67.8 (2019), pp. 5458–5473.

[185] Daniel Tunç Mcguiness, Stamatios Giannoukos, Stephen Taylor, and Alan Marshall. "Experimental and Analytical Analysis of Macro-Scale Molecular Communications Within Closed Boundaries". In: *IEEE Transactions on Molecular, Biological and Multi-Scale Communications* 5.1 (2019), pp. 44–55.

[186] Bon-Hong Koo, Ho Joong Kim, Jang-Yeon Kwon, and Chan-Byoung Chae. "Deep Learning-based Human Implantable Nano Molecular Communications". In: *ICC 2020-2020 IEEE International Conference on Communications (ICC)*. IEEE. 2020, pp. 1–7.

[187] A Oguz Kislal, Bayram Cevdet Akdeniz, Changmin Lee, Ali E Pusane, Tuna Tugcu, and Chan-Byoung Chae. "ISI-Mitigating Channel Codes for Molecular Communication Via Diffusion". In: *IEEE Access* 8 (2020), pp. 24588–24599.

[188] Mahmoud Abbaszadeh, Iresha Atthanayake, Peter J Thomas, and Weisi Guo. "Molecular Signal Tracking and Detection Methods in Fluid Dynamic Channels". In: *IEEE Transactions on Molecular, Biological and Multi-Scale Communications* (2020).

[189] Li Sun and Yuwei Wang. "CTBRNN: A novel deep-learning based signal sequence detector for communications systems". In: *IEEE Signal Processing Letters* 27 (2019), pp. 21–25.

[190] Shicai Xu, Jian Zhan, Baoyuan Man, Shouzhen Jiang, Weiwei Yue, Shoubao Gao, Chengang Guo, Hanping Liu, Zhenhua Li, Jihua Wang, et al. "Real-time reliable determination of binding kinetics of DNA hybridization using a multi-channel graphene biosensor". In: *Nature communications* 8.1 (2017), pp. 1–10.

[191] Yasuhide Ohno, Kenzo Maehashi, and Kazuhiko Matsumoto. "Label-free biosensors based on aptamer-modified graphene field-effect transistors". In: *Journal of the American Chemical Society* 132.51 (2010), pp. 18012–18013.

[192] Shimaa Eissa and Mohammed Zourob. "In vitro selection of DNA aptamers targeting β-lactoglobulin and their integration in graphene-based biosensor for the detection of milk allergen". In: *Biosensors and Bioelectronics* 91 (2017), pp. 169–174.

[193] Byeongju Kim, Hyun Seok Song, Hye Jun Jin, Eun Jin Park, Sang Hun Lee, Byung Yang Lee, Tai Hyun Park, and Seunghun Hong. "Highly selective and sensitive detection of neurotransmitters using receptor-modified single-walled carbon nanotube sensors". In: *Nanotechnology* 24.28 (2013), p. 285501.

[194] Fernando Patolsky, Gengfeng Zheng, and Charles M Lieber. *Nanowire-based biosensors*. 2006.

[195] Yinxi Huang, Xiaochen Dong, Yumeng Shi, Chang Ming Li, Lain-Jong Li, and Peng Chen. "Nanoelectronic biosensors based on CVD grown graphene". In: *Nanoscale* 2.8 (2010), pp. 1485–1488.

[196] Nithin V Sabu, Neeraj Varshney, and Abhishek K Gupta. "3-D Diffusive Molecular Communication with Two Fully-Absorbing Receivers: Hitting Probability and Performance Analysis". In: *IEEE Transactions on Molecular, Biological and Multi-Scale Communications* 6.3 (2020), pp. 244–249.

[197] Nithin V Sabu, Neeraj Varshney, and Abhishek K Gupta. "On the Performance of the Primary and Secondary Links in a 3-D Underlay Cognitive Molecular Communication". In: *arXiv preprint arXiv:2102.05812* (2021).

[198] S. Sun, Z. Cao, H. Zhu, and J. Zhao. "A Survey of Optimization Methods From a Machine Learning Perspective". In: *IEEE Transactions on Cybernetics* 50.8 (2020), pp. 3668–3681. DOI: 10.1109/TCYB.2019.2950779.

AUTHORS

Amit K. Shrivastava received a B.Tech. degree in Electronics and Communication engineering from the National Institute of Technology, Raipur in 2010; an M.Tech. degree in Digital Communication from Atal Bihari Vajpayee-Indian Institute of Information Technology and Management, Gwalior, in 2013, and is currently pursuing Ph.D. degree in Electronics and Communication engineering from Dr. SPM IIIT Naya Raipur.

Debanjan Das received a B.Tech. degree in applied Electronics and Instrumentation engineering from the Heritage Institute of Technology, Kolkata, in 2009, an M.Tech. degree in Instrumentation from Indian Institute of Technology, Kharagpur, in 2011, and a Ph.D. degree in Electrical Engineering from Indian Institute of Technology, Kharagpur, in 2016. He is an Assistant Professor with Dr. SPM IIIT Naya Raipur.

Neeraj Varshney received a B.Tech. degree in Electronics and Communication engineering from Uttar Pradesh Technical University, Lucknow, India, in 2008, an M.Tech. degree in electronics and communication engineering from the Jaypee Institute of Information Technology, Noida, India, in 2011, and a Ph.D. degree in electrical engineering from Indian Institute of Technology Kanpur, India, in 2018. Since Nov' 18 he is a international research associate with the wireless networks division at National Institute of Standards and Technology, Maryland, USA. His research interests are in signal processing, communications and networks which include mmWave and THz wireless communication, MIMO technology, molecular communication. From Oct '11 to Aug '12, he was a project research fellow at Jaypee Institute of Information Technology Noida, India. From May '18 to Sep '18, he was a visiting researcher with the department of electrical engineering and computer science at Syracuse University, New York, USA. He has served as a TPC member for 2019/2020 IEEE Globecom conferences in the track on Molecular, Biological, and Multi-scale Communications.

Rajarshi Mahapatra received a Ph.D. degree in Electronics and Electrical Communication engineering from the Indian Institute of Technology Kharagpur, Kharagpur, India, and a postdoctoral degree from the Commissariat à l'Énergie Atomique et aux Énergies, Grenoble, France. He is Associate Professor with the Department of Electronics and Communication Engineering, Dr. SPM IIIT Naya Raipur. He is also handling the responsibilities of Dean (Academics) of IIITNR.

BRAINWAVE ASSISTIVE SYSTEM FOR PARALYZED INDIVIDUALS

Md Ahnaf Shariar[1], Syeda Maliha Monowara[2], Md. Shafayat Ul Islam[3],
Muhammed Junaid Noor Jawad[4], Saifur Rahman Sabuj[5]
[1,2,3,4]Department of Electrical and Electronic Engineering, BRAC University, Bangladesh, [5]Department of Electronics and Control Engineering, Hanbat National University, South Korea

NOTE: Corresponding author: Md Ahnaf Shariar, md.ahnaf.shariar@g.bracu.ac.bd

Abstract *– The Brain-Computer Interface (BCI) is a system based on brainwaves that can be used to translate and comprehend the innumerable activities of the brain. Brainwave refers to the bioelectric impulses invariably produced in the human brain during neurotransmission, often measured as the action potential. Moreover, BCI essentially uses the widely studied Electroencephalography (EEG) technique to capture brainwave data. Paralysis generally occurs when there is a disturbance in the central nervous system prompted by a neurodegenerative or unforeseen event. To overcome the obstacles associated with paralysis, this paper on the brainwave-assistive system is based on the BCI incorporated with Internet-of-things. BCI can be implemented to achieve control over external devices and applications. For instance, the process of cursor control, motor control, neuroprosthetics and wheelchair control, etc. In this paper, the OpenBCI Cyton-biosensing board has been used for the collection of the EEG data. The accumulated EEG data is executed subsequently to obtain control over the respective systems in real-time. Hence, it can be concluded that the experiments of the paper support the idea of controlling an interfaced system through the real-time application of EEG data.*

Keywords – Action potential, brain-computer interface, brain wave, central nervous system, electroencephalography data

1. INTRODUCTION

The Brain-Computer Interface (BCI) has articulated a phenomenon that bridges the neural activities in the human brain with the computer system. The study of brainwave oscillations has been conducted by pioneers since the early 1900s. However, the research on BCI technology progresses towards non-traditional advancement in recent times due to the availability of wireless means of communication [1]. Nonetheless, the emerging research on implantation for interfacing with the neural system in [2], suggests an enhancement in the brainwave data acquisition process. In hindsight, the asserted techniques of accumulating data through conventional invasive methods can be substituted by biomedical treatments as discussed in [3]. The application of the Internet of Bio-Nano Things (IoBNT), expedited the implantation of the electrodes of artificial neurons to provide state-of-the-art technological facilities. Besides, [4] proposes how a nano-generated neural network can provide improved stimulation of brainwave signals for an optimized control system. Nevertheless, the high risk of tissue damage might considerably precede the favorable features of direct stimulation of prosthesis, muscles, and the spinal cord [3]. Provided the contingency factors, the non-invasive approaches have greater possibilities of being embraced, especially in the middle-income countries around the world.

The brainwave impulses generated during neurotransmission in the Central Nervous System (CNS) can be computed and interpreted using the BCI convention. Thus, the plausibility of the system is inherently conditioned to the user's brain functionality [5, 6]. BCI essentially uses the Electroencephalography (EEG) technique for the retrieval of the aforementioned signals, in the form of frequencies and electric bio-signals [7]. Recent studies suggest that the brain's peripheral mechanism for motor functionalities is not as imperative as anticipated over the years. Generally, the EEG data produced in a paralyzed individual is indistinguishable from that of a non-paralyzed person. Therefore, BCI can be employed to obtain Neurofeedback (NFB) of the complex brain activities by restoring the envisioned stimulation [8]. Consequently, successful task completion can be facilitated by utilizing brainwave signals alone, without requiring any physical actions. Hence, it can considerably assist paralyzed and physically

impaired individuals to regain self-sufficiency through technological breakthroughs; it can also benefit the field of clinical research and studies of neuroscience applications.

Furthermore, the collected ranges of data have boundless means of implementation if executed diligently. In [9] the primary focus has been the interpretation of the correlation between the brainwave activities while playing various computer games. The fundamental aspect of a different study [10] utilizes the Steady-State Visual Evoked Potential (SSVEP) based BCI system. Whereupon, the control over an automated wheelchair has been executed as a response to visual stimulation. On the other hand, [11] analyses the composition of music in correspondence to human feelings by employing the user interface of the BCI system. In our paper, the OpenBCI Cyton board has been operated as the EEG-based device for brainwave activity determination. Generally, such devices have been extensively used due to their advantageous factors of real-time responses, portability, and affordability [12]. Moreover, the techniques applied for data acquisition in our paper, and the respective ones in [10, 14, 19] were comparable, regardless of the indication of the stimulus. For instance, [14] coordinated the visual functioning alongside the pedaling action of the user and interfaced with the system. On the other hand, [10, 19] have rather depended on the user's response to visual stimulation. On the other hand, [18] has suggested a study for improvement in stroke patients by implementing the composed brainwave data.

Nevertheless, in this paper, we have accumulated the non-invasive EEG readings by placing electrode cups throughout the surface area of the scalp. The corresponding non-intersecting brainwaves exhibited are commonly classified as delta, theta, alpha, beta and, gamma frequencies. The delta (< 4 Hz) and theta (4-7 Hz) frequencies are observed in a relatively calmer state such as in the deep-sleep or relaxed state. Alpha (8-12 Hz) waves are commonly related to passive awareness and perception, they are generally discovered in the optical region of the brain. The beta (12-30 Hz) and gamma (30-100 Hz) waves are witnessed in the higher ranges due to the association with attention, cognition, and motor functionalities, related to the central and frontal lobes of the brain [12]. For our paper, the beta, and gamma ranges of frequencies have been exclusively centred for the implementation of cognitive functioning and control-based operations. Wireless networking methodology enables the successful communication of the EEG readings with the computer system. The OpenBCI Wi-Fi shield and RFDuino are both means of wireless communication. However, we have interfaced the Wi-Fi shield to transmit the gathered data through the medium of the Internet.

2. MOTIVATION AND CONTRIBUTION

In this paper, the proposed methodology would inherently enable the paralyzed people to overcome most of the technological barriers. As per the World Health Organization, a staggering 20-50 million individuals suffer from some degree of physical impediments caused by injuries and car accidents [6]. More often than not, the victims of paralysis and physical disabilities exhibit the immaculate generation of neuro-electrical impulses identical to that of a healthy brain. This implies that the brainwave signals obtained from the EEG data of an individual can be configured to be transmitted as input commands to retain control over a designated system. In order to ensure the performance of the system, we first scrutinized the numerous prospects of the EEG data obtained through the BCI technology. The continuous stream of data documented the ceaseless activity of brainwaves in an individual. However, the distinct functionalities of the brainwave at certain instances signified the constricted ranges of the collected data. Therefore, the perceptive administration in the cognitive frequency ranges has allowed attaining technological control in real-time. Our primary objective has been to enable physically impaired individuals to subdue certain limitations through the implementation of the BCI system. Moreover, the secondary objective is to utilize the invoked potential from the user's brain activity for different real-life implementations similar to that of [10]. Unlike the tactile operating system demonstrated in [16], which depends on an external control unit-our goal is to achieve command through the implementation of brainwave signals only.

Our contributions in this paper are as follows:

- To investigate the plausibility of the incorporation of the accumulated data to gain control over the proposed system.
- To discuss the possibility of the findings through the real-time implementation of the EEG data in an exploratory approach.

The paper holds the anticipation of providing ready-to-use technology without any modification. Although, the proposed system is yet to undergo multiple further steps of trial and error before it can be actively used. Nonetheless, the model has been partially established in order to experimentally incorporate the completion of specific tasks. In addition to that, there are challenges of managing and operating the innumerable brainwave data that is being constantly collected. Furthermore, the constricted period of data processing might challenge the efficiency and complexity during the application, which also needs to be considered. The proposed methodology of the system of our paper has been discussed elaborately in Section 3. This is succeeded by, the experimental feedback generation is presented in Section 4. Lastly, results and discussion are provided in Section 5.

3. PROPOSED METHODOLOGY

The proposed methodology section intricately represents the intended system architecture of our paper, as illustrated in Fig. 1. To ensure ample competency of the system, the pathway consists of data acquisition, data processing and data implementation. The data acquisition segment focuses on the processes of receiving the EEG signals from the brain. Hence, the accumulated data from the subject emphasizes optimizing its applications by eliminating any and/or all initial errors. Upon the collection of the data, the Wi-Fi shield instantly allows the transmission to a computer by means of wireless communication. The data processing further accumulates data in the next phase, whereby it is processed in order to filter and minimize external signals, noise, jitters, etc. Thus, it ensures that the acquired data can be further processed or preserved for future analysis and applications. Moreover, the data can be configured to be globally accessible at any instance through the wireless communication of 5G devices. Besides, the signals can also be transmitted to assigned wireless systems for the observation of the generated NFB. Eventually, the data implementation section illustrates how we have experimentally implemented the data through feedback generation of the control-specific data. In our paper, two dissimilar approaches have been observed for the experimental feedback of the control applications. The detailed discussion has been mainly segmented into the three aforementioned units which have been associated with each other and described henceforth:

3.1 Data acquisition

The fundamental component employed in our paper is the OpenBCI Cyton board. The board uses the EEG technique to extract the data from the brain's neural oscillations [17]. The neural impulses are initially analyzed as Action Potentials (AP) that are commonly measured as microvolts. The illustration of the AP, also known as bio-potential of the brainwave during various activities has been compared in association to [17]. The 8-channels of the board have 8 individual electrodes connected to them, which are used for the collection of the EEG data. The electrode gold-cups are placed on the scalp of the user according to the 10-20 arrangement as observed in [10, 19], this assures the accuracy of the obtained brainwave data. Moreover, to guarantee the precise transmission of the data, conductive pastes are applied along with the electrodes. We have accumulated the featured extraction of brainwave signals accordingly. Furthermore, in our paper, a WiFi-shield has been connected along with the Cyton board which allows signal transmission and networking. Therefore, the visualization of the signals in different instances and domains can be possible through the interface with suitable applications.

However, unlike the pedaling technique of brainwave stimulation associated in [14], our approach required little to no movement but only focus control. To ensure the elimination of the motor functionalities, the experiments conducted in our paper concentrated on the cognitive and visual aspects of the user. The number of

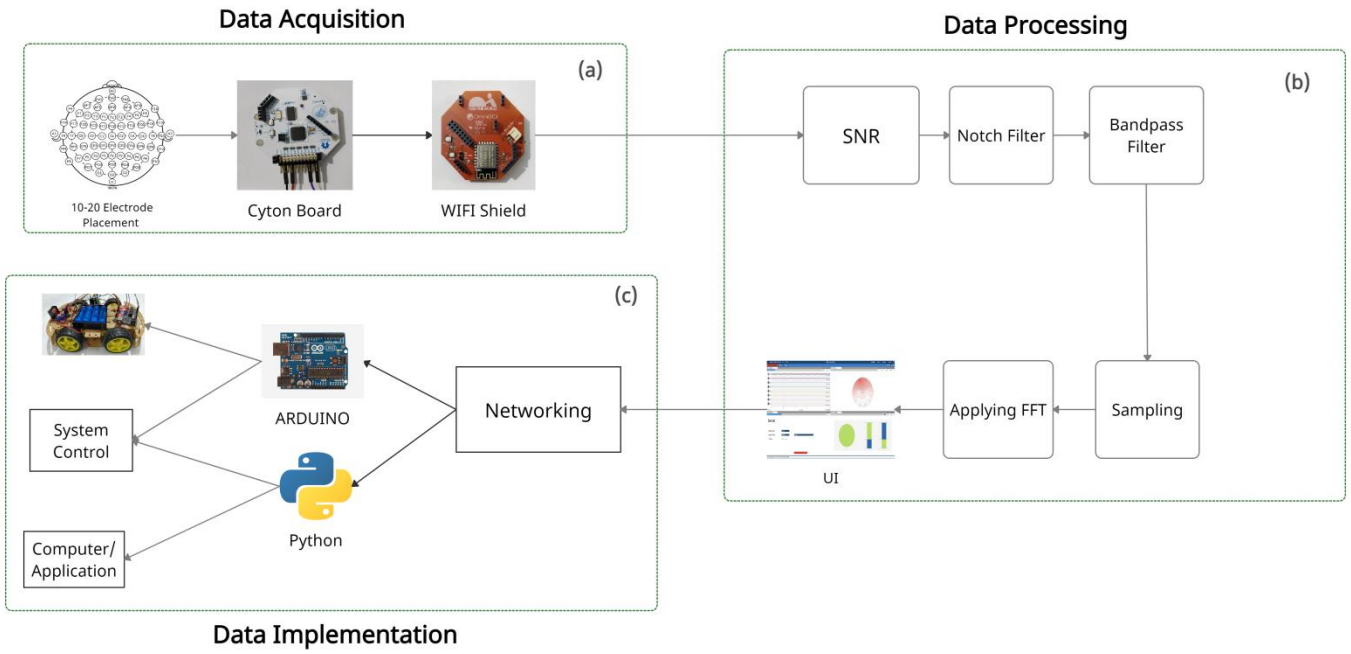

Fig. 1 – System architecture [20]

experiments we have administered thus far-essentially monitors the variations in EEG data during the motion of the arm or eye. It aspires to justify the objective of our paper by comparing the focus state and cognition to the developments in physical movement. The experiments directed in [21] have a comparable approach to that of ours. However, the control of an exoskeleton requires an expanded range of focus-control mechanisms which employs a considerable number of electrodes. In [21], the connectivity of the extensive driver circuits is maintained by the 16-electrodes channels that provide higher accuracy of brainwave data.

As discussed earlier, the inherent performance of the brain associated with the intellectual and comprehensive features remains consistent regardless of the capability of muscle control [6]. Although the subject of our paper exhibits the functionality of a healthy brain, the constrained ranges of the accumulated EEG data has facilitated the execution of the applications as designed. Consequently, [6] administered the control of brainwave frequency in the ranges 0.15-5 Hz in the time-span of 300-600ms by the commonly used P300 in the BCI system. On a similar account, [10, 14, 17-19] represents the manipulation of the acquired brainwave data in the targeted bandwidth for the respective allocations.

3.2 Data processing

As per Fig. 1, the acquired brainwave data requires extensive steps of processing and optimization before it can be analyzed. Thus, the discussion in [10] embodies the construction of the anticipated data processing operations through the user interface. Our foremost concern is the noise interferences associated with the raw brainwave data. Ordinarily, the non-invasive method contributes to the factors of noise since brainwave frequencies are not being directly extracted. Natural obstacles existing between the electrodes and the brain, i.e. the skull, skin, hair, etc. as well as artefacts (muscular movements) contribute to the noises [19]. To optimize the data, the user interface applies a Signal-to-Noise Ratio (SNR) for strengthening the signal that is estimated by applying the root-mean-square [10, 18]. Furthermore, signal filtering and sampling facilitate the selection of the desired ranges of data to be executed accordingly. The sampling theory of Nyquist-Shannon ensures that the accumulated EEG signals are sampled at a frequency of 250 Hz by the user interface applications [19]. Upon the passage of the frequencies through the Butterworth filters, the aspired ranges are separated for assigned requisitions. Additionally, the presence of electronic devices that emit electromagnetic waves of 50-60 Hz can cause distortion. Hence, to eliminate the specific bandwidth, notch filters are applied in the system.

Moreover, the Fast Fourier Transform (FFT) approach allows the observation of the brainwaves in the frequency-domain corresponding to the AP or bio-potential readings [10, 14]. Hence, this provides a more transparent comprehension of the acquired data when examined.

3.3 Data implementation

Henceforth, the accumulated data undergoes further networking for implementation purposes. For instance, a Lab Streaming Layer (LSL) networking protocol is employed to transmit the data from one application to another. Correspondingly, the optimized brainwave data in our paper has been transferred from the OpenBCI network to the Python application. This has permitted the user for visualization and controlled scrolling of newsfeed through EEG data. The communication between such applications yields the graphical representation of the brainwave AP in various domains as illustrated in [19].

In the case of interfaces with microcontrollers such as the Arduino, a serial communication protocol is exercised. The streaming of the brainwave signal in our paper has been enabled by the networking widget of the OpenBCI application. The successful serial communication has been sustained through the maintenance of the designated baud rate of EEG data streaming. Moreover, the transmission is implemented for NFB generation through the assigned receiving ports of the Arduino. As demonstrated in [10], the final implementation of controlling a wheelchair has been successfully achieved through the interfaced microcontroller. Therefore, it can be implemented for numerous other purposes such as robotics, neuroprosthetics, control of gadgets, appliances, and vehicles. Moreover, the use of diverse microcontrollers may as well accomplish related applications. For example, in [14] the pedaling bike was interfaced with the computer through the Raspberry Pi. Further discussion of the conducted experimental NFB generation in our paper is continued in the next section.

4. EXPERIMENTAL FEEDBACK GENERATION

4.1 Hardware implementation

The assertion of the earlier experiments depends on the support of the outcomes of the feedback generation observed. As orchestrated in Fig. 2, the Arduino relies on the serial communication networking protocol. In our paper, the NFB of EEG data was delivered through hardware implementation of the Arduino. Hence, it has allowed the accumulated data to be used for control and observation. Thus far, we have retained the motion of a small-scale car by utilizing the generated EEG feedback. The authority is maintained in the focus-state frequency ranges of the brainwave signals. Nonetheless, it is essentially a representation of the motion and direction control of a large-scale carrier, such as a wheelchair. In comparison to the electric wheelchair control in [10] and the bike pedaling in [14], where the visual stimulation required a cue/signal such as LED, stimulation as such was not imposed in our paper. Rather, the control of the car was perceived at the very instance the user accessed their focus-state. The user continued to operate the motion of the car upon the period of concentration and high cognitive functioning. It further enabled the user to control the direction of the car by propelling cognitive thought processes and absolutely no other means of administration. Eventually, the car immediately stopped when the focus state was departed.

4.2 Software control observation

Furthermore, the feedback generation of our paper was further observed through computer software applications. As illustrated in Fig. 2, LSL networking enables data transmission from the user interface to a Python application. Hence, the controlling of the newsfeed and computer screen has been conceivable. Similarly, in [5], cursor control was obtained by using the EEG data from the BCI. Suggesting that further precision in controlling virtual platforms can be achieved by enhancing goal-oriented or high-level programming language. For instance, the visual

cortex of the occipital lobe can enable the user to spell out the visualized words and letters as shown in [15]. However, to deliver such precise commands in any system, deep learning of the data is imperative. As associated in [13], the machine learning algorithm of deep learning concentrates on the advancements of precision-control in automated systems. This can benefit the obtained feedback generation of our paper to incorporate concrete real-life applications in the future.

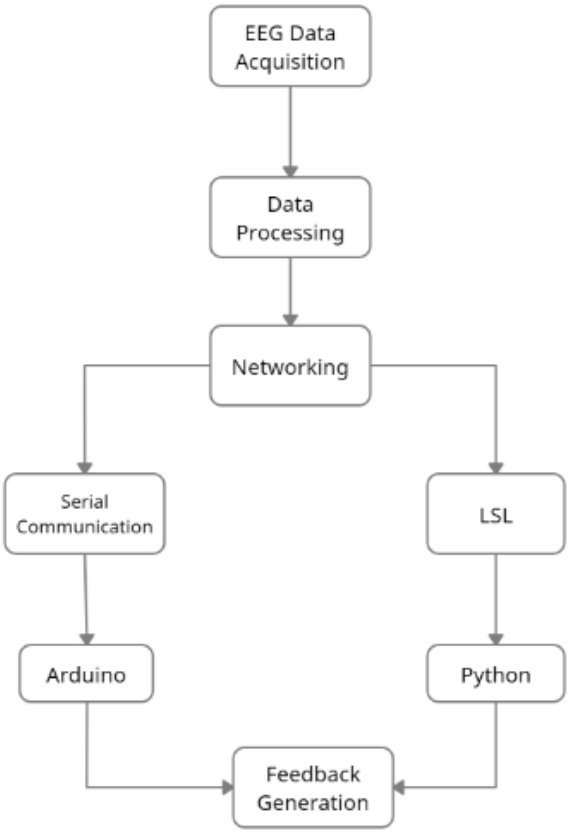

Fig. 2 – Experimental feedback generation

4.3 Parameter settings

In Section 4.1 and Section 4.2, hardware implementation and software control implementation were observed by utilizing the data streaming of an EEG reading from the person. Correspondingly, the EEG data generated from mostly the parameter setting depends on the pathway taken to filter the signal. Most of the time depending on the desired frequency range the filter setting changes to bandpass filter. For instance, to find out cognitive functioning EEG data, electrodes are attached to the frontal lobe, where to get rid of external electrical influence a notch filter is used. In addition, a bandpass filter of 5-50Hz is used, which is the brain activity wave except for the delta which is experienced during meditation or dreamless sleep and the amount of sample rate varies depending on the outcome expectation but mostly the used sample rate is 255Hz [18]. Moreover, maximum frequency can be opted for according to the preference which could be from 20Hz to 400Hz. Again, to make the data transmitted to Arduino or Python workable mapping of the data is required. Moreover to that, mapped data is used in the completion of tasks or controlling a system.

5. RESULT AND DISCUSSION

Continuing on from the previous discussion, motion control of a car with the assistance of Arduino has been successfully implemented by utilizing the acquired brainwave data exclusively. The Arduino-based robotic car has been through multiple trials for motion control where the brain wave signals were used to enforce the focus and concentration state on a real-time basis [20]. Looking at Fig. 3, we can see that 3(a) displays the bio potential of the brainwave in the frequency domain while 3(b) and 3(c) display the head region activity at the instances. In Fig. 3(a), 2 channels were attached to the frontal lobe while acquiring concentration state data. In 3(a) the FFT plot of the potential values are majorly active in the alpha (8-12 Hz) and beta (13-32 Hz) frequency ranges. This information implies that the focus state is activated in the aforementioned bandwidths and the car gains motion correspondingly. Thus, the motion and direction of the car can be controlled with concentration. However, the car immediately stops moving the very moment the focus state is departed. Furthermore, the head region plots 3(b) and 3(c), display high activity in the frontal and central lobe. The highlighted regions of the respective lobes are distinctly represented in the event of cognitive and motor functionalities.

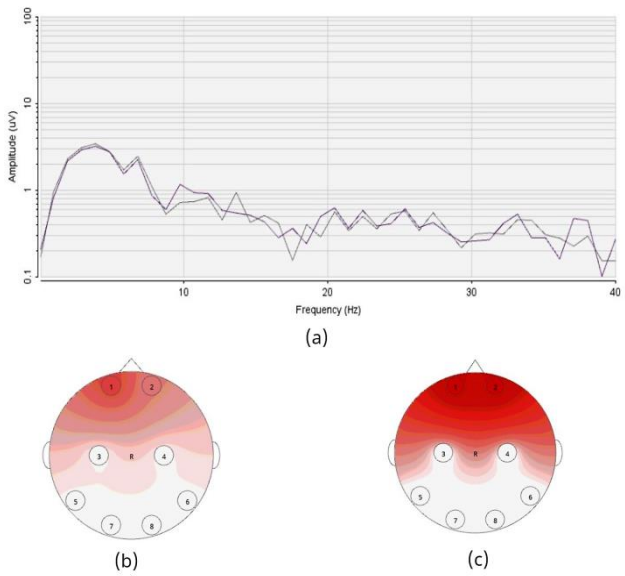

Experiment-1

Fig. 3 – Hardware implementation observation

Additionally, brainwave data has also been implemented in [20] for the control system of scrolling through computer applications. Thus, the user has been able to surf through a news feed or webpage while within the focus state as discussed earlier. In Fig. 4, 4(a) shows the FFT plot of the EEG data, 4(b) and 4(c) shows the head region plots during the monitoring and controlling of the virtual screen. For Fig. 4(a), on the head scalp near the occipital region one channel was attached to acquire the visualization data. As indicated in 4(a), the ranges of potential spikes are over a wider range of frequency. However, the head region plots display activity in the occipital region which wasn't as visible in the previous section. The mapping of the EEG data between the frontal and occipital lobe has enabled the opportunity to control the cursor by comparison of the action potentials. Further precision of the control can be enabled through deep learning techniques of the brainwave data.

The fundamental aspiration of the paper was to successfully acquire brainwave data with the assistance of the OpenBCI Cyton board in real-time. Upon the initial observation of the collected data, it emerged as a burst of reading due to the continuous brain activity. Since the brain is continuously generating signals, the data accumulation in the aspired range for application has been considerably challenging.

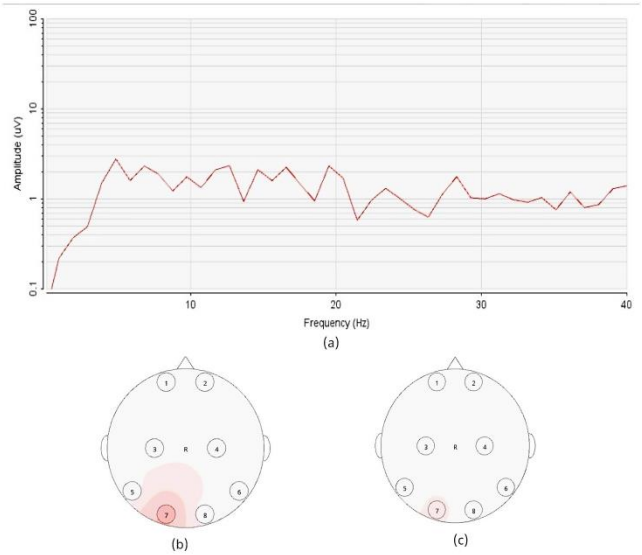

Experiment-2

Fig. 4 – Software control observation

Additionally, the noise factors are incorporated in the distortion of the quality of the raw data. The invariable muscular movements were incorporated as noise artefacts that required further extensive processing. Hence, the constraints over the potential values were challenging hindrances while attempting to accumulate the desired frequency ranges in order to implement certain requirements as per the respective cases.

Furthermore, the motion control of the car experiment suggested that the slightest deviation of the correspondence between the frontal and the parietal lobe can cause a significant disparity in the motion of the car. Similarly, the cursor control system may lack stability caused by equivalent factors. Hence, any inconsistency of focused cognitive functioning may disrupt the entire control system regardless of the system outcome. Nonetheless, our analysis establishes the fact that specific tasks can be performed up to a certain degree by utilizing EEG brainwave data. For further accuracy of the implementation of the feedback generation, more precision is required through machine learning approaches.

Table 1 – Data table for cognitive functioning

Channel 1	Channel 2
–8762.24	–1654.23
–8680.41	–1641.42
–7665.33	–2408.71
–7226.03	–2746.78
–7854.65	–2301.63
–8755.38	–1620.7
–8709.45	–1639.95
–7669.87	–2445.26
–7241.63	–2752.37
–7833.17	–2260.28
–8733.85	–1601.48
–8707.7	–1643.84
–7682.54	–2453.39
–7209.76	–2752.51
–7824.81	–2268.88
–8728.29	–1647.03
–8722.86	–1656.98
–7701	–2421.3
–7238.48	–2782.5
–7821.79	–2314.9
–8732.8	–1594.57

Table 1 illustrates the raw data of brainwave reading during cognitive functioning. The subject was asked to read and concentrate between the focus and out-of-focus state. During which, only the channels connected to the frontal region of the brain were kept activated. The collected data is transmitted to Arduino through means of serial communication, and thus, the motion of the car is controlled.

Furthermore, Table 2 demonstrates a portion of the data table from the acquired brainwave connected to a single channel in the occipital region of the brain. However, the tables provide the raw data that had been initially obtained. Henceforth, the use of Python and the lab streaming layer allowed the live streaming of the brainwave data, which was observed during the software control task.

Table 2 – Data table for occipital functioning

Channel 7	Channel 8
–45548	0
–45529.09	0
–45505.09	0
–45511.95	0
–45524.82	0
–45539.8	0
–45550.55	0
–45539.89	0
–45545.79	0
–45539.69	0
–45525.16	0
–45503.43	0
–45484.52	0
–45492.59	0
–45491.92	0
–45496.77	0
–45506.79	0
–45513.67	0

6. CONCLUSION

The analysis of the brainwave signals developed over the decades has laid the foundation for the notion of the BCI-based control system. The possibilities of implementing BCI can have a profound impact on all branches of science and technology, creating opportunities for every individual regardless of their physical capabilities. The IoT based brainwave assistive system for paralyzed individuals is designed to attain opportunities as such. The results achieved thus far, delivers beneficial analysis and provides insights on further potential of the brainwave data. However, our future aspects of the paper envisions precision control of large-scale automated devices such as a wheelchair. Hence, for expanding accuracy control through further propagation of the data, machine learning propositions will be incorporated to the current paper.

ACKNOWLEDGEMENTS

We would like to convey our heartfelt gratitude to the Department of Information and Communication Technology (ICT Division) of the Bangladesh Government, for their generous support as the sponsor of our paper.

REFERENCES

[1] F. Lotte, C. S. Nam, and A. Nijholt, "Introduction: Evolution of Brain-Computer Interfaces," Brain-Computer Interfaces Handbook: Technological and Theoretical Advance, Taylor & Francis (CRC Press), pp. 1–11, 2018, doi: 9781498773430 ⟨hal-01656743⟩.

[2] D. Accoto, M. T. Francomano, A. Rainer, M. Trombetta, P. M. Rossini, and E. Guglielmelli, "An implantable neural interface with electromagnetic stimulation capabilities," Medical Hypotheses, vol. 81, no. 2, pp. 322–327, May 2013, doi: https://doi.org/10.1016/j.mehy.2013.04.008.

[3] O. B. Akan, H. Ramezani, M. Civas, O. Cetinkaya, B. A. Bilgin, and N. A. Abbasi, "Information and Communication Theoretical Understanding and Treatment of Spinal Cord Injuries: State-of-the-art and Research Challenges," IEEE Reviews in Biomedical Engineering, Feb. 2021, doi: https://doi.org/10.1109/RBME.2021.3056455.

[4] S. Lee, H. Wang, Q. Shi, L. Dhakar, J. Wang, N. V. Thakor, S.-C. Yen, and C. Lee, "Development of battery-free neural interface and modulated control of tibialis anterior muscle via common peroneal nerve based on triboelectricnanogenerators (TENGs)," Nano Energy, vol. 33, pp. 1–11, Mar. 2017, doi: https://doi.org/10.1016/j.nanoen.2016.12.038.

[5] X. Gu, Z. Cao, A. Jolfaei, P. Xu, D. Wu, T.-P. Jung, and C.-T. Lin, "EEG-based Brain-Computer Interfaces (BCIs): A Survey of Recent Studies on Signal Sensing Technologies and Computational Intelligence Approaches and their Applications," IEEE/ACM Transactions on Computational Biology and Bioinformatics, Jan. 2020, doi: arXiv:2001.11337.

[6] A. Raj and S. M. Jaisakthi, "Analysis of Brain Wave Due to Stimulus Using EEG," 2018 International Conference on Computer, Communication, and Signal Processing (ICCCSP), Chennai, 2018, doi: 10.1109/icccsp.2018.8452823.

[7] K. Uno, G. Naito, Y. Tobisa, L. Yoshida,Y. Ogawa, K. Kotani and Y. Jimbo, "Basic Investigation of Brain–Computer Interface Combined with Augmented Reality and Development of an Improvement Method Using the Nontarget Object," Electronics and Communications in Japan, vol. 98, no. 8, pp. 9–15, Jul. 2015, doi: 10.1002/ecj.11715.

[8] S. Kono and T. M. Rutkowski, "Tactile-force brain-computer interface paradigm Somatosensory multimedia neuro-technology application," Multimedia Tools and Applications, vol. 74, pp. 8655–8667, Oct. 2015, doi: 10.1007/s11042-014-2351-1.

[9] A. G. Bakaoukas, F. Coada, and F. Liarokapis, "Examining brain activity while playing computer games," J Multimodal User Interfaces, vol. 10, pp. 13–29, 2016, doi: https://doi.org/10.1007/s12193-015-0205-4.

[10] Y. Li, K. K. Ang, and C. Guan, "Digital Signal Processing and Machine Learning," Brain-Computer Interfaces, The Frontiers Collection, Springer, Berlin Heidelberg, pp. 305–330, Sep. 2010, doi: 10.1007/978-3-642-02091-9_17.

[11] M. Numao, T. Nishikawa, T. Sugimoto, S. Kurihara, and R. Legaspi, "Constructive Adaptive User Interfaces Based on Brain Waves," Human-Computer Interaction, Springer-Verlag Berlin Heidelberg, vol. Part II, no. HCII 2009, pp. 596–605, 2009.

[12] Vaibhaw, J. Sarraf, and P. K. Pattnaik, "Brain-computer interfaces and their applications," An Industrial IoT Approach for Pharmaceutical Industry Growth, vol. 2, pp. 31–54, 2020, doi: https://doi.org/10.1016/B978-0-12-821326-1.00002-4.

[13] M. Rashid, N. Sulaiman, A. P. P. Abdul Majeed, R. M. Musa, A. F. Ab. Nasir, B. S. Bari, and S. Khatun, "Current Status, Challenges, and Possible Solutions of EEG-Based Brain-Computer Interface: A Comprehensive Review," Frontiers in Neurorobotics, Jun. 2020, doi: 10.3389/fnbot.2020.00025.

[14] M. A. Romero-Laiseca, D. Delisle-Rodriguez, V. Cardoso, D. Gurve, F. Loterio, J. H. PossesNascimento, S. Krishnan, A. Frizera-Neto, and T. Bastos-Filho, "A Low-Cost Lower-Limb Brain-Machine Interface Triggered by Pedaling Motor Imagery for Post-Stroke Patients Rehabilitation," IEEE Transactions on Neural Systems and Rehabilitation Engineering, vol. 28, no. 4, pp. 988–996, April 2020, doi: 10.1109/tnsre.2020.2974056.

[15] K. S. Mistry, P. Pelayo, D. G. Anil, and K. George, "An SSVEP based brain computer interface system to control electric wheelchairs," 2018 IEEE International Instrumentation and Measurement Technology Conference (I2MTC), Houston, TX, 2018, doi: 10.1109/ i2mtc.2018.8409632.

[16] Y. Y. Jang, T. H. Kim, and B. H. Lee, "Effects of Brain–Computer Interface-controlled Functional Electrical Stimulation Training on Shoulder Subluxation for Patients with Stroke: A Randomized Controlled Trial," Occup. Ther. Int., vol. 23, no. 2, pp. 175–185, Jun. 2016, doi: 10.1002/oti.1422.

[17] S. P. Zavala, J. L. L. Bayas, A. Ulloa, J. Sulca, J. L. M. López, and S. G. Yoo, "Brain Computer Interface Application for People with Movement Disabilities," International Conference on Human Centered Computing, vol.11354, pp. 35-47, Mar. 2019, doi: https://doi.org/10.1007/978-3-030-15127-0_4

[18] M. D. Novitasari, A. D. Wibawa, M. H. Purnomo, W. R. Islamiyah, and A. Fatoni, "Investigating EEG Pattern During Designed-Hand Movement Tasks in Stroke Patients," 2020 International Seminar on Intelligent Technology and Its Applications (ISITIA), Surabaya, Indonesia, pp. 141-147, 2020, doi: 10.1109/isitia49792.2020.9163680.

[19] A. Guerra, D. Caceres, F. Merchan, and K.-H. Jo, "Real Time Operator Focus Monitoring System Based on a Brain-Computer Interface," 2020 IEEE 29th International Symposium on Industrial Electronics (ISIE), Delft, Netherlands, pp. 1415-1420, 2020, doi: 10.1109/isie45063.2020.9152264.

[20] S. M. Monowara, M. A. Shariar, M. S. U. Islam, and M. J. N. Jawad, "IoT Based Brain-Wave Assistive System for Paralyzed Individuals", B.Sc. Thesis, Electrical and Electronic Engineering, Brac University, Dec. 2020.

[21] P. G. Vinoj, S. Jacob, V. G. Menon, S. Rajesh, and M. R. Khosravi, "Brain-Controlled Adaptive Lower Limb Exoskeleton for Rehabilitation of Post-Stroke Paralyzed," IEEE Access, vol. 7, pp. 132628–132648, 2019, doi: 10.1109/access.2019.2921375.

AUTHORS

Md Ahnaf Shariar is currently pursuing his degree of Bachelor of Science in Electrical and Electronic Engineering, BRAC University, Bangladesh. He is currently working as an intern as a software and architectural visualization developer in a software company. He is interested in robotics and has participated in numerous robotics competition and secured several prizes in those competitions. He had been in the position of General Secretary of the Robotics club of Brac University.

Syeda Maliha Monowara is currently pursuing her degree of Bachelors of Science in Electrical and Electronic Engineering, BRAC University, Bangladesh. She is interested in the research of robotics, neural networks and, neuroscience. She also aspires to work towards the betterment of humanity through applications of engineering.

MD. Shafayat Ul Islam as of late finished his graduation with a Bachelor of Science from BRAC University, Bangladesh. He is at present filling in as a data analyst in an outsourcing company. He is keen to work in the field of robotics and technology management.

Muhammed Junaid Noor Jawad is a recent graduate of BRAC University, Bangladesh with a Bachelor of Science degree in Electrical and Electronic Engineering. His current scientific interest include artificial intelligence, neural networks and intelligent robots.

Saifur Rahman Sabuj was born in Bangladesh. He is currently working with the Electronics and Control Engineering Department as a Postdoctoral Research Fellow at Hanbat National University, South Korea. He has been in the position of an assistant professor in the department of Electrical and Electronic Engineering at BRAC University, Bangladesh, since September 2017. From 2008 to 2013, he was a faculty member of Green University of Bangladesh, Metropolitan University, Sylhet and Bangladesh University. He received a B.Sc in Electrical, Electronic and Communication Engineering from Dhaka University, Bangladesh in 2007, an M.Sc at Engineering in the Institute of Information and Communication Technology, Bangladesh University of Engineering and Technology, Bangladesh in 2011, and a Ph.D. degree from the Graduate School of Engineering, Kochi University of Technology, Japan in 2017. His research interests include MIMO-OFDM/NOMA, Cooperative Communication, Cognitive Radio, Internet-of-things, Unmanned Aerial Vehicle and machine-to-machine for wireless communications.

RATE CONTROL FOR THERAPEUTIC APPLICATIONS IN INTERNET OF BIO-NANO THINGS USING MOLECULAR COMMUNICATION: A SURVEY

Shirin Salehi[1], Naghmeh Sadat Moayedian[2], Mohammad Taghi Shafiee[1]
[1]Communications Regulatory Authority, Ministry of ICT, Iran, [2]Department of Electrical and Computer Engineering, Isfahan University of Technology, Isfahan 84156-83111, Iran

NOTE: Corresponding author: Naghmeh Sadat Moayedian, moayedian@cc.iut.ac.ir

Abstract – *Molecular communication is transmitting and receiving chemical signals using molecules and is an interdisciplinary field between nanotechnology, biology, and communication. Molecular communication can be used for connecting bio-nano things. The connected nano-things build a nano-network. Transport mechanisms in molecular communication include free diffusion, gap junction channels, molecular motors, self-propelling microorganisms like bacteria and random collision of mobile nano-things. Free diffusion is the most widely used transport mechanism in the literature. Brownian motion is always available and its energy consumption is zero. This paper explores the therapeutic applications of rate control in the Internet of Bio-Nano Things and reviews the recent trends and advancements in the field of molecular communication. These methods aim to guarantee the desired rate of drug molecules at the target site and overcome the side effects of excessive emission.*

Keywords – Bio-nano things, molecular communication, release rate control, targeted drug delivery

1. INTRODUCTION

Nanomachines are the most basic operational units with dimensions of several hundred nanometers to a maximum of a few micrometers and have limited capabilities. They can perform simple tasks such as sensing, stimulating, calculating and storing information. In order to increase the capabilities of nanomachines and use them in real scenarios, a network must be formed between them. In this way, nanomachines are able to collaborate, combine or share information. The connection of these nanomachines is called a nano-network [1]. In fact, nano-networks are a new research branch that results from the use of nanotechnology in the field of digital communications [2, 3]. The very small size of nanomachines makes the physical telecommunication channels in nano-networks significantly different from traditional wireless and wired channels. Currently, there are two methods for connecting nanomachines: nano-electromagnetic communication and molecular communication [1].

Nano-electromagnetic communication is the sending and receiving of electromagnetic waves between nanoscale components. There is ambiguity about how nano-antennas can be achieved by shrinking existing antennas. The frequency released by the antenna comes from the $f \propto \frac{v}{L}$, in which v is wave propagation speed and L is antenna length, so in the expected size of a nanomachine, the frequency released by nano-antenna will be in the optical range (hundreds of THz). Although this frequency leads to a lot of bandwidth, it will also have a lot of loss, which causes the range of these nano-antennas to be almost zero, so traditional electromagnetic telecommunication methods must be deeply revised before using them in new scenarios [4].

To overcome these limitations, graphene-based nano-antennas are provided. Graphene is a form of carbon composed of flat sheets with the thickness of an atom in which atoms are placed as honeycomb lattices. Due to its specific properties, graphene-based nano-antennas will radiate at a lower frequency than the Terahertz band, and the channel attenuation will be much less at this frequency, therefore, graphene-based nano-antennas allow for nanoscale electromagnetic communication [5, 6].

Molecular communication is a new method that is inspired by the communication between living cells. In molecular communication, information is transmitted through message molecules [7]. The advantages of this solution compared to nano-electromagnetic communication are inherent nanoscale, biocompatibility and low energy consumption [8]. In molecular communication, chemical signals or molecules are sent and received. There are many differences between molecular communication and traditional communication: In molecular communication, the message is encoded in molecules, whereas in traditional networks, information is encoded in electromagnetic, audio and optical signals. The rate of wave propagation in traditional networks is much faster than the speed of the propagation of molecular messages. In addition, in molecular communication, most of the energy consumed is chemical and power consumption is low, while electrical energy is used in traditional networks.

Molecular communication can be effective in medical applications due to their biocompatibility [9, 10, 11, 12]. The components of molecular communication are: transmitting nanomachine, receiving nanomachines, messenger molecules, interface molecules and transport mecha-

nisms [13]. There are five transport mechanisms which include free diffusion, gap junction channels, molecular motors, self-propelling microorganisms and random collision of nanomachines. Molecular communication systems can be classified with various criteria as shown in Fig. 1:

a) Scale: The molecular communication scale refers to the distances at which bio-nanomachines interact with each other by releasing molecules and is divided into three categories: intracellular, intercellular and inter-organ [14]. Similarly, bio-nanomachines are divided into three categories, short-range such as molecular motors, medium-range such as ion signaling and transmission through diffusion, and finally long-range transmission such as transmission based on bacteria, neurons and pheromone signaling [7]. Pheromone is a chemical agent secreted or excreted, leading to the stimulation of a collective response in members of a species.

b) Energy consumption: Molecules are either dispersed in the environment or released directionally by chemical energy consumption, which is called Passive Molecular Communication (PMC) and Active Molecular Communication (AMC) [15, 14], respectively.

c) Communication type: Molecular communications can be divided into two categories: wired and wireless.

i) Wired: Refers to methods that require a physical link to transmit signals [8] and they are also called Walkway-based methods [16]. For example, microtubules are provided in micro-dimensions to connect nanomachines. Data transfer between nanomachines is done through the movement of molecular motors that walk on microtubules. Another example of wired molecular communication is neuronal messaging that is placed in the category of inactive molecular communication [17].

ii) Wireless: Wireless methods refer to methods that require only a fluidic medium (such as air, water and blood) without the need for electrical conductors or physical links to transmit information [8]. Most current molecular communication methods mimic wireless communication samples. This is due to the similarity of natural biological communication systems with wireless communication systems. Of course, the fundamental difference is that the distribution of molecules is slow compared to the propagation of radio waves. One example of this method is calcium signaling. In this method, the propagation of waves between cell junctions is carried out in densely packed cell tissue. Calcium waves are commonly used to transmit short-range information between cells where information is coded in the concentration of calcium ions. Another example of wireless data transmission is the use of bacteria [17]. The wireless method can be divided into two categories: A) Flow-based: In this method, molecules are released through diffusion in a fluidic medium such as blood flow. Intra-body hormonal communication is the most important example of this method [16]. B) Diffusion-based: In this method, molecules are propagated by diffusion in a fluidic medium and molecules only follow the rules of random walk. Pheromonal communications, calcium signaling and quorum sensing in bacteria are examples of this method [16]. Quorum sensing is a population-proportional stimulation and response system that bacteria use to coordinate with each other.

Medical applications, such as Targeted Drug Delivery (TDD), activation of the immune system and tissue engineering, are one of the most important application categories of molecular communication. In such scenarios, rate control mechanisms play an essential role. In TDD, rate control is indispensable to maintain the drug concentration between the Least Effective Concentration (LEC) and the Maximum Tolerated Concentration (MTC). Moreover, bio-nanomachines generally bear a limited resource, therefore releasing the drug molecules at the optimal rate is of significant importance. Controlling the rate of activators or antagonists is also indispensable in the immune system activity scenario i.e., to intensify or reduce the activity of the immune system. The rate control is required as well in tissue engineering scenarios to ensure the prolonged exposure of the damaged tissue to the growth factors. Considering the importance of rate control in therapeutics applications, this paper aims to review the state-of-the-art literature on rate control using molecular communication.

The organization of this paper is as follows: Rate control in molecular communication with a layer architecture perspective is investigated in Section 2. Section 3 presents the therapeutic applications of rate control. Section 4 reviews the recent advancements and current research on releasing rate control in DDS. Research opportunities are presented in Section 5. Section 6 concludes this paper.

2. RATE CONTROL IN MOLECULAR COMMUNICATION

Molecular communication architecture can be examined from the perspective of communication networks [18, 14, 19]: molecular physical layer, molecular link layer, molecular network layer, molecular transport layer and molecular application layer. Since our paper is focused on rate control in molecular communication, we review the existing works in the transport layer. This layer provides the functions needed for end-to-end transmission and is responsible for providing reliability, In-sequence delivery, congestion control and flow control. Rate control in molecular communication is carried out for two purposes: Flow control and congestion control.

2.1 Flow control

Flow control is a function in which the sender adjusts the transmission rate of the molecular transmission layer based on the receiver's characteristics. Flow control can be started by the sender or receiver [19]:

i) Transmitter initiated flow control: The easiest form of flow control is that the sender uses a very low transmission rate so that there are no losses. This requires prior

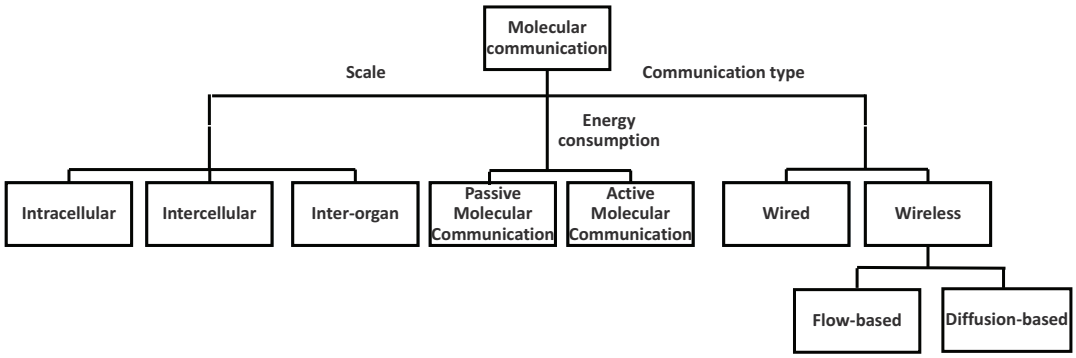

Fig. 1 – Classification of molecular communication based on scale, energy consumption and communication type

knowledge of the recipient's processing capabilities. A more complex shape requires the transmitter to be able to detect the losses of molecular frames. The transmitter may feel the existence or absence of expected chemical reactions in the receiver in the environment and adjust the sending rate accordingly.

ii) Receiver-initiated flow control: When the recipient's molecular storage is filling up, the receiver informs the transmitter by sending feedback. This form of flow control is commonly used in traditional communication. So far, only one method of flow control initiated by the receiver has been studied in [20, 18]. In order to control the flow of information in traditional networks, the recipient announces a window size to the sender, meaning that the unacknowledged number of bytes of the sender should not exceed that value at any given moment. If the recipient reads the information as fast as it reaches, the window will remain open, otherwise, the window size will be reduced by reaching each segment to eventually reach zero. In [18], N senders and M receivers are considered. First, an optimization problem is proposed to find the maximum throughput and efficiency according to the sender's transmission rate. Throughput is the number of molecules processed by receptors per unit time. Efficiency is throughput divided by the number of molecules sent per unit time. For simplicity, it is assumed that all transmitters are located at the origin and all receivers are located at a similar location. With this assumption, a mathematical expression is obtained for the upper bound of throughput and efficiency. Then, the optimal transmission rate that maximizes them is calculated numerically. It can be seen that there is a compromise between throughput and efficiency. In the following, [18] presents a method for controlling the transmission rate using positive and negative feedback. In this method, the receiver bio-nanomachine releases feedback molecules in the environment in response to the transmitter. The transmitter bio-nanomachine then regulates its transmission rate based on the concentration of feedback molecules. In the Negative Feedback (NF) the transmitter bio-nanomachine reduces the transmission rate by increasing the concentration of feedback molecules. In the Positive Feedback (PF), the opposite is true. Simulation results show that the negative feedback-based method provides maximin strategy by changing the number of transmitters, number of receivers, molecule degradation rate, diffusion coefficient and location, i.e. maximizes the minimum throughput. The positive feedback method is also a maximin strategy for efficiency by changing the number of receivers, diffusion coefficient and degradation rate of molecules, i.e. maximizes the minimum efficiency.

In [12], a TCP-like protocol is proposed to find the optimal transmission rate between the transmitter and receiver and prevent congestion in molecular communication. In this method, the transmitter is assumed to be very simple and the receiver acts as a control node and sends the connection signal to the transmitter. This triggers the transmitter to release molecules. The transmitted molecules are released in the environment and are absorbed by the receptors on the receiver surface. When the receiver absorbs the desired amount of the transmitter molecules, it releases a disconnection signal to prevent the transmitter from continuing the transmission. Similar to the TCP transmitter, which is not already aware of the maximum network capacity, the transmitter first increases the transmission rate. In TCP, this increase is done exponentially in the first step and in the stage of avoiding congestion linearly with the round trip time. In this scenario, for simplicity, only a linear rate increase is considered. Then, the receiver decides to halve or stop the transmission rate according to the round trip time.

2.2 Congestion control

Congestion control is used to regulate the number of molecular transfer data units in order to prevent congestion in the middle nodes. This can be done by setting the sender's transmission rate. By detecting an error, the sender's transmission rate can be reduced to a specified predetermined value. It is also possible to calculate the new transmission rate according to the amount of congestion. Congestion can be detected from the error rate. After the rate decreases, the sender may start to increase the sending rate again so that it can use the maximum channel capacity. The amount of this increase can be constant or

depends on a network parameter (e.g. how long the error hasn't occurred), in which case remembering the history is necessary.

In the past 30 years, the issue of congestion control in packet networks has been considered by many researchers. However, little attention has been paid to this issue in molecular networks [21]. In [21], congestion is defined as the inability of the receiver to accept all molecules in the receiver space and the congestion control problem has been investigated in a drug delivery scenario. This limitation occurs for two reasons: limited number of receptors at the receiver surface and significant trafficking time. Trafficking time is defined as the time required for a ligand to bind a receptor plus the time needed to internalize the complex. In [21], theoretical analysis of congestion reasons in a diffusion-based molecular communication is carried out and a receiving model including a set of queue systems is presented.

3. THERAPEUTIC APPLICATIONS OF RATE CONTROL

3.1 Targeted drug delivery

In drug delivery applications, if the transmitter sends molecules at a higher rate than what the receiver can process, these molecules will disperse in the environment and can lead to adverse side effects in other areas. Also, since drug molecules are expensive in some cases, it is important to prevent the loss of these molecules.

Molecular communication enables new methods of drug delivery by creating cooperation between nanomachines. For example, a large number of bio-nanomachines can be injected into a patient's body to perform massively parallel searches of the diseased site. When the bio-nanomachine detects the signal molecule secreted by the disease site, it will amplify the signal molecule, thereby increasing the concentration of the signal molecule in the environment, causing more bio-nanomachines to reach the disease site. A group of bio-nanomachines at the target site can also communicate via quorum sensing to estimate the number of bio-nanomachines in the environment and increase (or decrease) the rate of drug release if the number of nanomachines is small (or large) to achieve the continuous release of drug molecules into the environment. A group of bio-nanomachines with different functions can also be used to detect different environmental conditions, communicate to aggregate sensed conditions, and perform complex calculations such as logic calculations to determine whether drug molecules are released [14]. Another example of collaboration between nanomachines using molecular communication is encapsulated drug transmitters that help to increase the lifetime of a drug delivery system and solve the problem of limited reservoir capacity, as described in [22]. These methods are designed to maximize the therapeutic effects of drug molecules; therefore, a group of nanomachines must communicate with each other at the target site to adjust the rate of release of drug molecules based on different conditions, such as the spatial distribution of target cells and bio-nanomachines.

TDD enables local drug delivery, which is not possible with systemic drug delivery. By placing the drug delivery system near the tumor site, the drug is released only at the site of the disease and the drug level is low in other sensitive areas of the body [23]. On the other hand, other drug delivery systems that are injected intravenously may be rapidly excreted by cleansing organs such as the kidneys, which can lead to healthy tissue being exposed to toxic levels of the drug. To address these problems, local methods such as intra-tumor injection and drug release in the vicinity of unhealthy tissue have been studied, including [24, 25] to treat skin cancer and [26] for the treatment of bladder cancer.

3.2 Immune system

Rate control can also be used to activate the immune system. The immune system is made up of different types of cells that are able to perform specific functions against pathogens and threats. Each type of immune cell specializes in fighting a specific threat and is stimulated by a sequence of message molecules that are released by the immune cells responsible for detecting pathogens. The immune system is stimulated to kill bacteria or viruses, heal diseased cells, and eradicate cancerous tumors. Molecular communication and artificial nanomachines can stimulate the immune system and be used to intensify the response to a variety of threats [11]. In some cases, it is also necessary to prevent the immune system from responding by releasing molecules that can reduce the activity of the immune system. Synthetic antagonists can also be used to reduce the immune response. Therefore, similar to TDD, there is a need to monitor and control the rate of activators or antagonists.

3.3 Tissue engineering

Another application of molecular communications where the rate control is required is tissue engineering [14, 11, 27]. Tissue engineering can lead to organ construction and help patients with tissue or organ failure. By placing nanomachines in engineered organs, intelligent organs can be produced that can diagnose diseases.

Tissue engineering has a role in regenerative medicine. The goal of regenerative medicine is the replacement of damaged tissues and organs by using transplanted cells at the injured site. Cellular signaling plays an essential role in development of the tissue. This signaling is often based on diffusion and direct cell-to-cell interactions. Under such conditions, molecules such as peptides and proteins regulate the absorption of soluble growth factors, and the adhesion, migration, proliferation and differentiation of a large number of cell types. All these factors effectively control the response of the cells and ultimately the formation of the new tissues.

There is no doubt that growth factors are essential for the control of a multitude of biological processes, such as tissue regeneration; but these factors have a short life; because they are eliminated in the body immediately after release. The success of tissue regeneration depends on how long the tissue has been exposed to these factors. The highest rate of regeneration is achieved when the tissue is exposed to these factors throughout the whole repair process. For this purpose, a set of controlled delivery systems is considered that is able to release growth factors so that the tissue is continuously and for a long time exposed to such factors with an almost constant concentration [11]. Coordination between the nanomachines responsible for this operation can be done by molecular communication; In this way, the release and control of the place and time of growth factors can be done accurately. In this scenario, we need rate control methods as well to control the rate of growth factors.

4. CURRENT RESEARCH ON RELEASING RATE CONTROL IN LOCAL DDS

When the goal of delivering a drug at a target site like a tumor is considered, the drug should be released at an appropriate rate in such a way that the level of the drug is kept within the therapeutic limits during the duration of treatment [28]. In a sustained drug release system, nanotransmitters release drug molecules over a relatively long period of time to ensure long-term treatment of the target area. In this treatment method, the concentration of the drug should be placed between the two values of LEC and the MTC.

If the concentration of the drug at the target site is lower than the LEC, the drug is not effective enough, and if it is higher than the MTC, the drug can have harmful effects on healthy parts [29]. Rate control in this way can be used in other applications as well, such as tissue engineering, to control growth factors rates or to control the rate of activators in activating the immune system.

In recent years a great deal of research has been devoted to showing the application of molecular communication in order to enhance the efficiency of a TDD system by controlling the release rate of bio-nanomachines. A comparison of state-of-the-art literature on releasing rate control for TDD is shown in Table 1. The number of required type of molecules, nanomachine mobility, nanomachines configuration, receiver type and the transport mechanism are represented in this table.

To achieve this goal, in [30], a local multi-nanotransmitter drug delivery system at a constant rate is formulated as an image processing problem, and the minimum density required to get enough medicine to all parts of an arbitrary tumor of a certain size is obtained. The effect of distribution of nanomachines on system performance is also investigated. In this case, only the nano-transmitters located at the target site are activated. Therefore, the drug is confined to the target site and is not propagated in healthy parts of the body.

In [31], a single and multiple transmitter local drug delivery system with limited resources is designed at an optimal release rate. In this case, the nearest transmitters to a randomly located tumor are activated to provide the least effective concentration at the target site. In this scenario, the optimal rate of transmitter nanomachines is determined in such a way that the total release rate is minimized provided that the least effective concentration is available at the target site. Drug nano-transmitters have limited resources in terms of energy and reservoir and these limitations should be taken into account when designing a drug delivery system. Also, drug molecules may be expensive, and releasing a large number of them can lead to damage to healthy parts of the body.

A controlled-release drug delivery system with mobile drug carrier and absorbing receiver is proposed in [32, 33]. Mobile drug carriers are considered as mobile transmitters, the targeted disease cells as absorbing receiver and the channel between the transmitter and receiver as a time-variant channel. This leads to a time-dependent release rate of drug molecules. Numerical results show that the mobile transmitter controlled-release drug delivery system outperforms constant-release rate design.

In [34], the problem of joint optimization of molecules allocation and relay location is considered to minimize the error probability. Molecule allocation is necessary because of the finite availability of molecule synthesizing energy and limited storage capabilities of the reservoir.

Another release rate optimization problem is suggested in [35]. In this paper, an optimization problem is formulated to optimize the number of transmitters and transmit power such that the drug concentration at the receiver site is kept above LEC, while the interference at other receivers is maintained below the MTC threshold. The path loss of the human circulatory system is also taken into account.

Authors in [36] proposed a drug release rate optimization based on M/M/c/c queue for the purpose of local drug delivery. Drug reception model in this paper is based on M/M/c/c queue to simulate the interactions between ligands and receptors. The optimal release rate is derived from the LEC.

A drug release synchronization issue in a multiple transmitter local DDS is addressed in [37]. It is assumed that a trigger source transmits a signal to the transmitting nanomachines to initiate the drug release. However, the propagation delay causes the nanomachines to release molecules in a nonsimultaneous manner. The aim of this work is to minimize the release-time error considering the propagation delay.

In [38], the impact of feedback control is investigated in an Amplitude Shift Keying (ASK)-based Molecular Communication (MC) system, which is of great importance in DDS. In this paper, a one-dimensional channel with drift velocity caused by blood flow is considered. The receiver is assumed to be absorbing with a limit on ligand-receptor binding due to saturation. The input is limited by a toxicity constraint of injected molecules. It is shown that,

Table 1 – Comparison of state-of-the-art research on releasing rate control for TDD

Reference	Year	Required type of molecule	Nanomachines Mobility	Nanomachines configuration	Receiver type	Transport mechanism
[29]	2016	1	Static	MISO	Transparent	Diffusion
[30]	2017	1	Static	MISO	Transparent	Diffusion
[31]	2019	1	Dynamic	SISO	Absorbing	Diffusion
[32]	2019	1	Dynamic	SISO	Absorbing	Diffusion
[33]	2018	2	Static	SISO	Absorbing	Diffusion
[34]	2018	1	Static	MIMO	-	Diffusion-drift
[35]	2020	1	Static	SISO	Absorbing	Diffusion
[36]	2020	1	Static	MISO	Absorbing	Diffusion
[37]	2021	1	Static	SISO	Absorbing	Diffusion-drift
[38]	2018	2	Static	MISO	Transparent	Diffusion
[39]	2020	1	Dynamic	MISO	Absorbing	Diffusion-drift
[40]	2019	3	Dynamic	MISO	-	Diffusion

especially for higher values of toxicity constraint and sequence length, feedback, in terms of causal knowledge of the number of delivered molecules, improves performance of ASK-based molecular communication.

In [22], a multiple transmitter local drug delivery system associated with encapsulated drug transmitters is investigated in order to overcome one of the limitations of drug delivery systems, the reservoir capacity. In order to improve the lifetime of drug transmitting nanomachines, and, hence, the longevity of a drug delivery scenario, the system is associated with encapsulated drug transmitters. Encapsulated drugs are incapable of reaction with the environment unless they are unpacked in a drug transmitter nanomachine. Therefore, far-reaching transmitters do not have harmful effects on the healthy parts of the body. The advantage of this protocol is to increase the time interval between consecutive administrations without increased toxicity. As a result, it improves the mental health of patients and reduces the costs of treatment. The lifetime of this drug delivery system depends on the distribution and topology of encapsulated drug transmitters rather than their rates. Finally, a lower bound is derived on the expected lifetime of a Poisson distributed random network of nanomachines. The performance of this lifetime improvement protocol is compared with two other protocols which are the direct extension of the drug delivery system introduced in [31].

A TDD system with intelligent nanomachines which does not only rely on blood vessel circulation, is presented in [39]. A big intelligent nanomachine takes small intelligent nanomachines and drugs to the vicinity of the tumor area to release drug molecules there. The nanomachines are assumed to be resource constrained with simple intelligence. They collaborate to find the path between the home and destination. They then go back to the home, load the drug again and repeat the delivery process.

In[40], a single receptor is modeled as an M/M/1/1 queue considering the complementary blocking probability and the mean service time. Therefore, the stochastic nature of ligand-receptor binding, which comes from the incapability of a receptor to receive all molecules in its space; and also known as receptor occupancy is modeled. These findings can have a crucial role in designing drug delivery systems in which determining the optimal rate of the drug transmitting nanomachines is critical to avoid toxicity while maintaining effectiveness.

5. RESEARCH OPPORTUNITIES

Researchers are continuously exploring ideas to provide enhanced healthcare delivery in ways that either complements existing solutions or introduce entirely new technological solutions. In recent years, considerable research in the area of molecular communication has been devoted to design and implement a more effective drug delivery system. Considering the current research and advancements in the field of TDD using molecular communication, a number of research opportunities are suggested as follows:

1. Considering the dynamic conditions of the environment and the tumor in the TDD system so that the amount of drug released can be controlled according to the environmental conditions, size and activity of the tumor. The optimal drug delivery rate calculated in many works is with the assumption of stable environmental conditions and tumor characteristics. If the environmental conditions or characteristics of the tumor change, the drug delivery rate of the transmitter nanomachines should be adjusted accordingly automatically or by applying an external stimulus.

2. Investigating the rate control problem in similar applications such as tissue engineering and rate control of growth factors: Although the rate control problem in tissue engineering applications is very similar to rate control in a TDD system, details of the new problem should be considered in rate control system design.

3. Considering reflective spherical nano-transmitters instead of point nano-transmitters for directional gain in the TDD scenario: Having a directional gain can increase the gain of the drug delivery system and prevent the molecular dispersion in non-target environments.

6. CONCLUSION

Molecular communications is a promising paradigm to exchange information among bio-nanomachines and is realized through transmission, propagation and eventually reception of molecules. It is known as a practical solution for communication among nano-networks. This idea is inspired by nature and by observing successful molecular transmissions inside cells and between cells.
The transmission mechanism which is widely assumed in the related literature is free diffusion. Free diffusion is the most basic transmission mechanism in molecular communication. The advantages of this mechanism are zero energy consumption and no need for infrastructure. Of course, this method requires a large number of molecules and due to the random movement of molecules, the time needed to reach the destination is high.
In this paper, releasing rate control for therapeutic applications such as drug delivery using molecular communication is considered. In stable drug delivery systems, nano-transmitters must release drug molecules over a relatively long period of time to ensure target treatment. Therefore, transmitter nanomachines should use continuous release instead of instantaneous release of drug molecules. Also, the concentration of the drug at the target site should be between two amounts of minimum effective concentration and maximum tolerable concentration. Rate control is used in other applications such as tissue engineering and the immune system.

REFERENCES

[1] I F Akyildiz, F Brunetti, and C Blázquez. "Nanonetworks: A new communication paradigm". In: *Computer Networks* 52.12 (2008), pp. 2260–2279. ISSN: 13891286.

[2] Hoda ShahMohammadian. "System design for nano-network communications". PhD thesis. University of Calgary, 2013.

[3] Stephen F Bush. *Nanoscale communication networks*. Artech House, 2010.

[4] Ignacio Llatser. "Exploring the Scalability Limits of Communication Networks at the Nanoscale". PhD thesis. Universitat Politecnica de Catalunya, 2013, p. 182.

[5] Ian F Akyildiz, Josep Miquel Jornet, and Massimiliano Pierobon. "Propagation models for nanocommunication networks". In: *Antennas and Propagation (EuCAP), 2010 Proceedings of the Fourth European Conference on*. IEEE. 2010, pp. 1–5.

[6] Josep Miquel Jornet and Ian F Akyildiz. "Graphene-based nano-antennas for electromagnetic nanocommunications in the terahertz band". In: *Antennas and Propagation (EuCAP), 2010 Proceedings of the Fourth European Conference on*. IEEE. 2010, pp. 1–5.

[7] Mehmet S Kuran, Huseyin Birkan Yilmaz, Tuna Tugcu, and Ian F Akyildiz. "Modulation techniques for communication via diffusion in nanonetworks". In: *Communications (ICC), 2011 IEEE International Conference on*. IEEE. 2011, pp. 1–5.

[8] Lluís Parcerisa Giné and Ian F Akyildiz. "Molecular communication options for long range nanonetworks". In: *Computer Networks* 53.16 (2009), pp. 2753–2766.

[9] Ian F Akyildiz, Josep Miquel Jornet, and Massimiliano Pierobon. "Nanonetworks: A new frontier in communications". In: *Communications of the ACM* 54.11 (2011), pp. 84–89.

[10] Nariman Farsad, H Birkan Yilmaz, Andrew Eckford, Chan-Byoung Chae, and Weisi Guo. "A comprehensive survey of recent advancements in molecular communication". In: *IEEE Communications Surveys & Tutorials* 18.3 (2016), pp. 1887–1919.

[11] L. Felicetti, M. Femminella, G. Reali, and P. Liò. "Applications of molecular communications to medicine: A survey". In: *Nano Communication Networks* 7 (2016), pp. 27–45. ISSN: 18787789.

[12] Luca Felicetti, Mauro Femminella, Gianluca Reali, Tadashi Nakano, and Athanasios V Vasilakos. "TCP-like molecular communications". In: *IEEE Journal on Selected Areas in Communications* 32.12 (2014), pp. 2354–2367.

[13] Baris Atakan. *Molecular Communications and Nanonetworks*. Springer, 2016.

[14] Tadashi Nakano, Andrew W Eckford, and Tokuko Haraguchi. *Molecular communication*. Cambridge University Press, 2013.

[15] Baris Atakan, Ozgur B Akan, and Sasitharan Balasubramaniam. "Body area nanonetworks with molecular communications in nanomedicine". In: *IEEE Communications Magazine* 50.1 (2012).

[16] M Pierobon and I F Akyildiz. "Fundamentals of Diffusion-Based Molecular Communication in Nanonetworks". PhD thesis. Georgia Institute of Technology, 2013, pp. 1–147.

[17] Sasitharan Balasubramaniam, Sigal Ben-Yehuda, Sophie Pautot, Aldo Jesorka, Yevgeni Koucheryavy, et al. "A review of experimental opportunities for molecular communication". In: *Nano Communication Networks* 4.2 (2013), pp. 43–52.

[18] Tadashi Nakano and Yutaka Okaie. "Transmission Rate Control for Molecular Communication among Biological Nanomachines". In: *IEEE Journal on Selected Areas in Communications* 31.12 (2013), pp. 835–846.

[19] Tadashi Nakano, Tatsuya Suda, Yutaka Okaie, Michael John Moore, and Athanasios V. Vasilakos. "Nanomachines : A Layered Architecture and". In: *IEEE Transactions on Nanobioscience* 13.3 (2014), pp. 169–197.

[20] Tadashi Nakano, Yutaka Okaie, and Athanasios V Vasilakos. "Throughput and efficiency of molecular communication between nanomachines". In: *Wireless Communications and Networking Conference (WCNC), 2012 IEEE*. IEEE. 2012, pp. 704–708.

[21] Mauro Femminella, Gianluca Reali, and Athanasios V. Vasilakos. "Molecular communications model for drug delivery". In: *IEEE Transactions on Nanobioscience* 14.7 (2015), pp. 935–945. ISSN: 15361241.

[22] Shirin Salehi, Naghmeh S Moayedian, Shaghayegh Haghjooy Javanmard, and Eduard Alarcón. "Lifetime improvement of a multiple transmitter local drug delivery system based on diffusive molecular communication". In: *IEEE transactions on nanobioscience* 17.3 (2018), pp. 352–360.

[23] Narayan Bhattarai, Jonathan Gunn, and Miqin Zhang. "Chitosan-based hydrogels for controlled, localized drug delivery". In: *Advanced drug delivery reviews* 62.1 (2010), pp. 83–99.

[24] Abhijit Ray, Matthew A Williams, Stephanie M Meek, Randy C Bowen, Kenneth F Grossmann, Robert HI Andtbacka, Tawnya L Bowles, John R Hyngstrom, Sancy A Leachman, Douglas Grossman, et al. "A phase I study of intratumoral ipilimumab and interleukin-2 in patients with advanced melanoma". In: *Oncotarget* 7.39 (2016), p. 64390.

[25] Praveen K Bommareddy, Ann W Silk, and Howard L Kaufman. "Intratumoral approaches for the treatment of melanoma". In: *The Cancer Journal* 23.1 (2017), pp. 40–47.

[26] Shruti GuhaSarkar, Prachi More, and Rinti Banerjee. "Urothelium-adherent, ion-triggered liposome-in-gel system as a platform for intravesical drug delivery". In: *Journal of Controlled Release* 245 (2017), pp. 147–156.

[27] Prakriti Tayalia and David J Mooney. "Controlled growth factor delivery for tissue engineering". In: *Advanced Materials* 21.32-33 (2009), pp. 3269–3285.

[28] T. M. Allen. "Drug Delivery Systems: Entering the Mainstream". In: *Science* 303.5665 (2004), pp. 1818–1822. ISSN: 0036-8075. DOI: 10.1126/science.1095833.

[29] Juergen Siepmann, Ronald A Siegel, and Michael J Rathbone. *Fundamentals and applications of controlled release drug delivery*. Springer US, 2012.

[30] Shirin Salehi, Simon S Assaf, Raul G Cid-Fuentes, Naghmeh S Moayedian, Josep Solé-Pareta, and Eduard Alarcón. "Optimal deployment of multiple transmitter drug delivery system: A spatial sampling theorem approach". In: *Proceedings of the 3rd ACM International Conference on Nanoscale Computing and Communication*. 2016, pp. 1–2.

[31] Shirin Salehi, Naghmeh S Moayedian, Simon S Assaf, Raul G Cid-Fuentes, Josep Solé-Pareta, and Eduard Alarcón. "Releasing rate optimization in a single and multiple transmitter local drug delivery system with limited resources". In: *Nano Communication Networks* 11 (2017), pp. 114–122.

[32] Trang Ngoc Cao, Arman Ahmadzadeh, Vahid Jamali, Wayan Wicke, Phee Lep Yeoh, Jamie Evans, and Robert Schober. "Diffusive mobile MC for controlled-release drug delivery with absorbing receiver". In: *ICC 2019-2019 IEEE International Conference on Communications (ICC)*. IEEE. 2019, pp. 1–7.

[33] Trang Ngoc Cao, Arman Ahmadzadeh, Vahid Jamali, Wayan Wicke, Phee Lep Yeoh, Jamie Evans, and Robert Schober. "Diffusive mobile MC with absorbing receivers: Stochastic analysis and applications". In: *IEEE Transactions on Molecular, Biological and Multi-Scale Communications* 5.2 (2019), pp. 84–99.

[34] Satish K Tiwari, Tadi Ravi Teja Reddy, Prabhat K Upadhyay, and Daniel Benevides Da Costa. "Joint optimization of molecular resource allocation and relay positioning in diffusive nanonetworks". In: *IEEE Access* 6 (2018), pp. 67681–67687.

[35] Keishla D Ortiz-Lopez, Mahima Agumbe Suresh, and Radu Stoleru. "Transmitters location optimization for drug delivery systems". In: *Proceedings of the 5th ACM International Conference on Nanoscale Computing and Communication*. 2018, pp. 1–6.

[36] Qingying Zhao and Min Li. "Release Rate Optimization Based on M/M/c/c Queue in Local Nanomachine-Based Targeted Drug Delivery". In: *International Conference on Bio-inspired Information and Communication Technologies*. Springer. 2020, pp. 130–140.

[37] Tania Islam, Ethungshan Shitiri, and Ho-Shin Cho. "A Simultaneous Drug Release Scheme for Targeted Drug Delivery Using Molecular Communications". In: *IEEE Access* 8 (2020), pp. 91770–91778.

[38] Siavash Ghavami, Raviraj Adve, and Farshad Lahouti. "Information rate analysis of ASK-based molecular communication systems with feedback". In: *Nano Communication Networks* 28 (2021), p. 100339.

[39] Lin Lin, Fupeng Huang, Hao Yan, Fuqiang Liu, and Weisi Guo. "Ant-behavior inspired intelligent nanonet for targeted drug delivery in cancer therapy". In: *IEEE transactions on nanobioscience* 19.3 (2020), pp. 323–332.

[40] Shirin Salehi, Naghmeh S Moayedian, and Eduard Alarcón. "Diffusion-Based Molecular Communication Channel in Presence of a Probabilistic Absorber: Single Receptor Model and Congestion Analysis". In: *IEEE transactions on nanobioscience* 18.1 (2019), pp. 84–92.

AUTHORS

Shirin Salehi received a Ph.D. degree in electrical engineering, communication systems from the Isfahan University of Technology (IUT), Iran, in 2018. She was a visiting scholar with the NaNoNetworking Center in Catalunya (N3Cat), Universitat Politècnica de Catalunya, Spain, from 2016 to 2017. From 2018 to 2019, she was a Postdoctoral Researcher with the ECE Department, Isfahan University of Technology. Her research interests include cooperative communication systems, molecular communications with application in a medical field, and digital signal processing. She is currently affiliated with the communication regulatory authority, ministry of ICT, Iran.

Naghmeh Sadat Moayedian received B.S., M.S., and Ph.D. degrees in electrical engineering from the Isfahan University of Technology, Isfahan, Iran, in 1999, 2002, and 2009, respectively. She is currently affiliated with the ECE Department, Isfahan University of Technology. Her research interests include cloud networks, nano-networks, and wireless networks.

Mohammad Taghi Shafiee received a Ph.D. degree in human resources management from the Shakhespajouh Research Institute, University of Isfahan, Iran, in 2016 and M.Sc. degree in electrical engineering, communication systems from the K.N. Toosi University of Technology, Iran, in 1995. Since 1995, he has participated and contributed in various international events of of the International Telecommunication Union and Asia-Pacific Telecommunity. His research interests include leadership, radiocommunication systems, frequency spectrum management, ICT rules and regulations, spectrum monitoring, wireless networks and technologies.

INFORMATION THEORETIC MODELING OF PARANODAL REGIONS IN MYELINATED AXONS

Caglar Koca[1], Ozgur Ergul[2], Meltem Civas[3], Ozgur B. Akan[1,3]
[1]Internet of Everthing (IoE) Group, Department of Engineering, University of Cambridge, UK , [2]Gazi University, Faculty of Engineering, Department of Electrical and Electronics Engineering, Ankara, Turkey, [3]Next-generation and Wireless Communications Laboratory (NWCL), Department of Electrical and Electronics Engineering, Koç University, Istanbul, Turkey

NOTE: Corresponding author: Caglar Koca, ck542@cam.ac.uk

Abstract *– As a natural form of nanoscale communication, neuro-spike communication inspires the deployment of nanomachines inside the human body for healthcare. To this end, the identification of failure mechanisms in normal and diseased connections of nervous nano-networks is crucial. Thus, in this paper, we investigate the information transmission through a single myelinated axon segment. We introduce a realistic multi-compartmental model for a single myelinated segment by incorporating the axon's paranodal regions to the model. Next, we characterize the myelinated segment communication channel in terms of attenuation over the range of frequencies. Based on this, we derive the rate per channel use and upper bound on the information capacity. The performance evaluations reveal that our approach provides dramatic correction regarding frequency response. We believe that this result could have a significant effect on the characterization of demyelinated axons from the information and communication technology (ICT) perspective.*

Keywords – ICT-based treatment, intra-body nano-networks, Internet of Bio-Nano Things, demyelination, neuro-spike communication

1. INTRODUCTION

Advances in nanotechnology have opened the way for the deployment of nanomachines collaborating within the Internet of Bio-Nano Things (IoBNT) framework inside the human body as a new means of information and communication technology (ICT)-based treatment technique [1, 2]. IoBNT offers both the abstraction necessary for a deeper look into the evolution of intra-body communications [3] and the foundation for analyzing and interacting with living organisms. For example, as a large scale *intra-body nano-network*, the human nervous system bears an enormous potential to inspire architectures for such systems with novel applications in diverse areas, including smart healthcare [4].

Shannon's information theory is usually applied to existing intra-body nano-networks to analyze intra-body communication mechanisms, one of which is neuro-spike communication achieved via molecules [5]. Neuro-spike communication consists of consecutive stages, namely, spike generation, axonal and synaptic transmission. Understanding of communication failures within any of these stages due to nervous system diseases such as spinal cord injury and Multiple Sclerosis (MS) is crucial to the designs of assistive or replacement nanomachines [6]. Accordingly, an accurate communication theoretical analysis of intra-body communication channels requires realistic channel modeling of healthy and diseased connections, which is promising in understanding disease mechanisms in biological systems communicating via molecules [7].

Regarding axonal transmission, communication and computational models of axons exist in the literature. Communication models mostly assume the axon as an ideal all-pass filter [8]. In biologically detailed communication models, the axon is modeled as a low-pass filter, and modified second-order Butterworth filters [9, 10]. In more complex models, axonal propagation is represented with several state transitions in the case of hippocampal pyramidal neurons [11]. Moreover, an infinite transmission line model is also available [12]. The limitations of communication models include that they cannot fully capture the behavior of axons, which arises from the axon's physiology. The computational models, on the other hand, are accepted as biologically accurate. Thus, computational models can be used to construct the realistic channel model of axons, enabling accurate analyses. In this respect, multi-compartment models successfully describe the axonal transmission by dividing an axonal cable into compartments, where each compartment has the same membrane properties [13]. However, this approach neglects some parts of the axon, e.g., paranodal regions of myelinated axons, where the membrane properties are not uniform.

In many vertebrates, an insulating substance called myelin sheath surrounds axons. The myelin sheath is the extension of the plasma membrane of glial cells wrapping the axon, possibly in a multilayered structure. Myelin sheaths are formed in periodic segments. The short portions of the axon left uncovered by myelin are called the nodes of Ranvier. Axonal transmission is achieved by

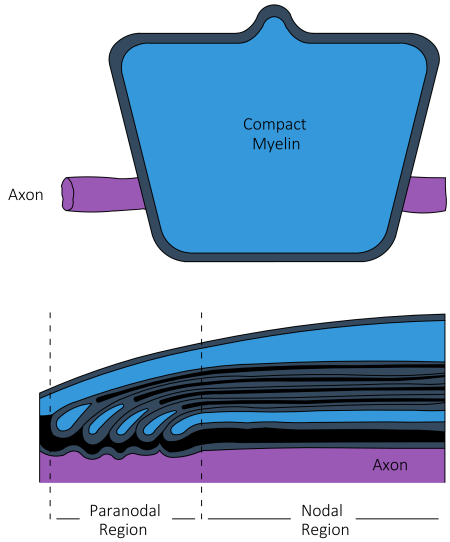

Fig. 1 – Paranodal and nodal regions of the myelin sheath.

impulse-like potential changes in the neuron membrane, called Action Potential (AP). Myelination increases the speed of signal propagation along the axon considerably by a process called saltatory conduction, which is simply the jumping of APs between the consecutive nodes of Ranvier. Successful saltatory conduction is strongly related to the structure and integrity of the myelin sheath [14]. In an intact and sufficiently thick sheath, ion leakage from the neuron membrane is minimal. As a result, attenuation at the membrane potential is also minimal. However, demyelination, which is the loss of myelin sheath, can increase ion leakage from the axon membrane to a level that the membrane potential attenuates too much when it reaches the next node. In this case, low membrane potential may not be sufficient to open Na^+ channels in the node, and consequently, AP propagation is blocked [15].

The myelin sheaths generally form in multiple layers. The sheath is wrapped around the axon starting from its short edge as shown in Fig.1. This structure of myelin forms intermediary regions called the *paranodal regions* between the nodes of Ranvier and the nodal regions of the myelin sheath. Assuming that the n-fold myelin sheath begins abruptly following a node of Ranvier causes inaccuracy when modeling the leakage resistance and capacitance of the region. Bearing in mind that there may be hundreds, even thousands of nodal and paranodal regions in a single axon, the importance of inaccuracy caused by oversimplistic modeling becomes apparent. Moreover, as shown in [16], even minor changes in the structure of paranodal regions can affect AP propagation significantly. This evidence shows that we should also consider paranodal regions to obtain a realistic model of myelinated axons.

In this paper, we propose a detailed model for the internode in a myelinated axon by taking paranodal regions into account, based on experimental evidence from the literature. Our aim is to investigate the frequency response properties of a single internodal channel. We perform frequency domain analysis of the system to quantify channel attenuation and compare the results with the classical cable model to show the effect of paranodal regions on information transmission. Then, we derive the rate per channel use and channel capacity when different forms of biological noise sources exist in the environment.

The rest of the paper is organized as follows. First, in Section 2, we describe the system model. Secondly, in Section 3, we define noise sources affecting the internodal channel and derive bounds on rate per channel use and capacity. Next, in Section 4, we provide numerical analysis of the channel's frequency domain properties. Finally, in Section 5, conclusions and future directions are summarized.

2. SYSTEM MODEL

A myelinated axon consists of active and passive compartments that sustain the active and passive spread of action potential through the axon, respectively. The nodes of Ranvier, which contain dense ion channels, are active compartments. In contrast, electrically neutral myelinated segments, i.e., *internodes*, with low ion channel density constitute passive compartments [17] as shown in Fig. 2. Due to the stochastic opening and closing of ion channels, which can be described via nonlinear differential equations of Hodgkin Huxley formalism, membrane resistance is time-varying at the nodes of Ranvier. On the other hand, since passive compartments have only a negligible number of ion channels, membrane resistance does not depend on time, and the axon acts linearly at internodes.

To investigate the linear response of an internode, we take paranodal regions into account. In this respect, classical cable theory, which is proven to be successful at explaining the behavior of AP propagation through the cylindrical structures such as dendrites and axons, is utilized [18].

2.1 The cable equation

According to cable theory, the membrane voltage is given by the following differential equation [13]

$$\frac{1}{r_f}\frac{\partial^2 V}{\partial x^2} = c_m\frac{\partial V}{\partial t} + \frac{V}{r_m}, \qquad (1)$$

where r_m, r_f and c_m are the membrane resistance, forward resistance and membrane capacitance of the axon, respectively. Using the length constant, $\lambda = \sqrt{\frac{r_m}{r_f}}$ and the time constant, $\tau = r_m c_m$, Eq. *(1)* becomes

$$\lambda^2\frac{\partial^2 V}{\partial x^2} = \tau\frac{\partial V}{\partial t} + V. \qquad (2)$$

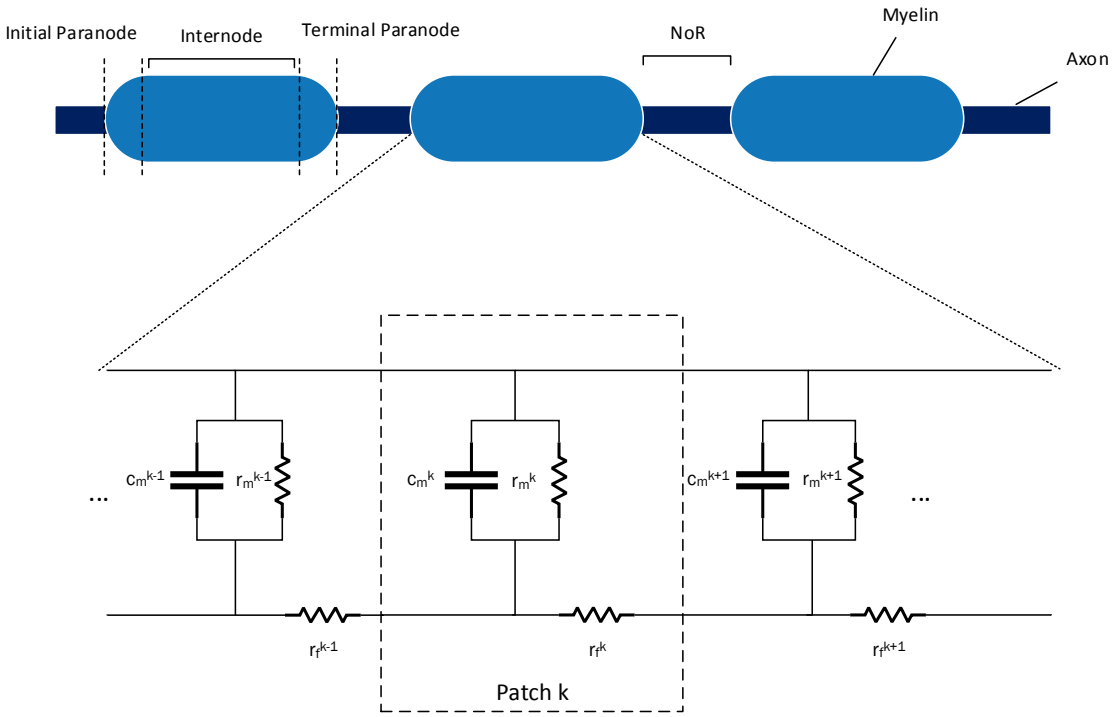

Fig. 2 – Two-dimensional diagram of myelinated axon and the circuit corresponding to a myelinated segment. The regions where axon is surrounded by myelin sheath are called internode and remaining parts without myelin are called Node of Ranvier (NoR). A myelinated segment consists of internodal region with constant myelin thickness, initial and terminal paranodes, where number of myelin wraps depends on the distance from and to NoR, respectively.

In the simplistic model of the myelinated axon, leakage resistance and capacitance are constant. However, due to the shape of the myelin sheath, paranodal regions do have different leakage resistance and capacitance values. Therefore, rather than taking r_m and c_m constant, we take them as a function of the distance from the start of the myelinated segment. Hence,

$$\lambda \sim \lambda(x) \tag{3}$$
$$\tau \sim \tau(x) \tag{4}$$

The lumped circuit approximation, valid due to the small dimensions of the myelinated segments compared to the wavelengths of the dominant components forming the action potential, helps us to assume any field effect is instantaneous throughout the entire segment. Therefore, to calculate attenuation values in the steady state, partial derivative of voltage with respect to the time variable becomes zero, i.e., $\frac{\partial V}{\partial t} = 0$. Hence, the resulting equation becomes

$$V = \lambda^2(x)\frac{\mathrm{d}^2 V}{\mathrm{d}x^2}. \tag{5}$$

This is the inhomogeneous heat flow equation for the steady state [19]. Apart from rare simple cases, the cable equation cannot be solved analytically but numerically [13].

Since solving this equation is hard, we employ the fi- nite difference method, by partitioning our model into N patches.

2.2 The discrete axonal cable

We consider a multi-compartment model of the myelinated axon to solve the inhomogeneous heat flow equation described in Section 2.1. Since this problem is hard to solve analytically, we attempt to solve this problem using the finite element method. By compartmentalizing the myelinated segment, where we assume the resistance and capacitance values are constant for the given compartment, we obtain a numerical solution to the heat flow problem.

Here, we divide a length-l myelinated segment into N compartments, where N is a large integer [20]. Each of these pieces consists of three circuit elements, i.e., a forward resistance, r_f, leakage resistance, r_m and leakage capacitance, c_m.

The equivalent circuit is shown in Fig. 2. Looking at Fig. 2, we see the $(k-1)^{th}$, k^{th} and $(k+1)^{th}$ compartments of the myelinated segment, which we divided into N compartments. The length of each compartment is $\Delta x = \frac{l}{N}$. Note that the smaller Δx is, the more accurate the finite element method will be.

2.3 Multilayer cell membrane

In the previous section, we described how the finite element method transforms the cable theory into a circuit with N different compartments. In this section, we present how circuit parameters for each compartment are calculated. There are three circuit elements we need to investigate, namely, forward resistance, r_f , leakage resis- tance, r_m, and leakage capacitance, c_m.

Forward resistance

The forward resistance for the k^{th} compartment is obtained as

$$r_f^k = R_f \frac{\Delta x}{2\pi a} \tag{6}$$

where R_f is the specific forward resistance of the axon. Note that $r_f^k = r_f \ \forall k$, as forward resistance is only due to the cytoplasmic resistance of axon, not on the myelin covers spanning the axon.

Leakage resistance

We calculate the leakage resistance of an unmyelinated segment of thickness Δx as

$$r_m = \frac{R_m}{2\pi a \Delta x}, \tag{7}$$

where a is the axon radius and R_m is the specific leakage resistance.

In order to calculate the leakage resistance of a myelinated segment, we first need to use the result in Eq. *(7)* to obtain the resistivity of axolemma, i.e.,

$$\rho = \frac{r_m}{2\pi a \Delta x} \frac{1}{\ln\left(\frac{a+d_a}{a}\right)} \tag{8}$$

$$= \frac{R_m}{\ln\left(\frac{a+d_a}{a}\right)} \tag{9}$$

where d_a is the axolemma thickness and we assumed axolemma to be cylindrical.

In case axolemma is covered with multiple myelin turns, we can assume each turn to be cylindrical resistors with inner thickness $a + n \times d_m$ and outer thickness $a + d_a + n \times d_m$ where d_m is the myelin layer thickness. Note that myelin tissue shows remarkable similarities with the axolemma. Hence, we model myelin as axolemma encapsulating some intracranial fluid, where d_m is the total layer thickness including the encapsulated intracranial fluid and the myelin itself, while d_a is only the thickness of myelin, equal to the axolemma thickness. The cross-sectional view of our model is depicted in Fig. 3. Since all

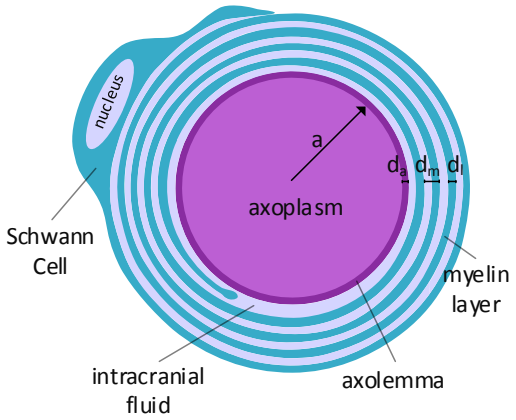

Fig. 3 – Cross-sectional view of myelinated axon.

myelin layers are connected in series, we can calculate the total axonal leakage resistance of a segment with length Δx and myelin cover n from axoplasm to the intracranial fluid as

$$r_m = \sum_0^n \frac{\rho}{2\pi\Delta x} \ln\left(\frac{a + d_a + n d_m}{a + n d_m}\right). \tag{10}$$

In the paranodal region, myelin turns wrapping a segment are not constant. If the last myelin layer is a partial turn, i.e., not covering the whole axolemma, we can still use Eq. *(10)* with a slight modification such that

$$r_m = \sum_0^{\lfloor n \rfloor} \left(\frac{\rho}{2\pi\Delta x} \ln\left(\frac{a + d_a + n d_m}{a + n d_m}\right)\right) + \tag{11}$$

$$(n - \lfloor n \rfloor) \frac{\rho}{2\pi\Delta x} \ln\left(\frac{a + d_a + \lceil n \rceil d_m}{a + \lceil n \rceil d_m}\right) \tag{12}$$

where the last part is due to the partial wrap. Note that here n is not an integer. Rather, $n - \lfloor n \rfloor$ gives us the ratio of the partial cover.

Finally, we can calculate the leakage resistance of the k^{th} piece of a length l, radius a and the paranodal region length d myelinated segment with Eq. *(11)* by switching n to n^k as

$$n^k = \begin{cases} \frac{Nk\Delta x}{d}, & k\Delta x \le d \\ \frac{N(d - k\Delta x)}{d}, & k\Delta x \ge l - d \\ N, & e.w \end{cases} \tag{13}$$

Leakage capacitance

Here we can pursue an approach similar to leakage resistance. Leakage capacitance of an unmyelinated segment of thickness Δx calculated as

$$c_m = C_m \Delta x (2\pi a). \quad (14)$$

Using Eq. *(25)*, we can calculate electric permittivity of axolemma as

$$\epsilon = \frac{c_m}{2\pi\Delta x} \ln\left(\frac{a+d_a}{a}\right) \quad (15)$$

$$= C_m a \ln\left(\frac{a+d_a}{a}\right). \quad (16)$$

Similar to the leakage resistance calculations, we can reach the leakage capacitance by modeling the myelin turns as concentric cylindrical capacitors with inner radii $a+n\times d_m$ and outer radii as $a+d_a+n\times d_m$. The resultant capacitance would be

$$c_m = \frac{2\pi\Delta x}{\sum_0^n \ln\left(\frac{a+d_a+nd_m}{a+nd_m}\right)}. \quad (17)$$

We can calculate the leakage capacitance of a segment with length Δx in case of partial myelin turns as

$$c_m = \frac{2\pi\Delta x}{\left(\sum_0^{\lfloor n \rfloor} \ln\left(\frac{a+d_a+\lfloor n \rfloor d_m}{a+\lfloor n \rfloor d_m}\right)\right) + \ln\frac{a+d_a+\lceil n \rceil d_m}{a+\lceil n \rceil d_m}}. \quad (18)$$

Similar to the leakage resistance, we can find the leakage capacitance at the k^{th} segment by using Eq. *(18)* with n^k instead of n as in Eq. *(13)*.

Outer resistance

Outer resistance, or extracellular resistance, is the resistance of the fluid between axons [21]. Here, we assume that outer resistance is due to the extracellular fluid enclosed by the endoneurium.

We calculate the outer resistance similar to the forward resistance, i.e.,

$$r_o^k = \frac{R_o \Delta x}{\pi(d_e^2 - (d_e - d_h)^2)}, \quad (19)$$

where R_o is the specific outer resistance, d_e is the radius of the endoneurium and d_h is the thickness of the endoneurium. Since endoneurium thickness and radius are accepted to be constant through the axon, r_o^k, similar to r_f^k, is independent of k.

3. INTERNODAL CHANNEL CAPACITY

In this section, we find the rate per channel use in internodal regions of myelinated axons.

Information transmission through axons is affected by noise sources including *channel noise* due to random fluctuations of voltage-gated ion channels at the node of Ranvier, *thermal noise* (Johnson noise) produced by membrane resistance, membrane capacitance, and cytoplasmic resistance, and *crosstalk noise* caused by axon-axon interactions such as ephaptic coupling [22, 23]. Concerning the internodal channel, we do not consider channel and crosstalk noise, since the former is effective at the nodes of Ranvier and the latter is specific to neuron types [24]. Here, thermal noise is the only noise source that affects the internodal transmission in general; therefore, we use it to offer an upper bound for the per-use rate of the internodal channel. Thus, the power spectral density of thermal noise voltage is given by

$$N_P(f) = 2kT\mathrm{Re}\{Z(f)\}, \quad (20)$$

where k is the Boltzmann constant, T is the temperature in Kelvin and Z is the total impedance of the system [23]. Since, Z depends on frequency, thermal noise is also frequency dependent.

Action potential, the input to the channel, is represented by voltage variable $x(t)$. The power spectral density of signal $x(t)$ over the finite time interval $[0, T]$ is given by

$$P(f) = \lim_{T\to\infty} \frac{1}{T}|X(f)|^2, \quad (21)$$

where $X(f)$ is the Fourier transform of $x(t)$. The input signal has power constraint that

$$\int_B P(f) \le P, \quad (22)$$

where P is the average transmitted signal power over given bandwidth B.

Hence, the rate per channel use of a myelinated segment under thermal noise is bounded by

$$R < \int_{-B/2}^{B/2} \log_2\left(1 + \frac{|G(f)|^2 P(f)}{N_P(f)}\right) \mathrm{d}f, \quad (23)$$

where $G(f)$ is the channel gain function and B is channel bandwidth. The channel capacity of a myelinated segment can be obtained by *water-filling*. However, due to the frequency-dependent gain function, first, we need to calculate the effective noise spectral density, i.e.,

$$N_P^{eff}(f) = \frac{N_P(f)}{|G(f)|^2}. \quad (24)$$

Thus, the capacity of the channel is found as

$$C = \Delta_f \sum_{i=1}^{M} \log_2\left(1 + \frac{P(f_i)}{N_P^{eff}(f_i)}\right), \quad (25)$$

where M is the number of sub-bands with each having a width of Δf that is sufficiently small. The power distribution that maximizes the capacity can be obtained by solving the Lagrange multiplier problem. Hence, the solution is given by [25]

$$P(f) = \begin{cases} K - N_P^{eff}(f) & f \in B \\ 0 & f \notin B \end{cases} \qquad (26)$$

where K value satisfies *(22)*.

4. PERFORMANCE EVALUATION

In this section, we first present the leakage resistance and capacitance trend graphically, and then the results of our frequency domain analysis of the internode.

The simulation environment for the results given in this section is Python. We choose Python over dedicated simulators such as *Comsol* or *Neuron* due to its flexibility in model building.

4.1 Leakage resistance and capacitance

Since the leakage impedance depends on the average number of layers, where each layer acts as another cell membrane, the leakage impedance in the paranodal region must increase linearly, as our model suggests. The difference between our model and the conventional model [18] is displayed in Fig. 4 and Fig. 5 for leakage resistance and leakage capacitance respectively.

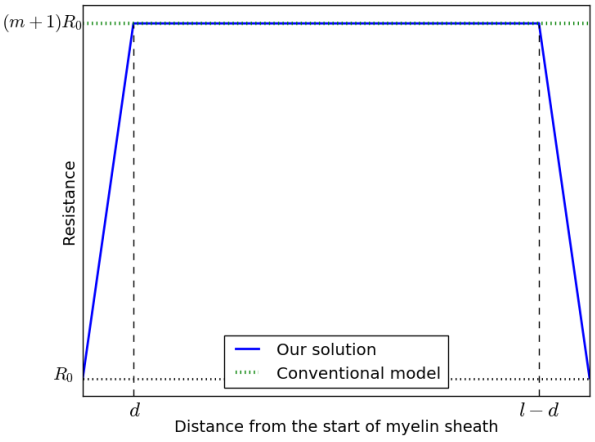

Fig. 4 – Leakage resistance trend between two Ranvier nodes.

As we can see in Fig. 4, the resistance gradually increases in the paranodal region, from R_0, the resistance of naked axolemma, to $(m+1)R_0$, axolemma covered with m layers of myelin, while the conventional model assumes it to be constant. For capacitance, however, the conventional model understates the capacitance, as can be seen in Fig. 5. The capacitance values drop from C_0 to $C_0/(m+1)$. In Fig. 4 and Fig. 5, d marks the boundary of the first

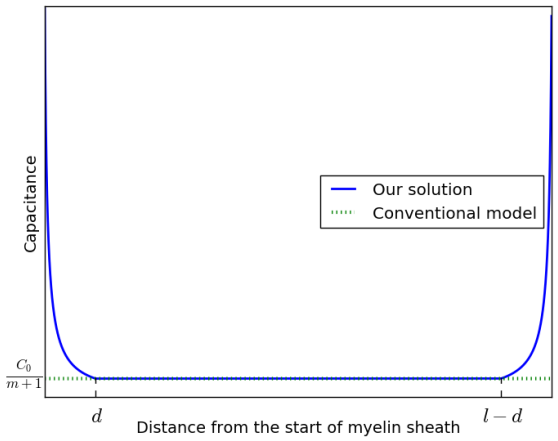

Fig. 5 – Leakage capacitance trend between two Ranvier nodes.

paranodal region, while $l-d$ marks the start of the end paranodal region.

Note that the effects of myelin layers on leakage resistance and leakage capacitance are the same because leakage capacitance being inversely proportional to the capacitance value while leakage resistance being linearly proportional to the resistance value.

4.2 Frequency response analysis of internode

In this section, we present the differences between our model and the conventional model. In this subsection, unless we are testing that specific variable, we use the simulation parameters given in Table 1. The frequency responses are simulated for the frequency range of $0-6000$ Hz.

First, we examine the attenuation depending on frequency over a single myelinated segment. The attenuation values are essential in determining the continuity of action potential through the whole axon because the voltage levels at the end of the segment determine whether the voltage-controlled channels in the Node of Ranvier are activated. Since the conventional method underestimates leakage in the paranodal regions by assuming a cylindrical myelin cover, the attenuation values are lower compared to our model. The frequency response of a single myelinated region is given in Fig. 6. Even though our solution traces a very similar path to the conventional method, the percent difference increases dramatically for higher frequency values, reaching 253% for $f = 6000$ Hz. As a result of this extreme difference, propagation of spontaneous high-frequency spikes, a complication related to axonal injuries may be underestimated using the conventional method. Furthermore, the discrepancy is not negligible for $f < 500$ Hz, where most of the spectrum of a normal action potential lies. Therefore, our model may correct the shape of a healthy action potential measured at the end of the myelinated segment.

Table 1 – Model and simulation parameters

Parameter	***Value***	***Unit***	***Symbol***
Specific forward resistance	*100* [26]	Ωm	r_f
Specific leakage resistance	10^6 [26]	Ωm^2	r_l
Specific membrane leakage capacitance	10^{-2} [26]	Fm^{-2}	c_m
Axolemma thickness	5×10^{-9} [27]	m	d_m
Length of myelinated segment	1×10^{-3} [28]	m	l
Length of paranodal region	1×10^{-4} [21]	m	d
Axon radius	10^{-5} [21]	m	a
Myelin turn number	20 [29]		n

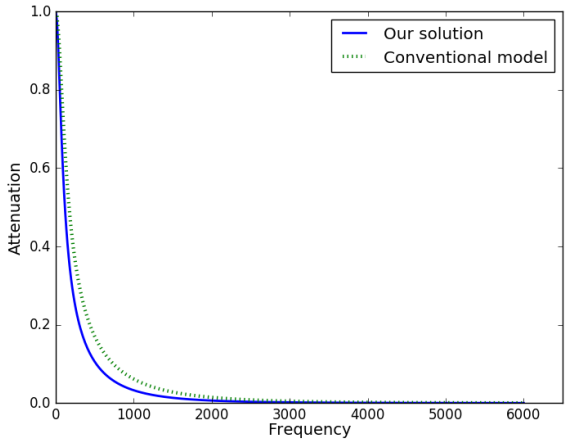

Fig. 6 – Attenuation vs frequency for a single myelinated segment.

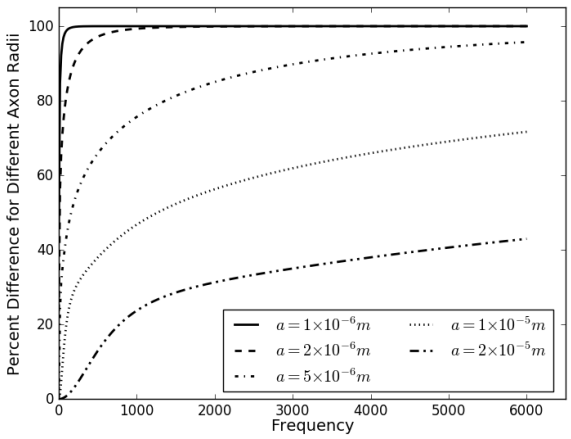

Fig. 7 – Percent difference between our model and conventional model for different frequency values depending on axon radii.

In Fig. 7, we show the percent difference for attenuation between our model and the conventional solution for different axon radii. For larger radii values, the effect of leakage is less so that our correction becomes insignificant. However, for typical and smaller radii values, our approach offers a dramatic correction over the conventional approach.

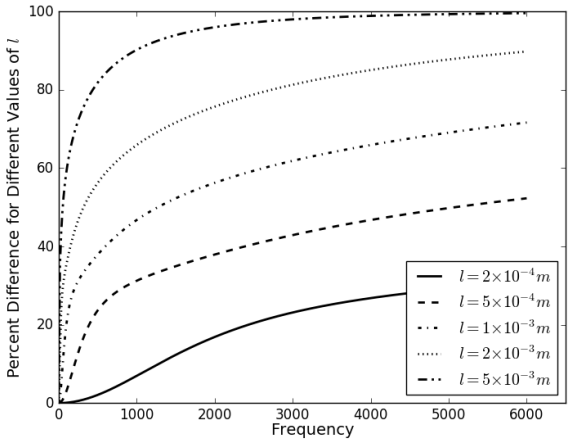

Fig. 8 – Percent difference between our model and conventional model for different myelin turn values.

In Fig. 8, we analyzed the percent difference between our model and the conventional solution in attenuation for different lengths of myelinated segments. Note that here we assumed the length of the paranodal regions are of the same ratio. That is, for longer myelinated segments, the paranodal regions were also assumed to be longer. As the length of the segment decreases, the overall leakage diminishes. As a result, our correction becomes less significant. However, for typical lengths of myelinated segments, the correction offers a tremendous change over the conventional method, especially for high-frequency values.

In Fig. 9, we focused on the effect of changing the ratio over the paranodal region length, d over the length of the whole myelinated segment, l. As expected, as the length of the paranodal segment diminishes, our correction becomes less significant. However, even for shorter paranodal regions, the correction may be important.

Fig. 10 analyzes the relationship between the maximum myelin cover, n, and the percent difference between our solution and the conventional cable theory approach. As expected, for low myelin cover, the paranodal regions are essentially similar to the rest of the segment. Thus, our correction becomes insignificant, especially for the low-frequency region.

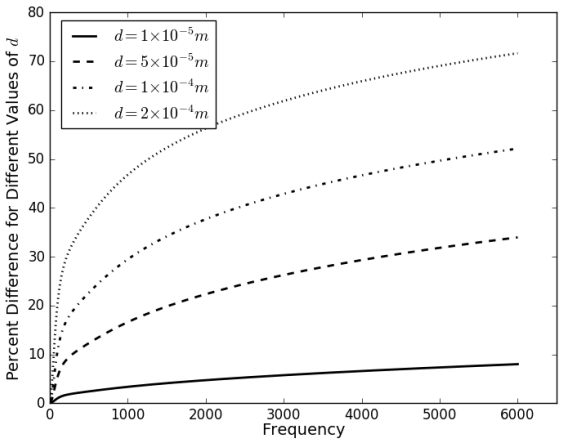

Fig. 9 – Percent difference between our model and conventional model for different frequency values depending on the length of the paranodal region.

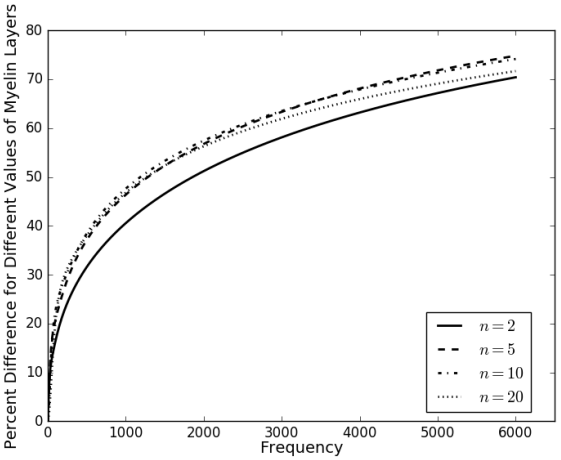

Fig. 10 – Percent difference between our model and conventional model for different frequency values depending on axon length.

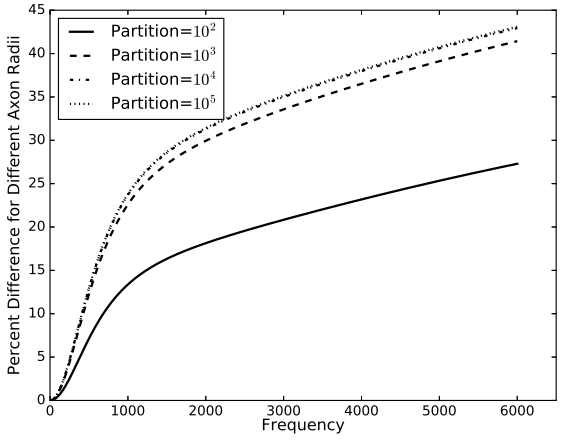

Fig. 11 – Percent difference between our model and conventional model for different step size values used for finite element analysis.

Fig. 11 shows the percent difference between our model and the conventional solution for different partition numbers. For the results presented above, we partitioned a single myelinated segment into 10^4 compartments. Note that, in Fig. 11, the percent difference values for 10^4 compartments and 10^5 compartments are indistinguishable, proving that our finite element method analysis has sufficient depth to offer accurate results, i.e.,

$$G_{\Delta x=\frac{l}{10^4}} \approx G_{\Delta x=\frac{l}{10^5}} \approx \lim_{\Delta x\to 0} G_{\Delta x}. \qquad (27)$$

5. CONCLUSION AND FUTURE DIRECTIONS

In this work, we developed a compartment-based model for the endpoints of the myelin sheath, i.e., the paranodal region, for the first time in literature. We believe our work paves the way to more complicated and realistic models to apply ICT-based treatments to conditions arising from deformities in the myelin sheath.

In future work, several issues will be investigated as follows:

- Incorporating nodes of Ranvier into the model to obtain end-to-end axonal channel characteristics,
- Extensive examination of axon's end-to-end model including delay and phase analysis,
- Calculation of digital and analog capacity for the axonal internodes,
- Modeling myelin-related diseases, e.g., paranodal detachment and demyelination, and determining the loss in internodal channel capacity due to a disease.

ACKNOWLEDGEMENT

This work was supported in part by the AXA Research Fund (AXA Chair for Internet of Everything at Koç University), ERC project MINERVA (ERC-2013-CoG #616922), and Huawei Graduate Research Scholarship.

REFERENCES

[1] IF Akyildiz, M Pierobon, S Balasubramaniam, and Y Koucheryavy. "The internet of bio-nano things". In: *IEEE Communications Magazine* 53.3 (2015), pp. 32–40.

[2] Ozgur B Akan, Hamideh Ramezani, Tooba Khan, Naveed A Abbasi, and Murat Kuscu. "Fundamentals of molecular information and communication science". In: *Proceedings of the IEEE* 105.2 (2017), pp. 306–318.

[3] Caglar Koca and Ozgur B Akan. "Anarchy versus cooperation on internet of molecular things". In: *IEEE Internet of Things Journal* 4.5 (2017), pp. 1445–1453.

[4] Tooba Khan, Meltem Civas, Oktay Cetinkaya, Naveed A Abbasi, and Ozgur B Akan. "Nanosensor networks for smart health care". In: *Nanosensors for Smart Cities*. Elsevier, 2020, pp. 387–403.

[5] Meltem Civas and Ozgur B Akan. "Rate of Information Flow Across Layered Neuro-Spike Network in the Spinal Cord". In: *IEEE transactions on nanobioscience* 19.3 (2020), pp. 368–377.

[6] Ozgur Baris Akan, Hamideh Ramezani, Meltem Civas, Oktay Cetinkaya, Bilgesu Arif Bilgin, and Naveed Ahmed Abbasi. "Information and communication theoretical understanding and treatment of spinal cord injuries: State-of-the-art and research challenges". In: *IEEE Reviews in Biomedical Engineering* (2021).

[7] Caglar Koca, Meltem Civas, Selin M Sahin, Onder Ergonul, and Ozgur B Akan. "Molecular Communication Theoretical Modeling and Analysis of SARS-CoV2 Transmission in Human Respiratory System". In: *IEEE Transactions on Molecular, Biological and Multi-Scale Communications* (2021).

[8] Mladen Veletić, Pål Anders Floor, Zdenka Babić, and Ilangko Balasingham. "Peer-to-peer communication in neuronal nano-network". In: *IEEE Transactions on Communications* 64.3 (2016), pp. 1153–1166.

[9] Eren Balevi and Ozgur B Akan. "A physical channel model for nanoscale neuro-spike communications". In: *IEEE Transactions on Communications* 61.3 (2013), pp. 1178–1187.

[10] Derya Malak and Ozgur B Akan. "A communication theoretical analysis of synaptic multiple-access channel in hippocampal-cortical neurons". In: *IEEE Transactions on communications* 61.6 (2013), pp. 2457–2467.

[11] Hamideh Ramezani and Ozgur B Akan. "A Communication Theoretical Modeling of Axonal Propagation in Hippocampal Pyramidal Neurons". In: *IEEE Transactions on NanoBioscience* (2017).

[12] Alireza Khodaei and Massimiliano Pierobon. "An intra-body linear channel model based on neuronal subthreshold stimulation". In: *Communications (ICC), 2016 IEEE International Conference on*. IEEE. 2016, pp. 1–7.

[13] Peter Dayan and Laurence F Abbott. *Theoretical neuroscience*. Vol. 806.

[14] R. Shi and W. Sun. "Potassium channel blockers as an effective treatment to restore impulse conduction in injured axons". In: *Neuroscience Bulletin* 27.1 (2011), pp. 36–44.

[15] A. Ochab-Marcinek, G. Schmid, I. Goychuk, and P. Hänggi. "Noise-assisted spike propagation in myelinated neurons". In: *Physical Review E* 79.1 (2009), pp. 011904-1–7.

[16] C. F. Babbs and R. Shi. "Subtle Paranodal Injury Slows Impulse Conduction in a Mathematical Model of Myelinated Axons". In: *PLoS ONE* 8.7 (2013), pp. 1–11.

[17] M. N. Rasband and J. S. Trimmer. "Developmental clustering of ion channels at and near the node of Ranvier". In: *Developmental Biology* 236.1 (2001), pp. 5–16.

[18] Wilfrid Rall. "Core conductor theory and cable properties of neurons". In: *Comprehensive physiology* (2011).

[19] O. N. Favorsky. *Thermal to Mechanical Energy Conversion : Engines and Requirements - Volume I*. Paris: Encyclopedia of Life Support Systems (EOLSS) Publishers, 2009.

[20] F. Gabbiani and S. Cox. *Mathematics for Neuroscientists*. London: Academic Press, 2010.

[21] Charles F Babbs and Riyi Shi. "Subtle paranodal injury slows impulse conduction in a mathematical model of myelinated axons". In: *PLoS One* 8.7 (2013), e67767.

[22] A Aldo Faisal, Luc PJ Selen, and Daniel M Wolpert. "Noise in the nervous system". In: *Nature reviews. Neuroscience* 9.4 (2008), p. 292.

[23] Amit Manwani and Christof Koch. "Detecting and estimating signals in noisy cable structures, I: Neuronal noise sources". In: *Neural computation* 11.8 (1999), pp. 1797–1829.

[24] A Aldo Faisal and Simon B Laughlin. "Stochastic simulations on the reliability of action potential propagation in thin axons". In: *PLoS computational biology* 3.5 (2007), e79.

[25] John G Proakis and Masoud Salehi. *Digital Communications 5e*. 2008.

[26] Ryosuke Matsumura, Hideaki Yamamoto, Takeshi Hayakawa, Shutaro Katsurabayashi, Michio Niwano, and Ayumi Hirano-Iwata. "Dependence and homeostasis of membrane impedance on cell morphology in cultured hippocampal neurons". In: *Scientific reports* 8.1 (2018), pp. 1–10.

[27] Srikantan S Nagarajan and Dominique M Durand. "Analysis of magnetic stimulation of a concentric axon in a nerve bundle". In: *IEEE Transactions on Biomedical Engineering* 42.9 (1995), pp. 926–933.

[28] Keiichiro Susuki. "Myelin: a specialized membrane for cell communication". In: *Nature Education* 3.9 (2010), p. 59.

[29] Nicolas Snaidero and Mikael Simons. "Myelination at a glance". In: *Journal of cell science* 127.14 (2014), pp. 2999–3004.

AUTHORS

Caglar Koca received a B.Sc. degree in electrical and electronics engineering from Middle East Technical University, Ankara, Turkey, in 2010, an M.Sc. degree in electrical and electronics engineering from Koc University, Istanbul, Turkey, in 2014, and is currently pursuing a Ph.D. degree at University of Cambridge. He joined the Next-Generation and Wireless Communication Laboratory (NWCL), Koc University in 2011 and he is currently a research assistant at the Internet of Everything (IoE) group, University of Cambridge since 2017. His research interests include Internet of Everything, Information Theory and molecular communications.

Ozgur Ergul received his M.S. degree from Middle East Technical University, Turkey, and Ph.D. degree from the Next-Generation Communication Laboratory, Koç University, Turkey respectively, both in electrical and electronics engineering. He is currently with the Department of Electrical and Electronics Engineering, Gazi University, Faculty of Engineering, Turkey. His current research interests include vehicular networks, visible light communications, and the Internet of Things.

Meltem Civas received her B.S. degree in Electrical and Electronics Engineering in Bilkent University, Ankara, Turkey, in January 2016, and her M.S. degree at the Electrical and Electronics Engineering Department, Koç University, Istanbul, Turkey in September 2018. She is currently a research assistant at the Next-generation and Wireless Communications Laboratory and pursuing her Ph.D. degree in Electrical and Electronics Engineering, Koç University. Her research interests include Internet of Everything and Molecular Communications.

Ozgur B. Akan received his Ph.D. degree in electrical and computer engineering from the Broadband and Wireless Networking Laboratory, School of Electrical and Computer Engineering, Georgia Institute of Technology, Atlanta in 2004. He is currently with the Electrical Engineering Division, Department of Engineering, University of Cambridge, United Kingdom, and also the director of the Next-Generation and Wireless Communications Laboratory in the Department of Electrical and Electronics Engineering, Koç University. His research interests include wireless, nano, and molecular communications, and the Internet of Everything.

EVOLUTIONARY GAME THEORETIC RESOURCE ALLOCATION SIMULATION FOR MOLECULAR COMMUNICATION

Caglar Koca[1], Meltem Civas[2], Ozgur B. Akan[1,2]
[1]Internet of Everthing (IoE) Group, Department of Engineering, University of Cambridge, UK , [2]Next-generation and Wireless Communications Laboratory (NWCL), Department of Electrical and Electronics Engineering, Koç University, Istanbul, Turkey

NOTE: Corresponding author: Caglar Koca, ck542@cam.ac.uk

Abstract *– Molecular Communication (MC) is an emerging technology using molecules to transfer information between nanomachines. In this paper, we approach the resource allocation problem in Molecular Nano-networks (MCN) from the perspective of evolutionary game theory. In particular, we consider an MCN as an organism having three types of nodes acting as a sensor, relay, and sink, respectively. The resources are distributed among the nodes according to an evolutionary process, which relies on the selection of the most successful organisms followed by creating their offspring iteratively. In this regard, the success of an organism is measured by the total number of dropped messages during its life cycle. To illustrate the evolution procedure, we design a toy problem, and then solve it analytically and using the evolution approach for comparison. We further simulate the performance of the evolution approach on randomly generated organisms. The results reveal the potential of evolutionary game theory tools to improve the transmission performance of MCNs.*

Keywords – Evolutionary game theory, molecular communication, nano-networks, resource allocation

1. INTRODUCTION

The Internet of Bio-Nano Things (IoBNT) is a novel paradigm based on the interconnection of nanoscale devices and biological entities. It enables novel applications ranging from intra-body sensing and actuator networks for the treatment and diagnosis of various diseases to the monitoring and control of environmental pollution [1, 2]. Molecular Communication (MC), which is inspired by the natural communication between biological entities, emerges as a promising communication technology to realize nano-networks for IoBNT applications [3], and recently recognized as an effective abstraction tool for understanding several diseases [4, 5, 6].

Research efforts in MC mainly focused on physical channel modeling, modulation, coding, and detection techniques [7, 8, 9, 10, 11]. Developing MC Nano-networks (MCN) acting and communicating cooperatively to perform IoBNT tasks still poses many challenges.

One of the most prominent challenges in MC is resource allocation. Relying on molecular dispersion instead of electromagnetic waves, MC devices need to preserve both energy and molecules to continue their operation. As a result, resource allocation is a more prominent problem for MC compared to EM, where preserving and/or harvesting energy is enough to guarantee high transmission efficiency.

Realizing the importance of resource allocation in MC, several works are proposed to overcome this problem. In [12], the optimal number of molecules released by the transmitter and the optimal detection threshold of the receiver minimizing the error probability of each hop in a multi-hop MCN are derived. In [13], the joint optimization of molecular resource allocation and relay location is investigated to improve the error performance of a cooperative MC system. Similarly, in [14], the optimal molecule allocation among molecular receivers is determined for a cooperative MC system. In [15], information molecules with different diffusion coefficients are considered optimizing molecular resource allocation in molecular multiple access networks.

MC is the primary communication mode for all organisms. It covers both short ranges as in synaptic communication and long ranges as in pheromones. It is used for both fast acting purposes such as adrenaline and slow acting purposes such as growth. DNA itself is an application of MC that transfers information through ages. Therefore, we turn to evolution, the driving factor of the MC utilization diversity, to find answers relating to the resource allocation problem. One way to tap into the power of evolution is using *evolutionary game theory*.

Game theory has been used as a tool to model networking problems and to investigate communication efficiency of MCN. Game theory principles can help one explore communication among molecular nanomachines when it is hard to obtain analytical solutions because of the size of MCN. Jiang *et al* [16] propose a game-theoretic approach for distributed research allocation for MC networks based on Nash equilibrium and Nash bargaining schemes. In [17], evolutionary game theory tools are used to explore the effect of transmitter behaviors, namely cooperation

or confrontation, regarding communication efficiency in MCN. Game theory has also been used to describe the behavioral dynamics of natural MCNs for sharing common resources such as bacteria populations [18] and plant microbiomes [19].

To the best of our knowledge, evolutionary game theory itself has not been considered in the literature for the MCN resource allocation problem. The success of evolutionary game theory in application to biological problems, including resource allocation in organisms [20] shows its applicability to the nature inspired MCN.

In this paper, we apply evolutionary game theory to the resource allocation problem in MCNs. The evolution procedure relies on selecting successful MCNs, where the success criterion is the total number of successful transmissions, followed by creating their offspring iteratively. By this approach, we have a population of MCNs which is *generally better* in terms of transmission count as we increase the iteration number. In a way, this approach resembles *machine learning*. In other words, our simulation behaves as an evolutionary machine learning algorithm based on mechanisms of evolutionary game theory. To illustrate the evolutionary approach, we use a toy problem for resource management in an MCN and then provide respective analytical and evolutionary solutions comparatively. We also demonstrate our simulation using a randomly generated MCN.

The rest of the paper is organized as follows. In Section 2, we describe the system model, i.e., the operation of the MCN and evolution procedure. In Section 3, we present an analytical and an evolutionary solution for a toy problem comparatively to illustrate how evolution works. In Section 4, we simulate a randomly generated MCN, using the evolutionary approach, and then discuss its performance. Finally, we conclude the paper in Section 5.

2. SYSTEM MODEL

We use an organism as an MCN. The organism consists of nodes communicating with each other using MC. In Section 2.1 we describe the organism in detail and in Section 2.2 we will present the system model for MC. Finally, in Section 2.3, we will illustrate the evolution procedure.

2.1 Organism

An organism has three types of nodes: sensor nodes collecting information about their surroundings, sink(s) operating as gateways to the Internet, and relay nodes transmitting the information they received from the sensor nodes to the sink(s). Because of the extremely small sizes of the relay nodes, they are randomly distributed in a volume. However, sensor nodes and the sink are larger, so they are not necessarily distributed randomly. Fig. 1 depicts the organism. We made the following assumptions regarding the operation of the nodes:

- The sensor nodes have an infinite number of molecules, while the relay nodes have a finite size molecule reservoir.
- The nodes have a good knowledge of each other and the location of the sinks, i.e., nodes use a localization algorithm prior to their operation.
- The existing nodes do not cause any obstruction for the nodes behind them.

The general operation of the organism is depicted in Algorithm 1. Firstly, one of the sensor nodes emits a message (lines 10-12). When a relay node receives the message, it relays the message to another node until the message reaches the sink (line 26). If several relay nodes receive the message, a random one among them, which is closer to the sink than the previously emitting relay node (lines 14-17), transmits the message (lines 18-19). The organism is considered *dead* if X messages are dropped consecutively or if reservoirs of $P\%$ of the relay nodes are exhausted (line 9). The latter condition is included to support the former. Without this condition, if the consecutive drop cycle is broken by a *lucky* transmission, at least X more attempts are made, which increases the drop counts and overall performance parameters are disrupted.

2.2 Molecular communication model

In this work, we use a simplistic model capturing all the essential mechanisms of MC without the computational burden. As with any MC model, our model comprises information carriers, medium, transmission, and reception, as described in detail as follows.

2.2.1 Information carrier

As the name suggests, the information carrier is a molecule that can diffuse and propagate in a medium. The molecules do not interact with each other, and they have a constant, isotropic diffusion constant, D. The half-life of the molecules is assumed long compared to the propagation time and short compared to the time between consecutive transmissions of the nodes. Therefore, the molecule count does not drop during propagation to other nodes. Moreover, we assume that the channel is cleared between consecutive transmissions.

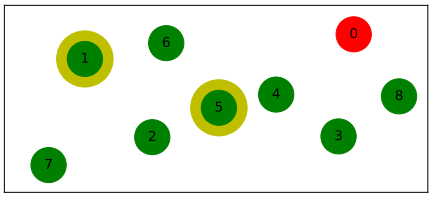

Fig. 1 – An example of an organism, with sink shown as red and sensors nodes shown with yellow rings around them. The other nodes are relay nodes.

Algorithm 1: Operation of the organism.

$\mathcal{S} = \{sensor\_set\}$
$\mathcal{R} = \{relay\_set\}$
$\mathcal{ES} = \{empty\_sensor\_set\} = \{\}$
$\mathcal{RS} = \{received\_set\} = \{\}$
$sink$
$drop\_count = 0$
$total\_drops = 0$
$total\_transmission = 0$
while $drop\_count < X$ *and* $\mathcal{C}(\{\mathcal{ES}\} < P \times \mathcal{C}(\mathcal{R})/100)$ **do**
  $sensor = \texttt{random}(\mathcal{S})$
  $sensor.\texttt{transmit}()$
  $previous\_node = sensor$
  while $sink.\texttt{received}() == FALSE$ **do**
    $\mathcal{RS} = \{node | node \in \mathcal{R}$
    and $node.\texttt{received}() = TRUE$ **and**
    $d(node : sink) < d(previous\_node : sink)\}$
    $next\_node = \texttt{random}(\mathcal{RS})$
    $next\_node.\texttt{transmit}()$
    $previous\_node = next\_node$
    if *drop* **then**
      $\mathcal{RS} = \{\}$
      $drop\_count++$
      $total\_drop++$
      `break`
    end
    if $sink.\texttt{received}() == TRUE$ **then**
      $\mathcal{RS} = \{\}$
      $drop\_count = 0$
      $total\_transmission++$
      `break`
    end
  end
end

2.2.2 Medium

The transmission medium is a 3D medium where molecules can diffuse. The medium is isotropic and homogeneous, i.e., the diffusivity of the molecules does not depend on the position or direction.

2.2.3 Transmission

Each node in the organism is capable of receiving and transmitting messages. The nodes transmit the message by releasing vesicles containing a fixed number of molecules. The release is assumed to happen in the center of the node in an omnidirectional manner.

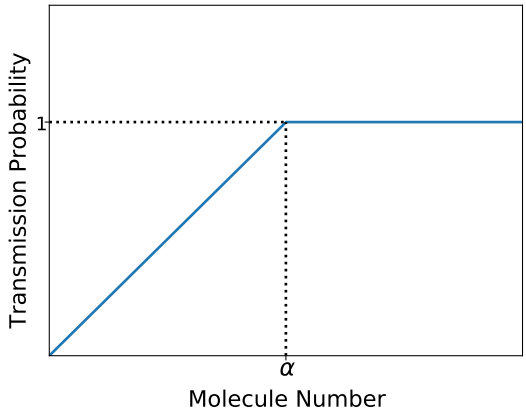

Fig. 2 – Reception behavior depending on molecule count in the vicinity.

2.2.4 Reception

Reception occurs when molecules are incident on the receptors located on the nodes. Considering a binding mechanism following the standard lock-and-key model, both the molecular concentration in the vicinity of the receptor and the orientation of molecules according to the receptor are important. In other words, while a single molecule with the correct orientation can bind the receptor, many molecules without the correct orientation may fail to trigger a reception. Hence, to capture the stochastic properties of reception, we use the following simple approach. If the maximum number of molecules exceeds a certain threshold, α, the binding probability approaches 1, so we assume successful transmission. If the number of molecules is below α, there is a non-zero chance of successful binding. This chance is directly proportional to the molecule count in the vicinity. Fig. 2 depicts the reception behavior. We can summarize reception with *(1)*,

$$P_1(t) = \begin{cases} 1, & \max\limits_{t \to t+\Delta T} M \geq \alpha \\ 0, & \max\limits_{t \to t+\Delta T} M = 0 \\ \frac{\max\limits_{t \to t+\Delta T} M}{\alpha}, & 0 \leq \max\limits_{t \to t+\Delta T} M \leq \alpha \end{cases} \quad (1)$$

where $\max\limits_{t \to t+\Delta T} M$ is the maximum number of molecules in the vicinity of the node and $P_1(t)$ is probabilities of successfully receiving the emitted signal.

2.3 Evolution

As stated in Section 2.1, the organism *dies* after it consecutively drops messages from its sensors. The total number of dropped messages during its life cycle measures the organism's success.

The more successful organisms, which are chosen according to the *selection* process, then produce their offspring, i.e., the *creation*. Iterated selection and creation stages constitute evolution. The evolution procedure is summarized in Algorithm 2. First, as the generation dies, the

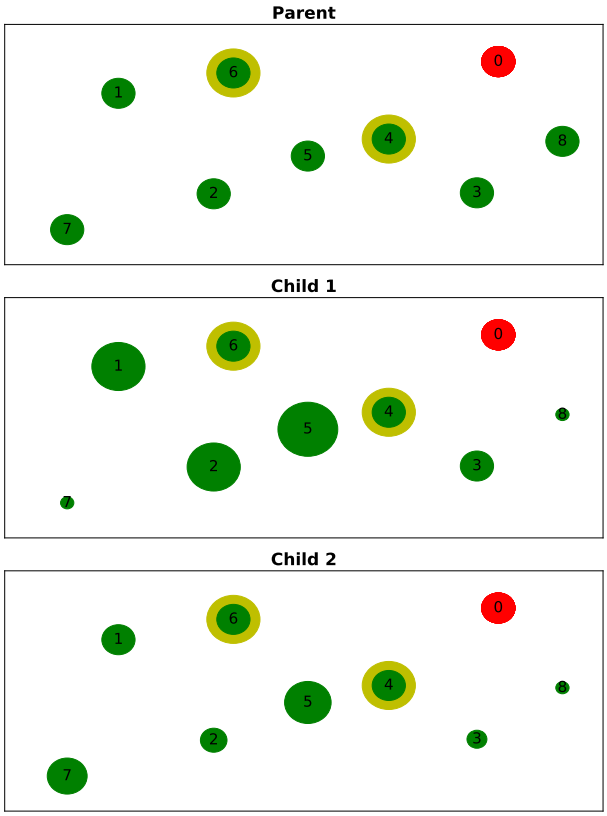

Fig. 3 – The parent, which has the same reservoir size in each node, evolves into two children. The radii of the nodes are proportional to the reservoir size. Note that for illustration purposes, the carried changes were not infinitesimal.

most successful R of organisms in the generation of N organisms are selected (lines 4-5). Then, the selections form their *offspring* (line 6). The nodes of these offspring have very similar reservoir distribution among their relay nodes compared to their parent. The resources are distributed among the relay nodes only with infinitesimal changes compared to the resource distribution of their parent. Hence, suboptimal distributions are eliminated, and better nodes are created. A parent with two offspring is presented in Fig. 3.

Note that during procreation, the resources available to each node of an organism changes by a random number k such that

$$k = \{-k_{max}, -k_{max}+1 \dots, -1, 0, 1, \dots, k_{max}\} \qquad (2)$$

If $k < 0$ and the node reservoir becomes smaller than 0, the resources are set to 0.

Note that the total resources distributed to all nodes are kept constant. Otherwise, organisms with a higher total number of resources would dominate the others, and we could not obtain any information regarding optimum resource distribution.

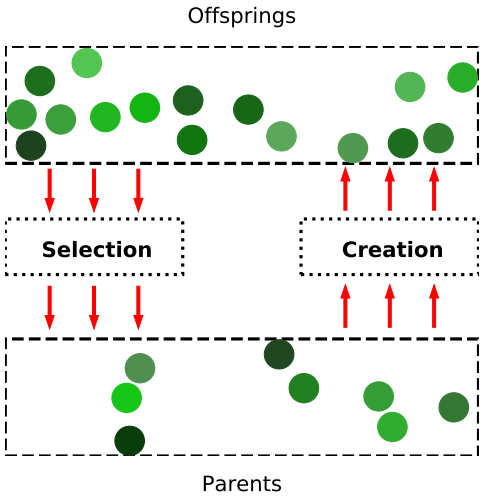

Fig. 4 – In the first stage, offspring of the previous generation are selected through the selection rules. In the second stage, selected parents create the next generation. In our approach, the selection rule is the higher total transmission count.

Algorithm 2: Evolution Procedure

1 $\{organisms\}$
2 $i = 0$
3 **while** $i < evolution\_iterations$ **do**
4 $\quad \{drops\} = \{organisms\}.\texttt{selection}()$
5 $\quad \{parents\} = \{org | org \in \{organisms\}$ **and** $org.\texttt{selection}() \in \texttt{sorted}(\{drops\})[0 : R-1]\}$
6 $\quad \{organisms\} = \{parents\}.\texttt{procreate}()$
7 $\quad i++$
8 **end**

3. EVOLUTIONARY GAME THEORY

Evolutionary game theory is an application of game theory for evolution and population dynamics. It suggests that the collective behavior of the individuals, whether they are rational, or not plays a vital role in the survival and continuation of the species.

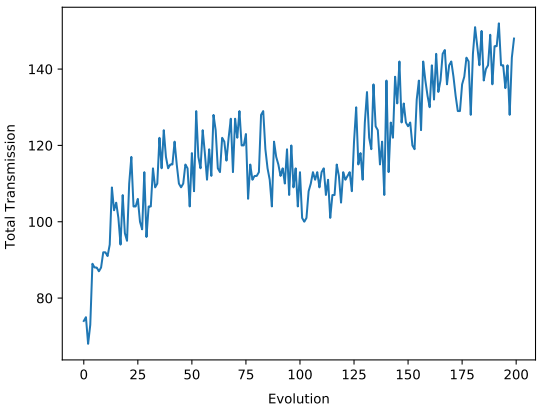

Fig. 5 – Total number of transmissions by the organism through stages of evolution.

Evolutionary game theory is a two-stage process. In the first stage, the population members undergo a selection process depending on the individual strategies of the pop- ulation. In the second stage, selected individuals create new offspring. The phases of evolutionary game theory are depicted in Fig. 4.

In this section, we first describe the toy problem and then present an analytic solution using the simple geometry of the toy problem. Then, we demonstrate an evolutionary solution for the same problem and compare the results with the analytic solution.

3.1 Problem description

To illustrate how evolution works, consider the toy problem given in Fig. 6. The parent consists of one sink node, two sensor nodes, $\mathcal{S} = \{n_4, n_6\}$ and six relay nodes. The goal, as described in Algorithm 1, is either to minimize the total number of dropped messages or maximize the total number of transmissions. Note that there might be other communication-related goals such as faster communication or communicating with fewer resources, however, for the sake of simplicity, we only focus on the maximum number of dropped messages from sensor nodes to the sink for this problem. As a result, organisms with a lower number of drops are selected to create offspring. Since we consider the organisms individually, we assume they do not interact with each other.

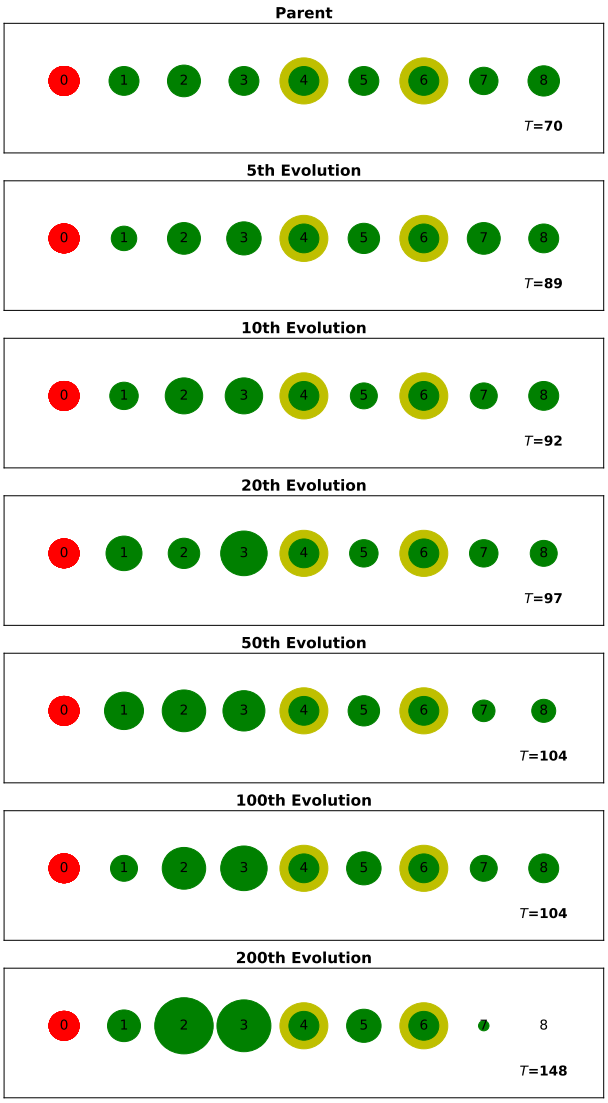

Fig. 6 – Snapshots of the resource distribution and total transmission, T after different evolution counts.

Without loss of generality, we assume that sensor nodes have unlimited resources, i.e., they safely outlast the relay nodes. Without this assumption, dried-up sensor nodes might stop creating messages before relay nodes stop transmitting them. Hence, such an assumption helps us only to focus on relaying the messages instead of their creation. This assumption is also justified because sensor nodes with extra hardware must be larger than the relay nodes.

Our final assumption is that each node knows the location of the sink and other nodes to a reasonable degree. Thus, nodes do not relay messages coming from a node closer to the sink than they are, as described in Algorithm 1. This assumption is justified as well since each node can include a stamp on the messages allowing the receiving nodes to learn the last transmitting node.

3.2 Analytic solution

Although most resource management problems do not have an easy analytic solution, we can attempt to find one for this problem because of its simple geometry. To this end, we evaluate the resource distribution of an optimal organism, using *Shapley Values* of individual nodes for the organism. A Shapley Value is defined as the performance difference in a system with and without the part under in- vestigation. In other words, we can find the Shapley Value of node $n_i \in \mathcal{R}$ using the formula

$$V(n_i) = P(\forall n_j \in \mathcal{R}) - P(\forall n_j \in \mathcal{R} - n_i), \qquad (3)$$

where $V(n_i)$ is the Shapley Value of node n_i and $P(\mathcal{X})$ is the cumulative performance of all members of set $\mathcal{X}$. Firstly, since they are located to the opposite side of the sink, i.e., *upstream* of all sensor nodes, n_7 and n_8 do not relay any messages. Hence,

$$V(n_7) = V(n_8) = 0. \qquad (4)$$

For the remaining relay nodes, we employ the probability of a drop to measure their performance.

$$V(n_i) = p_{drop}(\mathcal{R} - n_i) - p_{drop}(\mathcal{R}), \qquad (5)$$

where $p_{drop}(\mathcal{X})$ is the drop probability within the set $\mathcal{X}$. Note that since *(5)* focuses on drop performance, it is multiplied by a factor of -1, i.e., performance is measured as the negative of the drops.

Without loss of generality, we assume that transition between adjacent nodes is a certainty while there is still a non-zero chance of the next node receiving the message, as depicted in Fig. 2. The simulation parameters are also chosen to satisfy this assumption. Therefore, we expect no drop to occur if all nodes are present, which allows us to find $p_{drop}(\mathcal{R}) = 0$. Hence, only the first term of *(5)* remains.

We know that drops occur only if no other node receives the message. Otherwise, one of the receiving nodes, namely, $n_i \in \mathcal{RS}$ relays the message to the sink. Hence,

$$p_{drop}(i) = \lambda_{i+1}\left(1 - \prod_{k=2}^{i+1}(1-p_k)\right), \qquad (6)$$

where λ_i is the activation rate of n_i and p_k is the probability of a successful transmission between node n_i and n_{i+k}. Note that, $1-\prod(1-p_k)$ term gives the probability that no *downstream* node including the sink receives the message coming from n_{i+1} and if $\lambda_{i+1} = 0$ if $n_{i+1} \notin \mathcal{S}+\mathcal{R}$. Here, we also used the fact that the chosen simulation parameters *ensures* transmission between adjacent nodes, which renders drops possible only when one-step upstream node, i.e., n_{i+1} if $p_{drop}(i)$ is investigated, is transmitting.

Activation rates depend on the position of the node. While sensor node activation occurs independent of other nodes, relay nodes depend on the activation of sensor nodes. For example, n_5, which only has the burden of transmitting messages from n_6, is activated less than $n_1 - n_3$. As a result, λ_is can be solved recursively.
For a given node, we can find λ_{i+1} as

$$\lambda_{i+1} = \sum_{j>i+1, j\in\mathcal{S}+\mathcal{R}} \lambda_j \left(\sum_{\substack{n_0, n_i \notin \mathcal{RS} \\ n_{i+1}\in\mathcal{RS}}} \frac{1}{\mathcal{C}(\mathcal{RS})} p_{\mathcal{RS}} \right) + \sum_{n_j\in\mathcal{S}} \delta_{i+1,j}\lambda^S_{i+1}, \qquad (7)$$

where δ_{ij} is the Kronecker Delta, λ^S_i is the sensor activation rate of sensor node n_i, n_0 is the sink and p_{RS} is the probability of obtaining the particular $\mathcal{RS}$. It is calculated by

$$p_{\mathcal{RS}} = \prod_{n_j\in\mathcal{RS}} p_{6-j} \prod_{\substack{n_j\notin\mathcal{RS} \\ n_j\neq n_i}} (1-p_{6-j}). \qquad (8)$$

Although seemingly complicated, the first term of *(7)* describes the node acting as a relay probability by summing over all nodes, which might be relaying a message to node n_i. The second term describes the node acting as a sensor node. Note that second term becomes non-zero only when $n_j \in \mathcal{S}$.

Table 1 – Percent Shapley Values and resource distribution

	Analyic Results		Experimental Results	
Node	**Percent**	**Value**	**Percent**	**Value**
1	29.72	35.67	21.09	27
2	27.80	33.36	28.91	37
3	28.18	33.82	30.47	39
5	14.30	17.16	14.84	19
7	0	0	4.69	6
8	0	0	0	0

3.3 Evolutionary solution

In the previous subsection, we used the simplicity of geometry to find an analytic solution to an otherwise complicated problem. In this section, we allow the parent organism to continuously evolve as described in Section 2.3.

We can see in Fig. 6 that expectedly, the resources allocated to n_7 and n_8 are reallocated to the n_2 and n_3, even after a few iterations. n_5, which only has the burden of relaying messages originated at n_6, possesses fewer resources than the n_2 and n_3, relaying messages originated at both of the sensor nodes.

Inspecting Fig. 5, we observe that evolution does not guarantee increased performance after each iteration. This observation coincides with the fact that the evolution of species does not guarantee better offspring at every generation. Furthermore, similar to its counterpart in biology, evolution may be influenced by successful organisms with suboptimal resource distribution. For example, since the sensors are activated randomly, an organism with higher n_4 sensor activity would require fewer resources overall than an organism with higher n_6 sensor activity.

Note that there is also a systematic error in our simulation method promoting decreased performance in some iterations. We force an infinitesimal change in all nodes in the organism, i.e., nodes do not die off when they do not have any resources in an iteration. As a result, nodes having no reservoir either stay at no resources or slightly go up, causing the organism to approach a distribution just below the optimal.

Table 1 shows the comparison between analytical and evolutionary results after 200 iterations. Although they all start at resources enough for 20 transmissions, as expected, n_7 and n_8 lose their resources while other nodes thrive during the evolutionary process. However, as explained above, even though it approaches zero, n_7 is not yet quite zero, wasting some resources, which should be reallocated to other nodes. The only dramatic discrepancy is n_1 being lower than the expectations by the analytical solution. We expect that the discrepancy diminishes with an increasing iteration count.

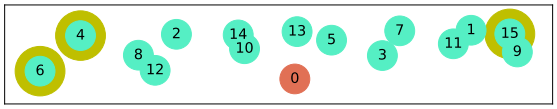

Fig. 7 – Layout for the simulation organism.

Table 2 – Simulation parameters

Name	Value	Unit
Vesicle size	40000	molecules
Diffusion constant	1×10^{-12}	m^2/s
Radius	0.5	μm
Exhausted node ratio	0.2	
# of Vesicles per node	40	
Offsprings	2	
Node count	16	
Dimensions	$1 \times 2 \times 10$	$\mu m \times \mu m \times \mu m$
Change amplitude	3	

4. VESICLE COUNT OPTIMIZATION

In this section, we use our approach to optimize a randomly generated organism. The only design constraint we have is introducing a separation between the sink and the sensors, i.e., the probability of any sensor successfully sending information to the sink without the relay nodes is small enough to be ignored. The simulation parameters and the simulation organism are given in Table 2 and Fig. 7 respectively. The selected simulation parameters are all arbitrary; however, one can alter the time scale, diffusion constant, radii, and the organism size easily to fit them to an actual organism.

Firstly, we investigate the effect of the number of offspring per organism. Since the population is kept constant, the selection rate is proportional to the inverse of the offspring per organism.

Child count change

Changing the child count for each stage has dramatic effects on the performance of the organism. These effects are visible in Fig. 8. A smaller number of offspring imply that more parents join in the creation of the next generation. As a result, there is less uncertainty in the next generation. More offspring increase the uncertainty. If one of the parents reached their performance mostly due to luck, most of the offspring in the next generation becomes inferior. This situation leads to huge discrepancies in performance between generations.

Amplitude change

Increasing the amplitude of change inter-generations has a dramatic impact on the system performance. For large amplitudes, the evolution fails to reach its potential. Once the organism reaches a certain performance, the huge

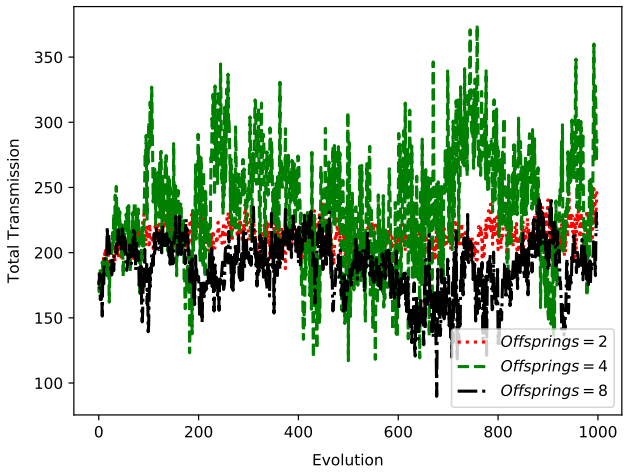

Fig. 8 – Performance of evolution with different child numbers.

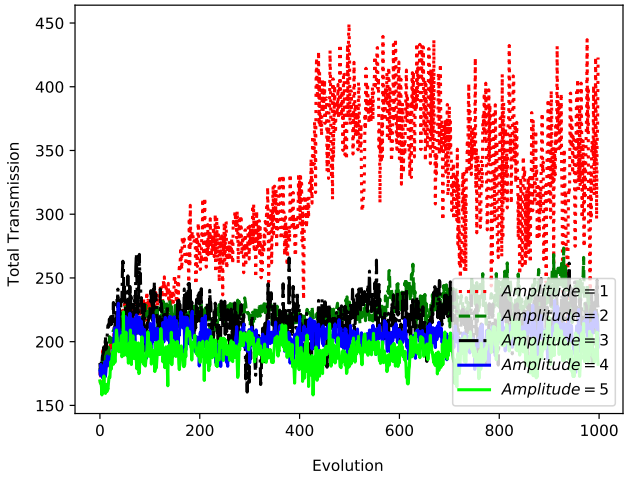

Fig. 9 – Performance of evolution with different amplitude values.

changes in the resource distribution set the organism back. Fig. 9 displays the performance of evolution with different change amplitudes.

Inspecting Fig. 9, we also realise that the performance of $Amplitude = 1$ line is inferior for the first hundred iterations of evolution. This is obviously due to the small increases due to the limited inter-generational changes. However, the same factor boosts the final performance of the organism, which verifies the biological evolution, i.e., small changes advance the organisms while huge changes are not sustainable.

5. CONCLUSION

In this paper, we simulate the resource allocation in an organism, having nodes communicating via MC, using evolutionary game theory. We propose a two-staged evolution process realized by selecting the organisms with

better transmission count and the creation of their offspring. Furthermore, we apply this approach to a simplistic MCN scenario, for which we also obtain an analytical solution. We simulate the performance of evolution concerning different parameters. Our work offers a simple demonstration of nature's solution to the resource management problem.

We believe our approach applies to many problems other than resource allocation. It also holds the potential of optimizing several different parameters to a reasonable degree. As future work, we will employ our method for node orientation, vesicle size, and receptor locations on the node surfaces.

ACKNOWLEDGEMENT

This work was supported in part by the AXA Research Fund (AXA Chair for Internet of Everything at Koç University) and Huawei Graduate Research Scholarship.

REFERENCES

[1] Ian F Akyildiz, Max Pierobon, Sasi Balasubramaniam, and Y Koucheryavy. "The internet of bio-nano things". In: *IEEE Communications Magazine* 53.3 (2015), pp. 32–40.

[2] Ozgur Baris Akan, Hamideh Ramezani, Meltem Civas, Oktay Cetinkaya, Bilgesu Arif Bilgin, and Naveed Ahmed Abbasi. "Information and communication theoretical understanding and treatment of spinal cord injuries: State-of-the-art and research challenges". In: *IEEE Reviews in Biomedical Engineering* (2021).

[3] Ozgur B Akan, Hamideh Ramezani, Tooba Khan, Naveed A Abbasi, and Murat Kuscu. "Fundamentals of molecular information and communication science". In: *Proceedings of the IEEE* 105.2 (2016), pp. 306–318.

[4] Caglar Koca, Meltem Civas, Selin M. Sahin, Onder Ergonul, and Ozgur B. Akan. "Molecular Communication Theoretical Modeling and Analysis of SARS-CoV2 Transmission in Human Respiratory System". In: *IEEE Transactions on Molecular, Biological and Multi-Scale Communications* (2021), pp. 1–1. DOI: 10.1109/TMBMC.2021.3071748.

[5] Saswati Pal, Nabiul Islam, Sudip Misra, and Sasitharan Balasubramaniam. "In Vivo Channel Characterization for Dengue Virus Infection". In: *Proceedings of the Sixth Annual ACM International Conference on Nanoscale Computing and Communication*. 2019, pp. 1–7.

[6] Meltem Civas and Ozgur B Akan. "Rate of Information Flow Across Layered Neuro-Spike Network in the Spinal Cord". In: *IEEE transactions on nanobioscience* 19.3 (2020), pp. 368–377.

[7] Murat Kuscu, Ergin Dinc, Bilgesu A Bilgin, Hamideh Ramezani, and Ozgur B Akan. "Transmitter and receiver architectures for molecular communications: A survey on physical design with modulation, coding, and detection techniques". In: *Proceedings of the IEEE* 107.7 (2019), pp. 1302–1341.

[8] Murat Kuscu and Ozgur B Akan. "Detection in Molecular Communications with Ligand Receptors under Molecular Interference". In: *arXiv preprint arXiv:2101.00081* (2020).

[9] Murat Kuscu and Ozgur B Akan. "Channel sensing in molecular communications with single type of ligand receptors". In: *IEEE Transactions on Communications* 67.10 (2019), pp. 6868–6884.

[10] Vahid Jamali, Arman Ahmadzadeh, Wayan Wicke, Adam Noel, and Robert Schober. "Channel modeling for diffusive molecular communication A tutorial review". In: *Proceedings of the IEEE* 107.7 (2019), pp. 1256–1301.

[11] Weisi Guo, Taufiq Asyhari, Nariman Farsad, H Birkan Yilmaz, Bin Li, Andrew Eckford, and Chan-Byoung Chae. "Molecular communications: Channel model and physical layer techniques". In: *IEEE Wireless Communications* 23.4 (2016), pp. 120–127.

[12] Arman Ahmadzadeh, Adam Noel, and Robert Schober. "Analysis and design of multi-hop diffusion-based molecular communication networks". In: *IEEE Transactions on Molecular, Biological and Multi-Scale Communications* 1.2 (2015), pp. 144–157.

[13] Satish K Tiwari, Tadi Ravi Teja Reddy, Prabhat K Upadhyay, and Daniel Benevides Da Costa. "Joint optimization of molecular resource allocation and relay positioning in diffusive nanonetworks". In: *IEEE Access* 6 (2018), pp. 67681–67687.

[14] Yuting Fang, Adam Noel, Nan Yang, Andrew W Eckford, and Rodney A Kennedy. "Symbol-by-symbol maximum likelihood detection for cooperative molecular communication". In: *IEEE Transactions on Communications* 67.7 (2019), pp. 4885–4899.

[15] Xuan Chen, Miaowen Wen, Chan-Byoung Chae, Lie-Liang Yang, Fei Ji, and Kostromitin Konstantin Igorevich. "Resource Allocation for Multi-User Molecular Communication Systems Oriented to The Internet of Medical Things". In: *IEEE Internet of Things Journal* (2021).

[16] Chunxiao Jiang, Yan Chen, and KJ Ray Liu. "Nanoscale molecular communication networks: a game-theoretic perspective". In: *EURASIP Journal on Advances in Signal Processing* 2015.1 (2015), pp. 1–15.

[17] Caglar Koca and Ozgur B Akan. "Anarchy versus cooperation on internet of molecular things". In: *IEEE Internet of Things Journal* 4.5 (2017), pp. 1445–1453.

[18] Adam Noel, Yuting Fang, Nan Yang, Dimitrios Makrakis, and Andrew W Eckford. "Effect of local population uncertainty on cooperation in bacteria". In: *2017 IEEE Information Theory Workshop (ITW)*. IEEE. 2017, pp. 334–338.

[19] Apostolos Almpanis, Christophe Corre, and Adam Noel. "Agent Based Modeling of the Rhizobiome with Molecular Communication and Game Theory". In: *Proceedings of the Sixth Annual ACM International Conference on Nanoscale Computing and Communication*. 2019, pp. 1–7.

[20] John Maynard Smith. *Evolution and the Theory of Games*. Cambridge university press, 1982.

AUTHORS

Caglar Koca received a B.Sc. degree in electrical and electronics engineering from Middle East Technical University, Ankara, Turkey, in 2010, an M.Sc. degree in electrical and electronics engineering from Koç University, Istanbul, Turkey, in 2014, and is currently pursuing a Ph.D. degree at University of Cambridge. He joined the Next-Generation and Wireless Communication Laboratory (NWCL), Koç University in 2011 and he is currently a research assistant at the Internet of Everything (IoE) group, University of Cambridge since 2017. His research interests include Internet of Everything, information theory and molecular communications.

Meltem Civas received her B.S. degree in Electrical and Electronics Engineering in Bilkent University, Ankara, Turkey, in January 2016, and her M.S. degree at the Electrical and Electronics Engineering Department, Koç University, Istanbul, Turkey in September 2018. She is currently a research assistant at the Next-generation and Wireless Communications Laboratory and pursuing her Ph.D. degree in Electrical and Electronics Engineering, Koç University. Her research interests include Internet of Everything and molecular communications.

Ozgur B. Akan received his Ph.D. degree in electrical and computer engineering from the Broadband and Wireless Networking Laboratory, School of Electrical and Computer Engineering, Georgia Institute of Technology, Atlanta in 2004. He is currently with the Electrical Engineering Division, Department of Engineering, University of Cambridge, United Kingdom, and also the director of the Next-Generation and Wireless Communications Laboratory in the Department of Electrical and Electronics Engineering, Koç University. His research interests include wireless, nano, and molecular communications, and the Internet of Everything.

ELECTRIC MANIFESTATIONS AND SOCIAL IMPLICATIONS OF BACTERIA AGGREGATION FROM THE BESSEL-KELLER-SEGEL EQUATION

Huber Nieto-Chaupis
Universidad Autónoma del Perú

Panamericana Sur Km. 16.3 Villa el Salvador, Lima PERÚ

NOTE: Corresponding author: hubernietochaupis@gmail.com

Abstract *– This paper proposes a fair extension of Keller-Segel equation based in the argument that bacteria exhibit proporties electric in their composition. The new mathematical form of this extension involves the integer-order Bessel functions. With this one can go through the electrodynamics of the representative scenarios in order to understand the social behavior of bacteria. From the theoretical side this paper demonstrates that, charged electrically, aggregation of bacteria would give rise to electric currents that hypothetically are the reasons for social organization and disruption among them. The electrical properties of bacteria from this mathematical proposal might be relevant in a prospective implementation of so-called Internet of Bio-Nano Things network, that aims to be characterized for having a very high signal/noise.*

Keywords – Bessel, classical electrodynamics, Keller-Segel, nanonetwork

1. INTRODUCTION

Evelyn Keller and Lee Segel in 1971 reported in [1] that bacteria exhibit some relative preference to move through the highest concentrations of substrate instead of the lowest ones. This phenomenon was projected onto the equation known as the Keller-Segel equation and it is written as:

$$\frac{\partial\, b(x,t)}{\partial t} = \frac{d}{dx}\left[\mu(s)\frac{db(x,t)}{dx}\right] - \frac{d}{dx}\left[b(x,t)\chi(s)\frac{ds}{dx}\right] \quad (1)$$

whose meaning of elements of this reads as follows:

- $b(x,t)$= bacteria density,
- $s(x,t)$ = substrate density,
- $\chi(s)$ = chemotactic coefficient,
- $\mu(s)$ = motility parameter.

Eq.1 can be seen actually as a kind of compensation. In effect, one can see that by putting $\chi(s,t)$ and $\mu(s)$ as constants, then the positive change $\frac{\partial\, b(x,t)}{\partial t} > 0$ demands that:

$$\frac{d^2 b(x,t)}{dx^2} > \frac{d^2 s(x,t)}{dx^2}\,. \quad (2)$$

That is valid over the allowed periods of bacteria substrate interaction. This has interesting consequences in the discipline of bacteria dynamics [2]. Clearly one can see that it encompasses the reason of the Keller-Segel equation, in the sense that bacteria can deplete substrate in an efficient manner. For example, Unluturk, Balasubramanian and Akyildiz [3] have used the Keller-Segel model in the study of social behavior of bacteria inside the framework of molecular communications as part of the fundamental postulates of the prospective Internet of Bio-Nano Things (IoBNT) [4]. Clearly one can appeal to physics of Eq. 1 for a robust application inside the molecular and phenomena at the nano-level. Since bacteria is transporting a net electric charge, then a plethora of ways to search their behavior represents an option to use theoretical scenarios of physics interactions and the implcations that would rise in a scenario of bio-nano technology. Thus, Eq. 1 opens various paths to understand both the physics and biophysics of bacteria dynamics. Of course, Eq. 1 can also be seen as a fair extension of diffusion equation [5]. In effect, Eq.1 to some extent can also be written as $\frac{\partial\, \rho(s,t)}{\partial t} = \mathrm{D}\,\frac{\partial^2 \rho(s,t)}{\partial s^2} + \mathrm{G(s,t)}$ with D the diffusion constant and G(s, t) enclosing a set of operations based at both spatial and time derivatives. Thus, emerges the questions: Are bacteria fully diffusive? What are then the physics of this possible diffusion? Here one can answer in terms of physics laws in: (i) Electricity, (ii) Thermodynamics, and (iii) Space-time propagation. The purpose of this paper is to extend Eq.1 when bacteria are composed by electrical material such as ions for instance, so that concrete electric interactions would take place.

In this manner a large amount of bacteria density might be described by micro-forces so that a combined description based in Newton forces and electrodynamics can add relevant information to the process of substrate degradation. In cases of complex dynamics, of course the usage of diffusion equation can be obsolete so that an upgraded version would have to be needed. For example, one can see the work of Rosen in 1984 [6] characterized by having differential equations inspired by the Navier-Stokes scenario in order to propose a theory of bacteria chemotaxis. The contribution of this paper is in essence the reformulation of the Keller-Segel equation containing the integer-order Bessel functions. With this an analysis about the implications of electrodynamics is derived. The rest of this paper is structured as follows: In the second section, the Bessel-Keller-Segel equation is derived. Once this equation is established then in the third section the eletrodynamics equations are derived in a closed-form manner. Here the instantaneous electric current is presented. It is seen that the resulting distributions exhibit a certain similarity with the discharge of a typical RC circuit. Finally, in fourth section the conclusion of the paper is presented.

2. EXTENSION OF THE KELLER-SEGEL EQUATION

Actually, one can exploit Eq. 1 in many ways by which one can extract the dynamics of any aggregation of bacteria in different scenarios while under interaction with substrates [7], [8]. Bacteria as a biological unit can require particular capabilities in order to guarantee an optimal colonization. Although it is not clear whether bacteria dynamics behave as a linear or nonlinear system, throughtout this document it will be assumed the linear assumption that allows for exact extensions.

Thus, for instance consider the case where $\boldsymbol{\mu(s) = g(s) \equiv g(x)}$ and $\boldsymbol{\chi(s) = h(s) \equiv h(x)}$ acquiring an explicit dependence on "$\boldsymbol{x}$" then from Eq. 1 one arrives at:

$$\frac{\partial\, b(x,t)}{\partial t} = g(x)\left[\frac{d^2 b(x,t)}{dx^2}\right] - h(s)\left[\frac{db(x,t)}{dx}\frac{ds}{dx}\right] - h(s)\left[b(x,t)\frac{d^2 s}{dx^2}\right]. \quad (3)$$

One interesting scenario is the stationary one with $\frac{\partial\, b(x,t)}{\partial t} = \mathbf{0}$. In this manner one can assume the following: $\boldsymbol{h(x)\, ds/dx = -x}$ in the second term in the right side of Eq. 3, yielding:

$$\frac{ds(x,t)}{dx} = \frac{-x}{h(s)} \Rightarrow \quad s(x,t) = -\int \frac{x}{h(s)} dx. \quad (4)$$

In this manner the Keller-Segel equation with $\boldsymbol{g(x) = x^2}$ one gets:

$$x^2\left[\frac{d^2 b(x,t)}{dx^2}\right] + x\left[\frac{db(x,t)}{dx}\right] - h(x)\left[b(x,t)\frac{d^2 s}{dx^2}\right] = 0. \quad (5)$$

2.1 Essential Assumptions

Eq.5 lends itself to being operated towards two known differential equations. Although one can apply unphysical procedures, it is clear that in a first instance the Bessel structure can be a good candidate. In this manner, in order to construct an integer-order Bessel differential equation [9], one needs to impose at the rigth-side the following:

$$h(s)\frac{d^2 s}{dx^2} = -\left(1 - \frac{n^2}{x^2}\right), \quad (6)$$

that implies that there is a direct relation between the function $\boldsymbol{h(s)}$ and the integer numbers $\boldsymbol{n}$. On the other hand one can take the definition of Eq. 4 to be inserted in Eq. 6 yielding:

$$-h(x)\,\frac{d}{dx}\left[\frac{x}{h(s)}\right] = \left(1 - \frac{n^2}{x^2}\right), \quad (7)$$

where the signs have been canceled in both sides. Subsequently by applying the derivative in a straightforward manner then Eq. 7 can be read as:

$$-h(x)\left[\frac{h(s) - x\frac{dh}{ds}\frac{ds}{dx}}{h^2(s)}\right] =$$

$$-\left[\frac{h(s) - x\frac{dh}{ds}\frac{ds}{dx}}{h(s)}\right] = \left(1 - \frac{n^2}{x^2}\right) \quad (8)$$

yielding a first-order differential equation that can be written as:

$$\Rightarrow\; x\frac{dh}{ds} - h(s) = h(s)\left(1 - \frac{n^2}{x^2}\right). \quad (9)$$

It was assumed the approximation given by $\frac{ds}{dx} \approx \mathbf{1}$, (resulting in a toy model for substrate dynamics that appears to be linear with x). It allows a direct solution of first-order differential equation that can be written as:

$$\frac{dh}{h} = \left(\frac{2}{x} - \frac{n^2}{x^3}\right) ds \quad \Rightarrow \quad h(s) = \mathbf{Exp}\left[s\left(\frac{2}{x} - \frac{n^2}{x^3}\right)\right]. \quad (10)$$

In this manner the chemotactic coefficient is expressed in terms of "x". A direct solution for it yields the exponential form and depends directly on the substrate density "s". Therefore, one arrives at:

$$\Rightarrow \chi(s) = \mathbf{Exp}\left[s(x)\left(\frac{2}{x} - \frac{n^2}{x^3}\right)\right] \quad (11)$$

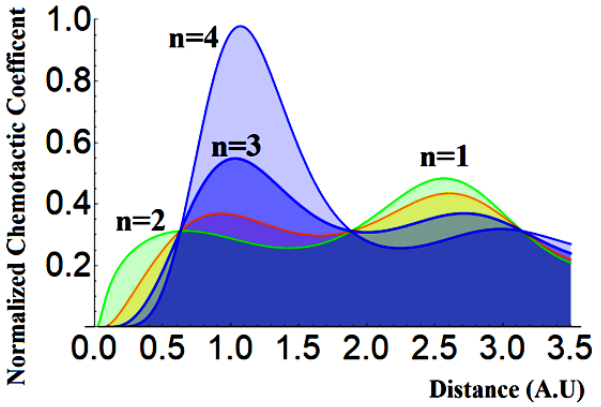

Fig. 1 – The normalized chemotactic coefficient from Eq. 11 for up to 4 values of number "n", denoting the order of Bessel functions. For this it is assumed the unidimensional representation of $s(x) = Cos[2.5x]Sin[0.1 * x^2]$.

2.2 Charged Bacteria Density

In Fig. 1 up to 4 different distributions of the normalized chemotactic coefficient are displayed under the assumption that the substrate density has the quasi-stochastic form given by $Cos(2.5\,x)\,Sin(0.1\,x^2)$ [10]. This mathematical approach comes from the fact that the existence of periodical manifestation of electric behavior would exhibit both attraction and repulsion, depending the state of pair: bacteria-substrate.

Thus, positive and negative values with rapid oscillation along the distances are expected to be allowed by the motility of bacteria. One can see that the higher order exhibits a well-shaped peak.

2.3 The Bessel-Keller-Segel (BKS) Equation

Therefore from Eq. 5 to Eq. 9 one arrives at a novel version of the Keller-Segel equation called BKS (Bessel-Keller-Segel), that is written below as:

$$x^2\left[\frac{d^2b(x,t)}{dx^2}\right] + x\left[\frac{db(x,t)}{dx}\right] + \left(1 - \frac{n^2}{x^2}\right)b(x,t) = 0 \quad (12)$$

that is solvable for the bacteria density yielding imminently the integer-order Bessel functions:

$$b(x,t) = B(x,t) = J_n(x,t) \quad (13)$$

Although a solid interpretation of Eq. 13 might not be adjusted to the scope of this paper, it is possible to some extent to adjudicate a meaning in terms of bacteria motility properties such as cooperative behavior. It is noteworthy that the negative values of Bessel functions are not describing physical solutions. Because of this, the positive values of bacteria density might be interpreted in terms of cooperative and competitive population, depending on the width of distribution. Clearly this requires the option of square of the Bessel functions that provides only physical meaning. Therefore from Eq. 13 one arrives a the solutions given by:

$$B(x,t) \propto |J_n(x,t)|^2 \quad (14)$$

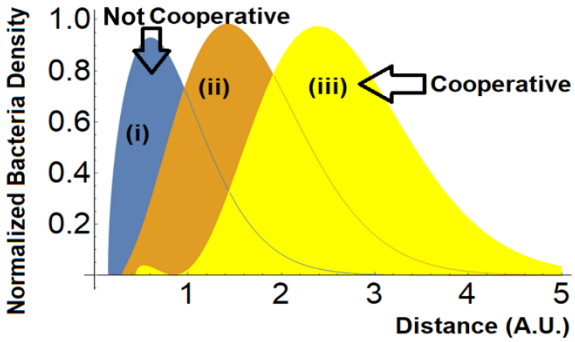

Fig. 2 – The normalized bacteria density $B(x,t)$ as a function of distance (in arbitrary units) for the first 3 orders of Bessel functions and their tentative interpretation in terms of cooperative population.

In Fig. 2 up to three possible bacteria density are displayed. For this a normalization function was opted, and it reads 2.9 $\lambda_B\sqrt{x - n \times \lambda_A}$ where λ_A is about the 5% of λ_B for this exercise (this is assumed both free parameters λ_A and λ_B, to illustrate Fig. 2). Clealrly, both can be changed in more analytic scenarios. Therefore the density spectra for s fixed time "T" reads:

$$B(x,T) = \lambda_B\sqrt{x - n \times \lambda_A}\ |J_n(x - n \times \lambda_A, t, T)|^2 \quad (15)$$

In fact, inspired at the criterion of [3] in which the bacteria densities have a steady-state profile centered in $x - n \times \lambda_A$ being this dependent on the integer "n". One can see that while the order of Bessel function increases then one would expect the cooperative population moves with distance; as seen in Fig. 2 the distributions moves to the right.

A compelling argumentation of why one calls cooperative population to the distribution (yellow color), can be directly seen in the width of each curve. Thus, when it is larger than the others, one arrives to the fact that bacteria join each other to perform a subsequent action ("Many make force"). A short width is perceived as The number of individuals along the time of interaction can be obtained from a simple integration $N(t) = \int dx B(x,t)$. Thus one can

speculate that from the spatial displacement the velocity can be dependent on the Bessel order. In this view, from Eq. 13 with the time derivative then one arrives at:

$$\frac{\boldsymbol{db(x,t)}}{\boldsymbol{dx}}\frac{\boldsymbol{dx}}{\boldsymbol{dt}} = \boldsymbol{v}\frac{\boldsymbol{db(x,t)}}{\boldsymbol{dx}} = \frac{dJ_n(x,t)}{dx} \qquad (16)$$

and the straighforward usage of the recurrence relation of the integer-order Bessel function, then one gets

$$\frac{\boldsymbol{db(x,t)}}{\boldsymbol{dx}}\frac{\boldsymbol{dx}}{\boldsymbol{dt}} \Rightarrow \frac{\boldsymbol{db(x,t)}}{\boldsymbol{dx}} = \frac{\boldsymbol{1}}{\boldsymbol{v}}[\boldsymbol{J_{n-1}(x)} - \boldsymbol{J_{n+1}(x)}]. \qquad (17)$$

Although not any direct interpretation can be extracted from Eq. 17, it is emphasized that only experimental data can provide a robust interpretation and matching if any, from the implementation of Bessel functions in the Keller-Segel scenario. Fig. 2 also exhibits a possible competitivity among bacteria along their displacements when all of them are under action of chemotaxis. This displacement per unit of time constitutes the aggregation bacteria velocity "$\boldsymbol{v}$" as written in right-side of Eq. 17. A tentative explanation about the origin of motility in certain types of bacteria, would be inside the territory of electricity where physics laws could explain inherent properties that are driven by electric forces, either attraction or repulsion. Some studies in the past about that have been reported, for example the one given in [11]. Under this view, the component ionic of bacteria emerges as the main point to board the problem of motility and chemotaxis. With this property, classic electrodynamics emrges as a sustained scenario to go through the bacteria motility properties.

Therefore, one can anticipate that the displacements done by aggregations of bacteria is dictated by classic physics and its corresponding electrodynamics. It is actually not valid for distances less than 0.001nm where quantum mechanics governs.

3. ELECTRODYNAMICS ANALYSIS OF BESSEL-KELLER-SEGEL EQUATION

A first view to be debated is about the BKS equation's solutions as done in Eq. 13 where the integer-order Bessel functions appear as the possible solutions of bacteria density. One can wonder if the volume integration returns the total electric charge. Actually, this fits well in electrodynamics in the sense that the total charge enclosed in a spherical volumen of radius "R" (for example, another spatial geometry can be opted as well). A straightforward integration: $\boldsymbol{Q(t)} = \int_0^R \boldsymbol{dV\, b(x,t)} = \int_0^R \boldsymbol{4\pi r^2\, J_n(x,t)\, dr}$ Is seen as the net charge. Below in Fig. 3 the different normalized total charge distributions as a function of sphere radius "$\boldsymbol{R}$" are displayed. One can see that the ampitude of distributions increases with the radius. For large radius, then one would expect strong attractions as well as repulsion forces, having direct implications with the highest and lowest levels in both cooperativity and competitivity.

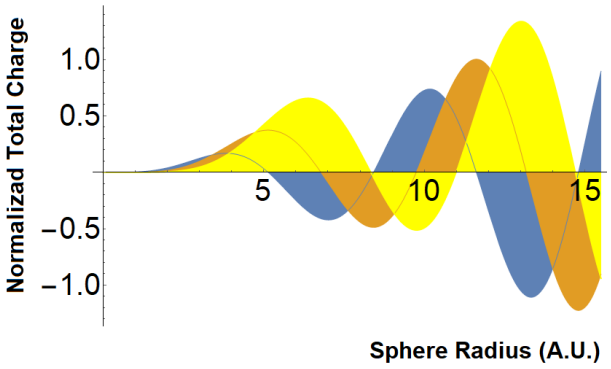

Fig. 3 – The normalized total charge of bacteria against the sphere radius exhibiting oscillations due to the Bessel-like behavior.

Thus in those scenarios of high electric charge for example, one can consider the role of electrodynamics in relation to the level of disruption among populations from the fact that large accumulation of ions would generate electric forces among them. It should be noted that electric interactions can be a reason to disturb the purpose of colonization. This might affect the "so-called cheaters" and other types of social manifestations of bacteria when carrying out actions of chemotaxis. Furthermore, engineered nanodevices recovered of ionic material would constitute an interesting window to attack the problem of infection and the respective diseases caused by bacteria (or virus).

With this background, it is feasible to derive a theory of classical electrodynamics from a BKS equation as expressed in Eq. 12. Thus, it can be written below in conjunction with time evolution as:

$$\frac{\boldsymbol{\partial\, b(x,t)}}{\boldsymbol{\partial t}} = \boldsymbol{x^2}\left[\frac{\boldsymbol{d^2 b(x,t)}}{\boldsymbol{dx^2}}\right] + \boldsymbol{x}\left[\frac{\boldsymbol{db(x,t)}}{\boldsymbol{dx}}\right] + \left(\boldsymbol{1} - \frac{\boldsymbol{n^2}}{\boldsymbol{x^2}}\right)\boldsymbol{b(x,t)}. \qquad (18)$$

As seen in previous works, bacteria can transport electrically charged proteins and any type of ions that microorganisms can bring on them. This constitutes an argument to analyze the Keller-Segel equation in terms of electric charge.

Mathematically speaking, one can integrate the volume in both sides of Eq. 18 , so that one gets:

$$\frac{d}{dt}\int \boldsymbol{b}(\boldsymbol{x},\boldsymbol{t})\boldsymbol{dV} = x^2\frac{d^2}{dx^2}\int \boldsymbol{b}(x,t)\,\boldsymbol{dV} + \boldsymbol{x}\frac{\boldsymbol{d}}{\boldsymbol{dx}}\int \boldsymbol{b}(\boldsymbol{x},\boldsymbol{t})\,\boldsymbol{dV} - \left(\mathbf{1}-\frac{\boldsymbol{n}^2}{\boldsymbol{x}^2}\right)\int \boldsymbol{b}(x,t)\,\boldsymbol{dV} \quad (\mathbf{19})$$

From the side of electricity, $\boldsymbol{b}(\boldsymbol{x},\boldsymbol{t})$ denotes the volumetric charge density transported by bacteria, fact that implies that its integration over the volume containing the charge turns out to be the net charge: $\boldsymbol{Q}(\boldsymbol{t}) = \int \boldsymbol{dV}\,\boldsymbol{b}(\boldsymbol{x},\boldsymbol{t})$. Under this view the left side of Eq. 19 is recognized as the instantaneous electric current. Thus, one arrives at:

$$\frac{\boldsymbol{dQ}(\boldsymbol{t})}{\boldsymbol{dt}} = \boldsymbol{I}(\boldsymbol{t}) = x^2\frac{d^2}{dx^2}\int \boldsymbol{b}(x,t)\,\boldsymbol{dV} + \boldsymbol{x}\frac{\boldsymbol{d}}{\boldsymbol{dx}}\int \boldsymbol{b}(x,t)\,\boldsymbol{dV} - \left(1-\frac{n^2}{x^2}\right)\int \boldsymbol{b}(x,t)\,\boldsymbol{dV} \quad (\mathbf{20})$$

By assuming the cylindrical coordinates system then the variable "x" is now changed to be the radial coordinate. Then one gets:

$$\boldsymbol{I}(\boldsymbol{t}) = \boldsymbol{r}^2\frac{\boldsymbol{d}^2}{\boldsymbol{dr}^2}\int \boldsymbol{b}(\boldsymbol{r},\boldsymbol{t})\,\boldsymbol{dV} + \boldsymbol{r}\frac{\boldsymbol{d}}{\boldsymbol{dr}}\int \boldsymbol{b}(\boldsymbol{r},\boldsymbol{t})\,\boldsymbol{dV} - \left(\mathbf{1}-\frac{\boldsymbol{n}^2}{\boldsymbol{r}^2}\right)\boldsymbol{Q}(\boldsymbol{t}). \quad (\mathbf{21})$$

Now special attention is paid on the first term of the right side. Since $\boldsymbol{b}(x,t)$ have been defined as the density of charge transported by bacteria, then this term is processed as follows:

$$\boldsymbol{r}^2\frac{d^2}{dr^2}\int \frac{\boldsymbol{Q}(\boldsymbol{t})}{\boldsymbol{A}\,\boldsymbol{r}}\boldsymbol{dV} = \frac{\boldsymbol{r}^2}{\boldsymbol{A}}\,\boldsymbol{\nabla}\int \boldsymbol{\nabla}\left(\frac{\boldsymbol{Q}(\boldsymbol{t})}{\boldsymbol{r}}\right)\boldsymbol{dV} \quad (\mathbf{22})$$

where the volume has been assumed to be $\boldsymbol{V} = \boldsymbol{r}\,\boldsymbol{A}$. The radial derivatives are actually the gradient operator that acts onto the electric potential [12] given by:

$$\boldsymbol{\Phi}(\boldsymbol{r}) = \frac{\boldsymbol{Q}(\boldsymbol{t})}{\boldsymbol{4\pi\varepsilon r}}. \quad (\mathbf{23})$$

With the balance of units and the incorporation of permissivity constant one arrives at:

$$\boldsymbol{r}^2\frac{\boldsymbol{d}^2}{\boldsymbol{dr}^2}\int \frac{\boldsymbol{Q}(\boldsymbol{t})}{\boldsymbol{A}\,\boldsymbol{r}}\boldsymbol{dV} = \frac{\boldsymbol{4\pi\varepsilon r}^2}{\boldsymbol{A}}\,\boldsymbol{\nabla}\int \boldsymbol{\nabla}\left(\frac{\boldsymbol{Q}(\boldsymbol{t})}{\boldsymbol{4\pi\varepsilon r}}\right)\boldsymbol{dV} = \frac{\boldsymbol{4\pi\varepsilon r}^2}{\boldsymbol{A}}\,\boldsymbol{\nabla}\int \boldsymbol{\nabla}\boldsymbol{\Phi}(\mathbf{r})\;\boldsymbol{dV}. \quad (\mathbf{24})$$

By which one can identify that in the last equation one has the field electric, thus one arrives at the divergence theorem , yielding that this contribution to the BKS equation is proportional to the square of cylindric radius. With this one gets that:

$$\frac{\boldsymbol{4\pi\varepsilon r}^2}{\boldsymbol{A}}\,\boldsymbol{\nabla}\int \boldsymbol{\nabla}\boldsymbol{\Phi}(\mathbf{r})\;\boldsymbol{dV} = \frac{-\boldsymbol{4\pi\varepsilon r}^2}{\boldsymbol{A}}\int \boldsymbol{\nabla}.\mathbf{E}\;\boldsymbol{dV} = \frac{-\boldsymbol{4q}(\boldsymbol{t})\boldsymbol{\pi\varepsilon r}^2}{\boldsymbol{Ae}} \quad (\mathbf{25})$$

Where Gauss's law was employed but in the form of:

$$\int \boldsymbol{\nabla}.\mathbf{E}\;\boldsymbol{dV} = \frac{\boldsymbol{q}(\boldsymbol{t})}{\boldsymbol{e}} \quad (\mathbf{26})$$

With "$\boldsymbol{e}$" a permissivity constant different to "$\boldsymbol{\varepsilon}$" because equipotential lines might not be inside the region of electric field in some points of space of bacteria displacement, so that only a single medium is not expected. Instead up two media or more can coexist together. A similar procedure can be applied to the second term of the right side of Eq. 21:

$$\boldsymbol{r}\frac{\boldsymbol{d}}{\boldsymbol{dr}}\int \boldsymbol{b}(x,t)\,\boldsymbol{dV} = \frac{\boldsymbol{4\pi\varepsilon r}}{\boldsymbol{A}}\int \boldsymbol{\nabla}\left(\frac{\boldsymbol{Q}(\boldsymbol{t})}{\boldsymbol{4\pi\varepsilon r}}\right)\boldsymbol{dV} \quad (\mathbf{27})$$

and again, one can construct the electric potential yielding finally that the term of Eq. 27 is linearly proportional to the cylindric radius:

$$\frac{\boldsymbol{4\pi\varepsilon r}}{\boldsymbol{A}}\int \boldsymbol{\nabla}\left(\frac{\boldsymbol{Q}(\boldsymbol{t})}{\boldsymbol{4\pi\varepsilon r}}\right)\boldsymbol{dV} =$$

$$\frac{\boldsymbol{4\pi\varepsilon r}}{\boldsymbol{A}}\int \boldsymbol{\nabla}\boldsymbol{\Phi}(\mathbf{r})\,\boldsymbol{dV} = \frac{-\boldsymbol{4\pi\varepsilon r L}}{\boldsymbol{A}}\int \mathbf{E}\,\boldsymbol{dA} = \frac{-\boldsymbol{4q}(\boldsymbol{t})\boldsymbol{\pi\varepsilon r L}}{\boldsymbol{Ae}}. \quad (\mathbf{28})$$

It should be noted again that $\boldsymbol{dV} = \boldsymbol{L}\boldsymbol{dA}$. Therefore, when previous resulting equations done above are inserted in Eq. 21 then one arrives at:

$$\frac{\boldsymbol{dQ}(\boldsymbol{t})}{\boldsymbol{dt}} = \left[-\frac{\boldsymbol{4q}(\boldsymbol{t})\boldsymbol{\pi\varepsilon r}^2}{\boldsymbol{Ae}} - \frac{\boldsymbol{4q}(\boldsymbol{t})\boldsymbol{\pi\varepsilon r L}}{\boldsymbol{Ae}} - \left(1-\frac{\boldsymbol{n}^2}{\boldsymbol{r}^2}\right)\right]\boldsymbol{Q}(\boldsymbol{t}). \quad (\mathbf{29})$$

Thus, one can see that all charges of the right side have a negative sign. Putting apart the total charge, then one arrives at:

$$\frac{\boldsymbol{dQ}(\boldsymbol{t})}{\boldsymbol{dt}} = \boldsymbol{Q}(\boldsymbol{t})\left[-\frac{\boldsymbol{4\pi\varepsilon r}^2}{\boldsymbol{Ae}} - \frac{\boldsymbol{4\pi\varepsilon r L}}{\boldsymbol{Ae}} - \left(\mathbf{1}-\frac{\boldsymbol{n}^2}{\boldsymbol{r}^2}\right)\right]. \quad (\mathbf{30})$$

One can see that the apparition of sign "-" on the right side is because the possible existence of a type of discharge because the straightforward solution of Eq. 30 yields the familiar negative exponential.

Electric interactions between compounds can be measured through the electric force as dictated by classical electrodynamics. To explore this, the total charge of bacteria should be explicitly done, thus from Eq. 30,

$$\frac{\boldsymbol{dQ}(\boldsymbol{t})}{\boldsymbol{Q}(\boldsymbol{t})} = \left[-\frac{\boldsymbol{4\pi\varepsilon r}^2}{\boldsymbol{Ae}} - \frac{\boldsymbol{4\pi\varepsilon r L}}{\boldsymbol{Ae}} - \left(1-\frac{\boldsymbol{n}^2}{\boldsymbol{r}^2}\right)\right]\boldsymbol{dt}, \quad (\mathbf{31})$$

whose integration yields the closed-form solution:

$$Q(t) = Q_0 Exp\left[-\int_0^T \frac{4\pi\varepsilon}{Ae}\left(r^2 + r + \eta\left[1-\frac{n^2}{r^2}\right]\right)dt\right] \quad (32)$$

With $\eta = \frac{Ae}{4\pi\varepsilon}$ and by specifying the upper limit by "T" the net charge that is transported by the bacteria with the change $R(r) = r^2 + r + \eta\left[1-\frac{n^2}{r^2}\right]$, then Eq. 32 can be written in compact form as:

$$Q(T,r) = Q_0 Exp\left[-\frac{4\pi\varepsilon T}{Ae}R(r)\right]. \quad (33)$$

With this result, now the electric current that involves a more general electric description of bacteria aggregation transporting ions is given by the instantaneous derivative of Eq. 33 and written as:

$$I(t=T,r) = -\frac{4Q_0\pi\varepsilon T}{Ae}\frac{dR(r,t)}{dt}\ Exp\left[-\frac{4\pi\varepsilon T}{Ae}R(r)\right]. \quad (34)$$

On the other hand in the simplest case by which "r" does not depend on time, then the integration over the time variable inside the exponential in Eq. 32 is trivial. In this manner the resulting electric current can be written in a simplified form as:

$$\frac{dQ(t)}{dt} = I(T) = -\frac{4Q_0\pi\varepsilon T}{Ae}R(r)Exp\left[-\frac{4\pi\varepsilon T}{Ae}R(r)\right]. \quad (35)$$

Actually the variable "T" can be understood as the period in the which the bacteria aggregation behaves as an electric current.

3.1 Biophysics Interpretation of Electrical Currents

Eq. 34 is displayed in Fig. 4 exhibiting a minimum for $r \approx 2$ a.u. For this plotting it was used as a numerical expression for Eq. 34 in the form of:

$$I(t=T,r) = 0.0001(2r + 0.01 + \frac{8}{(r)\text{^}3})Exp[-0.01(r\text{^}2 + 0.01r + (1 - \frac{4}{(r)\text{^}2}))]. \quad (36)$$

As indicated at Fig. 4, bacteria aggregation would exhibit a kind of disruption as seen in the minimum value of current distribution. In this manner, one can wonder if it is an inherent property of bacteria aggregation or if it is a pure speculative theoretical result that might not be matched with experiments. It should be noted that all these procedures have been done under the assumption of a 1-Dimension model. Of course, realistic simulations might be necessary in order to identify rupture of electrical properties. As done in [14], memory-based chemotaxis would exibit drift velocities. So that one can argue that this drift dynamics might appear from electric phenomena more than a pure biological reason.

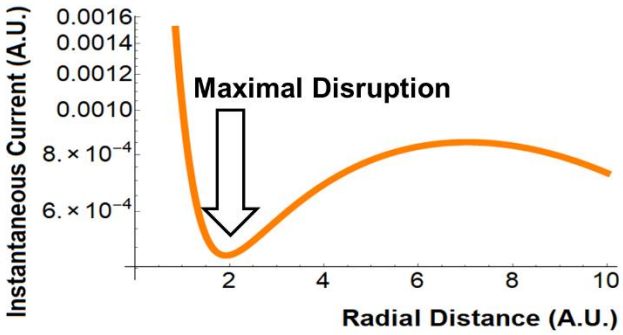

Fig. 4 – The instantaneous current as a function of radial distance (Eq.36), expressed in in arbitrary units. Two phases can be perceived.

Below in Fig. 5 the simplest scenario of Eq. 35 written as I(t)=tExp(-t) is illustrated. The qualitative shape of electric current indicates its maximal value. Clearly, it is directly interpreted as the inverse scenario of Fig. 4 establishing a kind of complementarity with it. This triggers logic scenario establishing that organization is first and disruption is after.

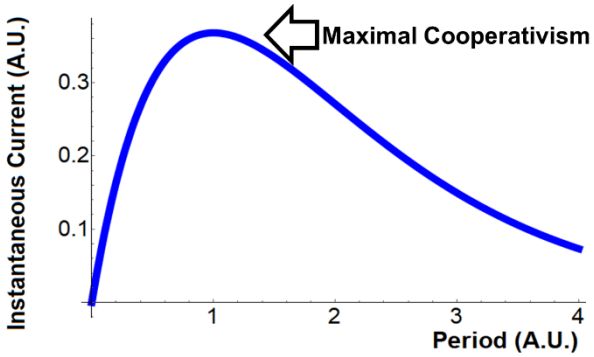

Fig. 5 – RC Discharge: The instantaneous current and period of electric interaction of bacteria as a function of radial distance, both expressed in in arbitrary units. This plot as well as Fig. 1, Fig. 2, Fig. 3 and Fig. 4 were done with the usage of Wolfram [13].

In this manner, one can see that from Fig. 4 and Fig. 5 the possible existence of well-defined phases. This would characterize the BKS model. These possible phases would emerge from the fact that the Eq. 5 exhibits a kind of electric discharge as a RC-circuit. It is in accordance to the negative exponential of Eq. 35. Therefore, bacteria aggregation and their social manifestations would be disrupted. In Fig. 5 the instantaneous current falls down as a fact that bacteria have "finshed" a social action leaving them to break down the possible molecular communications between them.

4. CONCLUSION

In this paper, an extension of the Keller-Segel equation has been established. It has taken advantage of having a second-order differential equation to establish a novel Bessel-Keller-Segel equation by which, at a first instance, it would give information about the electric behavior of bacteria and the possible implications of this in the social behavior. This appears to be crucial in prospective nanonetworks. Therefore, the electrodynamics of an electrically charged bacteria aggregation has been derived through closed-form equations. Interestingly, the shape of the curve of derived current exhibits a kind of discharge. Although a tentative interpretation in terms of social disruption because social behavior of the bacteria population is assumed, simulations and experimental studies should be done to corroborate the theory of this paper. The assumptions made throughout this paper have served to minimize the mathematical load that involves a second-order differential equation. Indeed the resulting curves have kept a close relationship with well-known electrodynamics.

In future work, some well-known families of bacteria and their data will be employed to explore the possible similarities with the present proposal.

REFERENCES

[1] E. F. Keller and L. A. Segel, Model for chemotaxis, J. Theor. Biol. 30 (1971) 225234.

[2] Michael Vilkhovoy, Mason Minot and Jeffrey D. Varner, Effective Dynamic Models of Metabolic Networks, IEEE Life Sciences Letters, Volume: 2, Issue: 4, 2016.

[3] Bige D. Unluturk, Sasitharan, Balasubramaniam, Ian F. Akyildiz, The Impact of Social Behavior on the Attenuation and Delay of Bacterial Nanonetworks, IEEE Transactions on NanoBioscience, Year: 2016 Volume: 15, Issue: 8.

[4] I. F. Akyildiz, The internet of Bio-Nano things, IEEE Communications Magazine Year: 2015, Volume: 53, Issue: 3, Pages: 32 - 40.

[5] X. Li, Y. Wang, Z. Xiang. Global existence and boundedness in a 2D Keller–Segel–Stokes system with nonlinear diffusion and rotational flux. Commun. Math. Sci., 14 (2016).

[6] Gerald Rosen, Navier-Stokes symmetry in the phenomenological transport theory for bacterial chemotaxis, Phys, Rev. A 29, 5, May 1984.

[7] Estrada-Rodriguez, Gissell, Gimperlein, HeikoPainter, Kevin. (2017). Fractional Patlak--Keller--Segel Equations for Chemotactic Superdiffusion. SIAM Journal on Applied Mathematics. 78. 10.1137/17M1142867.

[8] T. Xiang, "How strong a logistic damping can prevent blow-up for the minimal Keller-Segel chemotaxis system?," J. Math. Anal. Appl. 459, 1172–1200 (2018). https://doi.org/10.1016/j.jmaa.2017.11.022.

[9] Fournier, N., & Jourdain, B. (2015). Stochastic particle approximation of the Keller-Segel equation and two-dimensional generalization of Bessel processes. Annals of Applied Probability, 27, 2807-2861.

[10] T. Black. Sublinear signal production in a two-dimensional Keller–Segel–Stokes system Nonlinear Anal. Real World Appl., 31 (2016), pp. 593-609.

[11] Huber Nieto-Chaupis, Macrophage-Like Nanorobots To Anticipate Bacterial Dynamics, 2019 IEEE 9th Annual Computing and Communication Workshop and Conference (CCWC) Year: 2019, Conference Paper.

[12] J. D. Jackson, Classical Electrodynamics, 3rd Edition, Chap-I BoundaryValue Problems in Electrostatics: I. Wiley 1998.

[13] Wolfram Mathematica, www.wolfram.com.

[14] Gosztolai, A., Barahona, M. Cellular memory enhances bacterial chemotactic navigation in rugged environments. Commun Phys 3, 47 (2020). https://doi.org/10.1038/s42005-020-0312-8.

AUTHOR

Huber Nieto-Chaupis holds a Bachelor in Physics (1996) from the Universidad Nacional Mayor de San Marcos in Lima,Perú, a Licenciado in Physics (1999) from Universidad Nacional Mayor de San Marcos, a Master in Physics from Pontificia Univrsidad Católica del Perú (2003) and a Doktor in Rerum Naturalium Physik Experimental from Humboldt Universität in Berlin, Germany (2007). He has been a researcher at the Academia Sinica in Taiwan, Province of China (2007) and the University of Science and Technology of China in Hefeim, People's Republic of China (2009). In Perú, he has worked at the National University of Engineering UNI (2008-2011) and from 2011 to 2018 was an independent researcher working in various Peruvian private universities. In 2019, he joined the Universidad Autónoma del Perú as a senior principal investigator. He is interested in Nanomedicine, Internet of Bio-Nano Things, Photon science, Quantum Mechanics and Machine Learning.

INDEX OF AUTHORS

International
Telecommunication
Union

Telecommunication
Standardization Bureau (TSB)

Place des Nations
CH-1211 Geneva 20
Switzerland

ISSN: 2616-8375
Published in Switzerland
Geneva, December 2021